Development of a novel approach to influence the secretion of pathogenicity factors of *Staphylococcus aureus* by synthetic peptides

Von der Fakultät für Lebenswissenschaften

der Technischen Universität Carolo-Wilhelmina

zu Braunschweig

zur Erlangung des Grades eines

Doktor der Naturwissenschaften

(Dr. rer. nat.)

genehmigte

D i s s e r t a t i o n

von Jihad Mohammad Zakaria Jameel Al-Qudsi
aus Kuwait/ Emirat Kuwait

1. Referent: Professor Dr. Dieter Jahn
2. Referentin Privatdozentin Dr. Eva Medina
eingereicht am: 27.02.2012
mündliche Prüfung (Disputation) am 04.05.2012

Druckjahr 2012

Vorveröffentlichungen der Dissertation

Teilergebnisse aus dieser Arbeit wurden mit Genehmigung der Fakultät für Lebenswissenschaften, vertreten durch den Mentor der Arbeit, in folgenden Beiträgen vorab veröffentlicht:

Tagungsbeiträge (Conference contributions):

1. **[Poster presentation, 31st European Peptide Symposium, Copenhagen, Denmark, September 2010]**

Abstract: Al-Qudsi, J; Frank, R; and Tegge, W. Peptide constructs that interfere with the Sec pathway can reduce the secretion of bacterial pathogenicity factors. Journal of Peptide Science, 2010 Vol 16, Issue S1. DOI: 10.1002/psc.1303

2. **[Poster presentation, 1st North-Region-Day on Infection, Braunschweig, Germany, October 2010]**

Al-Qudsi, J; Frank, R; and Tegge, W. Disarming *Staphylococcus aureus* from secreting virulence factors by synthetic peptides.

3. **[Poster presentation, 7th Status Seminar Chemical Biology of the DECHEMA, Frankfurt, Germany, December 2011]**

Al-Qudsi, J; Frank, R; and Tegge, W. Peptide constructs that interfere with the Sec pathway can reduce the secretion of bacterial pathogenicity factors.

Acknowledgement

This PhD thesis is definitely and sofar the most important scientific accomplishment in my life and it would have been difficult to complete this work without support from the following. My special gratitude to Dr. Werner Tegge for his help in introducing me to this interdisciplinary theme, and for his unforgettable support in helping me understand medicinal, microbiological and molecular biology issues that pertain to this project. I thank Dr. Eva Medina for supporting this work until success. I am grateful to Prof. Dr. Dieter Jahn for his support and willingness to adopt this thesis under his supervision.

My gratitude to Dr. Jacek Miedzobrodzki (Krakow university, Poland) for providing me with *S. aureus* V8 strain, and to Dr. Christian Erk who facilitated the contact with Biogene GmbH for producing the anti rabbit-V8 protease, and to Dr. Lothar Gröbe for his support and engagement to perform the FACS analyses. My deep gratitude to Prof. Dr. John Colins, the English native-speaker, and to Dr. Lars Hillringhaus, the German native-speaker, who revised this dissertation. At this point, I would like warmly to thank the department of chemical biology for the creative discussions, thanks to all chemists and biologists in the teams of proteomics and infection biology at the Helmholtz Centre for the pleasant working atmosphere and their helpfulness not only in laboratory work.

Very special thanks to my parents, my sisters, and my brothers who always have been and are still supportive.

To my wife: Million thanks not only for supporting me in preparing this thesis, but also for your moral support.

Table of Contents

Abbreviations

The following abbreviations were used in this study, and were ordered alphabetically.

Abbreviation	Description
°C	degrees Celsius
ABz	3-Aminobenzoic acid
AcOH	Acetic acid
ADP	Adenosine diphosphate
agr	accessory gene regulator
AIPs	Auto-inducing peptides
AMP	methionine aminopeptidase
AMP	Adenosine monophosphate
AMP	Antimicrobial Peptide
ATCC	American Type Culture Collection
ATP	Adenosine triphosphate
Aur	Metalloprotease (aureolysin)
BHI	Brain Heart infusion
Boc	tert.-Butoxycarbonyl group
cap5	Polysaccharide capsule type 5
cap8	Polysaccharide capsule type 8
Cbz	Carboxybenzyl
CFP 10	Culture filtrate protein 10 kD (has no signal peptide)
CHCl3	Chloroform
clfA, clfB	Clumping factor A, Clumping factor B
CLSM	Confocal laser scanning microscopy
cna	Collagen Binding Protein
CnbP	Collagen Binding Protein
Coa	Coagulase
CPP	cell-penetrating peptides
CW	cell wall fraction
CWDS	Cell wall digestion supernatants
cyclo-	cyclic form of a peptide
Da	Dalton
DCC	N,N'-Dicyclohexylcarbodiimide (coupling reagent for amino acids in peptide synthesis)
DCM	Dichloromethane
dH_2O	distilled Water
DIC	N,N'-Diisopropylcarbodiimide (coupling reagent for amino acids in peptide synthesis)
DIPEA	Diisopropylethylamine
DMF	N,N-Dimethylformamide
DMSO	Dimethyl sulfoxide

DMSO	
DTT	Dithiothreitol
e.g.	for example
EDTA	Ethylenediaminetetraacetic acid
eq.	equivalent
ESAT-6	Early secreted antigenic target secretion system
ESI	Electrospray-Ionization
et al	and others, and elsewhere
Eta	Exfoliatin A
etb	Exfoliatin B
EtOH	Ethanol
EU	European Union
F5M	fluorescein -5-maleimide
FACS	fluorescence-activated cell sorter
Ffh	54 kD homologue of the SRP in eukaryotes, this homologue is found in prokaryotes
FITC	Fluoresceinisothiocyanat
Fme	FAME
Fmoc	N-(9-fluorenyl)methoxycarbonyl
FnbA, fnbB	Fibronectin Binding-protein A, Fibronectin Binding-protein B
FnbP	Fibronectin-binding protein
FtsZ	the bacterial cytoskeleton protein named after " Filamenting temperature-sensitive mutant Z"
g	Gram
geh	Glycerol ester hydrolase
GFP	green fluorescent protein
Glu-C	Glutamyl-C endoproteinase from *Staphylococcus aureus*
HAI	Health-care Associated infections
HATU	O-(7-azabenzotriazol-1-yl)-1,1,3,3-tetramethyluronium hexafluorophosphate
HCl	Hydrochloric acid
HEPES	N-(2-Hydroxyethyl)Piperazin-NS-2-Ethansulfonsäure
HIV	Human immunodeficiency virus that causes acquired immunodeficiency syndrome (AIDS
hla, hlb	α-Hemolysin, β-Hemolysin
hld, hlg	δ-Hemolysin, γ-Hemolysin
HOAt	1-Hydroxy-7-Azabenzotriazol
HOBt	Hydroxybenzotriazol
HPLC	High Performance Liquid Chromatography
hr	Hour/hours
Hys	Hyaluronidase
HZI	Helmholtz-Zentrum für Infektionsforschung, Braunschweig
i.e.	id est (latin) that is
IC50	50 % inhibition concentration
kDa	Kilodalton

Kg	Kilograms
L	Litre
LB medium	Luria-Bertani medium
LBP	Lactoferrin Binding-protein
LC-MS	Liquid chromatography-mass spectroscopy
lip	Lipase (butyryl esterase)
lukS/F	PVL leukocidin*
M	Membrane fraction
m/z	Mass to charge ratio
MALDI	Matrix Assisted Laser Desorption/Ionization
MeCN	acetonitrile
MeOH	Methanol
mg	Milligrams
MH medium	Müller-Hinton medium
min	Minute
ml	Millilitres
mM	Milimole
Mr	Molecular mass
MRSA	methicillin resistant *Staphylococcus aureus*
MS	Mass spectrometry
MTT	3-(4,5-dimethylthiazol-2-yl)-2,5-diphenyl tetrazolium bromide
Mw	Molecular weight
NADPH	Nicotinamide adenine dinucleotide phosphate
nm	nanometer
NMP	N-Methyl-2-Pyrrolidon
Nuc	Nuclease
OD	optical density
OD600	optical density at a wavelength 600 nm
P1	peptide-1 RSNNPFRARC-Fluor
P2	peptide-2
P3	peptide-3 YGRKKRRQRRRC-Fluor
Pbf	2,2,4,6,7-pentamethyldihydrobenzofuran-5-sulfonyl
PBS	Phosphate Buffered Saline
PDF	Peptide deformylase
PI	Propedium iodide
Plc	PI-phospholipase C
PMF	peptide mass fingerprinting
PMSF	Phenylmethylsulfonyl fluoride (serine protease inhibitor)
PNA	peptide nucleic acid
PS	Periplasm fraction
PVL	Panton Valentine Leukocidine

PyAOP	7-azabenzotriazol-1-yl-oxy-tris-pyrrolidino-phosphonium
PyBOP	benzotriazole-1-yl-oxy-tris-pyrrolidino-phosphonium hexafluorophosphate
QS	Quorum sensing
RBHE	Rhodamine B hexyl ester
RP	Reversed phase
rpm	Revolutions per minute
S	Supernatant fraction
S. aureus	*Staphylococcus aureus*
Sak	Staphylokinase
Sar	Staphylococcal accessory regulator
Scp	Staphopain (protease II)
sea, seb	Staphylcoccal enterotoxin A, Enterotoxin B
Sec	Major secretion pathway
Sec YEG	Hexamer protein that forms the membrane channel
Sec, sed	Staphylococcal Enterotoxin C, Staphylococcal Enterotoxin D
SecA	Dimer protein known as the secretory motor (ATPase)
seh	Staphylococcal Enterotoxin H
Spa	Staphylococcal Protein A
splA-F	Serine protease-like
SPPS	Solid-phase peptide synthesis
SPsB	Staphylococcal signal peptidase B
SRP	Signal recognition particle
SrtA	Sortase A
SrtB	Sortase B
ssp	staphylococcal serine protease (V8 protease)
sspB	staphylcoccal Cysteine protease
t But	tert-butyl
TAT	Twin Arginine Translocator
Tat-protein	Trans-Activator of Transcription
TBS-T	Tris-Bufferd Salin- tweened
TBTU	O-(Benzotriazol-1-yl)-N,N,N',N'-Tetramethyl-Uronium Tetrafluoroborate
TFA	Trifluoroacetic acid
TOF	Time of Flight
TRIS-HCl	tris(hydroxymethyl)amino methane
Trt	Tripheylmethyl (Trityl)
TSB	Tryptic Soy Broth
TSST	Toxic shock syndrom toxins
tst	Toxic shock toxin-1
Tween 20	Polysorbate surfactant 20
VISA	Vancomycin intermediate resistant *Staphylococcus aureus*
WST	Water soluble tetrazolume

λ	Wavelength
μl	microlitres
μm	Micrometer
μM	Micromole

Abstract

The emergence of antibiotic-resistant strains of *Staphylococcus aureus* including *MRSA* and *VISA* demands a modification in the attack strategy of antimicrobial agents. This prompted the search for novel compounds and new bacterial targets to combat infectious diseases that are associated with this pathogen. In this study, the major bacterial secretion pathway Sec was chosen as a novel target, because it has been identified as being responsible for secreting most of the staphylococcal proteins, which act directly and indirectly in the phases of infection processes. Depending on their signal sequences, the Sec-dependent proteins are directed in unfolded form through the bacterial membrane and displayed on the cell surface or secreted into the environment. We developed an approach, which should allow inhibition of secretion of a Sec-dependent protein (V8 protease). The approach utilizes chemically constructed peptides that represent the 29 amino acid secretion signal peptide of V8 protease (MKGKFLKVSSLFVATLTTATLVSSPAANA) conjugated to a cell penetrating peptide that facilitates the entry of the construct into bacterial cells. The signal recognition particle (SRP), the ATPase motor protein (SecA), and/or the signal peptidase (SpsB) were hypothesized as possible targets in the Sec system. Those are known to interact with the signal peptide of the secreted proteins, and thus may be competitively inhibited by the constructed peptides.

To test this hypothesis, it was necessary to chemically generate the potentially Sec-interfering peptides, and establish appropriate assays that facilitate monitoring their effect on inhibiting this type of secretion. For that purpose, the fluorescein-conjugated forms of three known cell-penetrating peptides (CPPs) were first synthesized. The uptake efficiency to these peptides by *S. aureus* was investigated using fluorescence microscopy and FACS analysis. The HIV-Tat derived peptide YGRKKRRQRRRC-F5M showed the most promising properties.

Based on this result, eight further peptidic constructs were chemically synthesized. A subset of these peptides contain the three different N-terminal forms of the secretion signal peptide of V8 protease as they may be found in prokaryotes during or after translation: with formylated methionine, with methionine, and without methionine, conjugated to the cell penetrating peptide (CPP). For control purposes, another subset of three forms of the V8 protease secretion signal peptide was synthesized without CPP. One construct was synthesized with a scrambled sequence of the secretion signal conjugated to the CPP, and one peptide was synthesized as unconjugated CPP. These peptide constructs were investigated with respect to their

ability to reduce the secretion of the Sec-dependent protein V8 protease. The secretion of V8 protease was evaluated by Western blot analysis, which provided a valid and reproducible quantitative detection. The investigated peptides did not show any effect on bacterial growth and viability. Only one peptide (KGKFLKVSSLFVATLTTATLVSSPAANAYGRKKRRQRRR-NH_2) among the different constructs showed a concentration-dependent effect in reducing the secretion of V8 protease, which was inhibited by up to 40% at 40 µM. This effect was not limited to V8 protease secretion. Inhibition of secreted hemolysins and other proteases was also observed. Subcellular fractionation reveiled that treatment of the staphylococcal cells with this peptide showed retention of V8 protease in the cell wall and periplasm fraction, which suggests an interference with the transport of the protease through the cell wall after its release from the membrane.

Although the underlying mode of action of this peptide in inhibiting the secretion is still not understood, a fluorescence-dependent analysis of the subcellular fractions showed a localization of the fluorescein-conjugated peptides in supernatant, cell wall and periplasm fraction, cytosol, and the membrane, with the highest abundance in the cytosol.

In conclusion, this study can be regarded as a preliminary positive insight that secretion of bacterial virulence factors can be inhibited by synthetic peptides. Although it requires further study, it supports the idea that such an approach may eventually provide a new strategy for antimicrobial intervention.

Zusammenfassung

Die Entstehung von Antibiotika-resistenten Stämmen von *Staphylococcus aureus* wie MRSA und VISA erfordert eine Änderung in der Angriffstrategie der antimikrobiellen Mittel. Dies veranlasste die Suche nach neuartigen Substanzen und neuen bakteriellen Targets um Infektionskrankheiten, die mit diesem Erreger verbunden sind, weiterhin wirksam bekämpfen zu können. In dieser Studie wurde der bakterielle Sekretionsweg Sec als neuartiges Ziel gewählt, da er für die Sekretion der meisten Staphylokokken-Proteine verantwortlich ist, die direkt und indirekt am Infektionsprozess beteiligt sind. In Abhängigkeit ihrer Signalpeptide werden die Sec-abhängigen Proteine in ungefalteter Form durch die bakterielle Membran transportiert und an der Zelloberfläche verankert oder in die Umgebung sezerniert. Wir entwickelten einen Ansatz, der die Hemmung der Sekretion eines Sec-abhängigen Proteins (V8-Protease) ermöglichen sollte. Dieser Ansatz nutzt durch chemische Synthese erzeugte Peptide, welche das aus 29 Aminosäuren bestehende Sekretions-Signalpeptid der V8-Protease (MKGKFLKVSSLFVATLTTATLVSSPA-ANA) enthalten und durch Konjugation mit einem Zell-penetrierenden Peptid (CPP) den Eintritt in die Bakterienzellen ermöglichen. Wir stellten die Hypothese auf, dass das Signalerkennungspartikel (Signal Recognition Particle, SRP), das ATPase Motorprotein (SecA) und/oder die Signalpeptidase (SpsB) mögliche Targets innerhalb des Sec-Systems sein könnten. Es ist bekannt, dass diese mit dem Signalpeptid der sekretierten Proteine wechselwirken und folglich durch die Peptidkonstrukte kompetitiv gehemmt werden könnten.

Um diese Hypothese zu überprüfen war es notwendig, potenziell Sec-interferierende Peptide chemisch herzustellen und geeignete Assays zu entwickeln, mit denen die Inhibition der Sekretion untersucht werden kann. Dazu wurden zunächst die Fluoreszenz-konjugierten Formen von drei bekannten zellpenetrierenden Peptiden (CPP) chemisch synthetisiert. Die Aufnahme-Effizienz dieser Peptide durch *S. aureus* wurde mit Hilfe der Fluoreszenzmikroskopie und FACS-Analyse ausgewertet. Das HIV-Tat Peptid YGRKKRRQRRRC(F5M)-NH_2 zeigte die vielversprechendsten Eigenschaften.

Auf diesem Ergebnis basierend wurden acht weitere peptidische Konstrukte chemisch synthetisiert. Drei Peptide davon enthielten die unterschiedlichen N-terminalen Formen des Sekretions-Signalpeptids der V8 Protease, wie sie in Eukaryoten während oder nach dem Translationsprozess vorkommen: mit formyliertem Methionin, mit Methionin und ohne Methioninin, jeweils konjugiert mit dem zellpenetrierenden Peptid (CPP). Für Kontrolluntersuchungen wurden drei weitere Formen des V8 Protease Sekretions-Signalpeptids

ohne CPP, ein weiteres Peptid mit einer gemischten Aminosäuresequenz des Sekretions-Signalpeptids in Konjugation mit CPP und ein weiteres Peptid als unkonjugiertes CPP synthetisiert. Die Peptide wurden bezüglich ihrer Fähigkeit, die Sekretion der Sec-abhängigen V8-Protease zu reduzieren, untersucht. Die Sekretion der V8-Protease wurde mittels Western Blot Analysen untersucht, was sich als valider und reproduzierbarer quantitativer Ansatz erwies. Die untersuchten Peptide zeigten keine Wirkung auf das Wachstum und die Lebensfähigkeit der Bakterien. Nur eines der acht Peptidkonstrukte (KGKFLKVSSLFVATLTTATLVSSPAANA-YGRKKRRQRRR-NH_2) zeigte eine konzentrationsabhängige Wirkung auf die Sekretion der V8-Protease mit einer Inhibition von bis zu 40% bei einer Konzentration von 40 µM. Dieser Effekt war nicht auf die V8-Protease beschränkt, sondern wurde auch bei den sezernierten Hämolysinen und anderen Proteasen beobachtet. In subzellulären Fraktionierungen von *S. aureus* zeigte sich eine durch das Peptidkonstrukt bewirkte Anreicherung der V8-Protease in der Zellwand und periplasmatischen Fraktion, was auf eine mögliche Interferenz des Transports der Protease durch die Zellwand nach der Ablösung des Proteins von der Zellmembran hinweist.

Obwohl der zugrundeliegende Wirkmechanismus dieses Peptids bei der Hemmung der Sekretion noch nicht verstanden ist, zeigte eine Fluoreszenz-abhängige Analyse der subzellulären Fraktionen eine Lokalisierung der Fluorescein-konjugierten Peptidkonstrukte im Wachstumsmedium, in der Zellwand-Periplasma Fraktion, im Zytosol und in der Membran, wobei sich die größte Menge im Zytosol befand.

Zusammenfassend kann diese Studie als positiver Ansatz für die Inhibition der Sekretion bakterieller Virulenzfaktoren durch synthetische Peptide gewertet werden. Auch wenn vertiefende Studien notwendig sind, wird die Idee bekräftigt, dass solch ein Ansatz möglicherweise eine neue Strategie für eine antimikrobielle Intervention darstellt.

1 INTRODUCTION

1.1 *Staphylococcus aureus*: commensal and pathogenic species

Staphylococcus aureus (*S. aureus*), a Gram-positive bacterium, can switch between two distinct lifestyles: *commensal and pathogenic.* In the commensal form *Staphylococcus aureus* is asymptomatic. This is the case for 30–40% of the general population. Since this species is part of the human normal flora, it is mostly harbored in the moist and sebaceous regions of the skin, such as the armpit and the perineum, or in the lining mucous layers, of mouth cavities, anterior nares, and pharynx. Figure 1.1 highlights the physiological colonizing niches of *Staphylococcus aureus* in and on the human body. Today, it is the leading cause of human infections worldwide, not only in the hospital environment but also in the community [1, 2].

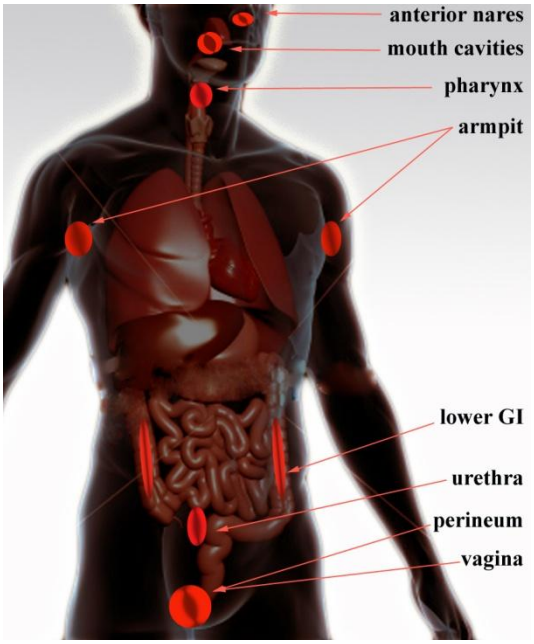

Figure 1.1 Major colonization and infection sites of *Staphylococcus aureus* in and on the human body.

1.2 *Staphylococcus aureus*: a major human pathogen

The pathogenic bacterium *Staphylococcus aureus* has the potential to cause a wide variety of human diseases, ranging from superficial abscesses and wound infections to deep and systemic infections such as osteomyelitis, endocarditis, and septicemia. This has been attributed to a large number of secreted toxins and digesting enzymes as well as to the bacterial surface proteins that bind various host molecules. These so-called virulence factors are accessory. It has been proposed that these are synthesized in response to the specific needs for maintaing an appropriate environment during the course of the infection process [3].[1]

[1] The bacterial factors and mechanisms that actively cause the damage of the host tissue are referred to as "virulence factors"

1.3 *Staphylococcus aureus*: infection mechanisms

Staphylococcus aureus is an adept pathogen in eluding the defense mechanisms of the host through its ability in orchestrating the expression of virulence factors in two major phases, namely the adhesion and the invasion phases. *S. aureus* modifies its phenotype from adhesive to invasive in order to disseminate within the host, and to escape from the changeable conditions during the phases of infection [4, 5]. The infection is established starting with bacterial adhering to the host tissue [6]**,** colonizing, building biofilm, surviving the host defense mechanisms and ending with crossing the tissue barriers and entering the tissues [7, 8]. In the adhesion phase, *S. aureus* promotes the expression of the specific extracellular adherence protein (EAP) and adhesins for extracellular matrix proteins (MSCRAMMs), such as collagen, fibronectin, and fibrinogen that are abundant in plasma, establishing persistent-binding colonies on the tissue [9]. In the invasion phase, *S. aureus* invades deeper tissues, including bone and joints, infecting every tissue and organ system of the body, sometimes ending with life threatening forms of infection (Figure 1.2). Due to its adaptive properties to grow in blood through subversion of plasma proteins and the tissue extracellular matrix, *S. aureus* can sustain the bacteremia [10]. The transition between the colonization and invasion phases is believed to be through expressing staphylococcal proteases [11-17].

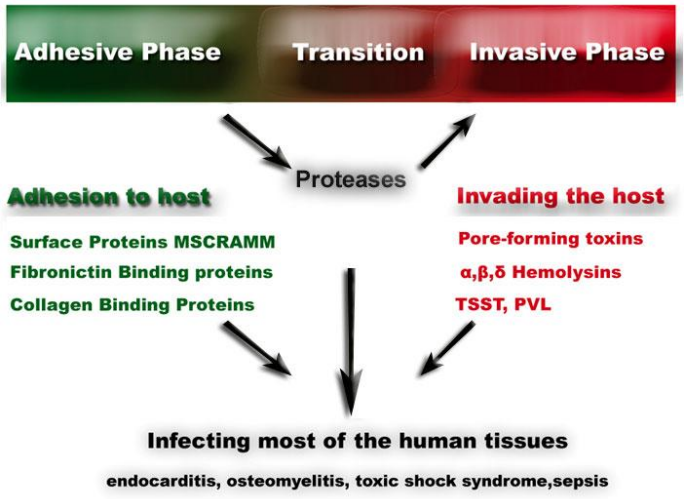

Figure 1.2 Characteristics of staphylococcal infection phases.
***S. aureus* is able to produce and excrete a variety of toxins, enzymes, and other extracellular or cell wall-associated proteins, that are required for the establishment and maintenance of an infection. Virulence factor expression occurs in a highly orchestrated manner. In the early stage of infection, the surface associated-colonization promoting factors are important, while the secreted proteins are up-regulated during the late stage, and are believed to be required for survival of the bacteria and dissemination of infection. The transition is regulated with the secretion of the proteases.**

1.4 Virulence factors in *Staphylococcus aureus*

Both surface and extracellular proteins represent the interface between the host and this pathogenic bacterium. Moreover, they play a key role in both colonization and subversion processes of the human host [18-20]. Table 1.1 summarizes the functions of the secreted virulence factors that have been identified in *Staphylococcus aureus*.

Table 1.1 Summary of the virulence factors involved in the staphylococcal pathogenesis. (source: Gustafsson, Thesis [21]).

ACTIVITY / FUNCTION	PRODUCT	GENE
Anti-immune, antiphagocytosis	Protein A	*spa*
	Polysaccharide capsule type 5	*cap5*
	Polysaccharide capsule type 8	*cap8*
Collagen binding proteins	Collagen BP	*cna*
Fibronectin binding proteins	Fibronectin BPA, Fibronectin BPB	*fnba, fnbB*
Fibrinogen binding proteins	Clumping factor A, Clumping factor B	*clfA, clfB*
Lactoferrin binding proteins	Lactoferrin BP	*lbp*
Hemolysins, cytotoxin	α-Hemolysin, β-Hemolysin	*hla, hlb*
	δ-Hemolysin, γ-Hemolysin	*hld, hlg*
Leukolysin	PVL leukocidin*	*lukS/F*
Food poisoning, TSST	Enterotoxin A, Enterotoxin B	*sea, seb*
	Enterotoxin C, Enterotoxin D	*sec, sed*
	Enterotoxin H	*seh*
Scalded skin syndrome	Exfoliatin A	*eta*
	Exfoliatin B	*etb*
Toxic shock syndrome	Toxic shock toxin-1	*tst*
Putative protease	Serine protease-like	*splA-F*
Spreading factors, nutrition	V8 protease	*ssp*
	Hyaluronidase	*hys*
Spreading, nutrition	Staphopain (protease II)	*scp*
	Glycerol ester hydrolase	*geh*
	Lipase (butyryl esterase)	*lip*
Nutrition	Nuclease	*nuc*
Fatty acid esterification	FAME	*fme*
	PI-phospholipase C	*plc*
Clotting, clot digestion	Coagulase	*coa*
Plasminogen activator	Staphylokinase	*sak*
Processing enzyme	Metalloprotease (aureolysin)	*aur*
	Cysteine protease	*sspB*

S. aureus like other prokaryotes depends on several protein transport pathways, among which the major secretory (Sec) pathway is the most well known and best described [22].

1.5 *Staphylococcus aureus*: challenges of disease and control in Europe

The methicillin-resistant *Staphylococcus aureus* (MRSA) is a major cause of healthcare-associated infections (HAIs). Over 380,000 HAIs were reported to be acquired annually in hospitals of the EU countries in 2008 [23]. These infections were due to selected antibiotic-resistant bacteria, including those of the bloodstream, lower respiratory tract, skin or soft tissues and urinary tract. In general, MRSA is responsible for 44% (n=171,200) of these infections, 22% (n=5,400) of attributable extra deaths and 41% (n=1,050,000) of extra days of hospitalization associated with these infections. The attributable extra in-hospital costs caused by MRSA are estimated to reach approximately 380 million EUR annually in Europe. Moreover, the vast extent of MRSA infections has both evoked fear and fuelled public distrust about healthcare. For many healthcare consumers, this has made MRSA bloodstream infection rates an indicator of both quality of care and outcome [23].

1.6 Emergence of the antibiotic-resistant strains requires modifying of the antimicrobial strategy

The development of antibiotics over the last decades was followed with a fast evolutionary resistance of the pathogenic bacteria. The emergence of staphylococcal antibiotic-resistant strains such as *MRSA* and *VISA (Vancomycin intermediate-resistant S. aureus)* demonstrates the urgent need for new therapeutics that are effective against multidrug-resistant bacteria (Figure 1.3). Although some treatment options remain, the search for new antibacterial compounds and novel bacterial targets is urgently needed to ensure that staphylococcal infections can be effectively treated in the future. The recently discovered antibacterial agents should be exploited. Moreover, focusing on the bacterial mechanisms and their gene products that are involved in essential cell functions can present novel targets [24].

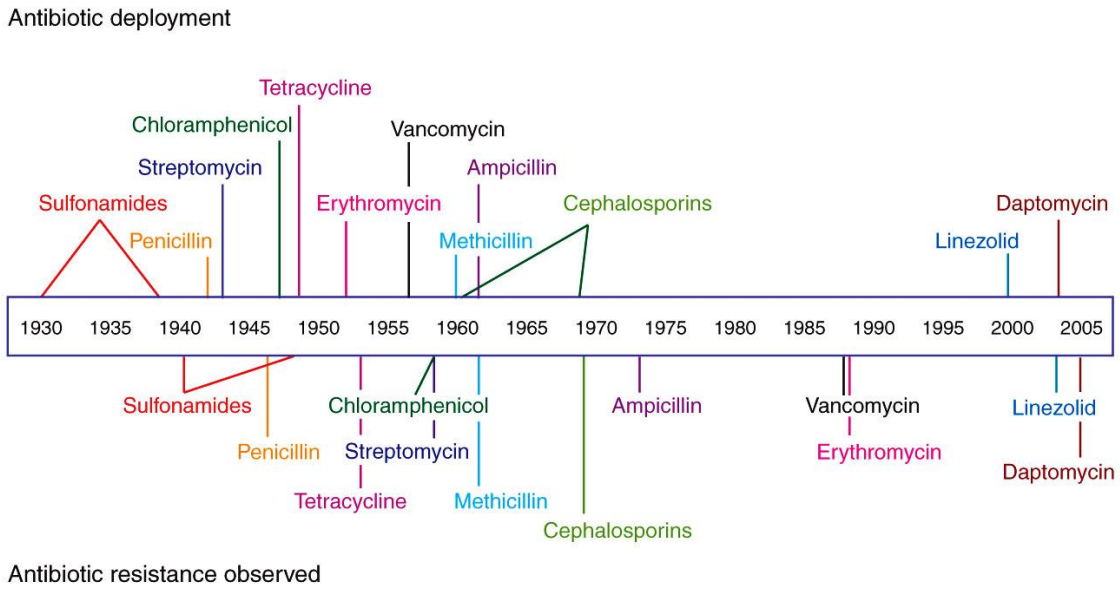

Figure 1.3 Timeline of antibiotic deployment and the evolution of antibiotic resistance.
Source: Clatworthy, *et al.* 2007 [24].

1.7 Peptide constructs: novel and promising potent antibacterial agents

Most conventional antibiotics, bacteriostatic and bactericidal, are principally designed to target bacterial functions or growth processes. Bacteriostatic antibiotics, such as the aminoglycosides, macrolides, and tetracyclines, are means for targeting protein synthesis, where those targeting the bacterial cell wall (penicillins, cephalosporins), or cell membrane (polymyxins), or interfere with essential bacterial enzymes (quinolones, sulfonamides) are usually bactericidal [25]. More recently, after a pause of 40 years in discovering new classes of antibiotic compounds, only a few new classes of antibiotics have been brought into clinical use. Daptomycin, as an example, is a cyclic lipopeptide used for Gram-positive infections [1, 26]. It has a distinct mechanism of action illustrated in disrupting multiple aspects of bacterial cell membrane function. It appears to bind to the membrane and cause rapid depolarization, resulting in a loss of membrane potential leading to inhibition of protein, DNA and RNA synthesis, which results in bacterial cell death [26, 27]. Recent research reveals that both cyclic peptides and the linear cationic peptides are potential alternatives to counteract the bacterial resistance to existing antibiotics [28, 29]. More than 1000 naturally occurring antimicrobial peptides have been described so far. These peptides are generally short (less than 50 amino acids in length), cationic, amphiphilic, demonstrate different three-dimensional structures, and appear to have different modes of actions. Some antibacterial peptides are summarized in Table 1.2.

Table 1.2 Selected natural cationic antimicrobial peptides. (Source: Hilpert *et al*., 2008 [29]).

Name	Source	Sequence	MIC (µg/ml)
Gramicidin	*Bacillus brevis*	cyclo-((D)Phe-Pro-Val-Orn-Leu)	3.1
Indolicidin	Bovine neutrophil	ILPWKWPWWPWRR-NH2	3.8
Lactoferricin H-20	Human, Lactoferrin	KCFQWQRNMRKVRGPPVSCI	128
Lactoferricin P-20	Porcine, derived from Lactoferrin	KCRQWQSKIRRTNP IFCIRR	32
LL37	Human neutrophils epithelial cells	LLGDFFRKSKEKIGKEFKRIVQRIKDFLRNLVPRTES	>32 (µM)
Magainin2	*Xenopus Laevisskin*	GIGKFLHSAKKFGKAFVGEIMNS	64
Bac7	Bovine Neutrophils	RRIRPRPPRLPRPRPLPFPRPGPRPIPRPLPFPRPGPTPIPRPLPFPRPGPRPIPRPL-NH2	200
Bactenecin	Bovine neutrophils	RLCRIVVIRVCR	32-64

Novel peptides as therapeutics for treating infections are being exploited. The possibility that peptides have multiple targets, in addition to their fundamental interaction with the bacterial membrane, means the chances of resistance by target modification are slight, as this would require the complete alteration of the membrane and/or several biochemical pathways to be circumvented [28, 30]. Table 1.3 explains the advantages of antimicrobial peptides on conventional antibiotics.

Table 1.3 Comparison of conventional antibiotics with cationic antimicrobial peptides (source: Marr *et al*, 2006 [30]).

Property	Conventional antibiotics	Cationic antimicrobial peptides
Spectrum of activity	Bacterial infections (often selective)	Bacterial, fungal and viral infections; septicemia; and/or inflammation
Uptake	Specific mechanisms	Relatively non-specific. Based on charge. Self-promoted uptake
Targets	Usually one dominating target or class of targets (e.g. penicillin-binding proteins, topoisomerases, ribosomes)	Relatively less specific (possibly multiple targets in any given cell)
Resistance rate and mechanism	Resistance development at frequencies of 10^{-7} to 10^{-10}, or after a few passages at sub-MIC. Resistance caused by mechanisms such as reduced uptake or increased efflux, chemical modification or degradation of antibiotic, or altered target	Resistance generally cannot be directly selected. Needs multiple passages on sub-MIC concentrations to induce resistance. Resistance caused by mechanisms such as an impermeable outer membrane or specific proteases (can be overcome by incorporating D-amino acids or backbone alterations)
Additional activities	No	Include anti-endotoxic and/or boosting of innate immunity
Pharmacokinetics	Varies but once per week antimicrobials under development	Short systemic half-life owing to proteolytic degradation
Toxicology	Antibiotics tend to be one of the safest groups of pharmaceuticals	No known topical toxicities; systemic toxicity issues remain undefined
Manufacturing costs	Can be inexpensive (e.g. $0.8 per gram for aminoglycosides)	Expensive ($50–400 per gram)

1.8 Novel antimicrobial targets in *Staphylococcus aureus*

The search for novel antibacterial targets in *S. aureus* has increased. Several research groups have e.g. investigated the possibility of inhibiting the two-component regulatory system in *S. aureus* [31, 32]. A model for novel discovered targets in *S. aureus* is the accessory gene regulatory system (Agr). Cyclic autoinducing peptides (AIPS), which have the conserved sequence YSTCAFIM, were considered as promising inhibitors for the transmembrane receptors AgrC of this regulatory system (Figure 1.4).

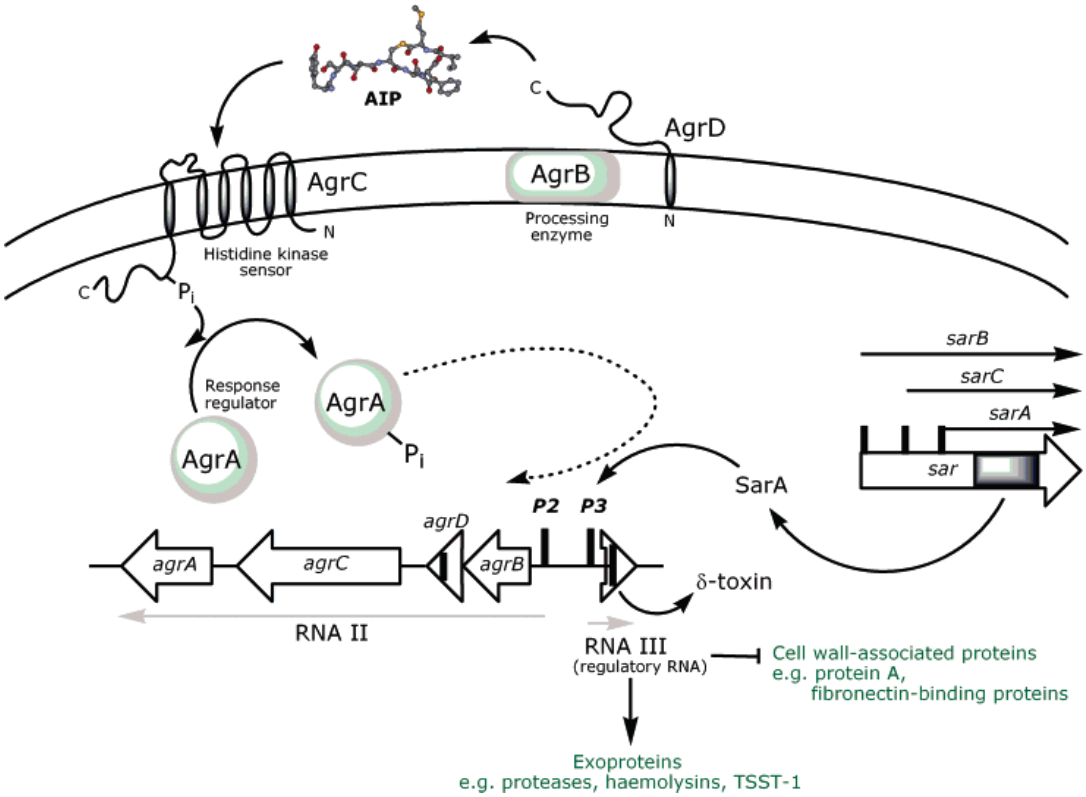

Figure 1.4 Schematic representation of the staphylococcal quorum sensing system shows the agr locus and its regulatory pathways.

The agr locus consists of two divergent operons, which is transcribed under the control of the promoters P2 and P3. The P2 transcript RNAII is polycistronic (agrBDCA) comprising the genes that encode proteins of a quorum sensing system that, at threshold concentration of the AIP, activates the transcription of P2 resulting in signal amplification) and P3-initiating production of the transcript RNAIII. Being the effector of the agr system, RNAIII initiates the transcription of genes that encode a variety of exoproteins, e.g. hla (encoding α-hemolysin), saeB (enterotoxin B), tst (TSST-1), ssp and spr (serine proteases), and represses the genes encoding cell surface proteins, e.g., spa (protein A) and fnb (fibronectin-binding protein). AIP result from the post-translational modification of AgrD by the membrane-bound AgrB. The AgrC-AgrA forms the crucial agr TCSTS. Source Chan *et al*., 2004 [33].

Upon AgrC inhibition, the quorum sensing of the staphylococcal bacteria will be switched off[2]. This will result in down regulating the expression of virulence factors and biofilm building. The discovery of this mechanism in *S. aureus* opened the doors to find more targets in other Gram-positive and Gram-negative bacteria. Similarly, the staphylococcal RNAIII, which is responsible for expressing the virulent exoproteins, hemolysins and proteases, was found to be inhibited by peptide analogues of the domain YSPWTNF. Developments were tried to optimize the inhibitory effect of this structure.

The peptides in the former examples are receptor-antagonists that in turn and consequently convey the inhibition to the gene transcription level. However, the inhibition can be designed to be on the protein level. Several research groups have been working on inhibiting the type I of the staphylococcal signal peptidase, SPsB, which is a membrane integrated peptidase processing the virulence factors on their N-terminus, facilitating their passage through the membrane from the cytoplasm to the periplasm and the cell wall [34].

The FtsZ, a bacterial cytoskeleton protein, which is involved in cell division, was found as novel target in *Staphylococcus aureus*. FtsZ assembles into protofilaments in a GTP-dependent manner, and forms a dynamic Z-ring at the mid-cell position. Haydon and others have found that FtsZ is a significant target for inhibitors like PC-190723. Several points were discussed suggesting the potential of FtsZ as a drug target for antistaphylococcal therapy [35]. Dubin and others have utilized hemocidin, an antibacterial peptide derived from hemoglobin and myoglobin, and products of enzymatic digestion of maternal proteins as specific inhibitors in targeting individual bacterial virulence factors, like the staphylococcal proteases [36]. Table 1.4 summarizes the active research in developing alternative antimicrobial strategies based on promising peptide antibiotics and synthetic small molecules.

[2] Quorum sensing is a type of decision-making process where bacteria coordinate their gene expression according to the local density of their population. In *S. aureus* the agr system, a two-component system, is responsible for reception of the chemical sensing in the individual components to assess the number of other components they interact with, and to trigger a standard response once a threshold number of components is detected.

Table 1.4 Novel targets that are essential in *Staphylococcus aureus* pathogenicity.

New compounds (peptide)	Novel target	Effect	Reference
Cyclic-YSTCAFIM-NH2 analogues	Agr C	inhibition of the transmembrane sensor Agr C (two component regulatory system) quorum quenching	[31, 32, 37-45]
YSPWTNF-NH2 Analogues	RNA III	Inhibiting the biofilm building	[37, 46-49]
Decanolyl LTPTAKAASKIDD α-ketoamid analogues	SpsB	Inhibiting the Type I signal peptidase	[50, 51]
Arylomycin	SPase	Inhibiting Type I signal peptidase	[52]
5-amino-thiazolo[4,5-d]pyrimidines	Sec A	Inhibiting the ATPase Translocation motor Sec A	[53]
PC-190723	FtsZ	Inhibit the Staphylococcus cell division	[35]
cis-5-phenyl proline	SrtA	Inhibiting the integration of the cell wall proteins.	[54, 55]
Hemocidins		Targeting of individual bacterial virulence factors	[36]
Staphostatins			
LBM-415	PDF	Inhibit the peptide deformylase and the maturation of proteins	[56]

Thus, it is clear from the former examples that peptides can contribute in inhibiting the virulence factors or in intervening with the pathogenicity mechanisms if they are utilized as novel therapeutics. Furthermore, they can have more potential if novel pathogenicity mechanisms are targeted. Based on these facts, it is believed that peptides can have a multiple potential impact against antibiotic resistant strains. This might reduce the selective pressure of the bacterial multidrug resistance. Targeting the secretion pathways of virulence factors that directly cause the harm to the host tissue in the infection process might be a successful approach in targeting virulence.

1.9 Sec pathway: a major bacterial route for secreting pathogenicity factors

One of the main reasons why *S. aureus* is able to infect almost every organ and tissue in the human body is that *S. aureus* cells can produce an arsenal of virulence factors that are exported to the cell surface and host milieu. The secreted proteins play key role in the interaction of bacteria with their environment [22]. These factors include proteins that are necessary for: 1) adherence to cells; 2) invasion and spreading throughout the host; 3) evasion of the immune system; and 4) damaging host cells, thereby contributing to the symptoms of septic shock (Table 1.1). *S. aureus* contains several protein secretion pathways of which the general Sec pathway seems to be most frequently used [57]. Other secretion pathways include the Twin arginine translocation (Tat) [58-60], Com and Ess pathways [61, 62]. See table 1.5.

Table 1.5 The major secretion pathways in staphylococci (modified based on Sibbald *et al*., 2006 [22]).

Secretion pathway	Major components	Hallmark of the signal peptide	Membrane translocation form	Secreted proteins
Sec-translocase	SecA, SecY, Sec E, SecG	NHC–extension-AAxA motif at C-terminus	Unfolded precursor protein	Serine, cysteine-proteases, α,β,γ-hemolysins; most proteins of secretome
Tat-translocon	Tat A, TatC	NHC-Extension - RR/KR Two consecutive arginines within N-terminal sequence	Folded precursor protein	Iron-dependent peroxidase FepB (Iron-binding lipoprotein)
ESAT-6 like (ESS-1)	Esa, EssA, EssB, EssC	WXG motives	Folded	EsxA, EsxB, CFP_{10}
Sort	StrA, SrtB	NHC-extension and LPTxG, YSIR motif at C-terminus	Unfolded Anchored to CW	FnbPA, FnbPB CnbP, ClfA

It has been suggested that the Tat pathway does not play a major role in protein secretion in *S. aureus*, rather it is functional and serves to translocate the iron-dependent peroxidase FepB [63]. The evolutionarily conserved general secretory (Sec) system mediates the secretion of many virulence proteins, in both Gram-positive bacteria like *S. aureus* as well as Gram-negative bacteria [57]. In Gram-negative bacteria, the Sec system exports unfolded proteins to the periplasm, where they are then recognized by other specialized systems for transport across the outer membrane, while in Gram-positive bacteria, Sec translocates unfolded proteins directly into the extracellular environment (Figure 1.5). The general secretory (Sec) system is the most used major secretion pathway in various bacterial species [64, 65]. In general, the N-terminus of the secreted proteins is a tripartite domain signal peptide, and it is needed to target them co-translationally together with the ribosome to the translocation machinery in the cytoplasmic membrane. After translation and channeling through the Sec complex, the N-terminal signal peptide will be removed by signal peptidase (SPase) and exoproteins will be either retained in an extracytoplasmic compartment of the cell or secreted into the extracellular milieu after its correct conformational folding [22]. The transport of the proteins through the Sec system occurs in a co-translational phase.

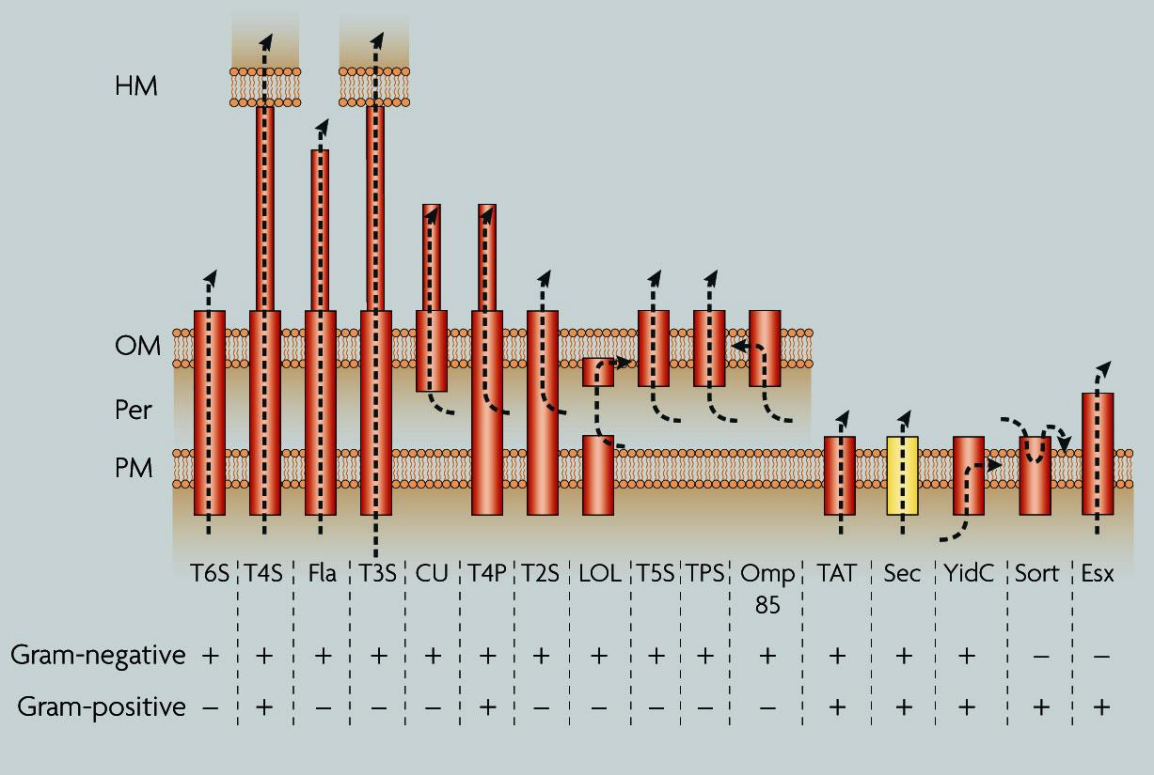

Figure 1.5 Secretion pathways in Gram-positive and Gram-negative bacteria.
The arrows indicate the taken path of the exported protein. Arrows that initiate in the periplasm indicate that Sec (or rarely TAT)-dependent translocation across the plasma membrane is a necessary first step for these systems. Bam: beta-barrel assembly machine. CU: chaperone–usher pathway. Esx: specialized secretion system that is found in Gram-positive bacteria (for example, mycobacteria). Fla: flagellum. HM: host cell membrane. LOL: lipoprotein outer-membrane localization. OM: outer membrane. Omp85: also known as YaeT. Per: periplasm. PM: plasma membrane. Sort: sortase. TPS: two-partner secretion. T2S: type II secretion. T3S: type-III secretion. T4P: type IV pili T4S: type IV secretion. T5S: type V secretion (autotransportation). T6S: type VI secretion (Source Papanikou *et al* 2007, [66]).

1.10 Stages of protein transport in the Sec system

The protein transport through the Sec system into the cell wall and the extracellular milieu can be divided into three stages. These stages include (a) targeting to the membrane translocation machinery by secretion-specific or general ribonucleic proteins; (b) translocation across the membrane via the Sec YEG, a heterotrimeric membrane protein complex, with the help of Sec motor ATPase SecA; and (c) post-translocational folding and modification [22, 66].

1.10.1 Targeting the protein from the cytoplasm to the cytoplasmic membrane

In Gram-positive bacteria, once the N-terminal signal peptide of the translated protein emerges from the ribosome it is recognized by a ribonucleic protein called signal recognition particle (SRP). The protein part of the SRP contains a homologue of the SRP 54 in eukaryotes

(Ffh). The hydrophobic sequence of the signal peptide is believed to bind to the M domain of the Ffh protein and thus the translated protein is targeted together with its ribosome to the membrane via the FtsY protein, which acts as a high affinity receptor for SRP [22]. This stage ends with docking the signal peptide of the preprotein with its ribosome to SecA (Figure 1.6).

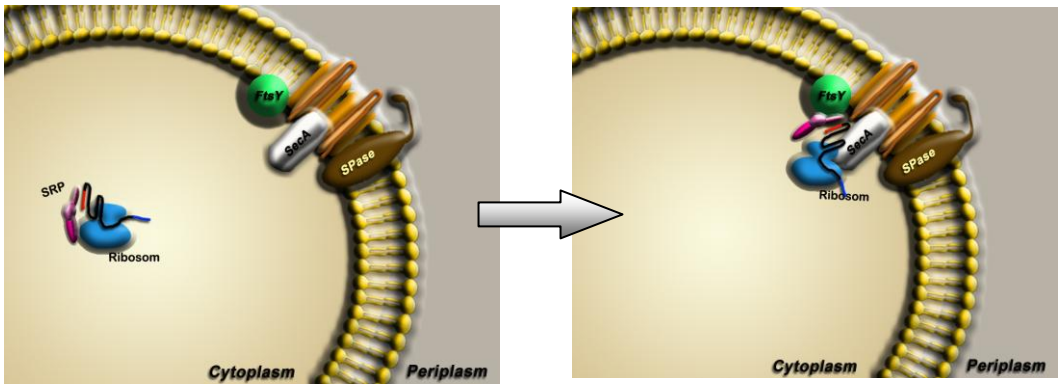

Figure 1.6 Stage 1: Preprotein targeting to the membrane in the Sec pathway of Gram-positive bacteria. The signal recognition particle (SRP) screens for the hydrophobic signal sequence of the nascent protein in co-translational phase, and locks on the ribosome to target the complex (nascent chain-ribosome) to the membrane receptor protein FtsY.

1.10.2 Transmembrane crossing of the preprotein through SecYEG

Once the SRP-ribosome-nascent protein complex is bound to its receptor protein FtsY, the ribosome is docked on the translocation pore. Thus, the non-folded protein is transferred to the SecA dimer, resulting in conformational rearrangements as the ATP molecules have bound to SecA, that promote their insertion of the non folded preprotein into the channel of SecYEG. Figure 1.7 explains the transmembrane crossing of a non-folded protein after it has docked to the SecA dimer. Upon the ATP molecules binding to SecA, conformational rearrangements of SecA promote the polypeptide insertion of the nascent protein into the channel of SecYEG [64]. Subsequent hydrolysis of ATP causes SecA to release the preprotein, return to its original conformation and disassociate from the translocation channel. The translocation of a peptide chain consumes many molecules of ATP. The polypeptide is further translocated across the cytoplasmic membrane via the proton motive force which is generated by binding and hydrolysis cycles of ATP molecules [66].

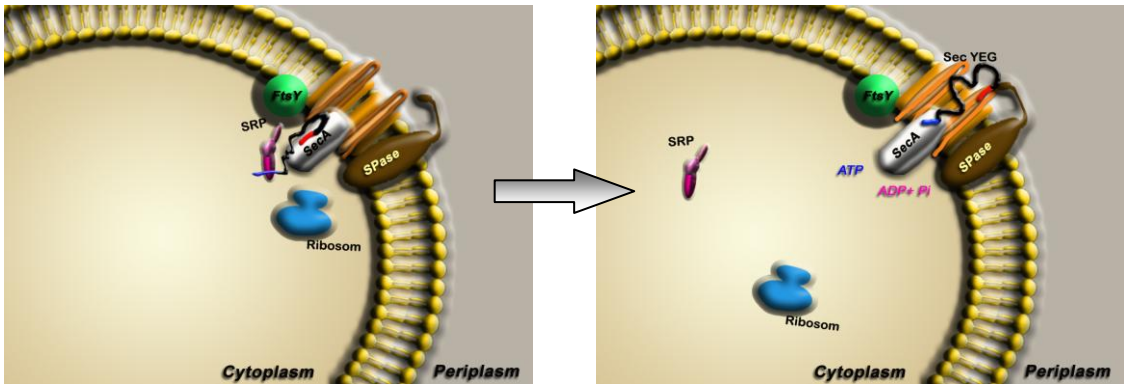

Figure 1.7 Stage 2: Translocation across the membrane in the Sec pathway of Gram-positive bacteria.
Transmembrane crossing of the unfolded protein with the help of SecA conformational changes: After binding of a preprotein to a SecA dimer, the SecA molecules will bind ATP, resulting in conformational changes that promote their insertion together with the preprotein into the membrane-embedded translocation channel. Subsequent hydrolysis of ATP causes SecA to release the preprotein, return to its original conformation, and reinsert it into the translocation channel.

1.10.3 Maturation and release of the translocated protein sequences

During transmembrane crossing, the junction between the signal peptide and the mature part of the translocating chain undergoes a cleavage at a specific catalytic site by the membrane signal peptidase SPase [22]. Figure 1.8 illustrates the signal peptidase action on the N-terminal recognition site of the unfolded protein through this stage.

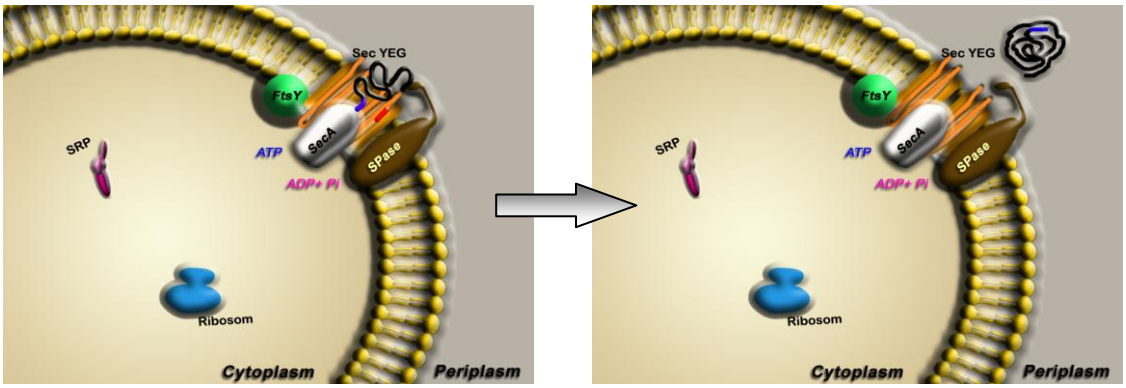

Figure 1.8 Stage 3: Maturation and release of the translocated non-folded protein.
The signal peptidase (Spase) recognizes the motif AxAA at the C domain of the secretion signal peptide while the preprotein is crossing the membrane and cleaves the protein causing the release and maturation of the preprotein. At this stage, another scenario might take place if the preprotein has a lipoprotein signal sequence at C-terminus that causes the insertion of the protein into the membrane via YidC.

1.10.4 Protein folding catalysts

Sec-dependent proteins that are transported across the membrane emerge at the extracytoplasmic membrane surface in an unfolded state. These proteins need to be rapidly and correctly folded into their native and protease-resistant conformation before they are degraded by

proteases in the cell wall or extracellular environment. PrsA is a lipoprotein, which shows homology to peptidyl-prolyl cis/ trans-isomerases, and is an important folding catalyst in *B. subtilis* and *S. aureus* [22]. Although no data have been published on *S. aureus* whether PrsA is also essential for the viability and virulence of this organism, studies on the effects of PrsA depletion in *B. subtilis* showed that the relative amounts of extracellular proteins from PrsA-depleted cells were significantly reduced [22].

Other proteins that are involved in proper folding of extracellular proteins in *B. subtilis* are the membrane proteins BdbC and BdbD, which are involved in the formation of disulfide bonds (Figure 1.9). Both proteins have been shown to be necessary for stabilization of the membrane- and cell wall-associated pseudopilin ComGC [22].

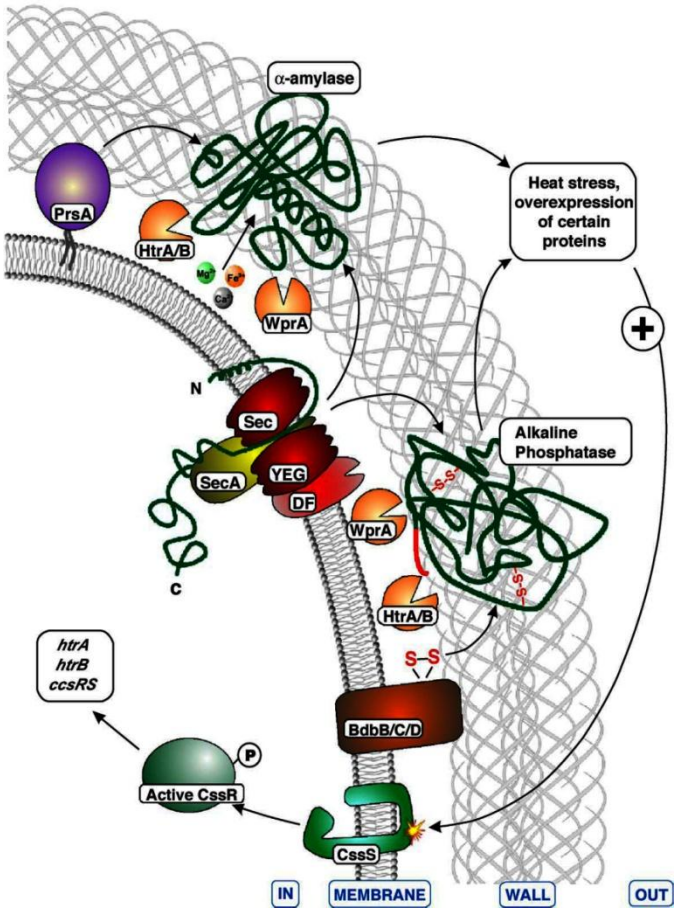

Figure 1.9 Protein-folding catalysts in the interface between the cytoplasmic membrane and the cell wall of *B. subtilis*.
Diagram shows the components of the Sec pathway and the elements involved in folding of secretory proteins and the degradation of misfolded proteins in Gram-positive bacteria. Two model proteins are shown: amylase from *B. amyloliquefaciens* and the alkaline phosphatase from *E. coli*. Source: Sarvas *et al.*, 2004 [67].

1.10.5 The role of signal peptides in targeting proteins

In *S. aureus*, the Sec-system signal peptides are consensus sequences and comprise on average the first 25 to 32 amino acids of the preprotein, and contain three distinguishable domains: the N, H, and C domain [22]. Figure 1.10 illustrates the nature of information that is localized within the signal sequences of the Sec-dependent proteins that have to be exported to different destinations.

The N-terminal domain contains positively charged amino acids, which are believed to interact with the secretion machinery, and/or with the negatively charged phospholipids in the membrane, whereas the H domain will provide the appropriate hydrophobicity to bind to the SRP, and will facilitate membrane insertion. Helix-breaking residues in the middle of the H domain may facilitate H domain looping during membrane insertion and translocation of the precursor protein. The subsequent unlooping of the H domain would display the SPase recognition and cleavage site at the extracytoplasmic membrane surface, where the catalytic domains of type I and type II SPases are localized. Helix breaking residues just before the SPase recognition and cleavage site would facilitate precursor processing by SPase I or II. Finally, the start and the end of C domain that includes the motif AXAA is defined by the helix breaking residues and the cleavage site for specific SPase, either SPase I or SPaseII [22, 68]. A conserved signal sequence, LPTXG, which is located at the C-terminus of the translocated sequences, sorts the proteins to be anchored to the cell wall by specific cell wall enzymes called sortases. In *S. aureus*, SrtA catalyzes the transpeptidation reaction that joins this LPTXG containing domain to the cell wall [69]. A set of about 20 surface proteins of *Staphylococcus aureus* were found to carry a YSIRK-G/S motif but this motif is not essential for surface protein anchoring to the cell wall envelope.

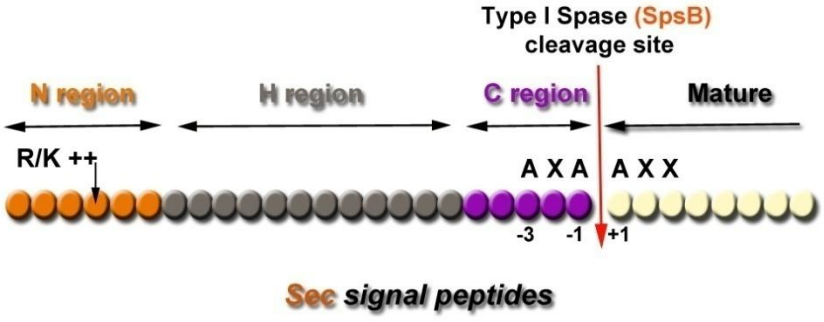

Figure 1.10 Tripartite domain of the signal peptide of the Sec-dependent proteins, comprises N, H, and C motives.

1.10.6 Destination of the virulence factors

The secreted virulence factors can be destined to one of the following positions: (1) secreted to the extracellular milieu, (2) retained to the cell surface by non-covalent or covalent binding to the peptidoglycan moiety of the cell wall or to cell membrane after they are sorted by sortase. Such proteins are protein A, clumping factors, fibronectin and fibrinogen binding proteins. The described details about the protein export stages via the Sec system reveal the pivotal role that signal peptides play in determining whether the exported protein will be secreted into the extracellular milieu or integrated in the cell wall or the cell membrane. In the Sec pathway, this signal peptide is likely to be recognized by three major players in different stages. First, it is recognized by the signal recognition particle SRP (ribonucleoprotein) in the cytoplasm in the targeting stage. Second, it is docked at the ATPase motor SecA, into the cytoplasmic membrane at the transmembrane crossing stage. Third, it is cleaved by the signal peptidase SPase (type I or type II) at the recognition site, which consists of small, aliphatic residues at positions -1 and -3 relative to the cleaved bond, and these correspondingly bind in the S1 and S3 binding sites of the SPase [22, 70].

1.11 Sec-pathway: a vital target for antivirulence therapy in former studies

The Sec pathway is considered a general pathway in Gram-positive and Gram-negative bacteria, through which the majority of all extracellular proteins are secreted. Most studies of the Sec pathway in Gram-positive bacteria have been carried out with *B. subtilis* Data on the *S. aureus* Sec system is scarce: SecA and SecY have been shown to be important, respectively essential, for growth by using antisense RNA [71]. Moreover, evidence is accumulating that mutation of some gene products of this pathway result in reducing the secretome in the supernatants associated with accumulation of some proteins in the cytoplasm. Sibbald *et al*. showed that a SecG mutant in *Staphylococcus aureus* results in affecting the extracellular accumulation of nine abundant exoproteins and seven cell wall-bound proteins, whereas deletion of secY2 exacerbated the secretion defects of secG mutants, affecting the extracellular accumulation of one additional exoprotein and one cell wall protein. Furthermore, a secG secY2 double mutant displayed a synthetic growth defect [72]. Other research groups showed that deficiency in SRP affect the biosynthesis [73, 74]. Proteome analysis of *B. subtilis* strains depleted of Ffh revealed a reduction of 13 extracellular proteins in the supernatant [73].

On the other hand, it has been shown that SecG, SecY mutations affect the amounts of the exoproteins. Baars *et al*. has studied the role of the Sec translocon in *E. coli* using subproteome

analysis of cells depleted of the essential translocon component SecE. The analysis showed that upon SecE depletion (i) secretory proteins aggregated in the cytoplasm and the cytoplasmic sigma-32-stress response was induced, (ii) the accumulation of outer membrane proteins was reduced, with the exception of some proteins, and (iii) the accumulation of a surprisingly large number of inner membrane proteins appeared to be unaffected or increased. Some individual studies on *E. coli* showed that depletion of SecA results in abolishment of the protein export through the membrane and a loss of cell viability. Since the prokaryotic SecA, SRP and type I Spase have structures that are different from their human counterparts, inhibitors for these key proteins have the potential to be of a novel class of antimicrobial agents with low toxicity [75].

1.12 Developing a novel approach for targeting virulence is an urgent demand

As described formerly, the resistance of pathogenic microorganisms like *S. aureus* to currently known antibiotics is constantly increasing due to a broad use of antimicrobials in medicine, animal husbandry and agriculture [36]. Yet with the exception of the recent development of the narrow-spectrum drugs, daptomycin and linezolid, there have been no new classes of clinically relevant antibiotics discovered in over 40 years. Traditional antibiotics have been identified for their ability to kill bacteria (bactericidal) or inhibit growth (bacteriostatic). They act by inhibiting bacterial functions (such as cell wall synthesis, DNA replication, RNA transcription and protein synthesis) that are essential for *in vitro*, logarithmic growth. However, through the use of antibiotic, lasting alterations are being made to a mutualistic relationship that has taken millennia to evolve: the relationship between the host and its microbiota [76]. Host–microbiota interactions are dynamic; therefore, changes in the microbiota as a consequence of antibiotic treatment can result in the dysregulation of host immune homeostasis and an increased susceptibility to disease [76]. A better understanding of both the changes in the microbiota as a result of antibiotic treatment and the consequential changes in host immune homeostasis is of vital importance, so that these effects can be alleviated (Figure 1.11). Since the conventional concept of virulence is defined by the ability of a pathogen to cause disease, and the virulence determinants are defined as the bacterial factors and mechanisms that actively cause the damage of the host tissue, developing antimicrobials that have novel modes of action should be considered in disarming the pathogens. This can be achieved by inhibiting the secretion of virulence factors that cause direct harm to the host tissue [24]. Over the past few decades, tremendous efforts to understand how bacteria cause disease have revealed new approaches.

Therefore, the next period of efforts in developing novel approaches should utilize the concept of virulence, and consider the balance between the microbiota and the changes in host immune homeostasis.

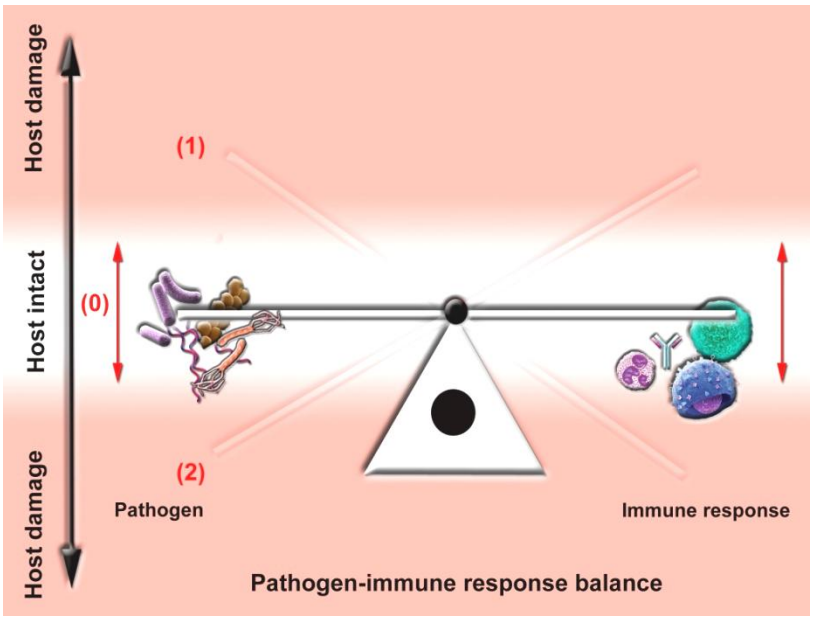

Figure 1.11 Interaction between pathogens and immune responses in the microbial pathogenesis.

Hypothesis of reducing the secretions of virulence factors might contribute in delaying the pathogen mechanisms in setting the infection or in causing the damage to the host tissue. The diagram depicts the damage to the host tissues caused by both factors (red area). In the normal case (state 0), which extends along the white area, there is a balance between the microbes and the immune response. In case the immune response abnormally sinks, (state 1), normal flora can cause a disease. For some pathogens, such as paramyxovirus (state 2), the immune responses rather than the microbial pathogen is primarily responsible for the tissue damage. For many pathogens, host with normal immune response may be colonized asymptomatically, but hosts with very strong/weak immune responses may suffer severe damage or even death.

Aim of the study

This study comes in the series of establishing alternative approaches to target functions essential for infection. The major bacterial secretion pathway (Sec) was put in the focus since it is dispensable for secreting proteins, most of which act as virulence factors in the infection process. The hypothesis of inhibiting or at least reducing the secretions of *S. aureus* carries a new approach that has several potential advantages including attenuating the damage caused to the host tissue by bacterial pathogen, expanding the repertoire of bacterial targets, preserving the host endogenous microbiome, and exerting less selective pressure, which may result in decreased resistance. Under the increasing needs to develop novel approaches and therapeutics for combating the infections caused by the antibiotic-resistant pathogens, several attempts have been made to discover novel targets in *S. aureus*. This pilot study aims at establishing a base for affecting the secretion efficiency of the bacterial virulence factors. This can be built on two major objectives:

1) Targeting the Sec-pathway in *Staphylococcus aureus*, using peptidic inhibitors, and monitoring the effect of the peptidic inhibitors on the bacterial growth, viability, and secretion.

2) Establishing biochemical and molecular assays that facilitate monitoring the success of the targeted process.

Under these two main objectives, the features of our research strategy are determined in the following parts:

- Synthesizing peptide constructs that are able to penetrate the *Staphylococcus aureus* cells and probing their extent of internalization

- Determining the optimal secretion conditions of proteases into the bacterial culture supernatants with focus on the V8 protease and establishing sensitive and quantitative detection methods as a model for the secretion of pathogenicity factors via the Sec pathway.

- Generating potential peptidic Sec-inhibitors that consist of the optimal internalizing sequence conjugated with the secretion signal sequence of V8 protease, including control sequences.

- Testing the effect of the peptides on the secretion through

    a. Quantifying the Sec-dependent V8 protease in the supernatant of bacterial cultures, and in different cellular compartments.

    b. Quantifying the total proteins in the supernatant of bacterial cultures (the secretome), and in different subcellular compartments to understand the mode of action of the peptides.

For a deeper understanding of the methods that were employed in this investigation the basic principles of solid phase peptide synthesis and the development and utilization of cell penetrating peptides will first be elaborated in the following chapter

2 Technical approaches

2.1 Solid phase peptide synthesis (SPPS)

Since their crucial role in biological, pharmaceutical, and in medical research, peptides, and their syntheses on a solid phase have been the major focus in this study. Solid phase peptide synthesis (SPPS) offers important advantages over the synthesis in solution, in that coupling reactions can be performed more rapidly and nearly to completion using an excess of the activated amino acid derivative, which is removed at the end of the reaction by simple washing operations. In contrast to ribosome protein synthesis, solid-phase peptide synthesis proceeds on the resin at a C-terminal to N-terminal manner. The N-termini of amino acid monomers are normally protected by Fmoc or Boc groups. These two groups are labile in base or acidic conditions, respectively. In this study, the automated technique of the peptide synthesizer PIONEER®, which works according to the Fmoc approach, was utilized. The advantages of Fmoc on Boc chemistry are known that the former generates peptides of higher quality and in greater yield than the latter [77]. The sequence, the amino acids content, and the length of a peptide influence whether correct assembly and purification are feasible. These factors also determine the solubility of the final product. Therefore, some important points that were considered in designing the peptide constructs are highlighted.

2.2 Description of the Fmoc solid-phase peptide synthesis process

In general, Fmoc solid phase synthesis can be performed by automated synthesizers that generate peptides from amino acids through coupling the amino acids in cycles. Each cycle consist of the following major phases (Figure 2.1):

1. Loading phase: loading of C-terminal amino acid to resin, this is only done in the first step

2. Deprotection phase: removal of the Fmoc protecting group from the N-terminus of amino acids after their coupling.

3. Activation phase: includes activating the carboxyl group of the next coupled amino acid e.g. by forming an uronium, phosphonium, or other onium salts.

4. Coupling phase: coupling new carboxyl-activated amino acid to the Fmoc-deprotected amine of the peptide chain, and washing the peptides.

5. Repeating the steps 2-4 again or cleaving the completed peptide from the resin.

The following chart depicts the major steps in the Fmoc solid-phase peptide synthesis.

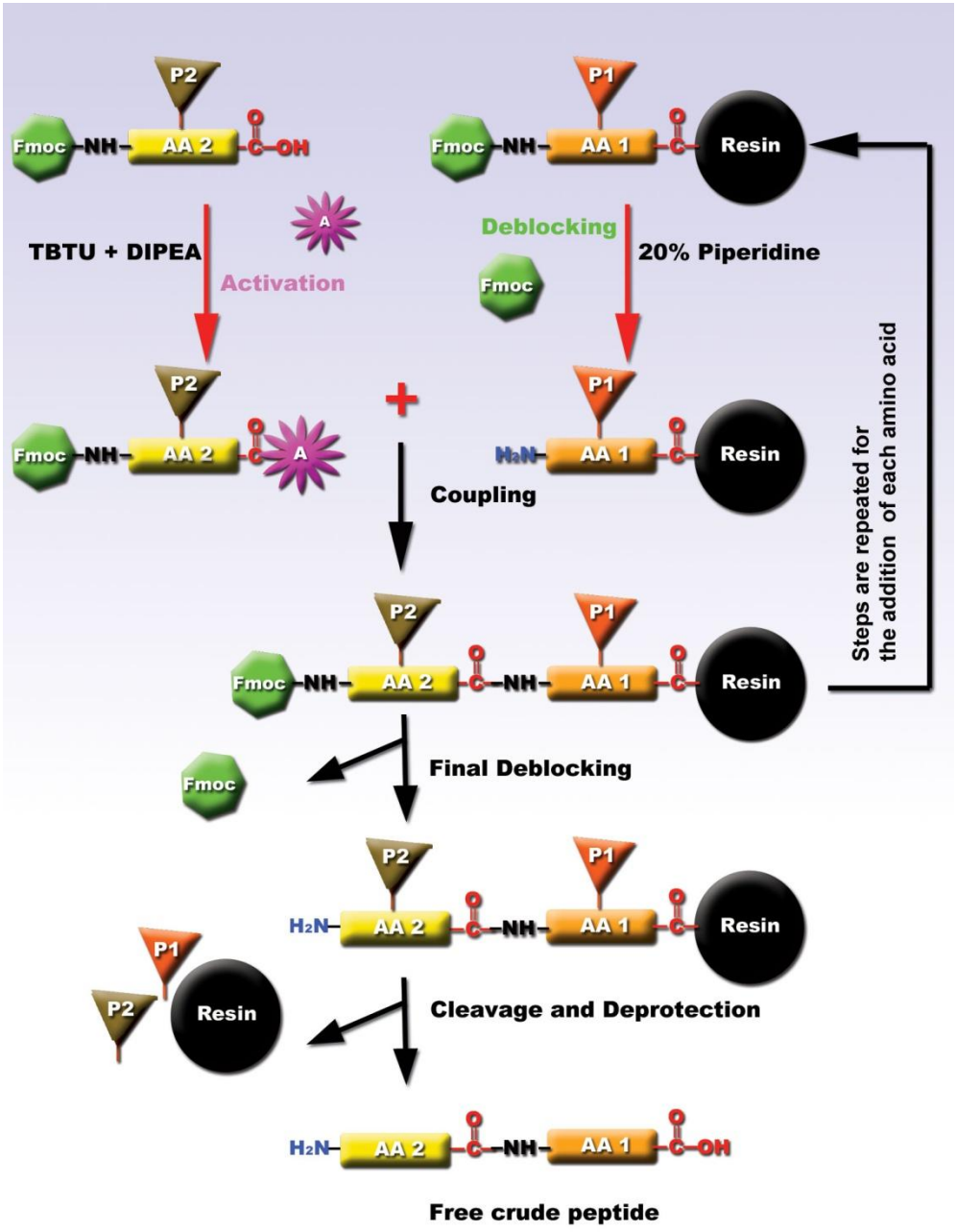

Figure 2.1 The steps and cycles of Fmoc solid-phase peptide synthesis.

2.2.1 Prediction of synthetically difficult sequences

Before starting the synthesis, a simple view at the peptide primary structure can be helpful to predict the degree of difficulty in coupling the amino acids along the peptide chain, especially

when synthesizing long peptides. For that purpose, the computer program, *Peptide Companion* from CSPS Pharmaceutical Inc, was utilized. This predictive view determines practically the coupling difficulties that can arise from the aggregation of some amino acids along the peptide chain. It additionally shows other measures, and predicts whether the coupling efficiency needs to be enhanced in the synthesis.

2.2.2 Loading the first amino acid to the solid support

Coupling the first amino acid to the resin occurs within the first cycle of synthesis. This requires detaching the Fmoc group from the resin in basic condition (20% piperidine), and activating the C-terminus of the first amino acid with coupling reagents (Figure 2.2).

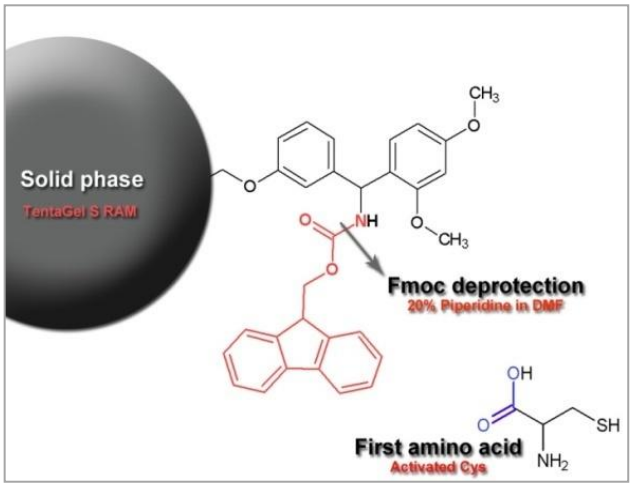

Figure 2.2 The rink-amide solid support for peptide synthesis.
TentaGel S RAM resin from RAPP POLYMERE can be used for all amide peptide syntheses. Here, the first amino acid to be coupled to the resin is cysteine.

2.2.3 Fmoc deprotection

The Fmoc (9*H*-fluoren-9-ylmethoxycarbonyl) is an orthogonal protecting group and used as common strategy in peptide synthesis. It is normally removed from the resin linkers and from the amino acid units in each coupling cycle of a peptide synthesis. It can be cleaved from the N-terminus of the peptide at the end of the synthesis process. The Fmoc protective group is generally labile under mild basic conditions, and stable under acidic conditions. This allows mild acid labile protecting groups that are stable under basic conditions, such as tert-butyl, benzyl oxycarbonyl (Boc) and trityl groups, to be used on the side-chains of amino acid residues of the target peptide. Piperidine is used for deprotecting the Fmoc from the resin when loading the first amino acid and, and before adding a new amino acid to the Nα-terminus of the peptide chain (Figure 2.3). Since the liberated fluorenyl group is a chromophore, Fmoc deprotection can be

monitored by UV absorbance of the overflow, a strategy that is employed in automated synthesizers.

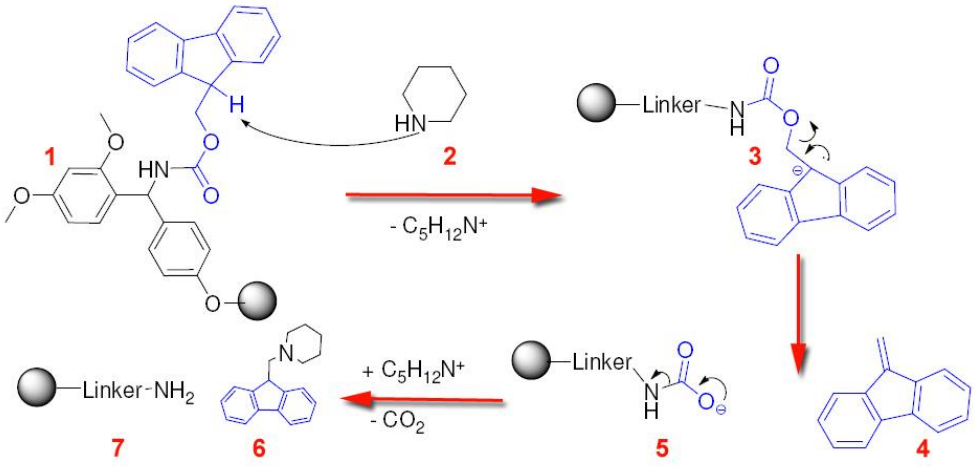

Figure 2.3 Mechanism of Fmoc deprotection with piperidine.

Rink amide resin is functionalized and protected as a carbamate 1. Piperidine 2, a nucleophilic base that deprotonates 1 forming 3, which then decomposes into 4 and 5. Carbamide acid 5 looses carbon dioxide, yielding in the free amine 7. Finally, piperidine (2) as scavenger adds a nucleophile to the produced methylene fluorene 4 yielding 6.

2.2.4 Coupling of amino acids

For coupling a new amino acid to the growing peptide chain in the synthesis column, the carboxyl group of the new amino acid needs to be activated after the Fmoc deprotection of the chain N-terminus. This is important for speeding up the reaction. In the last two decades phosphonium and uronium salts, like the reagent 2-(1-*H*-benzotriazole-1-yl)-1,1,3,3-tetramethyluronium tetrafluoroborate (TBTU), have been increasingly used instead of conventional activating groups like carbodiimides (DCC and DIC) and triazols (HOBt, HOAt). The activating reagents TBTU or HATU can introduce an active ester as uronium salt of a non-nucleophilic anion. Those coupling reagents can be dissolved in DMF, allow activating the carboxyl group of the amino acid in the synthesis column to couple it either to the resin or to the unprotected N-terminus of the added amino acid. The Fmoc group of the final amino acid is cleaved off by treating the resin with 20% piperidine at the end of the final cycle (Figure 2.4). The resin is normally washed and dried before the cleavage of the crude peptide from the support.

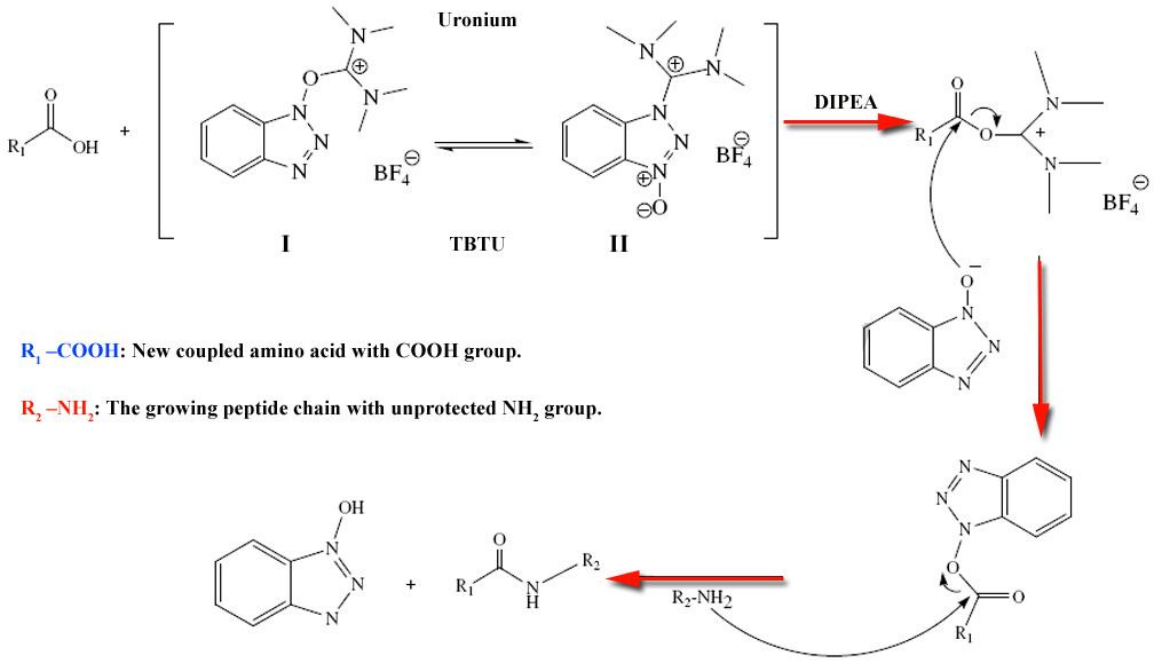

Figure 2.4 Proposed mechanism of the amide bond formation through TBTU (source: Balalaie *et al*., 2007 [78]).

2.2.5 Cleaving the synthesized peptide from the resin

In order to obtain the peptide in the free form without protective groups, the amide linkage to the resin is cleaved using strongly acidic conditions such as trifluoroacetic acid (TFA). Generally, cocktails of TFA are used with scavengers for removing the protective groups as well (Figure 2.5). Certain amino acids can cause problems during TFA cleavage and deprotection. These fall into three broad categories

1. Amino acids, whose protecting groups are easily removed, but whose deprotected side-chains are especially labile in acidic conditions (e.g., Met, Cys, His, Trp).
2. Amino acids, which need more than the normal two hours for complete removal of the side chain protecting groups (e.g., Arg(Pmc/Mtr), Asn/Gln(Mbh).
3. Amino acids whose side-chain protecting groups, once removed from the side-chain, are extremely reactive and must be scavenged to prevent reattachment or modification of the deprotected side-chains (e.g., Arg(Pmc/Mtr), Asn/Gln(Tmob))

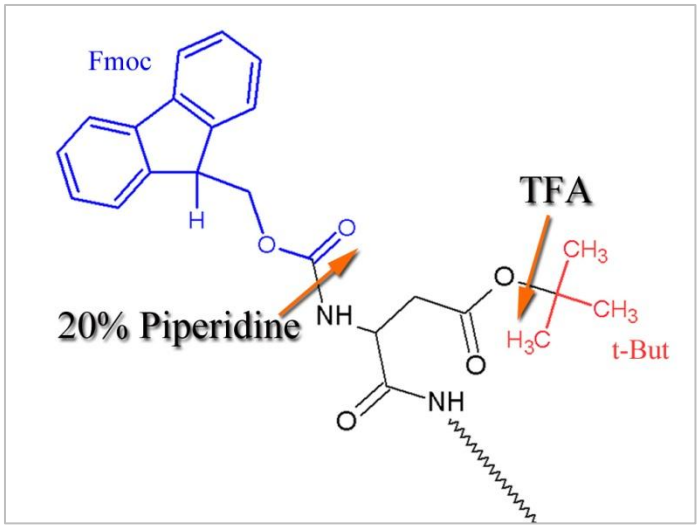

Figure 2.5 Deprotection of Fmoc at the N-terminus of an amino acid by 20% piperidine (basic conditions), and the cleavage of the side chain protective group (t-Bu) by TFA (acidic conditions).

2.2.6 Choosing the cleavage cocktail

The selection of the cleavage cocktail depends on (1) the nature of the cleavable linker attaching the peptide to the support, and (2) the nature of the protecting groups and the reactive properties of the unprotected side-chain. Various TFA cocktails can be prepared with chemical scavengers according to the presence and absence of some residues in the synthesized peptide.

2.2.7 Post cleavage preparations

Crude peptides should be cleaved off the resins in acidic conditions using TFA (in Fmoc chemistry), and then they should be further processed to obtain pure peptides. Figure 2.6 depicts the flow of major steps in the resin-peptide post cleavage process.

2.2.8 Peptide isolation and precipitation

Peptides are separated from the cleavage cocktail by precipitation. Hydrophobic and hydrophilic peptides that are dissolved in TFA can be isolated after evaporating the TFA by precipitation with the tert-butyl-methyl ether (MTBE). The resulting peptide can be isolated by centrifugation. Thereafter, it can be analyzed, lyophilized, and subjected to further purification processes (Figure 2.6).

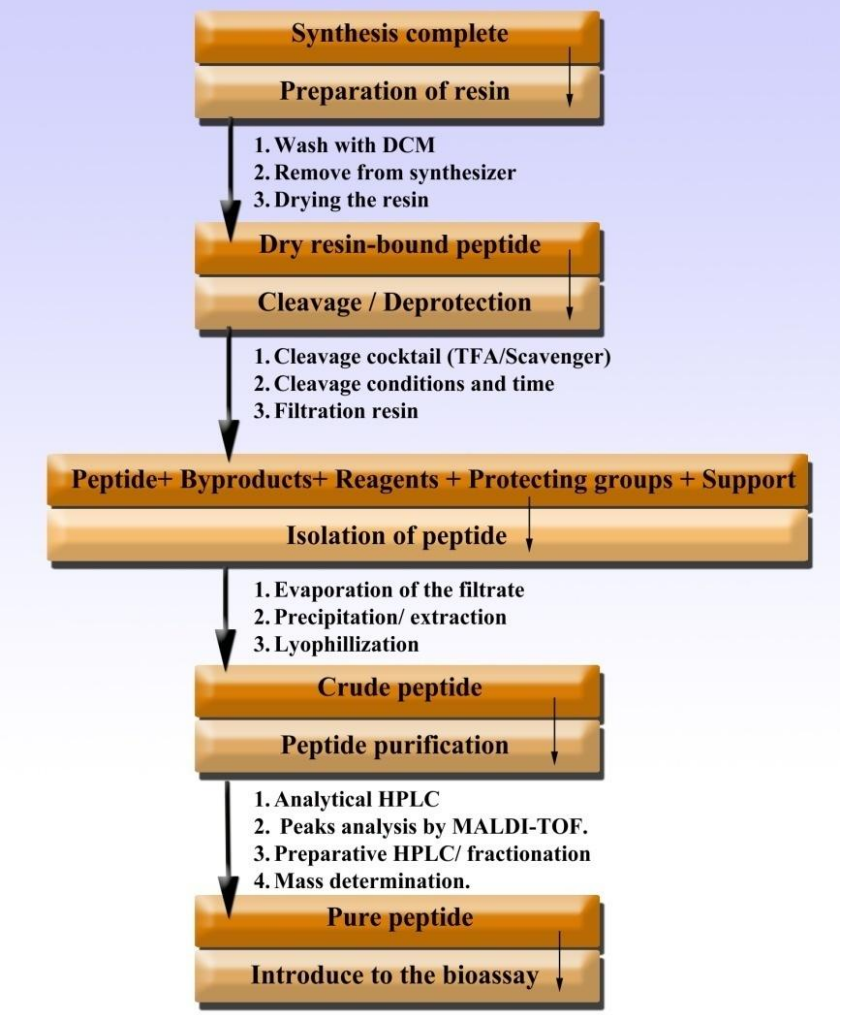

Figure 2.6 Scheme of the post synthetic workup in solid phase peptide synthesis.

2.2.9 Peptide analysis and purification techniques

The chemistry of peptide synthesis is well known with its different side reactions, accordingly, impurities can be generated with the crude peptide in form of diastereomers, hydrolysis products of labile amide bonds, deletion sequences formed predominantly in solid-phase peptide synthesis and insertion peptides and by-products formed during removal of protection groups in the final step of the synthesis. HPLC is one of the most powerful and rapid tools to analyze and purify peptides. The description of HPLC protocol varies according to the specifications of the synthesized peptides. The degree of hydrophobicity, the size, the constituent amino acids, the protective groups, the cyclic and linear form, and the solubility of the crude peptide are key determinants of the analytical and preparative HPLC-conditions. Various chromatography techniques can be used in large- and small scales. The majorly applied

techniques are reversed-phase chromatography (RPC) that is based on the hydrophobicity of the separated peptides, ion-exchange chromatography (IEC) that is dependent on the ionic interaction between the support surface and the charged group of the peptides, and gel-permeation chromatography (GPC) that separates the peptides primarily on the basis of size exclusion. In general, if the elution pattern of the peptide is unknown, a C-18 reversed phase column is used especially for small-to-medium-sized peptides (up to 20-30 amino acids) that are at least moderately hydrophilic. A shallow gradient and moderate flow rates can be used with a low percentage mobile organic phase (likely acetonitrile) at the start of the gradient. A polymeric reversed phase column C-8 or C-4 may perform better if the analyzed or the purified peptides are more hydrophobic or medium sized (40 amino acids). The mainly used buffers in the HPLC process are 0.1% TFA in water and 0.1% TFA in acetonitrile (ACN). Long peptides, or those having large amounts of similarly charged groups, may best be separated on either polymeric reversed phase or ion exchange columns. Some protecting groups, such an Mtr or Trt, absorb very strongly in the UV: even a small percentage of Mtr or Trt still remaining on the peptide will give disproportionately large peaks. Peptides, which have Mtr or Trt attached, will elute later than completely deprotected peptides. Peptides containing Tyr, Phe, or Trp can be monitored at 240-260 nm, due to the strong absorbance of the aromatic ring; otherwise, monitoring at wavelengths closer to the absorbance of the peptide (amide) bond (210-214 nm) is applied. If the crude peptide is hydrophobic, DMF is used as good solvent with a subsequent dilution with the HPLC gradient solution. In this case, a large peak at the beginning of the gradient is expected in the chromatogram. An optimal separation to the peaks and isolation of the fractions that contain the peptide of interest, followed by mass determination by MALDI-MS or by employing online HPLC-MS coupling is required. The peptide can then be lyophilized and introduced to the bioassay.

2.3 Cell penetrating peptides and their rules in delivering drugs into cells

Most “information-rich” molecules, such as, genes, oligonucleotides, proteins or peptides, are poorly taken up by cells since they do not efficiently cross the lipid bilayer of the plasma membrane. This is considered to be a major limitation for their *ex vivo* or *in vivo* use in possible clinical applications or in essential studies. The conventional techniques to deliver such compounds are limited to microinjection, electroporation, association with cationic lipids, liposome encapsidation, or receptor-mediated endocytosis. Various problems have been associated with the use of these techniques such as the low transfer efficiency, complex

manipulation, cellular toxicity, or immunogenicity, which would prohibit their routine use *in vivo* [79]. As an alternative technique to overcome this obstacle, several peptides have been successfully developed and used to improve the intracellular delivery of nucleic acids or proteins. These peptides are known as protein transduction domains or cell penetrating peptides (CPPs). They include Tat, Antennapedia, and arginine-rich peptides (Table 2.1). The common feature of these peptides is their highly cationic nature. The cellular uptake of many peptides and proteins coupled to Tat, Antennapedia, or Penetratin peptides has been reported [80, 81]. The ability to deliver molecules into cells is not limited to peptide moieties, since oligonucleotides, peptide nucleic acids or other compounds or structures with low and high molecular weight such as liposomes, phages and nanoparticle entities have been successfully internalized. Moreover, most of these examples have been accompanied by the expected biological response.

Table 2.1 Some CPPs and their physical properties.
source: Gräslund *et al.*, 2011 [81].

Peptide	Sequence	Total charge	No. of residues	No. of arginines	No. of lysines	Hydrophobicity *
R9	RRRRRRRRR	9+	9	9	0	2.58
TAT(48–60)	GRKKRRQRRRPPQ	8+	13	6	2	2.37
Penetratin	RQIKIWFQNRRMKWKK	7+	16	3	4	1.52
Pen-Arg	RQIRIWFQNRRMRWRR	7+	16	7	0	1.49
pVEC	LLIILRRRIRKQAHAHSK	8+	18	4	2	1.1
M918	MVTVLFRRLRIRRACGPPRVRV	7+	22	7	0	0.93
TP10	AGYLLGKINLKALAALAKKIL	4+	21	0	4	0.53

*Hydrophobicity calculated according to the values from von Heijne scale

Recent studies on the mechanisms of uptake of cell-penetrating peptides (CPPs) by mammalian cells provide evidence that one possible pathway for peptide entry involves initial cell-surface binding of the peptide carrying positively charged side chains followed by endocytosis and cytoplasmic trafficking [82]. This endocytotic uptake mechanism has been verified with various techniques, such as fluorescent peptide probes, flow cytometry, and confocal laser scanning microscopy (CLSM). Indeed, the uncertainty regarding the mechanism of entry extended for a long period. Data from several groups now argue for an energy-dependent process of entry [82]. The entry of most of these molecules is likely to be inhibited by low temperature incubation or in the presence of various drugs applied to inhibit the energy-dependent pathway of cell entry. Moreover, the binding of the highly cationic cell penetrating peptide to various anionic membrane components probably initiates the first step of the cell internalization process [80]. On the other hand, reports demonstrated that various putative endocytosis inhibitors,

low temperature, or cell-energy-depletion conditions could not effectively suppress peptide uptake [82, 83] ; this suggests a passive direct transfer of the CPPs through the plasma membrane (Figure 2.7)

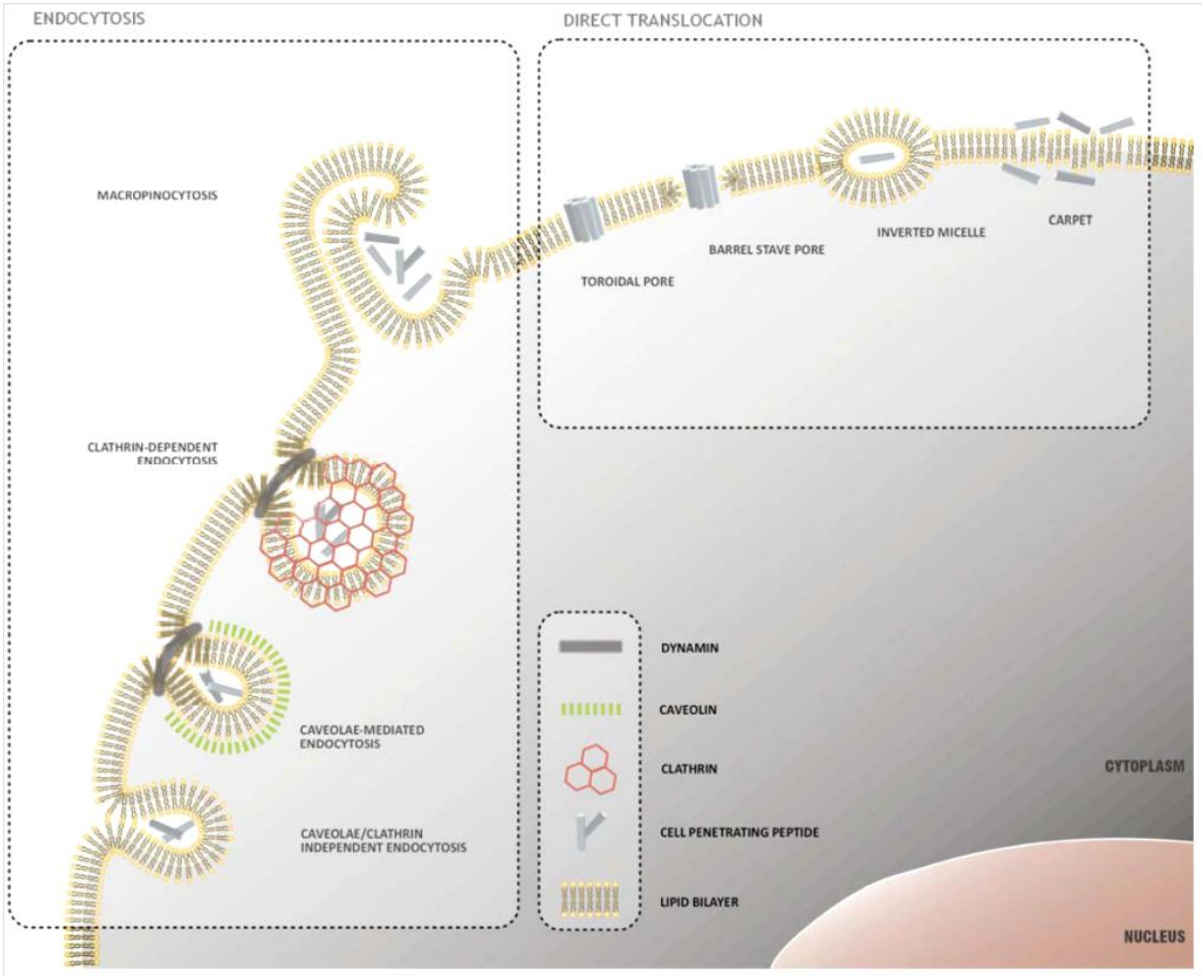

Figure 2.7 Mechanisms of peptide uptake across the cellular membrane.
A variety of internalization mechanisms have been proposed to explain cellular uptake of CPPs. These mechanisms include well-characterized energy-dependent pathways, based on vesicle formation and collectively referred as endocytosis, and direct translocation or cell penetration models, which involve the formation of hydrophilic pores or local destabilization of the lipid bilayer, (source: Trabulo *et al*., 2010 [82]).

In the last two decades, CPPs have been used as successful mediators for delivering a number of proteins, such as β-galactosidase, eGFP, Bcl-xL, human catalase, human glutamate dehydrogenase, Cu, Zn-superoxide dismutase, NF-κB inhibitor srIκBα and HSP70, among others [82]. With the exception of Pep-1 and MPG peptides that are short amphipathic peptides able to form stable nanoparticles with proteins and nucleic acids respectively, CPPs are usually coupled to proteins through covalent bonds or through fusion constructs [84]. Moreover, other studies

provided evidence that CPPs are able to mediate the delivery of proteins into a wide variety of cells, both *in vitro,* and *in vivo* [85]. Most importantly, these studies demonstrate that CPPs constitute a powerful tool that could be used to facilitate the delivery of protein-based therapeutics in pathological conditions, such as cancer, inflammatory diseases, oxidative stress-related disorders, diabetes and brain injury [82].

Little was known about the uptake of CPPs by microorganisms until recently, when it was reported that CPPs improve drug delivery into bacteria and fungi [85]. Data are accumulating that CPPs themselves possess biological activity beside their potential in penetrating a wide spectrum of cellular barriers [86]. Rajarao *et al*. revealed successful peptide constructs that mediate the delivery of green fluorescent protein GFP into *Bacillus subtilis*, *Escherichia coli* and *Staphylococcus aureus* [87]. In the present study, the potentiality of some constructs was investigated in penetrating the Gram-positive bacterium, *S. aureus*, and accordingly their internalization was evaluated.

3 Materials and methods

3.1 Materials

3.1.1 Technical devices

Peptide Synthesis, analysis and purification

Pioneer peptide synthesizer (Applied Biosystems, USA). Analytical HPLC-system (Merck-HITACHI, USA) consisted of the following units, (1) C18-RP separation column, 50 x 2.0 mm, 5 micron from Phenomenex®, (2) UV-detector of detection wavelength of 220 nm, (3) fraction collector and (4) a pump. The preparative HPLC system consisted of C18-RP separation column Nucleosil 250 x 40 mm from MACHEREY-NAGEL®, and UV-detector with detection wavelength of 220 nm. *Ultraflex* MALDI TOF MS (Bruker Daltonics, Germany), Universal 32R benchtop centrifuge (Hettich), a freeze-dryer (lyophilizer ALPHA 1-4 (Christ GmbH).

Cell culture

Incubation Shaker-Multitron 2 (INFORS HT, Switzerland), cell incubation chamber (Heraeus), Megafuge 3.0R™ benchtop centrifuge (Heraeus) Sterile GARD III™ work bench and laminar-flow cabinet (The Baker Company), Eppendorf Mixmate® vortexer (Eppendorf), multichannel pipettes (BioRad), blood agar plates (BD), Ultrafree-CL centrifugal filter units with microporous membrane 0.22μm (Millipore).

Biochemical assays

Spectrophotometer (HITACHI, Japan), microplate reader Biotek-FLI 600, supplied with different wavelength-filters (Biotek Instruments Inc, USA), Nunc 96- Microwell™ plates, fluorescence flat bottom (Thermo- Fischer scientific, Germany), Multichannel pipettes (BioRad, Germany), Optical density reader (NanoDrop 8000™ from Thermoscientific), a microplate reader (Fusion; PerkinElmer, USA), colonies-counting pen. Automated fluorescence microscope (ImageXpress microsystem®, Molecular Devices), flow cytometer (FACSCanto™, BD Biosciences). FluoView™ FV1000 Confocal laser scanning Microscope (Olympus, Japan).

SDS-PAGE and Immunoblotting

Mini-PROTEAN Tetra Cell from *Bio-Rad* ™, Power supply (Biometra, Germany), Fujifilm LAS-1000 Luminescent image analyzer system (FUJIFILM, Japan), supported with digital cooled CCD camera, micro lens over every pixel on CCD and UV-light table. Semi-Dry

Blotting Cell (Biometra), Low-voltage power supply from Biometra, X-ray BioMax™ light film (Kodak), X-ray film processor CURIX 60 (AGFA, Belgium), membrane exposure cassettes. Blotting *Protran Nitrocellulose-Membrane, Typ Protran® BA85** (Whatmann); 6 pieces of 60 x 90 mm area of *Whatmann*^{TM} filter paper per gel; SDS-PAGE home-made gels for resolving proteins bands, and incubation trays (Invitrogen).

Protein extraction

NanoDrop™8000 for monitoring the bacterial growth, Sonifer 450®-Homoginizer and cell disruptor (Branson), Biofuge (Heraeus), and ultracentrifuge Optima L8-50 M/E (Beckman Coulter Inc).

3.1.2 Computer programs and software

Table 3.1 Computer programs and software used in this study.

Computer program (software)	Source (Company)
Peptide companion	CSPS Pharmaceutical Inc
Pioneer workstation	Molecular Devices Inc
HPLC analyzer	Sigma
flexAnalysis Data analyzer for MALDI TOF	Bruker Daltonics
metaXpress	Molecular Devices
FlowJo for Flow cytometry analysis	BD Biosciences
FV Viewer	OLYMPUS
AIDA Advanced Image Data Analyzer	Raytest, Germany
ImageJ	Open source java software
Adobe Photoshop CS3	Adobe
Jalview (multiple alignment editor)	University of Dundee
W2 Clustal	EMB net –Clustal server

3.1.3 Chemicals

All chemicals that were used in the experimental part were at least of analytical grade

Table 3.2 Chemicals for peptide synthesis process and dyes for labeling peptides.

Substance	Source (Company)
Tenta-Gel S-RAM resins	RAPP POLYMER
N,N-Dimethylformamide (DMF), acetonitrile, methanol, and isopropanol	J. T. BAKER (Fluka)
tert-butylmethyl ether (MTBE), Dichloromethane (DCM)	J. T. BAKER (Fluka)
Pyridine, piperidine, and trifluoroacetic acid (TFA)	Carl Roth
N,N-Diisopropylethylamine (DIPEA)-Hünig Base	Carl Roth
Thioanisole and dithiothreitol (DTT)	Fluka
Triisopropylsilane (TIS), phenol, and dimethylsulfoxide (DMSO)	Sigma
O-(Benzotriazol-1-yl)-N,N,',N'-tetramethyluronium tetrafluoroborat (TBTU)	Sigma
Fluorescein and fluorescein-5-maleimide (F5M)	Pierce

Table 3.3 Fmoc protected amino acids from MultiSynTech GmbH used in peptide synthesis.

AA-Abbreviation	Fmoc-protected amino acid	Molecular weight[g/mol]	eq. 100µmol x4 excess [mg]
A	Fmoc-L-Ala-OH	311.3	125
R	Fmoc-L-Arg(Pbf)-OH	648.8	260
N	Fmoc-L-Asn(Trt)-OH	596.7	239
D	Fmoc-L-Asp(tBu)-OH	411.5	165
C	Fmoc-L-Cys(Trt)-OH	585.7	234
E	Fmoc-L-Glu(tBu)-OH	425.5	170
Q	Fmoc-L-Gln(Trt)-OH	610.7	244
G	Fmoc-L-Gly-OH	297.3	119
H	Fmoc-L-His(Trt)-OH	619.7	248
I	Fmoc-L-Ile-OH	353.4	141
L	Fmoc-L-Leu-OH	353.4	141
K	Fmoc-L-Lys(Boc)-OH	468.5	187
M	Fmoc-L-Met-OH	371.5	149
F	Fmoc-L-Phe-OH	387.4	155
P	Fmoc-L-Pro-OH	337.4	135
S	Fmoc-L-Ser(tBu)-OH	383.4	153
T	Fmoc-L-Thr(tBu)-OH	397.5	159
W	Fmoc-L-Trp(Boc)-OH	526.6	211
Y	Fmoc-L-Tyr(tBu)-OH	459.4	184
V	Fmoc-L-Val-OH	339.4	136

The chemical dyes SYBR green and propidium iodide were purchased from Pierce, Thermo-Fischer Scientific. The fluorescein-5-maleimide was ordered from Biozol-Diganostica. WST-8 was purchased from Sigma-Aldrich, Germany. Most buffering salts, acids and bases were ordered from Carl Roth, protease inhibitors such as benzamidine (HCl), Nα-p-tosyl-L-arginine methyl ester HCl, PMSF protease inhibitor, leupeptin hemisulfate salt, pepstatin A, polyethylene glycol tert-octylphenyl ether (Triton ® X-100), polyethylene glycol sorbitan monolaurate (Tween 20) were purchased from Sigma-Aldrich, Germany.

3.1.4 Kits

SuperSignal West Pico Chemiluminescent Substrate Kit (Pierce) was purchased from Thermo-Scientific, Germany. This kit was used to develop the enhanced chemiluminescence ECL on X-ray films for quantifying the Western Blotting protein bands.

3.1.5 Buffers

3.1.5.1 Buffers for peptide synthesis and labeling

Ammonium acetate buffer with isopropanol (1:1): ammonium acetate buffer (100 mM) was prepared by dissolving 7.708 g of ammonium acetate in 100 ml distilled H_2O. The pH was adjusted to 7.2. This buffer was mixed with isopropanol (1:1).

Phosphate buffered saline (10x PBS pH 7.0): 80 g NaCl, 2.0 g KCl, 14.4 g Na_2HPO_4, and 2.4 g KH_2PO_4 were dissolved in 800 ml distilled H_2O, the pH was adjusted to 7.4, the volume was completed to 1000 ml, and the buffer was sterilized by autoclaving. The 1xPBS buffer can be prepared by diluting the stock buffer with distilled H_2O (1:10) and then autoclaving.

3.1.5.2 Buffers for enzymatic assays

Phosphate buffer pH 7.8: 5.44 g of potassium phosphate, monobasic, anhydrous was dissolved in 300 ml distilled H_2O; pH was adjusted to 7.8 with 1 N KOH, diluted to 400 ml.

TRIS/HCl buffer pH 8.0: prepared by dissolving (12.1 g Tris base (MW 121.14) in 100 ml H_2O, pH was adjusted with concentrated HCl to 8.0.

HEPES buffer pH 7.2: prepared by dissolving 1.19 g of Hepes (N-(2-hydroxyethyl)-piperazine-N´-2-ethane sulfonic acid), Mw 238.3 g/mol) in 100 ml H_2O and adjusting the pH to 7.3 with 1 N KOH.

3.1.5.3 Buffers for subcellular fractionation and protein extraction

Lysis buffer L: 20 μg/ ml lysostaphin from *S. aureus* (Genmedics) was prepared in 50 mM Tris buffer pH 8.0.

Fractionation buffers: All chemicals and enzymes inhibitors were purchased from Sigma-Aldrich, Germany.

Buffer A:

Substance	Concentration	In 100 ml
Tris-HCl pH 8.1	40 mM	0.630g
NaCl	100 mM	0.585g
Sucrose	27%w/v	27g
$MgCl_2$	20 mM	0.191g
PMSF protease inhibitor	2 mM	0.035g
Benzamidine (HCl)	1 mM	0.016
Nα-p-Tosyl-L-arginine methyl ester HCl	0.2 mM	0.0075g
Leupeptin hemisulfate salt	10 μg/ ml	0.001g
Pepstatin A	10 μg/ ml	0.001g

Buffer B:

Substance	Concentration	In 100 ml
Tris-HCl pH 9.5	40 mM	0.630g
Benzamidine (HCl)	1 mM	0.0329g
Leupeptin hemisulfate salt	5 µg/ ml	0.5mg
Pepstatin A	5 µg/ ml	0.5mg
PMSF protease inhibitor	2 mM	0.035g
Nα-p-Tosyl-L-arginine methyl ester HCl	0.2 mM	0.0075g
Na-EDTA	2 mM	0.058 g

Buffer C:

Substance	Concentration	In 100 ml
Tris-HCl pH 8.1	50 mM	0.788g
NaCl	100 mM	0.585g
$MgCl_2$	2 mM	0.019 g
Triton-X	0.25%	250µl (TritonX-100)

3.1.5.4 Buffers for SDS-PAGE

Laemmli loading buffer: was ordered from Roth, Germany, known as Roti-Load 1, contains 2% (w/v) SDS; 10% (v/v) mercaptoethanol, 62.5 mM Tris-HCl, pH 6.8, 10% (v/v) glycerol, 0.01% (w/v) bromophenol blue.

Resolving buffer pH 8.8: 90.9 g Tris-HCl was dissolved in 500 ml distilled H_2O, pH was adjusted.

Stacking buffer pH 6.8: 30.2 g Tris-HCl was dissolved in 500 ml distilled H_2O, pH was adjusted.

10× Running buffer pH 8.6: 30 g Tris-HCl, 144 g glycine, and 10 g SDS were dissolved in 1000 ml distilled H_2O, pH was adjusted.

Tris-buffered saline with Tween, 10× (TBS-T): 80 g NaCl, 61 g Tris-base, 2 g KCl, and 1 ml tween 20 were dissolved in 1 liter of distilled H_2O and the pH was adjusted to 7.0 with 32% HCl.

Polyacrylamide gels: 10.5 × 7 cm, 1.0 mm thick of mini-gels were home-prepared. Mini slab gels consisting of 8-10% made of polyacrylamide/ bisacrylamide resolving gel (pH 8.8), and 4% polyacrylamide/ bisacrylamide stacking gel (pH 6.8) were used for resolving the proteins.

Destaining buffer: 300 ml ethanol and 100 ml acetic acid were diluted with distilled H_2O to a volume of 1000 ml.

RuPBs staining buffer: was prepared by adding 10 µl of the RuBPS stock solution (20 mM) to 1 litre of 20% ethanol.

3.1.5.5 Buffers for immunoblotting

Transfer buffer: 6 g Tris-HCl, 28.8 g glycine, and 400 ml methanol, completed to 2000 ml with distilled H_2O.

Membrane blocking buffer: 5% skimmed-milk in 1×TBS-T buffer.

Washing buffer: 0.05% TBS-T buffer pH 7.0.

Antibody diluting buffer: 1% bovine serum albumin in 1× TBS-T buffer.

3.1.6 Enzymes, antibodies, substrates, and proteins

Table 3.4 Enzymes, antibodies, substrates and proteins that were used in this study.

Substance	Usage	Source
Glu-C Endoproteinase from *Staphylococcus aureus*	Specific Control for enzymatic assay	Merck (Calbiochem)
Glu-C Endoproteinase from *Staphylococcus aureus*	Control protein for SDS PAGE	Roche Diagnostics
Lysostaphin from *Staphylococcus simulans*	Cell lysis	Sigma-Aldrich
Mutanolysin from *Streptomyces globisporus*	Cell lysis	Sigma-Aldrich
Rabbit anti serum of glutamyl-C endoproteinase	Primary antibody for detecting V8 protease	Biogenes GmbH
Polyclonal goat anti-rabbit immunoglobulin conjugated with horseradish peroxidase (HRP)	Secondary antibody for detecting V8 protease	Dako Cytomation
Biotin conjugated anti α-hemolysin	Primary antibody for detecting α-hemolysin	Abcam®
Streptavidin conjugated with horse reddish peroxidase (HRP)	Secondary antibody for detecting α-hemolysin	Pierce/ Thermoscientific
Peptide Z-Phe-Leu-Glu-*p*NA	V8-Specific chromogenic substrate	Sigma-Aldrich
Peptide Z-LLβNA	V8-Specific fluorogenic substrate	Sigma-Aldrich
Peptide ABz-AFAFEVFY(NO_2)D-OH	V8-Specific chromogenic substrate	Synthesized in house
Sheep erythrocytes in Alsever's solution	Hemolysis assay	Fiebig-Nährstofftechnik
Bovine serum albumin	Blocking buffer	Sigma-Aldrich
Skim milk powder	Blocking buffer	Difco
Precision Plus Protein Dual Color Standard	Standard protein	BioRad

3.1.7 Culture media

Luria-Bertani (LB)-Medium

Component	Weight (g) in 1 Litre	Source
Tryptone	10 g	Oxoid
Bacto yeast extract	5 g	BD Bioscience
Sodium chloride	10 g	Roth

BM-Medium

Component	Weight (g) in 1 Litre	Source
Soya peptone	10 g	Oxoid
Bacto yeast extract ™	5 g	BD
Sodium chloride	5 g	Carl Roth
KH_2PO_4*$3H_2O$	1 g	Carl Roth
Glucose	1 g	Carl Roth

Müller Hinton (MH)-Medium

Component	Weight (g) in 1 Litre	Source
Meat infusion	2 g	Carl Roth
Casein hydrolysate	17.5 g	Carl Roth
Starch	1.5 g	Carl Roth

Trypitcase Soy Broth (TSB)-Medium

Component	Weight (g) in 1 Litre	Source
Bacto tryptone	17 g	BD Bioscience
Bacto soy peptone	3 g	BD Bioscience
Dextrose	2.5 g	Carl Roth
Sodium chloride	5 g	Carl Roth
Dipotassium phosphate	2.5 g	Carl Roth

T-Medium

Component	Weight (g) in 1 Litre	Source
Tryptone	17 g	Oxoid
Soya peptone neutralized	3 g	Oxoid
Glucose	10 g	Carl Roth
MOPS	5.24 g	Carl Roth
NaCl	5.84 g	Carl Roth
KCl	0.149 g	Carl Roth
$CaCl_2$× 2 H_2O	0.294 g	Carl Roth

Brain-Heart Infusion (BHI)-Medium

Component	Weight (g) in 1 Litre	Source
Calf brain infusion solid	12.5 g	Oxoid
Beef heart infusion solid	5.0 g	Oxoid
Protease peptone	10 g	Oxoid
Glucose	2.0 g	Oxoid
Sodium chloride	5.0 g	Oxoid
Disodium phosphate	2.5 g	Oxoid

Chemically defined medium for *Staphylococcus aureus*

Component	Quantity per 1-Litre	Component	Quantity per 1-Litre
Aspartic acid	1.0 g	Cysteine	0.24 g
Glutamic acid	1.0 g	Phenylalanine	0.20 g
Proline	1.0 g	Tyrosine	0.18 g
Glycine	1.0 g	Methionine	0.18 g
Serine	1.0 g	Tryptophan	0.06 g
Threonine	1.0 g	Nicotinic acid	0.002 g
Alanine	1.0 g	Thiamin HCl	0.002 g
Lysine HCl	0.6 g	KH_2PO_4	1,34 g
Isoleucine	0.6 g	Na_2HPO_4	5.7 g
Leucine	0.6 g	$(NH_4)_2SO_4$	6.84 g
Histidine	0.48 g	NaCl	1.0 g
Valine	0.48 g	Glucose	4.0 g
Arginine	0.30 g	$MgSO_4$. 7 H2O	0.05 g

This chemically defined medium was described in Bhat *et al*, 1993 for optimal production of different exoproteins in the *Staphylococcus aureus* secretome [88]. This medium was used for producing the proteases, which can be later analyzed by mass spectrometry without the interference of the medium contents. All culture media above were filtered through 0.22 µm membrane filters into sterile bottles. The pH value of BM medium was adjusted to 7.2, and the pH values of MH, TSB, and T medium were adjusted to 7.4.

Preparation of 2% milk with BHI agar medium

Milk agar plates were used for detecting the optimal secretion of proteases. For preparing these agar plates, 26 g of BHI agar (Difco®) was weighed and transferred into 500 ml distilled H_2O, stirred by a magnetic stirrer. The content of the bottle was autoclaved. After autoclaving the agar medium, an amount of 10 g skim milk powder was added gradually, keeping stirring under the laminar flow cabinet (the agar medium should be hot enough in order to avoid the agglomeration of milk powder).

3.1.8 Bacterial strain

Staphylococcus aureus, V8 strain, a proteolytically hyperactive strain that was used in this study, was a generous gift from Dr. J. Miedozobrozki (University Krakow, Poland). He used this strain in a comparative study with isolated strains from atopic dermatitis patients. This strain was isolated by Dr. Arvidsons who reported about considerable production of V8 protease in this strain [89-97]. The strain was known as high-protease-producing strain from which the four major staphylococcal proteases (sspA, sspB, aur, and scp) were originally characterized [89-97].

3.2 Methods

3.2.1 Synthesis of peptides

14 peptides were chemically generated on a 100 µmol scale, starting from TentaGel S-RAM resin on the Pioneer synthesizer according to Fmoc-solid phase synthesis protocols (Table 3.5). All Fmoc-protected amino acids that were used in peptide syntheses were of the L-configuration and were coupled in a fourfold excess (Table 3.3). The peptides were assembled using TBTU and DIPEA as coupling agents and 20% piperidine in DMF as Fmoc-deprotecting agent.

Table 3.5 List of the chemically synthesized peptides that were utilized in this study.

Construct	Sequence	Usage
Peptide-1	VLTNENPFSDP-C(F5M)-NH_2	Cell-penetrating peptides (CPPs)
Peptide-2	RSNNPFRAR-C (F5M)-NH_2	
Peptide-3	YGRKKRRQRRR-C(F5M)-NH_2	
Peptide A	KGKFLKVSSLFVATLTTATLVSSPAANAYGRKKRRQRRR-NH_2	Potentially Sec-interfering peptides
Peptide B	**M**KGKFLKVSSLFVATLTTATLVSSPAANAYGRKKRRQRRR-NH_2	
Peptide C	**formyl- M**KGKFLKVSSLFVATLTTATLVSSPAANAYGRKKRRQRRR-NH_2	
Peptide D	YGRKKRRQRRRC-NH_2 (CPP)	
Peptide E	MKGKFLKVSSLFVATLTTATLVSSPAANA-NH_2 (Signal peptide)	
Peptide F	**M**KGKFLKVSSLFVATLTTATLVSSPAANA-NH_2 (Signal peptide)	
Peptide G	**formyl-M**KGKFLKVSSLFVATLTTATLVSSPAANA-NH_2 (Signal peptide)	
Peptide H	AAMGNSFVLSTLTKTKPAFLTLVASASVKYGRKKQRRR-NH_2 (Scrambled)	
Peptide I	**M**KGKFLKVSSLFVATLTTATLVSSPAANAYGRKKRRQRRR-C(F5M)-NH_2	Reporter peptides
Peptide J	**formyl-M**KGKFLTLVSSLFVATLTTATLVSSPAANAYGRKKRRQRRR-C(F5M)-NH_2	
Peptide K	ABz-AFAFEVFY(NO_2)D-OH	Substrate

(F5M) is the chemical dye fluorescein-5-maleimide, was abbreviated (F5M) in some parts of this dissertation.

After removal of the last N-α-Fmoc protecting group, the peptide-conjugated resins were transferred to filter syringes, washed three times with 3 ml dichloromethane (DCM), and left under the fume hood to be dried overnight. Peptides were cleaved from the resin by trifluoroacetic acid cocktails (Table 3.6). The resins were collected in a syringe with frit, and were treated with 2x 5 ml of the cocktail, with agitation over a period of 3-6 h. Then, the syringe was drained carefully and the filtrate was collected in a round bottom flask. The peptide-containing filtrate was concentrated on a rotatory evaporator and finally the peptides were precipitated with tert-butylmethyl ether.

Table 3.6 Two types of cleavage cocktails with high quality TFA and fresh scavengers were prepared.

Cleavage cocktail	Content	Cleavage time	Cleaving from resin of
A	(TFA/H_2O/triisopropylsilane) (9.5/0.3/0.2)	3-6 h	Peptides 1, 2, 3 and K
B	(TFA/H_2O/phenol/thioanisol/DTT) (8.25/2.5/2.5/2.5/1)	3-6 h	Peptides A to J

The suspended precipitation was transferred into 50 ml Falcon conical-centrifuge tubes, and centrifuged at 4500 rpm for 15 min. The ether layer was decanted and the precipitated peptide was dried overnight under the fume hood. The precipitated peptides were lyophilized and weighed to calculate their yields. The crude peptides were resuspended and analyzed by HPLC using various acetonitrile gradients in aqueous 0.1% trifluoroacetic acid. Masses of HPLC crude peaks were determined by MALDI TOF. Peptides were purified by preparative reverse phase HPLC. The collected fractions of the pure peptides were lyophilized and weighed to be subjected to the bioassay.

3.2.1.1 Analytical and preparative HPLC

All crude and purified peptides were analyzed using the Merck-HITACHI HPLC-system. An appropriate mobile phase gradient consisting of acetonitrile and water with 0.1% TFA was eluted with a flow rate of 0.7 ml/ min (Table 3.7).

Table 3.7 Gradient of analytical HPLC A: H_2O + 0.1 % TFA, B: MeCN + 0.1 % TFA, C: MeOH.

Time (min)	Flow rate (µl/min)	% A	% B	% C
0	700	95	5	0
1	700	95	5	0
12	700	50	50	0
13	700	40	60	0
14	700	0	100	0
15	700	0	0	100
19	700	0	0	100

Purification of peptides were done using an HPLC- Merck-HITACHI instrument, the pure peptide was eluted with an appropriate gradient using a mixture of mobile phase as acetonitrile: water with 0.1% TFA, product peaks were eluted with a flow rate of 25 ml/min. Fractions were collected and analyzed by MALDI-TOF. The fractions that correspond to the product were isolated, frozen, lyophilized, and then weighed to be used in specific concentration in the microbial experiment. The mobile phase gradient I in table 3.8 was eluted to purify

peptides 1, 2, and 3, whereas the mobile phase gradient II in table 3.9 was eluted to purify the peptides A to K.

Table 3.8 Gradient I of preparative HPLC A: H_2O + 0.1 % TFA, B: MeCN + 0.1 % TFA, C: MeOH.

Time(min)	Flow rate (ml/min)	% A	% B	% C
0	25	95	5	0
10	25	95	5	0
70	25	50	50	0
70.1	25	0	0	100
80	25	0	0	100

Table 3.9 Gradient II of preparative HPLC A: H_2O + 0.1 % TFA, B: MeCN + 0.1 % TFA, C: MeOH.

Time (min)	Flow rate (ml/min)	% A	% B	% C
0	25	95	5	0
10	25	95	5	0
15	25	80	20	0
75	25	40	60	0
75.1	25	0	0	100
85	25	0	0	100

3.2.1.2 Mass determination of peptides by MALDI TOF MS analysis

For the mass determination, 0.5 µl of the dissolved peptide mixture was analyzed by *Ultraflex* MALDI TOF MS (Bruker Daltonics) with a λ 337 nm N_2 Laser, equipped with a reflectron and employing alpha-cyano-4-hydroxycinnamic acid as the matrix. The obtained masses were externally calibrated using a mixture with standard peptides angiotensin-II (Mw 1046.54), angiotensin-I (Mw 1296.69), substance P (Mw 1347.73), bombesine (Mw 1619.82), ACTH clip 1–17 (Mw 2093.09) and ACTH 18–39 (Mw 2465.20), Somatostatin 28 (Burker Daltonics, USA). The covered mass ranges between 1000 to 5000 Da. Bruker Daltonics Ultraflex consists of two Time-of-Flight channels. The first separates the ions generated by laser beam on the basis of their molecular weights giving a mass fingerprint. The second TOF resolves the fragmented species generated by a collision chamber, which is present between the two TOFs.

3.2.1.3 Labeling the cell penetrating peptides with fluorescein-5-maleimide (F5M)

A stock solution (100 mM) of fluorescein-5-maleimide was prepared by dissolving 8.54 mg in 200 µl DMSO. A 100 mM ammonium acetate buffer was prepared by dissolving 7.708 g of

ammonium acetate in 100 ml water. The pH was adjusted at 7.2. This buffer was mixed with isopropanol (1:1). The peptide solution was prepared by dissolving 5-10 μmol of peptide with available sulfhydryl in 1 ml of the isopropanol buffer (pH 7.2), this will result a 5-10 mM peptide solution. For labeling the peptide with the fluorescein-5-maleimide, a 10% molar excess of fluorescein-5-maleimide was added onto the molar amount of sulfhydryl to be coupled. The reaction was allowed to proceed in dark vessel overnight at room temperature. Analytical HPLC was performed, a shifting of the retention time in the main peaks was observed. Mass analysis for the labeled peptide was determined by MALDI-TOF. The labeled peptide was purified by preparative HPLC, and the collected fractions were isolated, lyophilized, and weighed.

3.2.1.4 Labeling the Sec-interfering peptides with fluorescein-5-maleimide (F5M)

The potentially Sec-interfering peptides were chemically generated with a cysteine residue at the C-terminus (table 3.6). Due to their low yields, the cysteine containing peptides were labeled with F5M and purified in one pot according to Vive's, *et al.* [98]. In summary, the peptide was incubated with the F5M in buffer conditions, and purified by adding the acetone in the same reaction tube, which was kept in darkness for 18 hours. The reaction mixture was under vacuum evaporated, lyophilized, and analyzed.

3.2.1.5 Fmoc-Solid phase synthesis of ABz-AFAFEVFDY(NO_2)D-OH as a fluorogenic substrate for V8 protease

This fluorogenic substrate was prepared according to the published procedures of Singh *et al.* [99]. Briefly, the peptide was prepared according to Fmoc chemistry, the side reaction was entirely prevented upon treatment of the resin bound peptide with piperidine prior to final TFA cleavage. After deprotection, the peptide was purified and characterized by analytical HPLC and MALDI-TOF spectrometry. The lyophilized pure peptide was dissolved in DMSO then diluted with aqueous solution to be introduced to the supernatant enzymatic assay.

3.2.2 Bacterial strain and culture conditions

3.2.2.1 Preparation of strains in glycerol stocks

Glycerol stock of *S. aureus* V8 strain was prepared from exponentially overnight growing cultures in BM broth, at 37 °C with constant agitation (180 rpm) and stored in cryogenic vials in 20% glycerol at -80°C.

3.2.2.2 Subculture the bacterial strain on the blood agar plate

By means of a sterile inoculating loop, a portion from the top of the frozen glycerol stock was scraped off and streaked onto the blood agar plate under laminar flow hood. The agar plate was incubated for 24 h at 37º C. The next day, the plate was taken and wrapped with paraffin film keeping it sterile in low temperature 4ºC. The subcultured strains were used for up to 4 weeks from the date of subculture.

3.2.2.3 Culture conditions of the *S. aureus* V8 strain

Main cultures of *Staphylococcus aureus* V8 strain were prepared by inoculating aliquots of the overnight culture in 5 ml growth broth. Sterile screw-cap glass tubes of 15 ml-volume were used for this purpose. The optical densities of bacterial cultures were started at 0.05, measured at λ 600 nm. The peptides were immediately inoculated to the cell suspensions in each tube. The growth of staphylococcal cells was allowed at 37ºC with agitation on a shaker 180 rpm until the stationary phase was reached. The optical densities were monitored throughout the bacterial growth. 24 hours after starting the growth, the bacterial cells were harvested and equal volumes of supernatants were collected by filtration through 0.22 µm Millipore filter units. Pellets were isolated in the cups of filters. For some particular experiments, bacterial cells were resuspendend with phosphate buffered saline (PBS) to an optical density of 1.0. Thereafter, they were either undergone complete lysis for testing the cellular and extracellular protein contents, or undergone subcellular fractionation for testing the protein contents in different cellular compartments. The resulting extracellular and intracellular proteins were denatured, profiled on 8% SDS-gels. Western-blot was used specifically for quantifying V8 protease on the X-ray images.

3.2.3 Investigating the entry of the cell penetrating peptides into *S. aureus*

Bacterial cells of *S. aureus* V8 strain were cultivated in BM broth in an overnight culture. The cell suspension was filtered through 0.22 µm Millipore filters. The pelleted cells in the top of the filter were rinsed with 3× 2-ml PBS buffer. The rinsed cells were diluted with PBS buffer to an $OD_{\lambda 600}$ of 1.0 in three individual tubes. The fluorescein-conjugated peptides 1, 2, and 3 were incubated with the three bacterial suspensions at a concentration of 100 µM at 30ºC. After 1 hour of incubation, bacterial cells were collected by 0.22 µm Millipore filters (3500 rpm, 5 min), washed with 3×2-ml PBS buffer to remove extracellular fluorescent-peptides and the background fluorescence. After diluting the bacterial suspensions with PBS (1:10) in a black 96-well plate (Greiner), fluorescence microscopy measurements were performed by the automated microscope *ImageXpress* with excitation and emission wavelengths of 488 and 518 nm, respectively. The

images were analyzed using the Transfluor mode of the *metaXpress* software that can count the pits of the fluorescent cells and consequently calculate the average intensity of the fluorescence. In order to get better image-resolution to the internalized peptides, confocal laser microscopy was used. Rhodamine B hexyl ester (RBHE) was added in a concentration of 5µM as control to detect the internalization of the fluorescent-peptides.

For quantifying the staphylococcal uptake of 100 µM fluorescent peptides, samples were prepared in the same previous procedures for FACS analysis with diluting the cell suspension to an OD_{600} of 0.250. Propidium iodide was supplemented into the cell suspensions to determine the dead cells, SYBR green was used for staining the total cells. Since the flow cytometer FACSCanto was equipped with variable excitation laser lines, 488 nm and 633 nm for the green and red fluorescence channels, respectively, it was used for counting the corresponding bacterial populations. The calculations were deduced by comparing the count of cells that have internalized the peptides to the whole cell population in each sample.

3.2.4 Identifying the optimal medium for producing proteases

Staphylococcus aureus V8 strain was cultivated in five different media, as described in the procedures under 3.2.2.3, namely MH, LB, BM, TSB, and T medium. At 24 h of growth, supernatants were collected by filtration through 0.22 µm Millipore filters. Plates of 2% skimmed-milk in brain-heart-infusion agar were used in qualitative and semi-quantitative evaluation of extracellular proteases. Small (3 mm diameter) sterile discs were soaked with 20 µl aliquots of staphylococcal supernatants. The diameters of the proteolytic zones on milk agar plates were measured after overnight incubation at 37°C.

3.2.5 Quantification of V8 protease in the supernatants

3.2.5.1 Quantification of V8 protease using the chromogenic peptide Z-FLEpNA

The enzymatic activity in bacterial culture supernatants was assayed in procedures based on Yabuta *et al*., 1995. V8 protease activity was measured at 30ºC in a 96 well plate (Nunc-flat buttom), each well containing 4 mM of Z-Phe-Leu-Glu-*p*NA in a volume of 200 µl 50 mM TRIS-HCl buffer (pH 8.0). Initial velocity values were determined by monitoring the absorbance of the released *p*-nitroaniline at 405 nm with a Biotek FL 600 microplate reader. Serial dilution of the commercially available enzyme was utilized to determine the limits of detectable activity [100].

3.2.5.2 Quantification of V8 protease using the fluorogenic peptide Z-LLE-βNA

The enzymatic activity of the purchased V8 protease was investigated by preparing solutions of 0, 2.5, 5, 10, 25, and 50 µM of the substrate Z-LLE-β-NA in 100 mM of phosphate buffer pH 7.8. The substrate solutions were assayed with 100 ng/ml of the commercially available V8 protease in 96 well plates. The enzymatic activity of the bacterial supernatants was assayed according to the same procedure. Each assay well contained 100 µl of 100 mM phosphate buffer (pH 7.8), 80 µl of the substrate solution and 20 µl of supernatant. The reaction was carried out for 30 min at 25°C. The released amount of β-naphthylamide was determined at 410 nm. A unit (U) of enzyme is defined as the change of the fluorescence unit per min under the given assay conditions. In contrast to Nickerson *et al*. 2007, our approach was modified in using the free secreted V8 protease instead of covalently immobilizing the enzyme to silicon AFM tip (ATEC-CONT) or silicon particles via amide bonds [10].

3.2.5.3 Quantification of V8 protease using the synthetic fluorogenic peptide (ABz)AFAFEVFY(NO_2)D-OH as substrate

The assay was performed based on intramolecular fluorescence quenching according to Breddam, 1992 [101]. It utilizes a 96-well plate setup and fluorescence microplate reader. In order to optimize the sensitivity of this method, different buffers were first investigated, namely HEPES at pH 7.4 and phosphate at pH 7.8. The assay was further run according to the optimal conditions. In summary, the commercially available V8 protease (Glu-C endoproteinase from *S. aureus*) at the concentrations 0, 0.1, 0.5, 1.0, 5.0, 10, 20 µg/ ml was assayed with a solution of 200 µM of the synthetic substrate (ABz-AFAFEVFY(NO_2)D-OH) in HEPES buffer pH 7.4 and at room temperature conditions. The fluorescence was read each 1 min for 60 min. The isolated supernatants, 24 h after growing the bacterial cultures, were assayed with the synthetic substrate at the same conditions. In order to get better fluorescence detection, supernatants, were diluted with HEPES buffer (1:10) in a volume of 100 µl. The initial rate of the enzymatic activity, which is dependent on the concentration of V8 protease, was measured in milli-fluorescence unit per min (mFU/ min), it was determined from the first 5 min of the fluorescence increase that resulted from the cleavage of the substrate. The emission of fluorescence was measured at 410 nm using the fluorescence spectrophotometer FLI-600 (Bio-Tek).

3.2.5.4 Quantification of V8 protease using SDS-PAGE

Different concentrations of the commercially available V8 protease, Glu-C endoproteinase, were prepared, (0, 2.5, 5, 10, 25, 50, and 100 µg/ml), then denatured by treatment

with Laemmli buffer, for 10 min at 95˚C. 10 µl of protein samples were loaded into the wells of home-made slab gels, which consisted of a 10% polyacrylamide/ bisacrylamide resolving gel, and a 4% polyacrylamide/ bisacrylamide stacking gel. SDS-PAGEs were run in a Bio-Rad Miniprotean electrophoresis chamber at 90 Volts for about 1 hour at room temperature. Power was stopped when the bromophenol blue dye was leaving the gel. Subsequently, the gels were incubated overnight with buffer (30% ethanol and 10% acetic acid), washed 3× with 20% ethanol for 30 min, stained with RuBPS in 20 % ethanol for 6 hours, and destained with 30% ethanol and 10% acetic acid. The next day, the gel was washed with water and set on a UV plate to generate a photo by the CCD camera (Fujifilm, Raytest).

3.2.5.5 Quantification of V8 protease bands by using Western blots

For Western blot analysis, 10 µl of each supernatant was resolved by 10% sodium dodecyl sulfate-polyacrylamide gel and was transferred to nitrocellulose membranes (Whatmann) using a semi dry electroblotting apparatus (Biometra) with 20% methanol in the blotting buffer. The membranes were blocked with 5% skimmed milk, and incubated with the rabbit V8 protease-anti serum at 1:10000 (Biogene GmbH). The membranes were washed with Tris-buffered saline containing 0.05% Tween-20 (TBS-T), and probed with an HRP-conjugated anti-rabbit antibody (1:10000 Dako Cytomation). For ECL detection, the kit (SuperSignal West Pico Chemiluminescent Substrate, Thermo Scientific) was used. Upon the ECL activation on the membrane, the membrane was incubated in the dark with the X-ray film inside a film-cassette. The exposed X-ray film was processed and scanned to produce TIFF-format images. The resulted bands were quantified based on densitometry scale using AIDA image analyzer (Raytest) and Photoshop CS3 (Adobe), and were normalized to 10 µg/ ml of endoproteinase Glu-C from Merck Bioscience.

3.2.6 Testing the effect of the peptides on bacterial growth and viability

In order to investigate the toxicity of the utilized peptides towards the bacterial cells, the cell viability test can give a good estimation. In this context, two assays were performed to serve this purpose. (1) Counting the colonies forming units (CFU/ ml), and (2) the water-soluble tetrazolium WST-8 assay.

S. *aureus*, V8 strain, suspensions were prepared as described above in 3.2.2.3. Bacterial suspensions were treated with 10 µM of peptides (A to H) in individual culture tubes. One bacterial culture tube was left without peptide treatment as a control. After 24h of growth,

bacterial cell suspensions were well homogenized by a vortexer, 1 ml of each culture suspension was undergone serial dilution (1:9) with phosphate saline buffer (PBS pH 7.0). At the ninth dilution step, 100 µl of homogenized suspension was plated on BHI agar plate, and incubated overnight at 37ºC. On the next day, the colonies-forming units in the plates were counted as a parameter representing the viable cells in the suspension 24 hours after starting the growth.

In the WST assay, the metabolic activity of the living bacterial cells was spectroscopically measured using a test wavelength of 460nm and a reference wavelength of 620 nm. Bacterial cultures were individually treated with 10µM of peptides A to H, and one culture was left without peptide treatment, 24 h after the growth 1ml of each bacterial culture was serially diluted with PBS in 96-well plates. Aliquots of 100 µl of WST-8 solution were added to each well. After 4 h of incubation the absorbance was read.

3.2.7 Investigating the peptides effect on the secretion of V8 protease

Overnight cultures of *S. aureus V8* strain were diluted in BM medium to an OD_{600} of 0.05, and treated with 10 µM of peptide A, B, and C. One culture was left without peptide treatment as a control. Cultures were parallel grown at 37ºC under aerobic conditions (as described in 3.2.2.3). To monitor the growth, samples were taken every 6 hours and the OD_{600} was measured. Samples for subsequent experiments were taken after 24 hours. Cells were separated from the medium by centrifugation (2 min, 3500 rpm). Proteins in the supernatant were denatured, and subsequently introduced to SDS-PAGE and Western blotting. Comparisons between the protein bands in lanes of the peptide-treated cells and the other lanes of the untreated cells were performed by the software AIDA from (Raytest Company). The densitometry of the protein bands was used as comparison parameter for the protein abundance. The secreted amounts of V8 protease in supernatants were standardized to the optical density parameter at 24 h of growth.

3.2.8 Investigating the optimal peptide construct that reduces the secretion of V8 protease

The levels of the secreted V8 protease were analyzed using Western blotting. Briefly, *S. aureus* cultures were prepared as described in 3.2.2.3, bacterial cultures were treated with 10µM of peptides A to H. One bacterial culture was without peptide treatment. Supernatants were isolated by centrifuging the suspensions through 0.22µm Millipore filter units, and then introduced to the SDS-PAGE and Western blotting. The quantified amounts of the V8 protease were standardized to the optical density of the corresponding bacterial culture.

3.2.9 Investigating the effect of peptide A on the secretion of V8 protease

As described in 3.2.2.3, bacterial cultures were individually treated with 2.5, 5, 10, 20, 30, and 40 µM of peptide A. One bacterial culture was left without peptide treatment. Supernatants and cells were isolated from the growth medium after 24h by 0.22 µm Millipore filters units. Bacterial cells were resuspended in cold PBS in the same volume of the suspension, and then incubated for 1 hour at 37 ºC with the lysis buffer L. Subsequently, cell debris was homogenized by ultrasonifier for 30 seconds. Cell lysates were centrifuged at 10,000× g for 20 min at 4 °C. Both cell lysates and supernatants were introduced to SDS-PAGE and Western blotting to evaluate the levels of the cellular and secreted V8 protease, respectively.

3.2.10 Investigating the effect of peptide A on α-hemolysin

3.2.10.1 Quantification of secreted and the cellular α-hemolysin using Western blot analysis

Based on the streptavidin-biotin specific binding on Western Blot analysis, an approach was established using different concentrations of the commercially available α-hemolysin from *S. aureus* (Sigma) ranging between (2.5–100 µg/ml). Both standards and samples were profiled on a gel, and were blotted onto a nitrocellulose membrane. The membrane was blocked with 5% bovine serum albumin for 1 h, and subsequently treated with the biotin conjugated staphylococcal α-hemolysin antibody (Abcam) for 1 h, then washed 6× 5 min with Tris-buffered saline containing 0.05% Tween-20 (TBS-T) and probed with high sensitivity streptavidin-HRP antibody (Pierce). The kit (SuperSignal West Pico Chemiluminescent Substrate, Thermo Scientific) was used for ECL detection. The ECL TIFF-format image was developed from the X-ray film. The densitometry of each protein band was quantified using AIDA image analyzer (Raytest) and Photoshop CS3 (Adobe), and were normalized to 25 µg/ml of α-hemolysin from *S. aureus* (Sigma).

3.2.10.2 Investigating the secreted hemolysins using the hemolysis assay

This method estimates the content of hemolysins (Sec-dependent proteins) in supernatants, upon treating 3 staphylococcal cultures individually with 0, 10, and 40 µM of peptide A. The secreted hemolysins in the supernatants were assayed in 96 well plates with sheep erythrocytes. Upon the lysis of sheep erythrocytes, the absorbance was read at λ440 nm. Briefly, under aseptic conditions, sheep erythrocytes were washed 3× 10 ml PBS buffer and resuspended after centrifuging (3000× g for 5 min), the resulting red blood cells solution (2%RBC) was seeded into

a 96-well plate (U-bottom, Greiner). Each well in the RBC-plate contains 100 µl of RBC suspension. Separately, a 96-well preparative control- plate was prepared: each well of this plate was filled with 25 µl PBS buffer, and the first position of row A was filled with 100 µl of Triton-X 1% (positive control), and the first position of row E in this plate was filled with 100 µl of PBS buffer (negative control). The first positions in rows B, C, and D in this control plate were filled with 100 µl of supernatants of the suspensions that treated with (0, 10, and 40 µM) of peptide A, respectively. Serial dilutions (3:4) with PBS buffer were made in each row by transferring the content from each well to the next. For the hemolysis reaction, 20 µl of the content of each well in the control plate was pipetted onto their counterparts in the RBC plate. The RBC plate was incubated for 30 min at 37ºC on agitator in order to homogenize the wells content, allowing the erythrocytes to be lysed. The RBC plate was centrifuged for 5 min, and the lysates were pipetted from the RBC plate onto a reading plate. The lysates containing plate was measured at wavelength λ 440 nm by a light spectrophotometer.

3.2.11 Investigating the effect of peptide A on the supernatant and subcellular proteins

Two bacterial cultures were cultivated as described in 3.2.2.3. One culture was treated with 40µM of peptide A and the other was without peptide treatment. To quantify the proteins in different cellular compartments, a published fractionation protocol by Pieper *et al.*, 2006 was used with slight modification [102]. In summary, after 24h of *S. aureus* growth, supernatants were isolated through the 0.22 µm Millipore filters, taken in equal volumes (3 ml), frozen and lyophilized to be concentrated. Cell pellets were washed with PBS and centrifuged at 6000×g for 15 min at 20ºC. The cell pellets were resuspended at OD_{600} of 1.0 in buffer A. Bacterial cell walls were digested by incubating the cells at 37ºC in a buffer A containing the enzymes lysostaphin (100 mg/ ml), and mutanolysin (50 mg/ ml). Ten-microliter aliquots were removed prior to and following 1.5 h and 3 h incubation times to monitor the decrease in A_{600} indicative of cell wall degradation. The preparations were centrifuged at 6000×g for 20 min at 4 ºC to separate the cell wall digestion supernatants (CWDS) from the protoplasts. CWDS samples were collected to be applied to SDS-PAGE experiments. Samples were frozen at - 20ºC until further analysis. The intact protoplast pellets were resuspended in buffer B. Addition of the hypotonic buffer caused rapid protoplast lysis. Cell aggregates were homogenized by ultrasonifier for 30 seconds (5 ml, 0.01mm clearance, ten strokes). The lysates were chilled on ice and centrifuged at 100 000×g for 20 min at 4 ºC. The supernatants containing cytosolic proteins were centrifuged and isolated. The

membrane non-dissolved debris was suspended in buffer C and homogenized by the ultrasonifier to be analyzed by SDS-PAGE.

3.2.12 Subcellular localization of the effective peptides

Three bacterial cultures were prepared as described in 3.2.2.3. The cultures were individually supplemented with fluorescein-conjugated peptides, namely peptide -3, peptide I, and peptide J. The supernatants were isolated through the 0.22 µm Millipore filters, and the pellets were undergone subcellular fractionation as described in section 3.2.11. The distribution of the peptides in each fraction was determined by measuring the fluorescence intensity of each fraction using the Fusion fluorescence reader. The background disturbance of each buffer fraction was subtracted from the corresponding fluorescence value.

4 Results and discussion

Since the general bacterial secretory nano-machine, Sec, is indispensable for secreting most of the surface and extracellular virulence factors, a major interest in this pilot study was to establish a solid base for targeting this system. This focuses on the generation of novel compounds that have a high likelihood of inhibiting this system and thus reducing the secretion of pathogenicity factors. The strategy in this study includes three interdependent tactics: (1) Synthesizing cell penetrating peptides (CPPs) that potentially penetrate the staphylococcal cells and subsequently evaluating this potential. (2) Synthesizing the Sec-interfering peptides conjugated with the optimal CPP and their variants and consequently evaluating their effect on the secretome level, specifically Sec-dependent proteins, like V8 protease and α-hemolysin. (3) Having found one or more peptides showing inhibitory activity to characterize the underlying modes of action by which these peptides exert their activity. The first part of the results describes the selection and syntheses of the CPPs emphasizing their cellular uptake by *Staphylococcus aureus* using automatic fluorescence microscopy, confocal laser scanning microscopy and fluorescence activated cell scanning (FACS) analysis. The second part describes the syntheses of both the Sec-interfering peptides and their control peptides. The third part explains the attempted approaches for quantifying secreted proteases into the staphylococcal growth cultures (further on termed 'supernatant'). In this part, several results discuss the most effective peptide, and present an evidence for its capability in reducing the secretion of Sec-dependent proteins. The last part of the results discusses the possible mode of action of the Sec-interfering peptides through (1) quantifying the total proteins in the supernatant and three different subcellular fractions of *Staphylococcus aureus*, namely, the periplasm and cell wall; the cytosol; and the cytoplasmic membrane; and (2) quantifying the fluorescein-conjugated forms of these peptides in these subcellular compartments.

4.1 Design of the utilized peptide sequences

In this pilot study, the model of intervention with the Sec pathway utilizes peptidic inhibitors that mimic the signal peptide of a particular Sec–dependent protein (like V8 protease). Based on the described machinery and the significant role of the signal peptide in exporting proteins via the Sec system, these peptidic inhibitors are expected to bind competitively to at least one of three significant Sec members SRP, SecA, and/ or SpsB, in the same manner that the signal peptides of the exported native proteins do. Thus, the intervention with the secretion of the

Sec-dependent virulence protein can theoretically occur in the cytosol or in the cytoplasmic membrane in the co-translational phase. In order to facilitate their entry into the bacterial cells, these peptidic inhibitors can be synthesized with a transduction domain at their C-termini. These transduction sequences are known as cell-penetrating peptides (CPPs) and classically facilitate the cellular uptake of various molecular cargoes [74, 103] (see introduction, chapter II).

The purpose in linking the internalizing sequence to the C-terminus of the signal peptide is to keep the N-terminus of the peptidic inhibitor exposed for competitive binding to SRP or SecA in the cytoplasm, and/ or to the signal peptidase SPsB in the cytoplasmic membrane and thus affect the secretion of one or several Sec-dependent proteins (Figure 4.1).

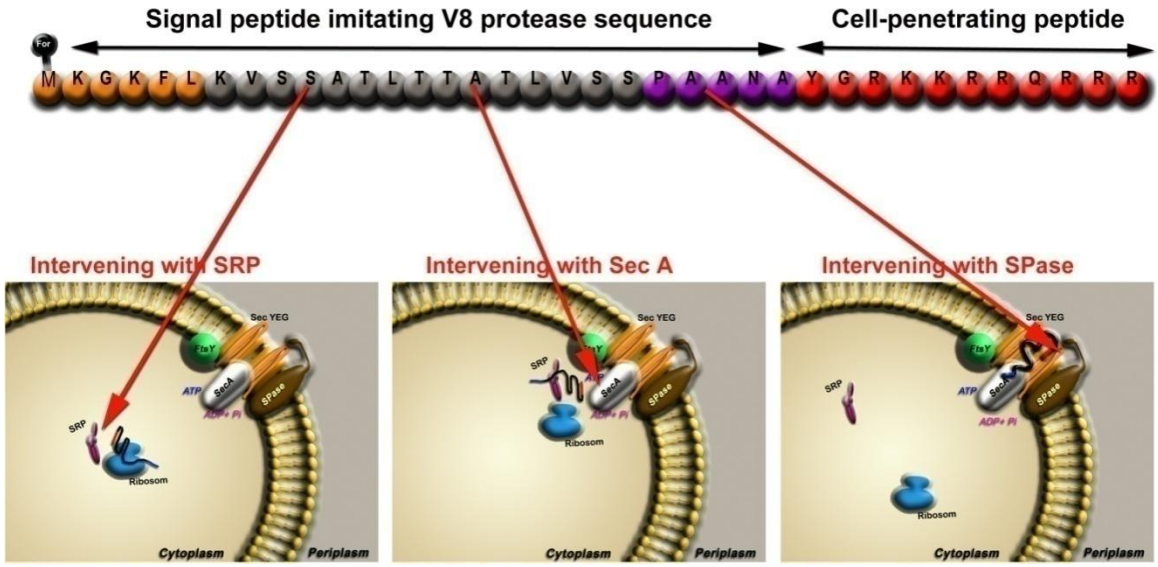

Figure 4.1 The hypothesized strategy of targeting the bacterial Sec-pathway.
A design was constructed to contain the V8-protease-secretion signal peptide conjugated with a CPP. Three positions in the cell are potential targets to be competitively attacked by the signal peptide imitative after internalization.

This template is a unique design to mimic the signal sequences at the post-translational modification that occur during or after ribosomal protein synthesis in prokaryotes. In prokaryotes, every protein translation is initiated with formylated methionine. During expression, the formyl group is cleaved by specific peptide-deformylases (PDF). The methionine of the majority of the translated proteins is then cleaved by specific methionine aminopeptidases (AMP) [104]. Since it is not known yet to which form the signal recognition particle SRP binds, these three variants of the peptide construct were proposed. In other words, mimicking the native signal peptide in the cytosol and cell membrane required synthesizing three forms of this signal peptide. This includes (a) signal peptide without methionine at its N-terminus; this mimics the final-cleaved form of the

prokaryotes native preprotein, (b) signal peptide with methionine that mimics the deformylated prokaryotic preproteins, and (c) signal peptide with formylated methionine, which mimics the initiated prokaryotes preprotein in the cytoplasm.

In this pilot study, 14 linear peptides were generated according to Fmoc chemistry. They vary in their lengths from 8 to 40 amino acid residues, and in their hydrophobic stretches. Each set of these peptides was assigned to play one of the following roles:

(1) A set of cargo delivery peptides that is able to penetrate the cellular membranes of *Staphylococcus aureus*. Rajarao, *et al.* published a group of cell penetrating peptides that showed variable efficiency in mediating the delivery of green fluorescent protein (GFP) into prokaryotes, including *Bacillus subtilis*, *Escherichia coli* and *Staphylococcus aureus* [87]. These peptides were fused to green fluorescent protein (GFP) in modified plasmids, expressed in *Escherichia coli*, partially purified and incubated with growing cells (Table 4.1).

Table 4.1 The cell penetrating peptides that showed successful delivery of GFP into prokaryotes.

Sequence	Charge	Naturally occurring proteins	Reference
VLTNENPFSDP	2-	Endocytosis signal in Saccharomyces cerevisiae	[87, 105]
RSNNPFRAR	3+	EH domain affinity	[87, 105]
YGRKKRRQRRR	8+	HIV-Tat protein	[74, 87]
YKKSNNPFSD	1+	EH domain affinity	[87, 105]
CFFKDEL	1-	Endoplasmic reticulum localization	[87, 105]

In our study, based on Rajarao's findings, three of these peptides were chosen and chemically synthesized with an added cysteine at their C-termini that was used for fluorescence labelling (Table 4.2).

Table 4.2 Chemically synthesized CPPs to investigate the uptake efficiency by *S aureus.*

Construct	Sequence (labeled with F5M)	Molar mass (Mw*)
Peptide-1	VLTNENPFSDPC(F5M)-amide	1760.6
Peptide-2	RSNNPFRARC(F5M)-amide	1645.6
Peptide-3	YGRKKRRQRRRC(F5M)-amide	2088.9

***Mw: is the monoisotopic mass calculated by Peptide companion software."F5M" stands for the labeling with fluorescein-5-maleimide.**

(2) A set of potentially Sec-interfering peptides (peptides A to C), with a subset of five variants (peptides D to H) that were designed as control (Table 4.3).

All peptides that are listed in table 4.3 were synthesized in amide form at their C-termini to avoid introducing a charge where there is none in the native sequence, and to minimize the influence of any added molecule to the peptide N and C-termini on the folding of the peptides.

Table 4.3 Chemically synthesized peptides to serve as Sec-interfering peptides and control peptides.

Construct	Sequence	Mw *
Peptide A	KGKFLKVSSLFVATLTTATLVSSPAANAYGRKKRRQRRR-NH_2	4361.5
Peptide B	**M**KGKFLKVSSLFVATLTTATLVSSPAANAYGRKKRRQRRR-NH_2	4492.6
Peptide C	**formyl-M**KGKFLKVSSLFVATLTTATLVSSPAANAYGRKKRRQRRR-NH_2	4520.6
Peptide D	YGRKKRRQRRRC-NH_2 (CPP)	1659.9
Peptide E	KGKFLKVSSLFVATLTTATLVSSPAANA-NH_2 (Signal sequence)	2820.6
Peptide F	**M**KGKFLKVSSLFVATLTTATLVSSPAANA-NH_2 (Signal sequence)	2951.7
Peptide G	**formyl-M**KGKFLKVSSLFVATLTTATLVSSPAANA-NH_2 (Signal sequence)	2979.6
Peptide H	AAMGNSFVLSTLTKTKPAFLTLVASASVKYGRKKQRRR-NH_2 (Scrambled)	4492.6

***Mw: is the monoisotopic mass calculated by Peptide companion software.**

(3) A set of fluorescein-conjugated peptides (peptide I and peptide J). Both peptides end with a cysteine residue at their C-termini (Table 4.4). The two peptides were chemically generated in order to investigate their localization in the staphylococcal subcellular compartments.

Table 4.4 Chemically synthesized peptides that serve as reporter peptides.

Construct	Sequence	Mw*
Peptide I	**M**KGKFLKVSSLFVATLTTATLVSSPAANAYGRKKRRQRRRC(F5M)-NH_2	5021.6
Peptide J	**formyl-M**KGKFLKVSSLFVATLTTATLVSSPAANAYGRKKRRQRRRC(F5M)-NH_2	5049.6

***Mw: is the monoisotopic mass calculated by Peptide companion software. 'F5M' stands for the labeling with fluorescein 5-maleimide.**

(4) A fluorogenic substrate (peptide K), ABz-AFAFEVFY(NO_2)D-OH (Mw: 1272.1). This peptide was used as specific substrate to monitor the secretion of the Sec-dependent protein (V8 protease), and consequently assess the potentiality of the peptides in affecting the Sec system of *Staphylococcus aureus*. According to Singh, *et al.* the serine V8 protease has a specific substrate consisting of nine amino acids [99]. This peptide has a nitrotyrosine as a fluorophore, and 4- aminobenzoic acid (ABz) as a quencher at the N-terminus. Upon specific cleavage at the alpha-carboxyl of glutamic acid, the distance between the fluorophore and the quencher increases, resulting in the amplification of the fluorescence intensity.

4.2 Fmoc synthesis of the cell penetrating peptides

Rajarao, *et al.*, illustrated the efficiency of several peptides in delivering GFP into bacteria and yeasts [103, 106]. Based on this result, we chemically generated three CPPs (Table 4.5). In order to investigate their uptake by the staphylococcal cells, the peptides were generated with a cysteine residue at their C-termini. The free sulfhydryl group of the cysteine residue was conjugated with fluorescein-5 maleimide (F5M). The fluorescent-peptides were purified, and utilized to assess their uptake by *S. aureus* using appropriate fluorescence techniques

Table 4.5 CPPs synthesized according to Fmoc chemistry with their yields.

Peptide	Non-labeled sequence	*Mw	Theoretical weight+ (mg)	Practical weight	Yield after purification
Peptide-1	VLTNENPFSDPC-NH_2	1332.6	167.5	30	17.9%
Peptide-2	RSNNPFRARC-NH_2	1217.6	190.2	35	18.4%
Peptide-3	YGRKKRRQRRRC-NH_2	1660.9	280.1	48	17.1%

***Mw is the monoisotopic mass of calculated by Peptide companion software. + based on the TFA salts that were obtained.**

The Fmoc chemistry showed a feasible approach to synthesize these CPPs. Dimeric forms of the desired peptides were generated as byproducts, particularly associated with the cysteine-containing peptides that might form disulphide bonds. Therefore, purification was necessary to produce peptides that were appropriate for the bioassays. The eluted peaks from the analytical and preparative HPLC of both crude and purified products, respectively, showed the expected masses of the synthesized peptides according to MALDI TOF MS. (Figure 4.2)[3].

[3] The chromatograms and MALDI determinations of peptide-3 are shown in this chapter, while that of peptide-1 and peptide-2 can be seen in appendix-I of this dissertation.

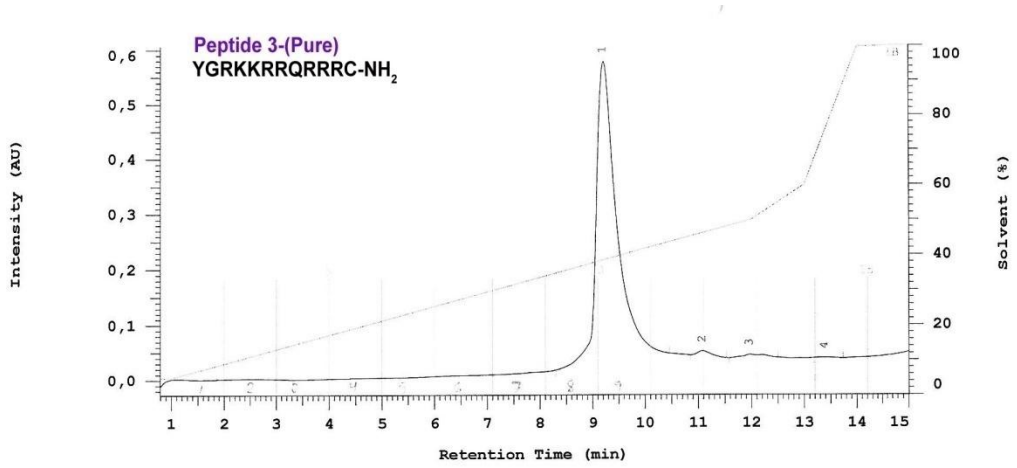

Figure 4.2 HPLC chromatogram of the purified Tat-derivative peptide before labeling with the fluorescein-5-maleimide (F5M).

The purified forms of the cell penetrating peptides were chemically coupled to fluorescein-5-maleimide according to the procedure in 3.2.1.3. Mass determinations of the crude peptides showed a minor peak of double labeling with the fluorescence groups due to the addition of the fluorescein-5-maleimide to the cysteine and probably to the amine of lysine residues or the free N-terminus. The analytical HPLC showed a shifting of the retention time in the main peaks that is due to the acquired hydrophobic properties to the molecule upon coupling the fluorescein. The mono-labeled peptides were purified by preparative HPLC with a reversed phase column RP-18. See figures 4.3 and 4.4.

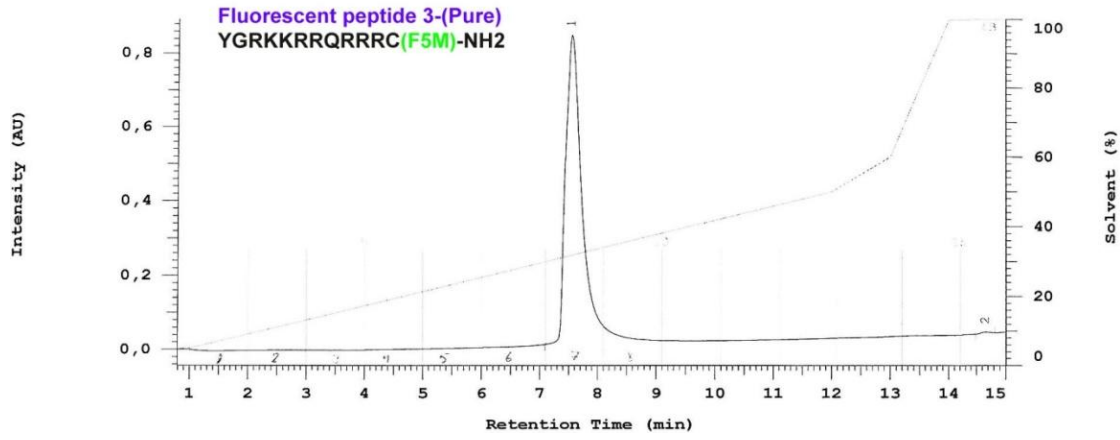

Figure 4.3 HPLC chromatogram of the purified Tat-derivative peptide after labeling with the fluorescein-5-maleimide (F5M).

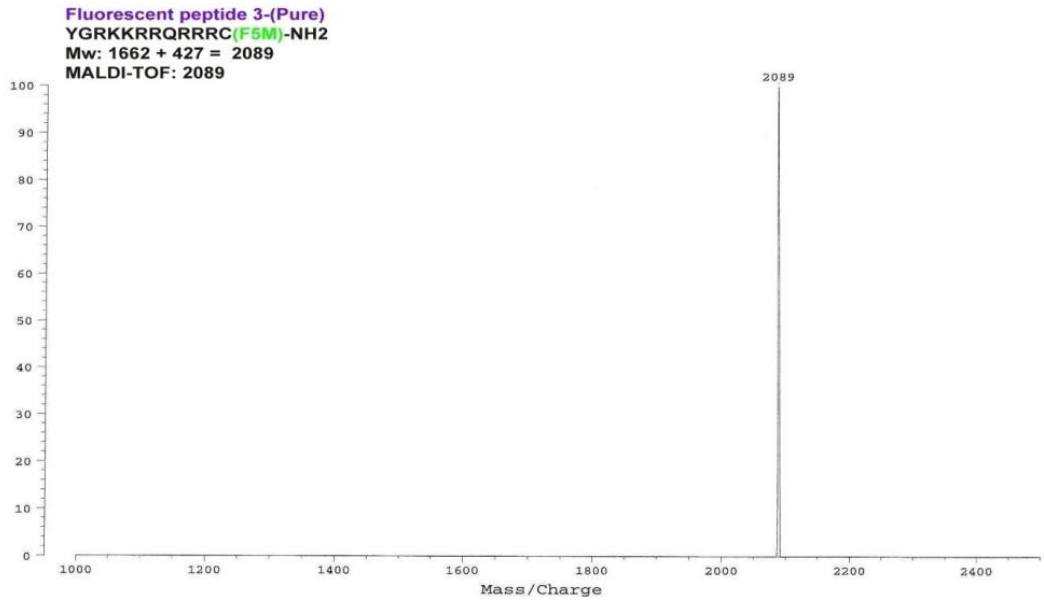

Figure 4.4 MALDI-TOF mass spectrum of the purified Tat-derivative peptide after labeling with fluorescein-5-maleimide (F5M).

4.3 Investigation of the uptake of the fluorescein-conjugated CPPs by *Staphylococcus aureus V8 strain*

Following the encouraging results obtained for peptide-mediated delivery into yeasts and bacteria from Rajarao, our study was extended to assess the uptake of fluorescein-conjugated CPPs by *S. aureus*. Peptides have been used to carry cargo molecules into bacteria previously, as described in the technical approach chapter, however we do not know about attempts to use the peptides described here for bacterial applications, and only few data are known about delivering proteins into bacteria using carrier peptides. Therefore, we synthesized here these peptides chemically, and conjugated them with fluorescein-5 maleimide to investigate the potentiality of CPP uptake by *S. aureus*, and to facilitate later the uptake of the Sec-interfering peptides.

In this approach, freshly grown *S. aureus* cells were prepared at 1.0 OD. Three cell suspensions were individually incubated with three fluorescein-conjugated peptides at 30 ˚C for 1 h in PBS buffer. Following incubation, cells were rinsed and examined for fluorescein distribution using confocal laser microscopy. The fluorescence average intensity was quantified for each peptide using automated fluorescence microscopy (Figure 4.5).

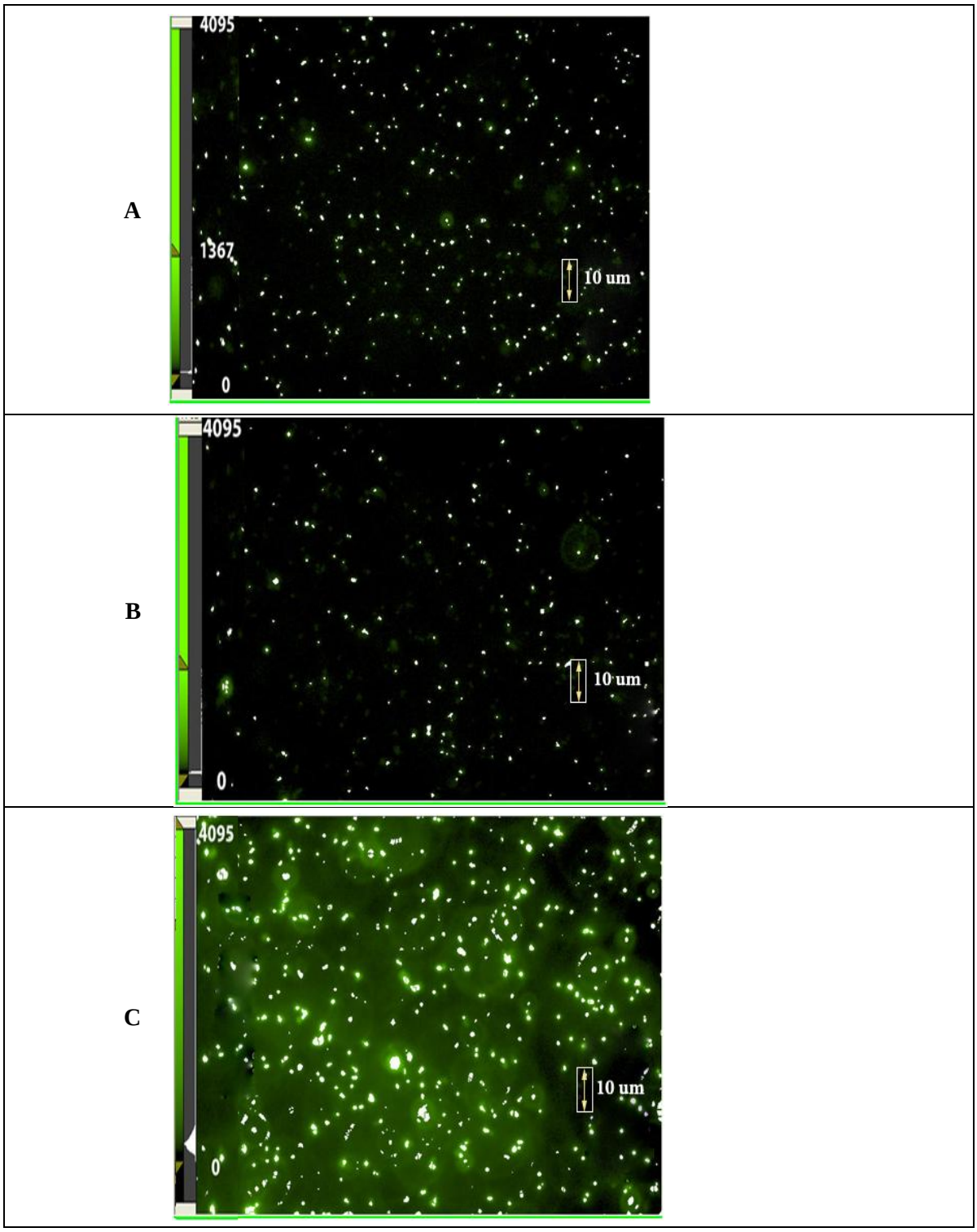

Figure 4.5 Fluorescence microscopy analyses of *Staphylococcus aureus* suspensions at 0.5 OD600. Bacterial cell dilutions with phosphate buffer saline (1:10) were incubated at 37°C for 1 hour with 100 µM (A) peptide-1, (B) peptide-2 and (C) peptide-3. Fluorescence intensity of the cells is represented as white pits.

In addition, the uptake efficiency of the fluorescein-conjugated CPPs by *S. aureus* was evaluated using FACS analysis (Figure 4.7).

A	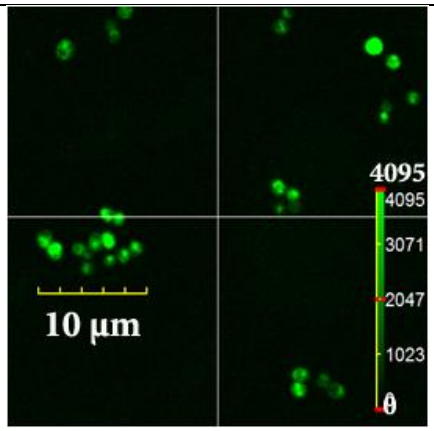	Fluorescent peptide-3
B	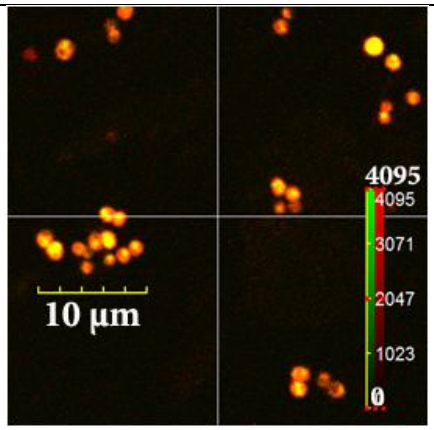	Fluorescent peptide-3 + Rhodamine B hexyl ester
C	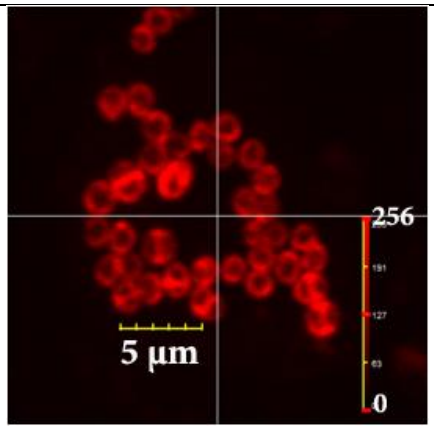	Rhodamine B hexyl ester

Figure 4.6 Confocal laser microscopy revealed the 3D distribution of peptide-3 at a specific z-value.
(A) Fluorescent peptide-3 in the core of *Staphylococcus aureus* (green filter). (B) The bacteria after incubation with the fluorescent peptide-3 and rhodamine B hexylester (shown in green and red, respectively). (C) The bacteria were incubated only with rhodamine B hexylester (red). Confocal microscopy was performed and z-series measurements were acquired with 70-nm increments. Three-dimensional (3D) projections were created from stacks using OLYMPUS FV1000 Viewer software.

The results show the highest average intensity of fluorescence when incubating the bacterial cells with the internalizing peptide-3 (HIV-1 Tat transduction domain), as shown in Figure 4.5. [4]

A verification of the peptide-3 uptake into *Staphylococcus aureus* was performed by confocal laser microscopy (Figure 4.6). Rhodamine B hexyl ester (RBHE), which is known to interact with the bacterial membrane but does not internalize [107, 108] was used as a control to stain the cell membrane of the staphylococci. The 3D imaging, at specific z level, shows the distribution of the fluorescein-conjugated peptide concentrated in the core of the *Staphylococcus aureus* cells (green), where Rhodamine B, the lipophilic dye, is distributed on the cell surface, visualized as a ring in some views of the 3-D scan (red)[5].

Fluorescence activated cell scanning (FACS) was used as an alternative technique for quantifying the cellular uptake of the cell penetrating peptides. Data analysis confirmed the optimal cellular uptake of peptide-3 (YGRKKRRQRRRC(fluor)-NH_2). Figure 4.7 shows an appropriate quantification of population's count resulting from three different cultures. These cultures were first adjusted to OD_{600} = 0.250 before adding the peptides and were supplemented with propidium iodide (PI) and with 100 µM of fluorescent peptides-1, -2, and -3, respectively. For performing this quantification, SYBR green was used in a separate culture of the same conditions to stain the total bacterial cells (positive control). The counted population of this culture represents the total cell count of the live and dead cells. The FACS analysis of the gated area shows the population's count of the corresponding dye. The highest count was observed in bacterial culture that contains peptide-3. The gated area in column B shows a clustering of the enhanced fluorescence which might result from aggregated counted cells when adding the peptide, this clustering might indicate a change of the cell morphology. The clustering is most strong in the presence of peptide-3, which has the highest positive charge +9 of the three peptides, whereas peptides 1 and 2 have the charges -1 and + 4, respectively. The aggregation of the cells may be due to an interaction of the cationic peptides with the anionic charges of the membrane. (For more details, see appendix -IV).

[4] For more images from the confocal laser microscopy, about cellular uptake of peptide-3 see appendix-IV

[5] More images of the confocal laser microscopy that show the cellular uptake of peptide-3 (YGRKKRRQRRRC(F5M)-NH_2) can be seen in appendix-IV of this dissertation.

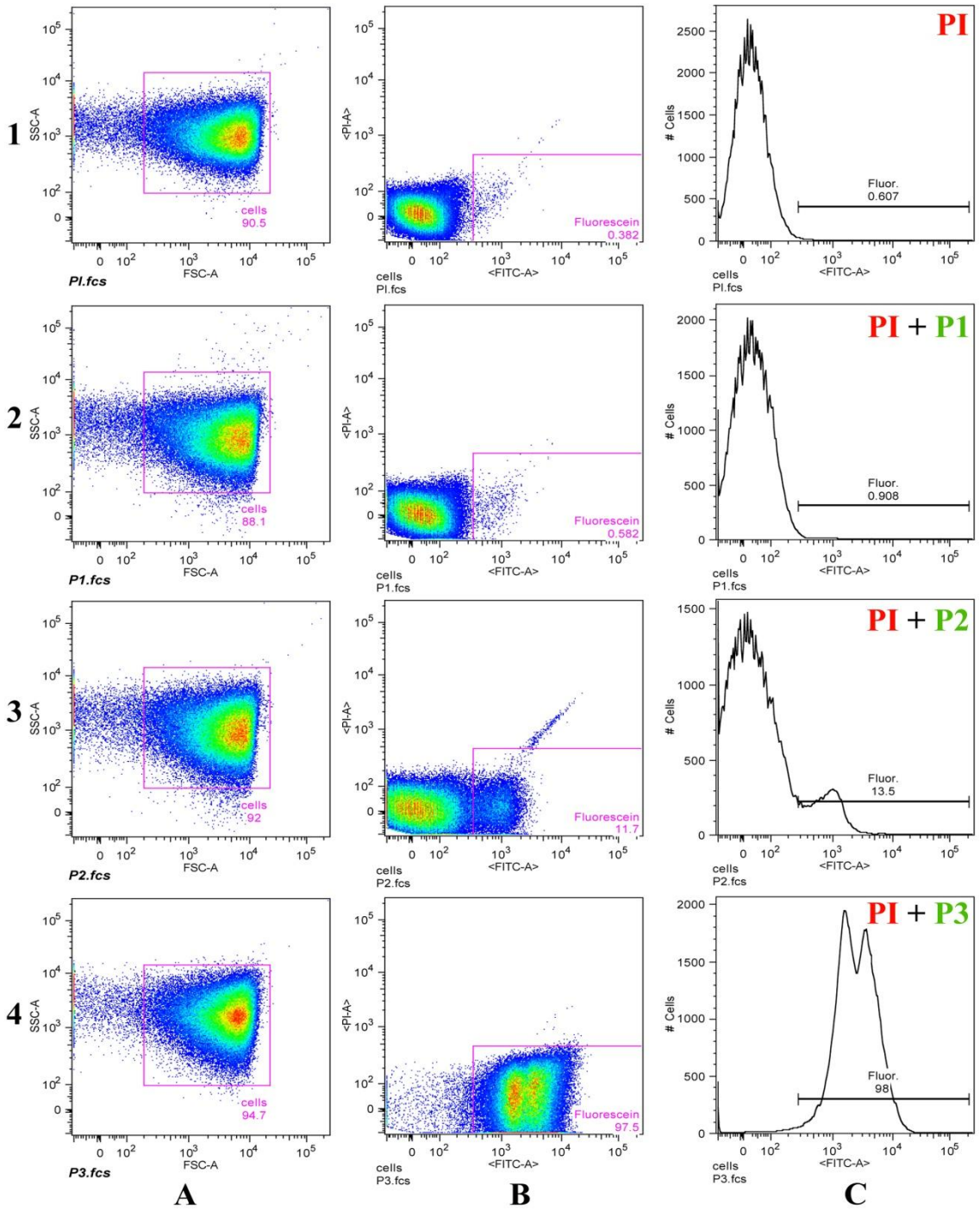

Figure 4.7 Fluorescence activated cell scanning after incubating the bacteria with fluorescein-conjugated peptides (P_i) and propidium iodide (PI).
Column A: sideward fluorescence scattering (SSC) *vs*, forward scattering (FSC). Column B: gated populations from the labeled cell *vs*, dead cells. Column C: visual peak of the population for the counted cells in the gated area. The rows 1, 2, 3, and 4 represent the cells that were incubated with PI, PI+peptide-1, PI+peptide-2, and PI+peptide-3, respectively. All dot plots were produced by FlowJo software.

The fluorescence microscopy analysis of the bacterial populations, which were incubated with the fluorescein-conjugated CPPs, showed an average fluorescence-intensity that is proportional to the bacterial cell count resulted from FACS analyzer. From these data, the efficiency of the bacterial uptake to these three fluorescein-conjugated CPPs can be evaluated (Figure 4.8).

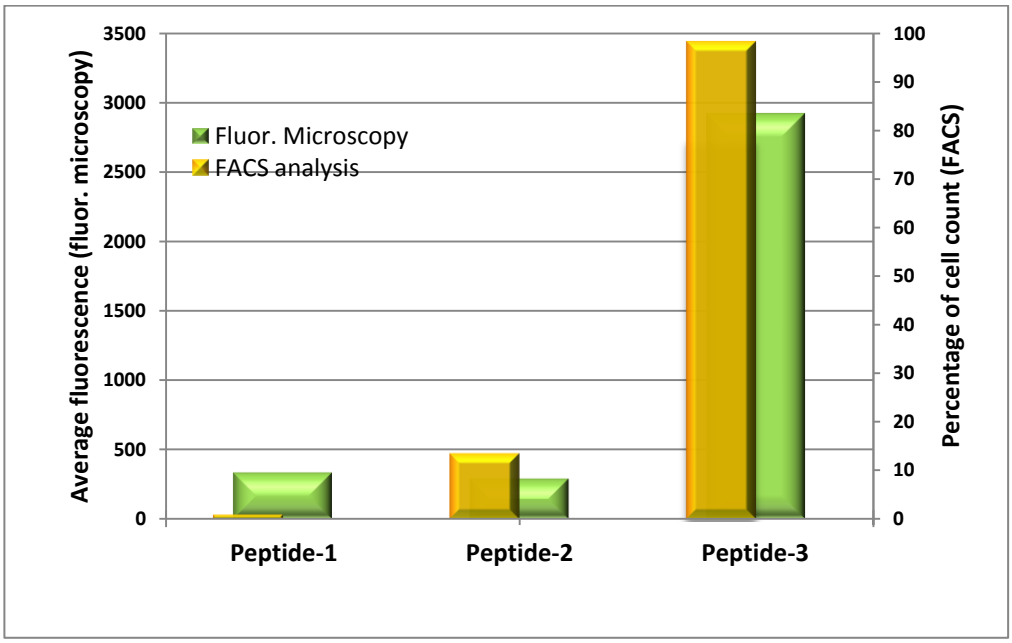

Figure 4.8 The efficiency of the bacterial uptake to the fluorescein-conjugated CPPs.
The diagram shows the efficiency of the staphylococcal uptake to the CPPs, quantified by FACS (yellow bars) and the average fluorescence intensity, quantified by the fluorescence microscope (green bars). Data were obtained from staphylococcal suspensions at OD 0.250. The three fluorescein-conjugated CPPs were incubated with *S. aureus* at a concentration of 100 µM for 2 hours, the quantification was done for the 3× washed bacterial cultures.

In Rajarao's publication, the three investigated CPPs have already shown successful delivery of the green fluorescent protein GFP into prokaryotes and yeasts [87]. Furthermore, the three peptides had shown efficient internalization into *S.aureus*, and the peptide VLTNENPFSDP has shown an efficient deliverey of GFP into *Candida albicans* and *Staphylococcus aureus*, while YKKSNNPFSD has been most efficient for *Bacillus subtilis* and CFFKDEL for *Escherichia coli*. In the present study, data analysis from the automatic fluorescence microscope and FACS revealed the successful uptake of these three fluorescein-conjugated peptides with the highest uptake of peptide-3 (YGRKKRRQRRRC(F5M)-NH_2) by *Staphylococcus aureus*. This observation gives further evidence of the influence of the delivered cargo on the internalization process, and is in excellent agreement with the other cell-based assays performed in studies that

utilized peptide-3 with other cellular species [74]. The higher uptake of this peptide compared to the other two CPPs can be due to the unique arginine-rich primary structure of peptide-3, which promote the cationic properties in initiating the penetration of the anionic cell walls and membrane components. Furthermore, peptide-3 mimics the transduction domain of the HIV-1 transcriptional activator protein (Tat) with a similarity of 8 basic amino acids RKKRRQRRR. This unique structure was already used for a successful entry of different cargoes, ranging from small particles to proteins, peptides, and nucleic acids [74, 79, 109]. The mode of action of this and other CPPs is still discussed and investigated, but data from different researches argue for an energy-dependent process of entry [80, 103]. Therefore, the incubation of the labeled penetrating peptides with the staphylococcal cells was conducted at 37˚C. The addition of agents that are known to inhibit energy-dependent uptake pathways like omeprazole which inhibits the ATPase, or adding endocytosis inhibitors like wortmannin, cytochalasin, colchinine, nocodazole, taxol, brefeldin A, and chloroquine [110] was not investigated. Since the scope of these experiments was concentrated on finding a specific tool for delivering the Sec-interfering peptides the mode of action of the delivery peptides was not addressed. Based on the published data about the entry of the HIV-1 Tat conjugated proteins, this transduction domain was synthetically coupled to the C-terminus of the secretion signal sequence of the V8 protease, conveying the cell penetrating properties to the Sec-interfering peptides. As a summary, incubating the three fluorescein-conjugated peptides individually with the staphylococcal cells for 2 hours indicated the entry of all three of these peptides into the cells. Measuring the fluorescence properties by fluorescence microscopy and FACS analysis showed best results with uptake of the HIV-1 Tat mimetic, peptide-3.

4.4 Fmoc syntheses of the potentially Sec-interfering peptides and their control peptides

The Sec-dependent protein, *V8 protease* is a significant target in this study because there are several known pathogenic aspects associated with its secretion throughout the transition phase of the infection process. It plays a key role in moderating the adhesion to fibronectin by degrading cell surface fibronectin-binding proteins**,** and it regulates pathogenesis in controlling the microbial adhesion to the host cells [16, 96]. Moreover, V8 protease plays a key role in eluding phagocytosis by eliminating protein A, which is recognized by immunoglobulins (IgG) of the host [16, 111]. Furthermore, V8 protease is also participating indirectly in the pathogenicity, by

activating other bacterial cysteine proteases like SspB and Scp that are needed in cell homeostasis and the destruction of foreign or target cell proteins, thereby promoting bacterial invasion [12]. V8 protease also degrades neutrophil defensins, IgG and α-1-antichymotrypsin [112], in addition to its role in altering the α_1-proteinase inhibitor that keeps neutrophil elastase balance in blood [113, 114]. In *S. aureus* culture supernatants, the pore-forming α-toxin is cleaved also by the coexpressed V8 protease and aureolysin [17, 115]. Figure 4.9 illustrates the cascade role of the staphylococcal proteases.

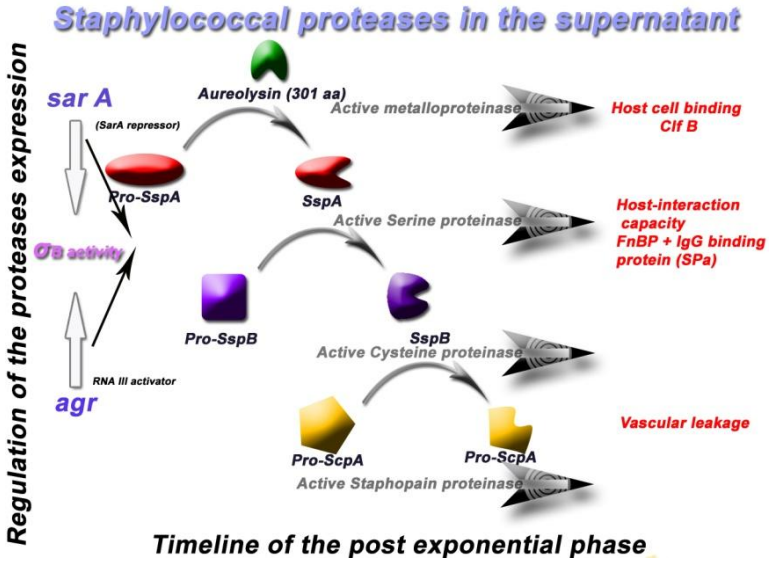

Figure 4.9 Role of protease expression in staphylococcal pathogenicity.
The four types of proteases that are found in V8 strain contribute directly and indirectly in the pathogenicity. The figure was established based on published results [12, 19, 97].

Another important reason for choosing this enzyme was the expectation to develop an easy peptide based assay, which facilitates evaluating the outcome of the secretion when treating *S. aureus* with the Sec-interfering peptides. The staphylococcal serine protease, V8 protease, is well known with its action to specifically cleave peptide bonds at the carboxyl group of the acidic amino acid residues aspartic acid and glutamine acid. Therefore, fluorogenic substrates were procured and generated to evaluate the secretion of V8 protease at specific conditions.

In this pilot study, the secretion signal sequence of the staphylococcal glutamyl endoproteinase (V8 protease) was chemically synthesized to play the inhibitor role for the Sec-system. It consists of the 29 amino acid sequence MKGKFLKVSSLFVATLTTATLVSSPAANA [111, 116]. Since the interference with the Sec-system is expected to be co-translational in *S. aureus*, the Sec-interfering peptides should principally contain two domains, the C-terminal

domain (11 amino acids of peptide-3, based on the previous results) for transport into the cell, and the N-terminal domain: the secretion signal peptide of V8 protease (29 amino acid stretch). Since we do not know which, if any, form of the V8 protease-secretion signal peptide can optimally perform interference, three forms of the V8 protease signal peptide were generated. (Table 4.3, peptides A, B, and C):

1. The formylated methionine form: this is a common preprotein form, which is found in the prokaryotic cytosol, and is observed upon the emergence of the preprotein from the ribosome (peptide C).
2. The methionine form: normally found in the cytoplasm in prokaryotes after they are processed by the peptide deformylase (PDF) (peptide B).
3. The final cleaved form (without methionine): commonly exists in prokaryotes after the signal peptides processed by the PDF and the amino-methionine peptidase AMP for protein maturation (peptide A).

Another subset of peptides was synthesized as controls. They consist of the transduction domain (peptide D), the V8 protease secretion signal peptide (three forms, peptides E, F and G), and in addition a scrambled sequence of the V8 secretion signal sequence with the transduction sequence (peptide H). Table 4.6 shows the molecular mass of the peptides and their determined MALDI masses of the obtained peaks. The purpose of probing these control peptides is to study the effect of the structure activity relationship (SAR) of any of these peptides upon the inhibition of secretion.

Table 4.6 List of the Sec-interfering peptides and the control peptides with their molecular masses.

Construct	Sequence	Monoisotopic mass [M]	MALDI mass $[M+H]^+$
Peptide A	KGKFLKVSSLFVATLTTATLVSSPAANA-YGRKKRRQRRR-NH_2	4362.5	4362
Peptide B	MKGKFLKVSSLFVATLTTATLVSSPAANA-YGRKKRRQRRR-NH_2	4492.6	4493
Peptide C	For-KGKFLKVSSLFVATLTTATLVSSPAANA-YGRKKRRQRRR-NH_2	4520.6	4521
Peptide D	YGRKKRRQRRRC-NH_2	1659.9	1662
Peptide E	KGKFLKVSSLFVATLTTATLVSSPAANA-NH_2	2820.6	2821
Peptide F	MKGKFLKVSSLFVATLTTATLVSSPAANA-NH_2	2951.7	2951
Peptide G	For-KGKFLKVSSLFVATLTTATLVSSPAANA-NH_2	2979.6	2980
Peptide H	AAMGNSFVLSTLTKTKPAFLTLVASASVK-YGRKKRRQRRR-NH_2	4492.6	4494

Fmoc syntheses of the Sec-interfering and control peptides were successful. Figures 4.10 and 4.11 represent the obtained data from the synthesis and analysis of peptide A, namely the analytical HPLC chromatogram for the purified peptide; and the mass determination spectrum for the pure peptide, respectively.[6]

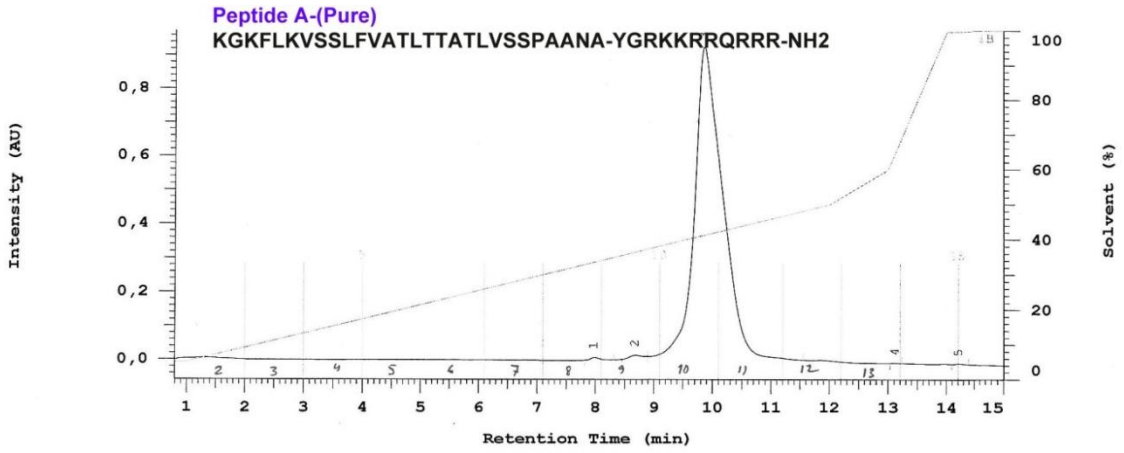

Figure 4.10 HPLC chromatogram of the purified peptide A shows a single peak.

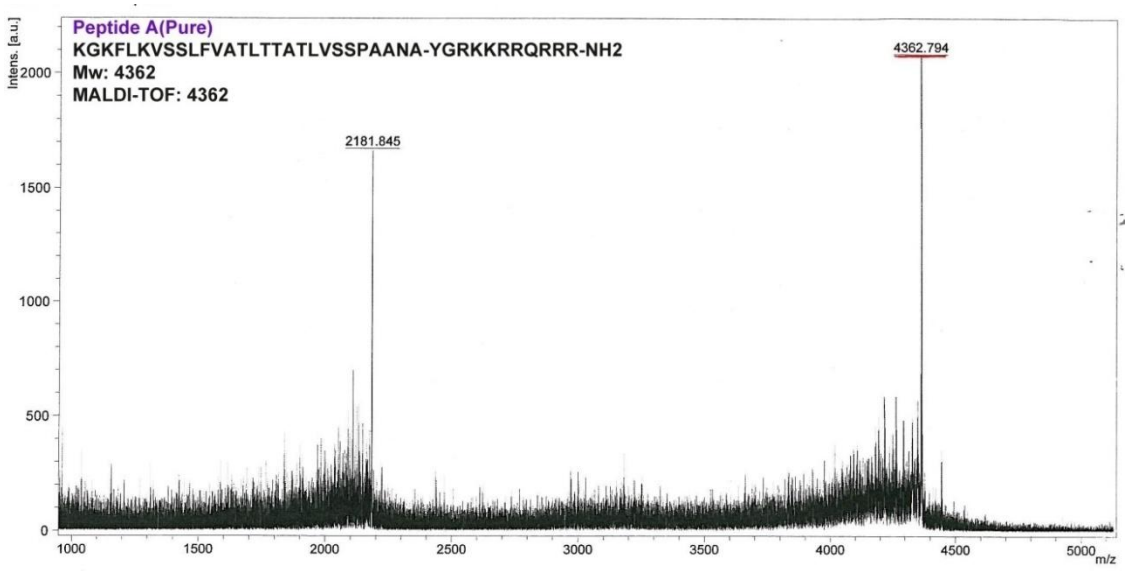

Figure 4.11 MALDI-TOF mass spectrum shows a corresponding mass of the purified peptide A. A double charged mass detection $[M+2H]^{2+}$ appears at m/z 2181.84.

[6] The analytical data (chromatograms and mass spectra) of all synthesized peptides can be seen in the appendix II and III.

The solid phase syntheses of all peptides according to Fmoc chemistry were feasible by employing the automated Pioneer synthesizer, but with low yields of the purified products ranging between 3-10%. These results could be due to the aggregation of the hydrophobic residues along the peptide chains, which plays a motive force for peptide folding, resulting in difficulties by HPLC purification, especially for peptide E, peptide F and peptide G, where the preparative HPLC was not efficient enough for separating these highly hydrophobic folded structures. Nevertheless, several batches were prepared after the consumption of the peptide in the biochemical assay. Sometimes, the quality of the newly synthesized peptide was not high, like peptide C that showed deviated results in the second batch (Table 4.7). Therefore, optimizations of the Fmoc-solid phase syntheses was necessary, this was achieved by doubly coupling the amino acids where the hydrophobic aggregates are increased, especially for all peptides that contain the secretion signal sequence of V8 protease. The double coupling of the amino acids starts mainly after coupling the 6th amino acid where the adjacent hydrophobic residues are found. Synthesis optimization strategies were based on predictions of difficult couplings from the analysis of the sequences by the software program Peptide Companion.

Table 4.7: List of the synthesized Sec-interfering peptides and the control peptides with their yields.

Construct	Sequence	Theoretical wt+ TFA*	Practical wt	Yield after purification %
Peptide A	KGKFLKVSSLFVATLTTATLVSSPAANA-YGRKKRRQRRR-NH_2	584.5 mg	68 mg	11.6
Peptide B	MKGKFLKVSSLFVATLTTATLVSSPAANA-YGRKKRRQRRR-NH_2	597.6 mg	55 mg	9.2
Peptide C	For-M KGKFLKVSSLFVATLTTATLVSSPAANA-YGRKKRRQRRR-NH_2	589.1 mg	24 mg	4.1
Peptide D	YGRKKRRQRRRC-NH_2	280.1 mg	48 mg	17.1
Peptide E	KGKFLKVSSLFVATLTTATLVSSPAANA-NH_2	339.1 mg	19 mg	5.6
Peptide F	MKGKFLKVSSLFVATLTTATLVSSPAANA-NH_2	352.1 mg	15 mg	4.3
Peptide G	For-MKGKFLKVSSLFVATLTTATLVSSPAANA-NH_2	343.6 mg	16 mg	4.7
Peptide H	AAMGNSFVLSTLTKTKPAFLTLVASASVK-YGRKKRRQRRR-NH_2	597.5 mg	23 mg	3.9

* At each free N-terminus and at every arginine, histidine, and lysine residues, peptide has a trifluoroacetic acid (TFA) as a counter ion of a mass 114 g/mol. These were considered in the theoretical weights.

4.5 Identifying the optimal medium for inducing *S. aureus* protease activity on milk agar plates

It is reported that *S. aureus* secretes four types of proteases; they are namely, serine proteases, cysteine proteases, metalloproteinases, and papain proteases [10, 12]. A milk agar assay was assigned to evaluate the total secreted proteases: The action of supernatant proteases on milk casein substrate, has been generally used to quantify the proteolytic activity of the secreted proteases of *S. aureus* [89, 117]. When 10 µl of supernatants of the cultured bacteria were applied on 3 mm sterile discs, proteolysis took place on the agar plate, resulting a white precipitation surrounded by a transparent zone (halo). This zone is generated by the action of extracellular proteases, which degrade insoluble casein of the medium into soluble peptides and insoluble substances that precipitate around the disc. The extent of proteolysis exhibited by the supernatants is represented by the type and size of the transparent zone, whereas the white zone of precipitation represents the first stage of casein breakdown that mainly consists of insoluble para-κ-casein around the disc [89, 118, 119].

S. aureus V8 strain was cultivated in five different media, BHI, BM, LB, T, and TSB respectively. The supernatants were collected 24 h after starting the culture, and were investigated on 2% milk agar plates. The investigated supernatant that was isolated from bacterial culture in BM medium showed the largest proteolytic zone (Figure 4.12).

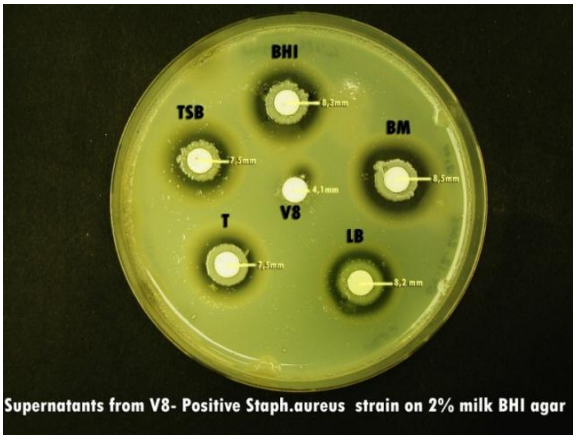

Figure 4.12 Proteolytic activities on milk agar plates (milk was used as substrate for the staphylococcal proteases).
The isolated supernatants after 24 h of culturing *S. aureus* (V8 strain) in 5 different media were assayed on 2% milk-agar plates to investigate the optimal conditions for secreting the proteases.

This finding agrees with the finding of Coleman *et.al.*, who found that glucose was essential for expressing the proteins in V8 strain, whereas a high concentration of glucose (> 1%) suppressed

the production of extracellular proteins [117]. Based on this result, BM medium with less than 1% glucose, was used as optimal medium for producing the proteases in the culture media. In addition to the milk agar plates, casein agar plates were utilized. However, the results with milk plates had better resolution than the casein plates. Furthermore, in all cases the proteolytic zones showed white precipitation, which was due to the cleavage of casein into insoluble κ-casein [89, 118, 119].

On the same milk agar plate, applying 10 µl of V8 protease up to a concentration of 100 µg/ml did not show any proteolytic zone (figure 4.12 the disc in the middle). This might be due to an insufficient concentration of this protease, or the protein contents in milk are not cleaved by the V8 protease. Consequently, this method cannot be used for quantifying the secreted V8 protease at this concentration. However, this assay can be utilized as a semi-quantitative determination of the optimal medium for expressing the total staphylococcal proteases that are secreted into the supernatant.

4.6 Testing growth and viability of the staphylococcal cells

Two assays were performed to check the viability of the cells 24 h after treating the bacterial suspensions with 10 µM of the peptides, (1) colony forming unit (CFU) assay, and (2) water soluble tetrazolium (WST) assay.

S. aureus, V8 strain, suspensions were treated with 10 µM of peptides A to H in individual culture tubes. One bacterial culture tube was left without peptide treatment as a control and another tube was treated with 0.05 µg/ml of V8 protease. The homogenized 24 h-cell suspensions were serially diluted with PBS (up to $1:10^9$). 100 µl of the resulted suspensions were plated on BHI agar plates, and incubated overnight at 37ºC to count the colony forming units (CFU/ml) that resulted from the viable cells. Comparing the colonies count of the peptide-treated cells with the one of the non-treated cells presents an evaluation for the effect of the peptides on bacterial viability.

In the water-soluble tetrazolium assay (WST), the metabolic activity of the living cells can be spectroscopically measured using a test wavelength of 460 nm and a reference wavelength of 620 nm. Incubating the bacterial suspensions with WST-8 will cause the bioreduction of 2-(2-methoxy-4-nitrophenyl)-3-(4-nitrophenyl)-5-(2,4-disulfophenyl)-2H-tetrazolium by cellular dehydrogenases to an orange formazan product that is soluble in the cell culture medium

(Appendix VII). The amount of formazan produced is directly proportional to the number of living cells [120]. Data from the WST assay were similar to that from the CFU-count assay. In addition to that, the CFU test showed stable values even when treating the bacterial cultures with 40 µM of the peptides. Up to this concentration, no toxic effect was observed on bacterial viability. On the other hand, the lowest growth and CFU values were observed when treating the staphylococcal cells at the early growth phase with 0.05 µg/ml of the commercially available V8 protease (Figures 4.13 and 4.14).

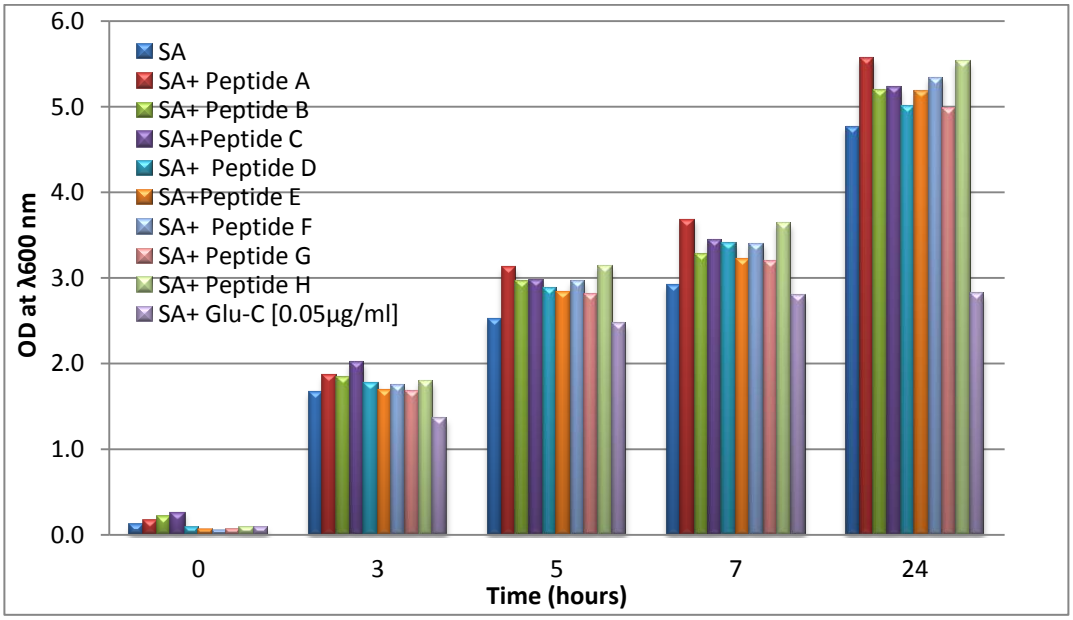

Figure 4.13 The effect of peptides A to H and external V8 protease on bacterial growth at different time points. Cell suspensions were treated with 10 µM of peptides A to H. One cell suspension was left without peptide treatment, and an extra suspension was treated with 0.05 µg/ ml of V8 protease (Glu-C Endoproteinase).

This observation is in excellent agreement with McGavin's results that showed a sensitivity of the staphylococcal fibronectin binding proteins (FnbP) and a limited number of other high-molecular-weight cell surface proteins to V8 protease [16, 96, 121]. Published data showed that both adhesive phenotype and cell surface protein profile of *S. aureus* could be modified by V8 protease activity [16] [7]. Our result suggests that the early addition of the activated V8-protease to

[7] V8 protease and other proteins are reported to be secreted and activated in the late exponential phase of growth. In this study, supernatants of bacterial suspensions were isolated at different time points of growth, then profiled by SDS-PAGE. An evidence introduced in this study (appendix-II) indicates that some proteins are expressed after 12 hours of growth, which corresponds to the late exponential phase.

the bacterial culture affects the adhesins and binding of bacteria to each other and to the environmental biomaterials [16]. The specific action of the V8 protease on the glutamyl and aspartyl residues at their Cα-carboxyl probably disturbs the adhesion of the bacterial cells to each other, which consequently affects the bacterial density in the culture medium. In addition, the result shown in Figure 4.14 suggests another mechanism for V8 protease: it seems to suppress growth.

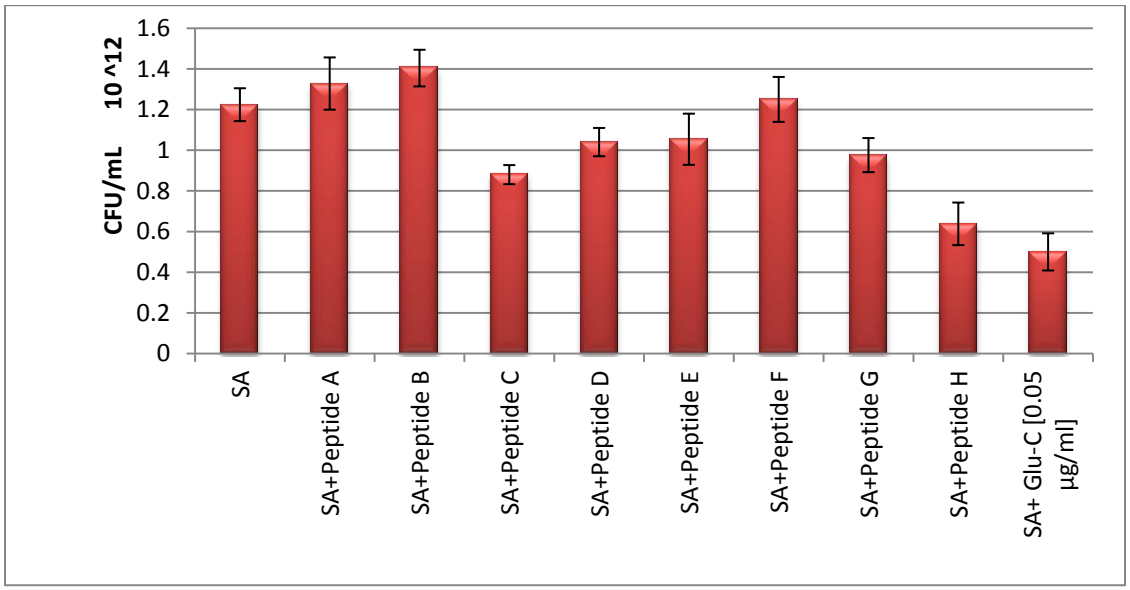

Figure 4.14 The effect of peptides A to H and V8 protease on cell viability after 24 h of growth. Toxicity of the peptides was determined at a concentration of 10 µM and later at 20, 30, and 40µM of peptide A (data not shown).

In summary, the optical density at λ 600 nm was used to monitor the cellular growth. On average, the apparent optical density values were 10% higher in the presence of the peptides than in their absence. This was due to the limited solubility of the peptides, which contributed to the turbidity at higher concentrations. However, this slight change in the optical density can be neglected when standardizing the secretion-amounts to the parameter of colonies forming units, which represents the intact and viable bacterial cells. In all experiments, no toxic impact was observed when incubating the peptides up to a concentration of 40 µM. Both bacterial growth and bacterial cell viability parameters remained stable in the presence and absence of the peptides. Based on this fact, the quantified secretome was standardized to the optical density parameter at the time of harvesting the bacterial cells and isolating the secretome.

4.7 Quantifying the Sec-dependent protein, V8 protease, in bacterial growth media

To investigate the impact of the peptides on the secretion of *Staphylococcus aureus* proteins, a precise quantitative determination of the secreted V8 protease and the Sec-dependent proteins was required. Since the amounts of the synthesized peptides were limited, the secretome was investigated in culture volumes of 5 ml. Several approaches were experimented to quantify the secreted proteins, and especially V8 protease in culture supernatants of 5ml-volume. Among the secretome of *S. aureus*, several extracellular proteases with proposed roles in virulence were described. The major proteolytic enzymes secreted by *S. aureus* consist of a metalloproteinase (aureolysin, Aur), a serine glutamyl endopeptidase (V8 serine protease, SspA) and two related cysteine proteinases referred to as staphopain (ScpA) and the cysteine protease (SspB) [12]. V8 protease is secreted in a pro-form, which is proteolytically cleaved to produce a mature and functional enzyme, possibly in an Aur dependent manner [10, 92] (Figure 4.9). In addition to its important role in pathogenicity, V8 protease possesses the potential advantage of its convenient detection and quantification by utilizing chromo- and fluorogenic substrates. V8 protease specifically cleaves the Cα-carboxyl of glutamic acid or aspartic acid under specific conditions (buffers of pH 7.4-7.8).

In order to estimate the secretion status of this Sec-dependent protease among other proteases, the activity of the secreted V8 protease was assayed with synthesized or commercially available peptides. These peptides in general contain a glutamic acid residue and carry either a chromogenic group or a fluorogenic group with a quencher at an appropriate intramolecular distance, which make them specific substrates to V8 protease. When the V8 protease is secreted to the supernatant, it specifically cleaves the Cα-carboxyl of the glutamyl residue. Consequently, the quenching effect is reduced causing an amplification of absorbance or fluorescence. Based on this principle, the following assays were used to serve this purpose.

4.7.1 Chromogenic assay of the secreted V8 protease

Supernatants were first assayed with the commercially available substrate benzyloxycarbonyl-Phe-Leu-Glu-*p*-nitroaniline (Z-Phe-Leu-Glu-*p*NA), the release of the *p-nitroaniline* causes an intensive absorbance at λ405 nm [122]. The chromogenic assays in the present investigation failed due to a low sensitivity of the method, and due to the interference caused by the supernatant components that has an absorbance at the same wavelength.

4.7.2 Fluorogenic assays of the secreted V8 protease

Two fluorogenic assays were experimented to detect the secreted V8 protease within the supernatant. The first assay utilized a trimeric peptide, benzyloxycarbonyl-Leu-Leu-Glu-βNA (Z-LLE-βNA, which contains a glutamic acid residue attached to the fluorophore β-naphthylamine (ßNA) at the C-terminus [123]. This commercial substrate was incubated with the supernatant to principally release the fluorophore β-naphthylamine, which can be measured at the emission wavelength 410 nm upon excitation at λ 345 nm (Figure 4.15). Assaying the secreted V8 protease with this substrate was expected to give better results, but the detection of fluorescence was disturbed by the supernatant contents. This issue was investigated by diluting the supernatants with PBS ten times until a better fluorescence was detected.

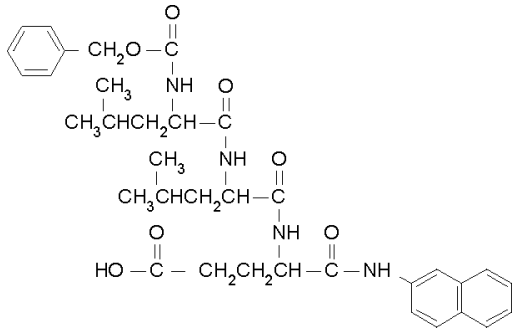

Figure 4.15 Z-LLE-βNA as a fluorogenic substrate for detecting the secreted V8 protease.

The second fluorogenic assay utilized a synthetic fluorogenic peptide that carries a fluorophore (3-nitrotyrosine) close to the C-terminus, and a quencher (N-terminal anthraniolyl group) in an appropriate intramolecular distance (Figure 4.16). This Glu-Xaa-containing substrate previously showed specificity to different enzymes from *Staphylococcus aureus* (V8), *Bacillus licheniformis* and *Streptomyces griseus* [101].

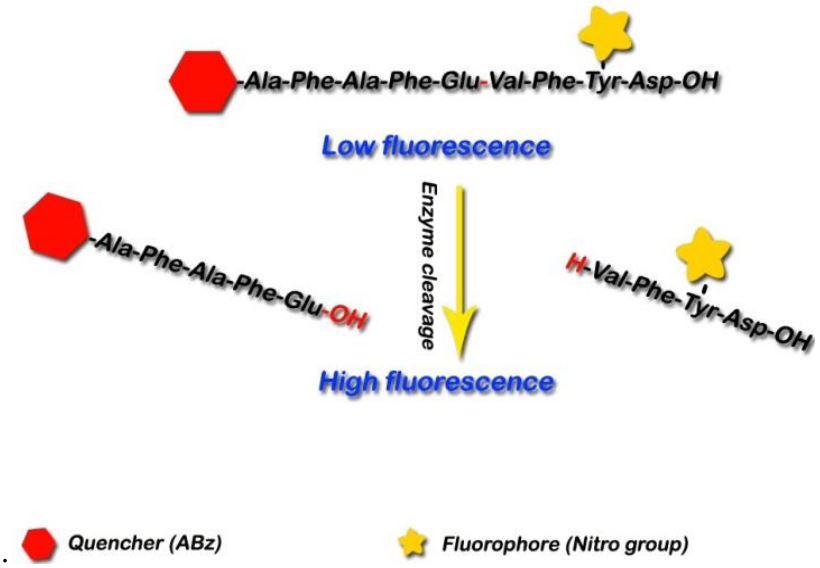

Figure 4.16 A fluorogenic substrate was synthesized for detecting the secreted V8 protease. The cleavage product of this substrate produces increased fluorescence.

The hydrolysis of such substrates has been fluorometrically monitored and Glu-Xaa peptide bonds showed approximately 1000-fold faster cleavage than Asp-Xaa bonds, where a decrease in intramolecular quenching was associated with the resulting hydrolysis [101].

Based on these findings, the fluorogenic substrate ABz-AFAFEVFFY(NO_2)D-OH was chemically synthesized in the Glu-Xaa form and assayed with the secreted V8 protease.

The fluorogenic assay with ABz-AFAFEVFDY(NO_2)-D-OH showed a sensitive detection of V8 protease (detection limit 0.352 µg/ ml) only in HEPES buffer and not in any culture medium, because the components of the culture medium were likely contributing in inhibiting the secreted V8 protease.[8] This conclusion was drawn after diluting the enzymatic supernatants by HEPES buffer; accordingly, the assay showed better increase in the fluorescence and the V8 protease reactivity was optimally detectable after a dilution (1:9) with HEPES buffer. Despite our expectation about the efficiency in evaluating the secreted V8 protease in supernatants, the previous assays in general showed shortcomings due to the low sensitivity, and the interfering-effect of the culture medium.

[8] More evidences about the inhibitory effect to the secreted V8 protease by medium-contents can be seen in the appendix V of this dissertation, in addition to several non-reproducible results of the fluorogenic assay.

Several precipitation trials failed in isolating the proteins of interest from the culture supernatant due to the low culture volumes, and due to the co-precipitation of the nutrition medium content. A chemically defined medium was also used to eliminate the effects of the medium and the co-precipitation, but the concentration of the secreted proteases was too low to be detected by the fluorogenic assay. Therefore, an SDS-PAGE approach was experimented to have a better quantification of the V8 protease. The stain Ruthenium (II) tris (bathophenantroline disulfonate) (RuBPS) was utilized to visualize bands of the secretome on gels, which were subsequently quantified by densitometry. In general, ruthenium complexes offer the possibility for very sensitive detection. Despite this fact, V8 protease could not be detected in a concentration below 30 µg/ ml.

Further SDS-PAGE experiments revealed a valid and robust quantification of other secreted proteins only after concentrating the supernatants by lyophilization, and recover them with fewer amounts of aqueous buffers.

For these reasons, and to reduce the experimental errors in quantifying the V8 protease, a Western blot approach was further investigated. Accordingly, a polyclonal antibody for V8 protease was generated from two rabbits by the company Genmedics, and experimented for optimal results. The rabbit-antiserum of V8 protease was used as primary antibody, and the commercial antibody, horseradish peroxidase (HRP)-conjugated to goat-anti-rabbit IgG, was used as secondary antibody. The detection limits in this approach can be promoted depending on the enhanced chemiluminescence resulting from activating the V8 protease bands. With this approach the V8 protease was linearly detectable in the range between 0.5 – 20 µg/ ml. Table 4.8 summarizes the direct and indirect quantitative approaches that were experimented for quantifying the secreted V8 protease on a µg scale.

On the other side, further investigations for quantifying V8 protease in the supernatants by WB proved the validity and reproducibility of the method even without concentrating the supernatants. The quantification was made for the collected supernatants 24 h after growing the cells in culture media containing the tested peptides (according to culture procedures 3.2.2.3). The quantified secreted proteins were standardized to the optical density of the respective culture. The supernatant of the 24 h culture without peptides was used as a control for quantifying the other assays.

Table 4.8 Biochemical assays for detecting the secreted V8 protease in the supernatants.

Assay	Substrate	Detection method	Reference
Milk agar plates	Milk	visible transparent zone	[89, 119]
Chromogenic	Z-FLE-pNA	absorbance λ 405 nm	[122]
Fluorogenic	Z-LLEβNA	fluorescence λ 410 nm	[123]
Fluorogenic	ABz-AFAFEVFDY(NO_2)D-OH	fluorescence λ 410 nm	[101]
SDS-PAGE	RuBPS staining	visible illuminated bands	[124]
Western blot	Rabbit anti serum of V8 protease	enhanced chemiluminescence on X-ray film	[125]

4.8 Quantification of V8 protease on Western blots by the enhanced chemiluminescence signals (ECL) approach

The success of quantifying the V8 protease bands by Western blotting depends on calibrating signals from the chemiluminiscent labels in a simple and reproducible manner over a usable range of protein concentrations. This quantification approach depends on the sensitive chemiluminescence detection, by means of the Horseradish peroxidase-conjugated secondary antibody, that gives a hard copy image on X-ray film. An accurate quantification of this signal can be obtained upon densitometry scanning of the V8 protease bands. Chemiluminescent systems based on horseradish peroxidase (HRP) offer rapid highly sensitive results with excellent signal-to-noise ratio. Since the ECL images were developed on a film, it was important that several exposure times were taken to ensure that the signal from the blot falls within the dynamic range of the film. A concentration gradient of the commercial V8 protease (Glu-C endoproteinase from Calbiochem®) ranging from 2.5 to 100 µg/ ml was investigated on the Western blot to determine the dynamic range of the ECL image. Subsequently to the immunodetection and imaging, the results were analyzed using AIDA and Adobe Photoshop CS3® to determine the pixel intensities of the bands by integration. With the data a standard curve was generated, which was used for the quantification of the secreted V8 protease from the bacterial cultures (Figure 4.17). All Western blot experiments showed a detectable concentration of the secreted V8 protease within the dynamic range of the ECL image, particularly below 12 µg/ ml, whereas the corresponding bands were not detectable on the SDS-PAGE gel after RuBPS staining due to insufficient sensitivity of this method.

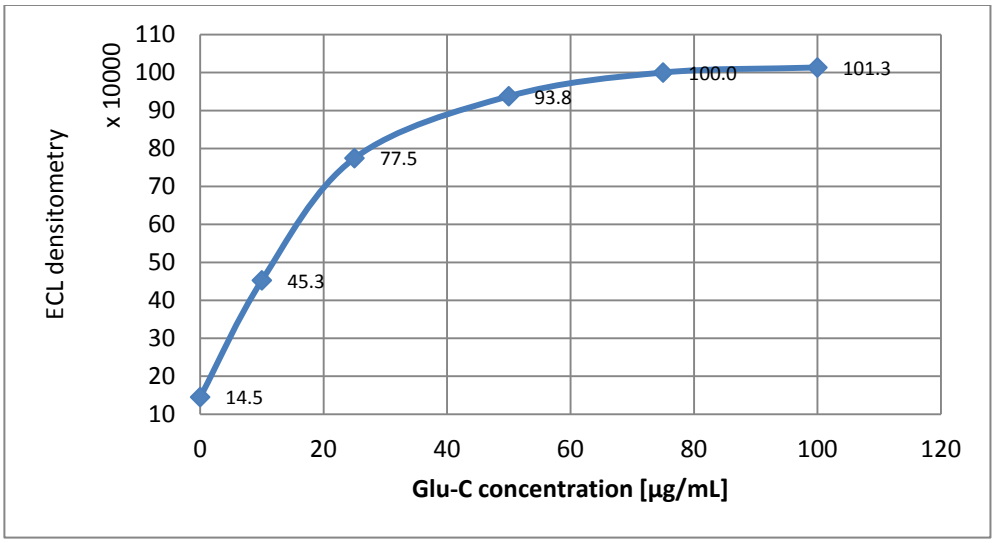

Figure 4.17 ECL dependencies on the concentration of V8 protease (Glu-C endoproteinase) standard. The dynamic range of the ECL images that resulted from V8 protease (Glu-C) standard is broad enough to quantify the light output of the V8 protease bands in a concentration between 0- 60 µg/ ml.

The detection limit of the V8 protease by Western blot using the ECL reagents is in the range of µg/ml.

4.9 Standardizing parameters to quantify the secretions of V8 protease

For optimal quantification of the secreted V8 protease, it is important to standardize the secreted V8 protease to an associated-parameter such as the colonies forming units (CFU), the optical density (OD), total secreted proteins, or to any other appropriate parameter. In this study, values were normalized to the optical density unit of the culture suspension at 24 h.

4.10 Efficiency of peptide A and peptide C in reducing the secretion of the Sec-dependent protein V8 protease

Upon treating the staphylococcal cultures with 10 µM of the early batches of the peptides A, B, and C, the supernatants were collected after 24 hours of growth, and profiled by Western blot analysis. A reproducible effect of peptide A and peptide C in reducing the secreted amount of V8 protease was observed in three different experiments (Figures 4.18 and 4.19).

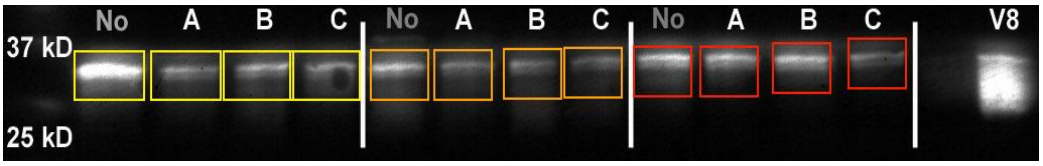

Figure 4.18 Western blot analysis of secreted V8 protease in four bacterial cultures of three individual experiments.
Supernatants were collected after 24 h of growth. The lanes No represent the supernatants of the non-treated bacterial cells. The lanes A, B, and C represent three supernatants of bacterial cells treated with 10 µM of peptide A, B and C, respectively; lane V8 represents a standard of 10 µg/ml V8 protease.

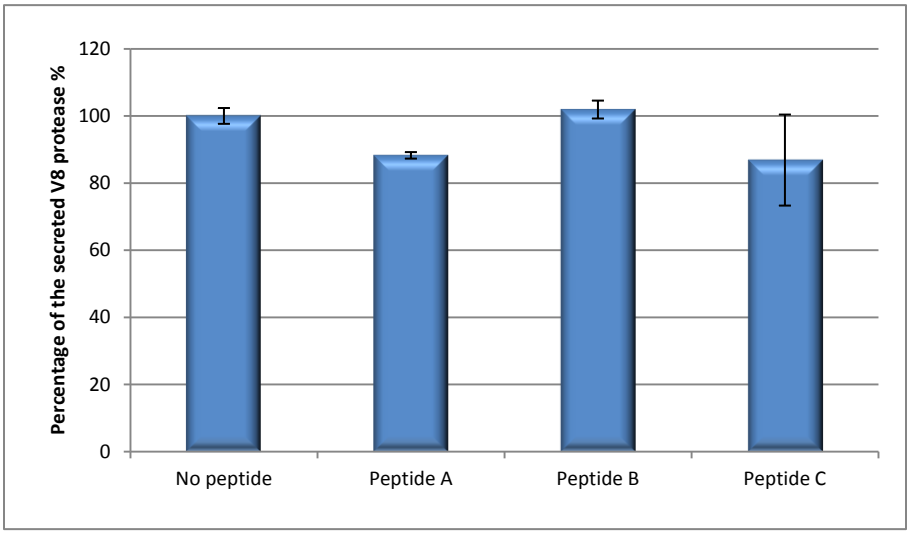

Figure 4.19 Effect of the Sec interfering peptides A, B, and C on the secretion of V8 protease.
The diagram shows error bars taken from the standard deviation of three individual experiments.

The early batches of the experimented peptides A, B, and C showed no impact on bacterial growth and viability, and a small to moderate impact on reducing the secretion of V8 protease into the supernatants. The strongest effect was observed for peptide A and peptide C (the mean values of reduction were 12% and 13% respectively). These findings suggest that conjugating V8 protease signal sequence with the HIV-1 transduction domain may be a promising tool in reducing the secretion of V8 protease.

4.11 Effect of peptide A in reducing the secretion of V8 protease

Beside the three peptidic constructs A, B and C, another five control constructs were examined in parallel to determine whether the two-domain structure of the peptide is essential for reducing the secretion of V8 protease from *Staphylococcus aureus*. Briefly, 8 staphylococcal cultures were treated with 10 µM of the peptides A to H and one culture was without peptide treatment. The amount of secreted V8 protease that resulted from 24 h culture supernatants was analyzed by Western blotting (WB; Figure 4.20). Densitometry of the bands was used for

quantifying the secreted proteins and then normalized to the optical density parameter (cell mass) of the culture (Figure 4.21).

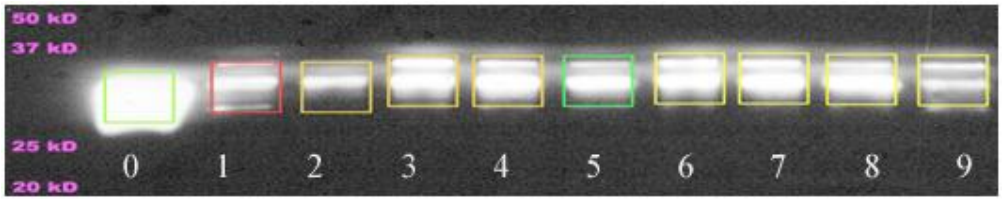

Figure 4.20 WB analysis of the secreted V8 protease in 9 individual bacterial culture supernatants.
The ten positions on the blot represent the bacterial supernatants that were treated with: (1) no peptide, (2) peptide A, (3) peptide B, (4) peptide C, (5) peptide D, (6) peptide E, (7) peptide F, (8) peptide G and (9) peptide H at 10 µM each. Lane (0) contains 10 µg/ml of Glu-C endoproteinase (V8 protease).

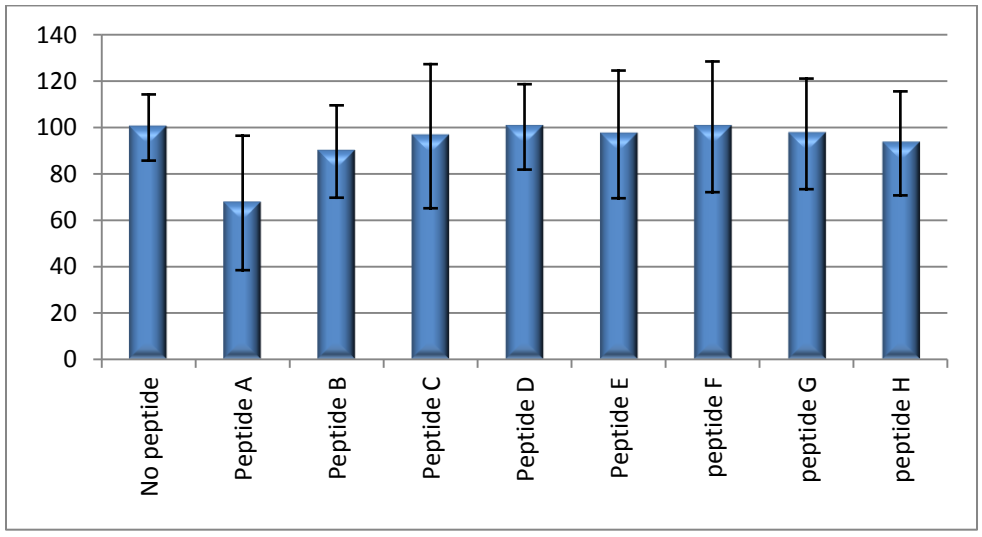

Figure 4.21 Diagram of the quantified V8 protease in the supernatants.
The error bars were taken from the standard deviation of six individual experiments.

In six individual experiments, peptide A showed a fluctuating impact in reducing the secretion of V8 protease (the reduction was fluctuating between 12– 38%). This finding, in principle, asserts that the main structure of the effective peptide should contain the signal peptide domain and the transduction domain. The control peptides D to H did not reduce the secretion of V8 protease in the staphylococcal supernatant.

When the second batch of peptide C was tested (Figure 4.21), it did not show the same effect in reducing the secretion of V8 protease. This may be due to a poorer quality of this batch in which the synthesis was carried out without using a double coupling of amino acids. Therefore, it resulted with more purifying difficulties, and consequently with higher content of impurities and lower peptide quality than the first batch (figure 4.19). Because of the lower quality of peptide C as compared to peptide A, further experiments were carried out only with peptide A.

Peptides containing formylated methionine at their N-terminus, as peptide C, are known to be strong inducers of inflammation and stimulators of the human innate immune responses [126, 127]. For these reasons, we continued probing the effect of peptide A, correlating the reduction of the secreted V8 protease with the concentration of peptide A.

4.12 The concentration-dependent effect of peptide A in reducing the secretion of V8 protease

For further investigations on the effect of peptide A, five individual culture tubes of V8 strain were started as described in 3.2.2.3. At an optical density of 0.05 OD, the five tubes were supplemented with 0, 10, 20, 30 and 40 µM of peptide A, respectively. No effect was observed on the growth or on the viability of the bacteria over the tested concentration range. The secreted V8 protease in the supernatants was profiled and quantified on WB. The quantified amounts of the V8 protease were standardized to the optical density of the cultures after 24 h of growth (Figure 4.22 and 4.23).

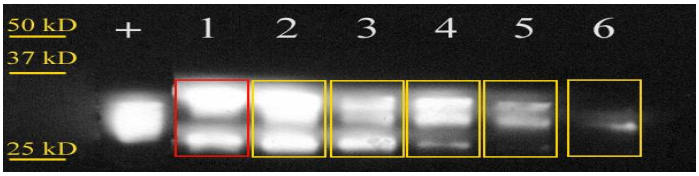

Figure 4.22 WB profile of the secreted V8 protease in supernatants.
The cell cultures were treated with different concentrations of peptide A: position (1) No peptide, position (2) 5 µM, position (3) 10 µM, position (4), 20 µM, position (5) 30 µM, position (6) 40 µM, position (+) shows the commercial V8 protease at a concentration of 10 µg/ml.

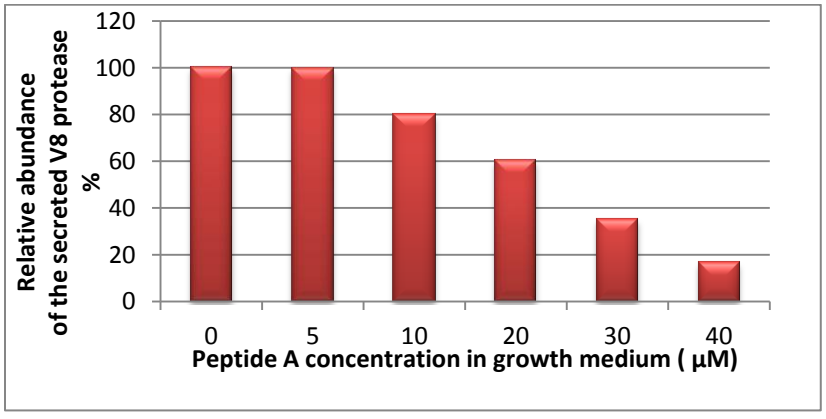

Figure 4.23 Concentration-dependent effect of peptide A in reducing the secretion of V8 protease.
The diagram represents the relative abundance of V8 protease in the supernatants. The percentage was calculated as a ratio of the V8 protease secreted by the peptide-treated cells to the V8 protease from non-treated cells. This diagram shows the values of quantified V8 protease bands after standardization to their respective optical densities at 24 h (A/OD_{600}).

The IC_{50} value for reducing the secretion of V8 protease is approximately 25 µM. Furthermore, SDS-PAGE analysis of these supernatants showed that treating the bacterial cultures with higher concentrations of peptide A was associated with less secretions not only of V8 protease, rather of the supernatant proteins that have masses between 20-50 kD, and this reduction was observed in a concentration-dependent manner (Figure 4.24)

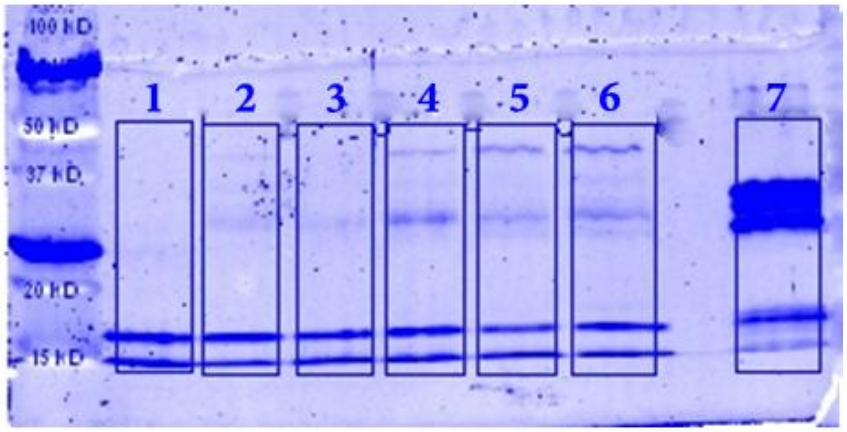

Figure 4.24 SDS-PAGE analysis of supernatants isolated from 24 h staphylococcal cultures.
Bacterial cultures were treated with different concentrations of peptide A. Position (1) with 40 µM, (2) with 30 µM, (3) with 20 µM, (4) with 10 µM, (5) with 5 µM, (6) without peptide A, (7) control of mixture of α-hemolysin and V8 protease (100 µg/ ml each).

The concentration-dependent effect of peptide A was also investigated on the secretion of all proteases by milk agar assay. 10 µl of supernatants that were isolated from cultures treated with increasing amounts of peptide A (0, 20, and 40 µM) showed proteolytic clearance zones of 15.5, 11.5, and 9.5 mm, respectively (Figure 4.25).

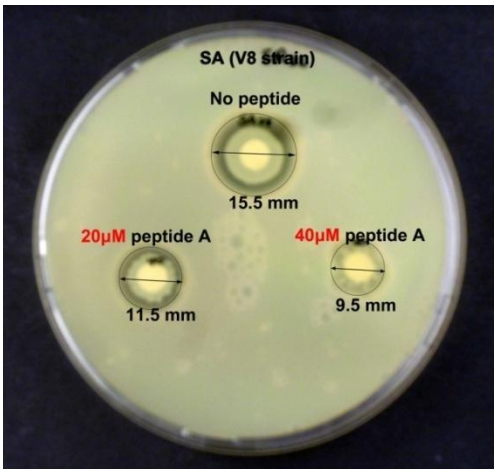

Figure 4.25 Effect of peptide A on the secreted amounts of staphylococcal proteases.
Cleavage zones on milk agar plates of supernatants isolated from cultures that have been treated with 0, 20, and 40 µM peptide A.

When treating the bacterial cultures at the start of growth with peptide A, the secretion of V8 protease and probably of other proteases into the extracellular matrix showed to be reduced in a concentration-dependent manner. In contrast, the successive additions of peptide A at different time points after the start of growth, namely, at 3, 6, 9, and 12 hours at a concentration of 10 µM each did not show any further reduction of the secretion compared to that found with a single initial dose (data are not shown). This observation suggests that peptide A is likely to be effective only in the early exponential phase of staphylococcal growth.

4.13 Quantification of cellular and extracellular V8 protease after treatment of the staphylococcal cultures with different concentrations of peptide A

In order to verify the ability of peptide A to affect the secretion of V8 protease, it was necessary to extend investigation specifically to the cellular V8 protease. To this end, V8 protease was determined in a Western blot. The distribution between the secreted and the cellular form was determined by analyzing both supernatant and lysed cell pellet fractions. Three individual bacterial cultures were grown in the presence of 0, 10, and 20 µM of peptide A. After 24 hours of growth, supernatants and bacterial cells were separated by centrifugation, and the cells were lysed by lysostaphin. Both supernatants and lysates were subjected to SDS-PAGE and WB analysis. The two figures 4.26 and 4.27 show the quantified bands of the extracellular and intracellular V8 protease.

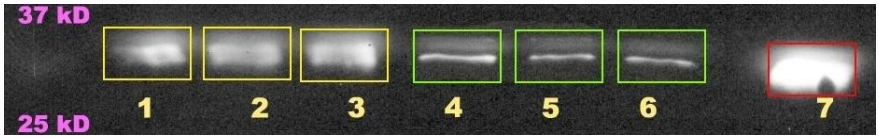

Figure 4.26 WB analysis of V8 protease from cell lysates and supernatants, respectively.
Positions 1, 2, and 3 represent the cellular V8 protease from the cell pellet lysates. Positions 4, 5 and 6 represent the secreted V8 protease in the supernatants. Positions 1 and 4: no peptide was added to the bacterial culture. Positions 2 and 5: 10 µM of peptide A was added. Positions 3 and 6: 20 µM of peptide A was added. Position 7: 10 µg/ ml of a commercially available V8 protease.

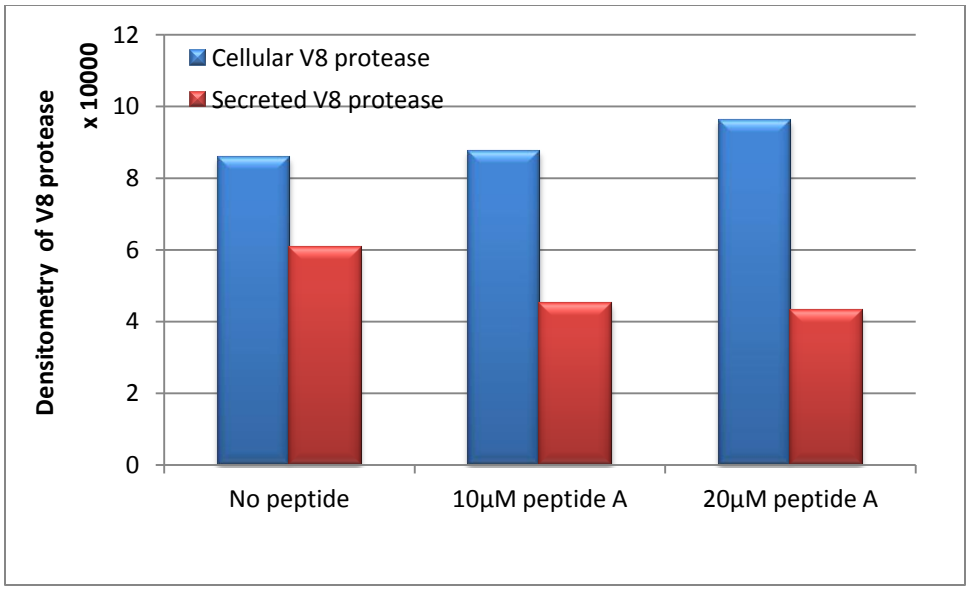

Figure 4.27 Effect of peptide A on the cellular and extracellular V8 protease.
Two bacterial cultures were treated with 10 and 20 µM peptide A, and one culture was without peptide treatment. The supernatant and the lysate were collected from 24 h cultures. The blue columns represent the cellular V8 protease (cell lysates), and the red columns represent the extracellular V8 protease (supernatants).

Peptide A showed a concentration-dependent reduction of the secretion of V8 protease and correspondingly a concentration dependent retention of the V8 protease inside the bacterial cells. However, this presentation shows only the secreted V8 protease and the total cell-bound V8 protease in general, V8 protease from subcellular compartments is still not addressed. Therefore, this observation is not a sufficient evidence for the interference of peptide A with the secretion process, because there are still more possibilities that suggest a retention of the V8 protease in the membrane or in the cell wall. This issue requires addressing the V8 protease in subcellular compartments e.g. the cytosol, the cytoplasmic membrane, and the cell wall. This might give a better understanding to the underlying mode of action.

4.14 The effect of peptide A on the secretion of α-hemolysin

In order to probe whether the effect of peptide A has specificity to the Sec-system in general, it was necessary to investigate further Sec-dependent proteins as well. α-Hemolysin is another major *S. aureus* pathogenicity factor that is also transported through the bacterial membrane via the Sec pathway [22, 123]. Besides the successful quantification of the V8 protease, a similar Western blot approach was developed to investigate the effect of peptide A on α-hemolysin. For that purpose, a Western blot experiment was established based on streptavidin-biotin specific binding. The biotin conjugated anti α-hemolysin from *S. aureus* was utilized as

primary antibody, and streptavidin conjugated with horseradish peroxidase (HRP) was used for detection. The secretion of α-hemolysin was investigated in 24 h-culture supernatants that had been treated with/without peptide A. Standard solutions (2.5, 5, 10, 25, 50, and 100 µg/ml) of α-hemolysin were prepared, and analyzed together with cellular/secreted α-hemolysin by WB (Figure 4.28).

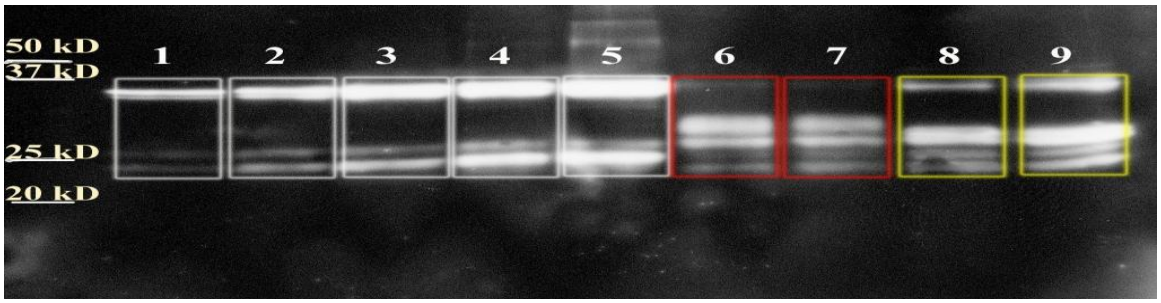

[22, 128]Figure 4.28 WB analysis and quantification of cellular and extracellular α-hemolysin.
Positions 1 to 5 contain commercially purchased α-hemolysin (2.5, 5, 10, 25, 50 and 100 µg/ml), respectively. Positions 6 and 7 contain the supernatants of cultures that were treated with 0 and 40 µM peptide A, respectively. Positions 8 and 9 contain the isolated and lysed cell pellets of cultures that were treated with 0 and 40 µM peptide A, respectively. The rectangles show the areas that were integrated densitometrically.

Three major bands were recognized for the commercial α-hemolysin, whereas four bands were recognized for the secreted α-hemolysin. This observation can be explained through the possible action of enzymes (V8 protease and aureolysin) that might participate in activating α-hemolysin in the supernatants to help it in a self-oligomerization process that is needed to promote the formation of the pore-forming α-hemolysin [112]. The observed amounts of the secreted α-hemolysin were limited between 5 and 25 µg/ml in all experiments.

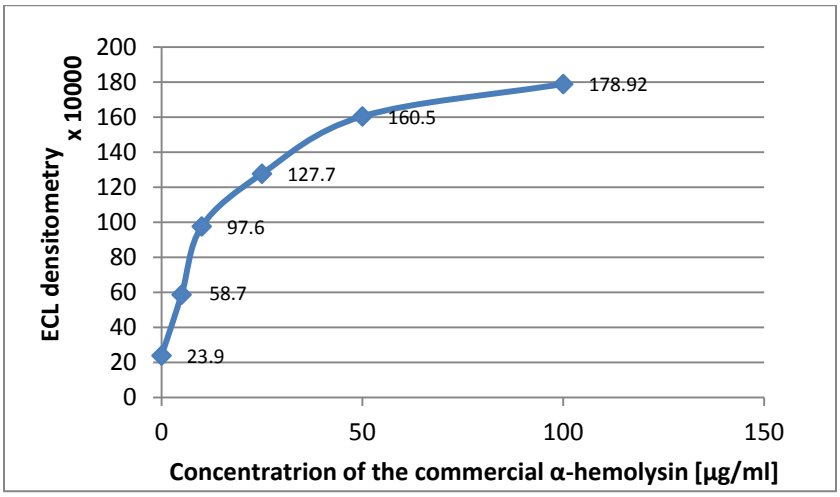

Figure 4.29 ECL dependencies on the concentrations of α-hemolysin.
The dynamic range of the ECL images that resulted from α-hemolysin standard allows the quantification of α-hemolysin bands on the Western blots in a concentration between 0-100 µg/ml.

A comparative WB analysis for the secreted and cellular α-hemolysin between the non-treated cultures and cultures that were treated with 40 μM of peptide A shows a concentration-dependent effect similar to the one that was observed for V8 protease. In other words, peptide A showed a concentration-dependent reduction of the secretion of α-hemolysin and correspondingly a concentration dependent retention of α-hemolysin inside the bacterial cells (Figure 4.30).

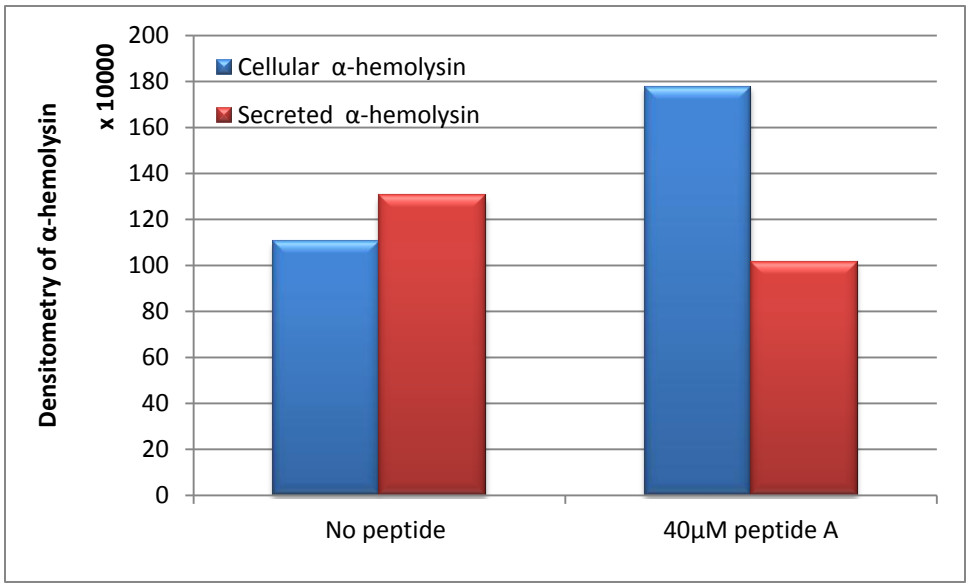

Figure 4.30 Effect of peptide A on the secretion of α-hemolysin in bacterial cultures after 24 hours of growth. The percentages of the extracellular and the cellular α-hemolysin were taken as a ratio of the peptide-treated cultures to the non-treated cultures.

In order to substantiate those results, a hemolysis assay was developed based on the hemolytic effect on erythrocytes as an alternative in quantifying the total secreted hemolysins instead of α-hemolysin.

As an independent control experiment, the total hemolysins that were secreted by the bacteria were estimated with a hemolysis assay that is based on a literature procedure with slight modification [129]. In summary, the staphylococcal supernatants were isolated 24 hours after treating the cultures with peptide A at concentrations of 0, 10, and 40 μM, and assayed in 96-well plates with sheep erythrocytes (2% suspension). Fifty microliters of supernatant from each growth culture was transferred to a flat-bottom 96-well microplate and the absorbance of the released hemoglobin in the wells supernatants was determined at 440 nm. Zero hemolysis (blank) and 100% hemolysis controls were determined using erythrocytes suspended in PBS medium and in 1% Triton X-100, respectively. A standard curve was established by assaying solutions of commercially available α-hemolysin with the erythrocyte suspension (Figure 4.31).

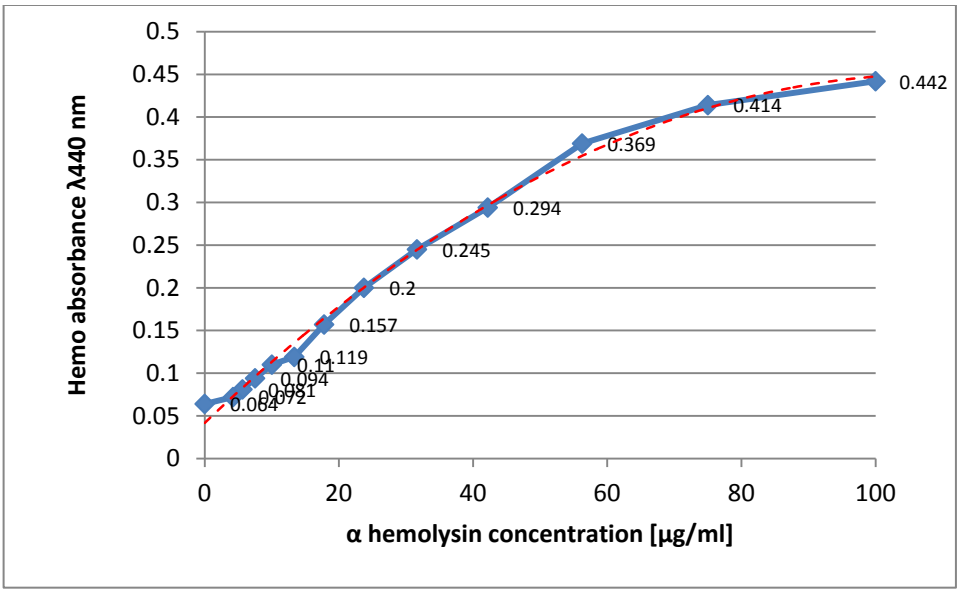

Figure 4.31 The standard curve represents the functionality of the hemolysis assay to the concentration of α-hemolysin
The standard solutions of α-hemolysin (0, 5.6, 7.5, 10, 13, 18, 24, 32, 42, 56, 75, and 100 µg/ml), and staphylococcal supernatants of cultures that were treated with different concentrations of peptide A were assayed with a suspension of 2% sheep erythrocytes.

Assaying the supernatants of bacterial cultures that were treated with different concentrations of peptide A showed a concentration-dependent effect of peptide A on lysis of the sheep erythrocytes (Figure 4.32).

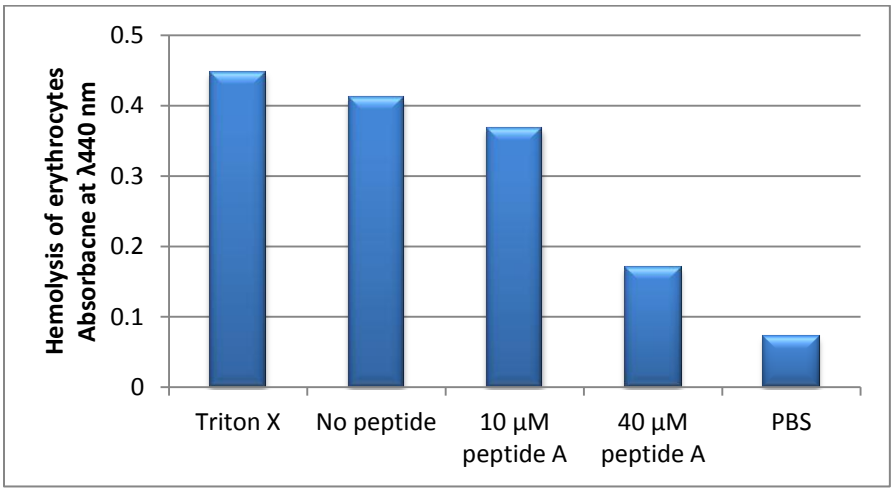

Figure 4.32 Hemolysis assay with sheep erythrocytes after the addition of growth culture supernatants with and without peptide A.
Triton X-100 and PBS buffer were used as positive and negative controls, respectively.

Hemoglobin-lysate measurements showed a maximum absorbance of 0.420 at 440 nm. The absorbance value for the supernatant without peptide A is higher than the absorbance value of supernatant with 10 µM of the compound, and these are higher than the absorbance value of the culture with 40µM of peptide A. Correlating this data to the concentration of α-hemolysin in the standard curve, and to the WB data, we can deduce that a concentration-dependent effect of peptide A on the secretion of this toxin might happen, i.e. the higher the concentration of peptide A, the less α-hemolysin is secreted.

In order to answer the question if this reduction in the secretion is based essentially on an interference of peptide A with the Sec-system, the investigation of the secretion of Sec-independent proteins should be addressed. No commercial antibody for known Sec-independent proteins was available and in the time frame of the present investigations it could not be generated.

4.15 Determining the effect of peptide A on the concentration of V8 protease in different cell compartments

In order to obtain a better understanding of the underlying mode of action of peptide A, and to address if the intervention of peptide A occurs within the membrane, the cell wall, or within the cytosol, a comparative analysis of the staphylococcal V8 protease and the proteome in different cellular fractions was carried out. If peptide A blocked one of the Sec components: SRP, SecA, or SpsB, an accumulation of the Sec-traslocated protein would be observed in the corresponding cellular compartment. To this end, two staphylococcal cultures containing 0 and 40 µM of peptide A were grown for 24 h followed by a subcellular fractionation. Based on published procedures [102], the successive subcellular fractionation was performed using three buffers of specific contents and specific pH values to keep the physiological conditions for the extracted proteins optimal, and to keep the fraction content intact (Figure 4.34).

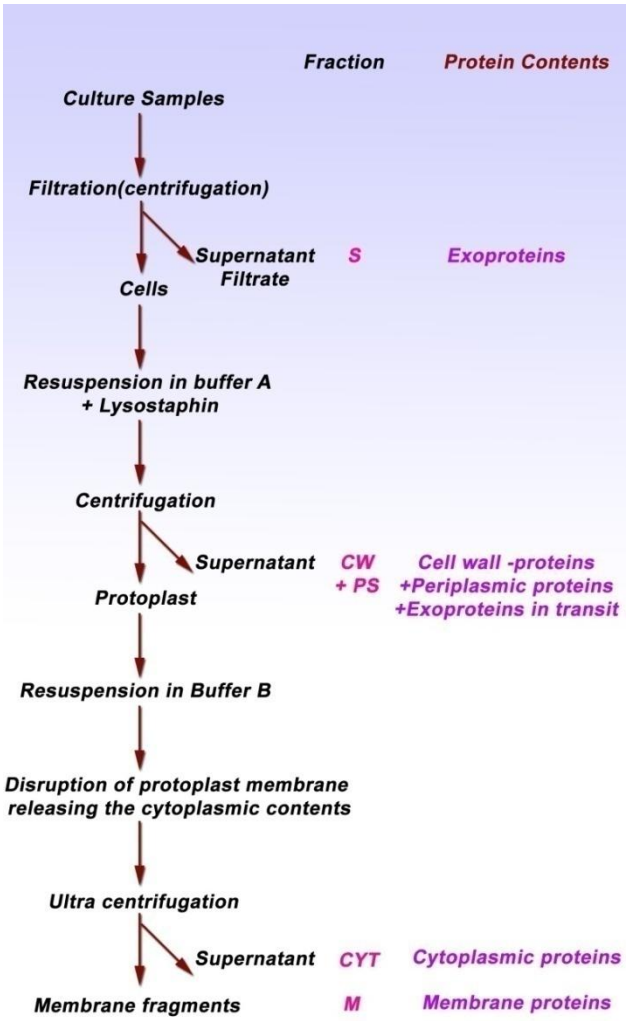

Figure 4.33 Schematic representation of the cell fractionation procedure.
S, CW, CYT and M represent culture supernatant, cell wall with periplasmic space, cytoplasm and membrane, respectively. Membrane fragments were dissolved later in buffer C.

Moreover, it was important to keep the lysis process of the pellets under mild conditions: supplementing the lysis buffer with a cocktail of protease-inhibitors, keeping the protoplast intact, and generating a precise determination of the protein content of the cytoplasm and the cytoplasmic membrane. Lysostaphin (25kD) was used in this procedure as a lysis factor due to its known specificity in digesting the staphylococcal pentaglycine bridges of the cell wall. According to Park *et al*. [130] EDTA and an alkaline medium function as inhibitor for the zinc-metalloproteinase (lysostaphin). Therefore, EDTA was supplemented to further buffers as an inhibitor for lysostaphin. Furthermore, a cocktail of protease inhibitors was utilized to inhibit the action of the existing proteases. Triton X was used as a detergent that is well known to solubilize membrane proteins and to separate them from hydrophilic proteins via phase partitioning at physiological temperature. The membrane fraction was isolated from the cytosol by

ultracentrifugation at 100,000× g. This approach resulted in four different fractions; they are namely, the supernatant, the cell wall/ periplasm, the cytoplasm, and the cytoplasmic membrane. The resulting four fractions were introduced to SDS-PAGE and WB analysis to develop the ECL images and subsequently quantify the extracellular and subcellular V8 protease bands (Figures 4.34 and 4.35).

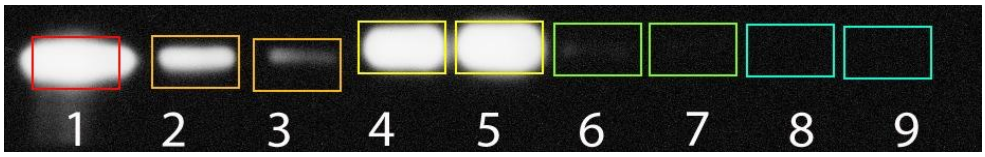

Figure 4.34 WB analyses for V8 protease in different subcellular fractions and culture supernatant.
Position (1) 10 µg/ml of V8 protease, positions 2 and 3: V8 protease of supernatants. Positions 4 and 5: V8 protease of the cell wall and periplasm. Positions 6 and 7: V8 protease of cytosol. Positions 8 and 9: V8 protease of membrane fractions. Positions 2, 4, 6, and 8 were of the non-treated cells, while positions 3, 5, 7, and 9 were of the cells that were treated with 40 µM peptide A. The supernatants were standardized to an OD600 of 5.0, while the subcellular fractions were standardized to OD600 of 1.0.

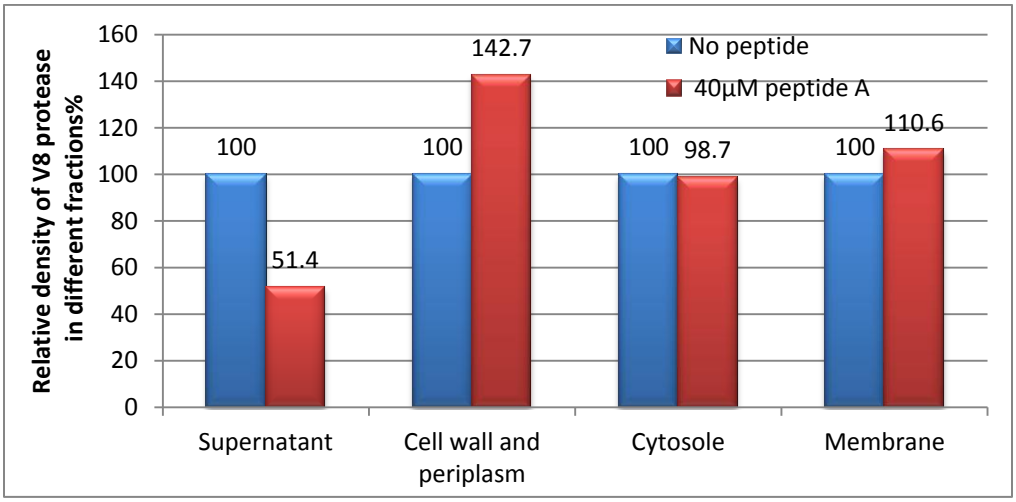

Figure 4.35 Effect of peptide A on V8 protease accumulation in supernatant and subcellular compartments of staphylococcal cells.
The values from the culture with peptide A were related to the values from the culture without peptide addition.

Since the protein is co-translationally secreted through the membrane, and based on results that revealed the reduction of V8 protease amounts in the supernatant when using peptide A, an accumulation of V8 protease would be expected to be found in cytosol or cytoplasmic membrane when Sec system is blocked. A comparative study of V8 protease in different fractions was performed for the peptide treated cells and the non-treated cells. Western blot analysis showed that less V8 protease was secreted into the supernatant than without peptide treatment, and more retained in the periplasm/ cell wall of the peptide-treated cells, while only very small

amounts of V8 protease in the cytoplasm and the cytoplasmic membrane can be detected. A possible explanation to this finding might be that the matured or non-matured protein that was secreted into the periplasmic space during the 24 h of growth is only slowly released from the membrane, possibly after completion of maturation. In addition, it would be expected that nascent protein would be degraded in the cytoplasm. These findings are so far in agreement with peptide A interfering with secretion during the co-translational phase, whereby peptide A may also be either blocking or slowing the transport or migration through the cell wall.

4.16 Determining the effect of peptide A on the cellular proteome in different cell compartments

For a better understanding of the underlying mode of action of the peptide construct, and to address if the peptide A has a general effect on accumulating other proteins in cellular compartments, an analysis of the total staphylococcal secreted and subcellular proteins was carried out. For that purpose, a comparative SDS-PAGE analysis of the total proteins was performed in parallel under two conditions, with/ without peptide treatments. The staphylococcal cells were grown according to procedure 3.2.2.3, supernatants were obtained by filtering the cell suspensions, pellets were resuspended in the original culture volume, and undergone a fractionation according to procedure 3.3.7. The cellular fractions were collected in equal volumes to allow quantitative comparison of the proteins in each fraction and thus, get a comprehensive analysis of all proteins. Since the sensitivity of SDS-PAGE analysis is not as high as WB analysis, the supernatant and the membrane fraction were of high importance to be detected. Therefore, it was found advantageous to carry out a concentration enhancement before the electrophoretic separation, which was achieved by lyophilizing a defined aliquot of the solution and redissolving the solid remainder in a smaller amount of water. The supernatants were concentrated 6-fold this way and the membrane fractions 2-fold. Samples were profiled on large 8% SDS-PAGE gels (Figure 4.36).

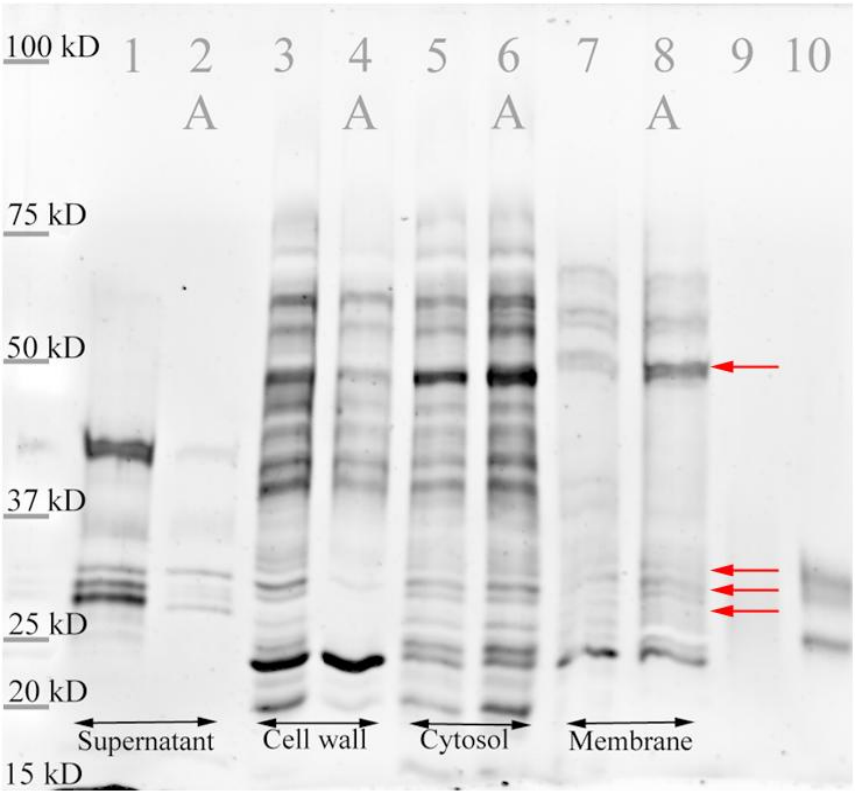

Figure 4.36 SDS PAGE profile of total proteins in four fractions with/ without peptide A treatments.
Protein contents of four fractions were profiled on 8% SDS-PAGE, namely supernatants and the 3 subcellular fractions cell wall, cytosol, and cytoplasmic membrane. Using the lyophilization approach, supernatants were 6 fold concentrated, while the membrane fractions were 2 fold concentrated. Lanes 1-2: supernatant fractions, lanes 3-4: cell wall fractions, lanes 5-6: cytoplasmic fractions, lanes 7-8: membrane fractions, lanes 9-10 are controls of 100 µg/ ml of commercial V8 protease and α-hemolysin, respectively. Lanes marked with A represent the fractions resulting from cells treated with 40 µM peptide A. Staining with RuBPS.

The comparative analysis of the supernatants and cellular compartments of the peptide-treated/ non-treated cultures showed a general reducing effect on the secretion of proteins. In general, proteins that are transported across the membrane in a Sec-dependent manner emerge at the extracytoplasmic membrane surface in an unfolded state. These proteins need to be rapidly and correctly folded into their native and protease-resistant conformation in order to protect them from cleavage by proteases in the cell wall or extracellular environment [67]. The highest abundance of proteins was observed in the periplasm and cell wall and the cytosolic fractions in this experiment.

Upon treating the bacterial cells with 40 µM of peptide A, no effect was observed on bacterial growth, or on cell viability, but a substantial effect in reducing the amounts of secretions into the supernatant and the periplasm/ cell wall. In comparison with WB analysis of the quantified V8 protease in four fractions, treating the bacterial cultures with peptide A lead to a reduction in the

secreted amounts of V8 protease and to an accumulation of V8 protease in cell wall. This accumulation of V8 protease in the cell wall compartment can be detected by WB but not by SDS-PAGE approach. This may be due to the retention of the Sec-dependent proteins in the periplasm and the cell wall compartment, which are secreted as non-folded proteins and are folded to form the mature proteins. Although SDS-PAGE analysis is still insufficient tool to detect low concentrations of the V8 protease and other Sec-dependent proteins in comparison to WB analysis, it showed a reduction of the amounts of some proteins in cell wall compartments associated with the bacterial culture treatments with peptide A. Moreover, a slight enhancement of some proteins was observed in the membrane at ca. 28 and 48 kD regions. This latter finding calls for further investigations to determine whether these proteins (28 and 48 kD) are Sec-dependent proteins. Not all membrane proteins use SecYEG for insertion, rather a small subset of integral membrane proteins are targeted to YidC where they are inserted into the membrane in a Sec independent manner [131, 132].

4.17 Investigating the subcellular targeting of the potentially Sec-interfering peptides

Based on the previous findings, our research interest was stimulated towards investigating the possible targets of the peptide constructs and their subcellular localizations in *S. aureus*. A preliminary experiment was established to serve this purpose. Three fluorescein-conjugated constructs were chemically synthesized, namely peptide-3, peptide I, and peptide J. (Tables 4.2 and 4.4). These peptides were incubated with the bacterial cultures for 24 h. The supernatants were isolated and the bacterial cells were collected and fractionated into four fractions as described above. The fractions were collected in equal volumes to facilitate an optimal evaluation of the measured fluorescence in each fraction. This evaluation can serve as a preliminary map of the potential subcellular targets that can be interfered by these peptides. The fluorescence properties were measured in supernatant, cell wall, cytosol, and membrane fractions (Figure 4.37).

The fluorescence was observed in all cellular compartments (Figure 4.37). This asserts the potential entry of the peptide into the staphylococcal cells. The highest fluorescence value for the bacterial compartments was observed in the cytoplasm fraction. However, it is still yet not known if a potential intervention of these peptides with one of the cytoplasmic or membrane components has occurred. Therefore, the binding affinity of these peptides to the signal recognition particle

SRP, to the molecular motor SecA, and to the signal peptidase SpsB in the cytoplasmic membrane should be investigated in future studies. This may be addressed by utilizing peptide or protein microarrays. The array requires preparing a piece of glass on which different expressions of the SRP or SecA proteins have been affixed at separate locations in an ordered manner thus forming a microscopic array. The known expressed sequences of the staphylococcal SRP, or SecA protein are used as capture molecules to detect any specific binding to the labeled peptide A. This approach is still limited because no enough libraries of such proteins are commercially available at the time of this study. Therefore, it would be much easier to establish an ELISA-type assay or use SPR-based methods (e.g. the Biacore instrument) if only a few proteins and their interaction with peptide A are to be investigated.

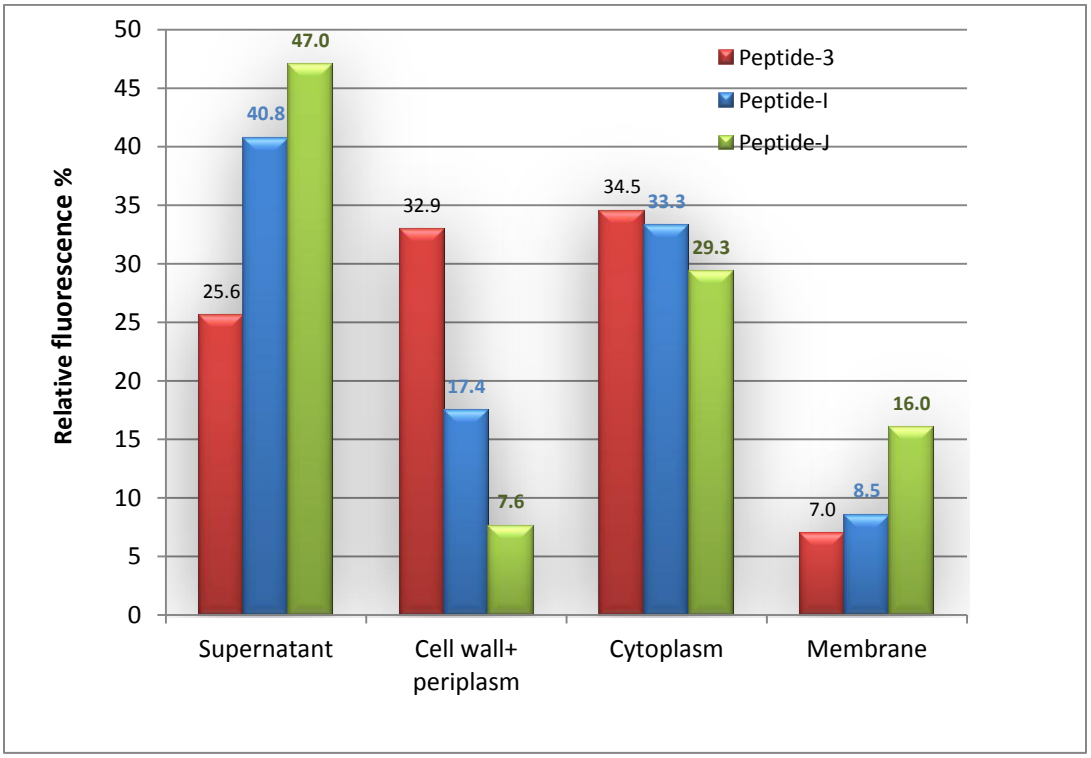

Figure 4.37 Relative distribution of fluorescein conjugated peptides in supernatants and in different subcellular fractions.
The sum of fluorescence in all fractions was considered as 100%, and accordingly the distribution was evaluated.

.

5 Conclusions and recommendations

These studies were initiated in the face of an urgent unmet need to develop novel approaches to combat the infections caused by antibiotic-resistant bacteria. Specifically the problem was approached to find novel active compounds and targets in *S. aureus.* This study investigated establishing a base for affecting the secretion efficiency of the bacterial virulence factors. Our study presents new peptides that play a double role. On one side, they penetrate the staphylococcal cells. On the other side, they were designed to interfere with the secretion of specific Sec-dependent proteins that might act in the pathogenesis of infection. Little data has so far been accumulated with respect to developing antimicrobial agents as specific inhibitors fo the signal peptidase SpsB, and Sortase A in *Staphylococcus aureus* [50, 51, 54, 55, 69]. These trials in interfering with the secretion of the cell wall integrated proteins were novel at that time. In this work, the general secretion pathway Sec was put on the focus due to its essential role in secreting most virulence factors through the cell membrane. Based on the description of this pathway in Gram-positive bacteria, it is believed that the signal recognition particle SRP, the secretory motor Sec A, and the signal peptidase SpsB play the key role in interacting with the signal peptide of the secreted preprotein, and thereby translocating unfolded virulence proteins from the cytoplasm into the extracellular milieu. Therefore, this study hypothesized that these three Sec- components can be significant targets to synthetic peptides, which potentially compete with the secretion signal sequence of a Sec-dependent protein (V8 protease). In order to internalize these peptides into *S. aureus*, three cell-penetrating peptides (CPPs) were chemically generated, and investigated whether they are efficient in delivering fluorescein-5-maleimide into *S. aureus*. Fluorescence-based methods revealed an optimal cellular uptake of the peptide YGRKKRRQRRR. Based on this finding, potentially Sec-interfering peptides were chemically generated by Fmoc chemistry. These peptides consist mainly of two domains, the signal peptide mimetic of the V8 protease (29 amino acids), and the transduction domain mimetic of the HIV-1 Tat protein (11 amino acids). Another subset of control peptides was chemically synthesized. Their potential in affecting the secretion of Sec-dependent proteins was investigated.

The experimental work in this study proved that the Fmoc solid-phase synthesis was a feasible approach for generating the required peptide constructs, despite the relatively low yields of the pure products. As discussed before, automated synthesizers can chemically regenerate these 40mer constructs. Both quality and yields of these long peptides might be improved if

newer synthetic strategies and techniques were utilized, e.g. synthesizing nona- or decapeptides and subsequently ligating them chemically as longer peptide might be a good alternative to improve the yield, since this synthesis strategy might bypass the aggregation of the hydrophobicity along the synthesized chain and give higher yields and purity of the final products [133]. Another possibility is the utilization of pseudoproline (dipeptide) building blocks in the synthesis process. Dipeptides are known to minimize the aggregation in the peptide chain through providing the temporary side-chain protection especially for Ser, Thr, and Cys on one hand, and providing the fast solubilized building blocks leading to increase the solvation and the coupling rates of the peptide synthesis on the other hand [134]. This strategy might improve the yield of the syntheses through promoting the coupling efficiency. Microwave-assisted peptide synthesis technique could be another way to improve that quality and yield of the peptides because this approach is known to keep the long synthesized peptides receiving homogenous microwave energy field, providing them with optimal temperature for coupling of the amino acids with lower racemization degrees [135, 136]. These techniques can be successful alternatives to the conventional technique if they were applied in this study.

Investigating the staphylococcal uptake of three cell-penetrating peptides showed optimal properties for the HIV-Tat protein derivative, YGRKKRRQRRR. Three techniques were used in parallel to investigate this phenomenon: automatic fluorescence microscopy to quantify the internalization of the fluorescently labeled peptides, FACS analysis to quantify the uptake of the fluorescent peptides into the *Staphylococcus aureus* cells, and the fluorescence quantification of four different subcellular fractions.

One of the major objectives in this study was to establish robust assays for both qualitative and quantitative determinations of Sec-dependent proteins and total secreted proteins. This was set to facilitate evaluating the state of secretion upon the peptide treatments. The quantified amounts of Sec-dependent proteins were correlated in each experiment to the bacterial growth and viability parameters.

The semi-quantitative determination on milk agar plates showed the BM medium as optimal growth medium for inducing the secretion of the staphylococcal proteases. Therefore, it was used in all experiments to cultivate the V8 strain in this study. The attempted quantitative determination of the secreted V8 protease in the supernatant by using colorimetric and chromogenic assays with special peptide substrates was not useful due to the low sensitivity of

the approaches. Therefore, this technical approach was replaced by alternative experimental settings. Gel electrophoresis followed by Western blot was found to be an optimal and valid tool for quantifying the secretion of the Sec-dependent proteins V8 protease and α-hemolysin.

Investigating eight generated peptides showed a reproducible impact of peptide A (KGKFLKVSSLFVATLTTATLVSSPAANAYGRKKRRQRRR) in reducing the secretion of two Sec-dependent proteins, V8 protease, and α-hemolysin, and on the hemolysis properties of bacterial growth supernatants. This finding was not limited to these two Sec-dependent proteins, rather it includes other proteases and probably additional proteins [9].

Investigating the secretion of Sec-independent proteins could not be addressed explicitly because no commercial antibody for known Sec-independent proteins was available or could be generated in the time frame of the present investigations. Therefore, this issue was left unanswered. Nevertheless, we developed a comparative approach, comparing specific protein contained in cellular fractions of non-treated and peptide-treated cells. This was expected to provide a better understanding on how the peptide constructs affect the secretion of V8 protease in different fractions, namely; the supernatant; the periplasm and cell wall; the cytosol; and the cytoplasmic membrane.

Based on these results, an incomplete picture emerged which left many questions still open. A comparative secretome study of the supernatants and probably also of the different cell compartments in the presence and absence of peptide A should yield a more complete picture but was considered to be beyond the present scope of this study. This approach can be built on two-dimensional gel electrophoresis and mass spectrometry, where the spots of the secretome, from the supernatants or cell compartments, can be identified by mass spectrometry and quantified. This approach will reveal a comprehensive view about all Sec-dependent and independent proteins and other cell components.

The fluorescein-conjugated form of peptide A was distributed in all subcellular compartments. The high abundance of the fluorescein-conjugated peptide in the cytosol fraction calls to a further investigation whether the mode of action of this peptide was based upon a competitive binding to one of the cytosolic components, in particular SRP and/ or SecA. However, further studies are

[9] The effect of this construct in reducing the secretion of this number of proteins could be due to the similarities of the peptide A sequence to the signal peptides of these proteins. A multisequence alignment analysis showed a similarity between the signal peptides of the Sec-dependent proteins in general (See appendix VI).

still required to identify the mode of action of this product. A protein-function microarray might be helpful to investigate the specific binding of the signal sequence or the peptide constructs to the M domain of the fifty four homologue (Ffh protein) in the SRP that is binding to the signal peptide [137]. This is more important issue because of the promiscuity of the SRP, and because only one type of SRP is present in the bacteria, and this is processing all Sec destined proteins with their different secretion signal sequences.

This approach might also be used for the optimization of binding affinities and the activity profile of the peptide constructs by investigating sequence modifications. Such a study could include generating combinatorial libraries of the successful signal peptides attached to a solid-phase and testing their specific binding to some known expressed cytosolic proteins. Following such a study, further successful structures might be candidates for drug discovery.

The stability of the peptides in serum should further be addressed. This will determine the potential of such constructs to enter further clinical trials if they show promising stability and non-toxic effect against eukaryotic cells. Many drugs which exhibit promising pharmacological activities fail to show convincing effects in vivo. This is due to various reasons, including low stability or unexpected immunogenicity and toxicity. One main problem is that several therapeutic peptides and proteins exhibit a short plasma half-life time in the range of a few minutes to a few hours. Half-life times of only a few minutes are in most cases not effective in order to deliver sufficient drug amounts to the target tissue. Therefore, strategies to prolong the half-life of peptide A to enter clinical studies might require replacing some L-amino acids by D-amino acids or other nonproteinogenic amino acids, to enhance the stability of the peptide towards degrading plasma enzymes.

The utilizied CPPs are not specific for bacteria. They are known to internalize efficiently and rapidly into eukaryotic cells [83]. Thus, a rapid clearance of the serum from the peptide constructs can not only be expected because of degradation but also due to uptake into the host tissue. Before a pharmacological systemic application of such constructs can be considered, bacteria-specific CPPs need to be developed. So far those are not known.

Since the L-amino acid construct of peptide A had no effect on bacterial growth, and the viability of the staphylococcal cells, it cannot be classified as a conventional antibiotic. Nevertheless, it might be useful as an anti-virulence agent that interferes with the Sec-system, thus, disarming the bacterial cells by competing secretion of virulence factors like V8 protease

and α-hemolysins. The non-toxic effect of peptide A on the bacterial cells provides a preliminary insight on a new strategy. This new strategy might create an *in-vivo* scenario that is similar to vaccination with a live, attenuated strain. The bacteria are eventually cleared by the host immune response, with little to no impact on the normal human microbiota (Figure 1.11).

However, this approach, in targeting virulence, can introduce a new generation of potent drugs that principally consists of the cell penetrating peptides conjugated with chemical warheads, whose intervention with the bacterial virulence factors and mechanisms might slow the proceeding of the infection process. With this strategy, more chance can be given for the infected tissue to regulate its immune response clearing out the pathogen with less damage. The strategy of interfering with the secretion of pathogenicity factors rather than with the viability of the bacteria may impose weaker selective pressure for the development of antibiotic resistance relative to current antibiotics. Although all the advantages of such a novel strategy are highly desirable the results presented rather suggest that it would be extremely difficult to achieve drugs with clinical potential with this approach.

1. Ohlsen, K., *Novel antibiotics for the treatment of Staphylococcus aureus.* Expert Review of Clinical Pharmacology, 2009. **2, No. 6**(November 2009): p. 661-672.
2. Ohlsen, K. and U. Lorenz, *Immunotherapeutic strategies to combat staphylococcal infections.* International Journal of Medical Microbiology, 2010. **300**(6): p. 402-410.
3. Wisell, K.T., *Regulation of virulence gene expression in Staphylococcus aureus*, in *Microbiology and Tumor Cell Biology*. 2000, Karolinska Institutes: Stockholm.
4. Manfredi, R. and S. Sabbatani, *Novel pharmaceutical molecules against emerging resistant gram-positive cocci.* Brazilian Journal of Infectious Diseases. **14**(1): p. 96-108.
5. Shompole, S., et al., *Biphasic intracellular expression of Staphylococcus aureus virulence factors and evidence for Agr-mediated diffusion sensing.* Molecular Microbiology, 2003. **49**(4): p. 919-927.
6. Calander, A.M., et al., *Staphylococcus aureus infection triggers production of neutralizing, V8 protease-specific antibodies.* FEMS Immunology and Medical Microbiology, 2008. **52**(2): p. 267-272.
7. Calander, A.-M., *Proteases in Staphylococcal Arthritis.* Thesis in Sahlgrenska Academy, Göteborg University, Sweden, 2007.
8. Sinha, B. and M. Fraunholz, *Staphylococcus aureus host cell invasion and post-invasion events.* International Journal of Medical Microbiology, 2010. **300**(2-3): p. 170-175.
9. Thompson, K.M., N. Abraham, and K.K. Jefferson, *Staphylococcus aureus extracellular adherence protein contributes to biofilm formation in the presence of serum.* FEMS Microbiology Letters. **305**(2): p. 143-147.
10. Nickerson, N.N., et al., *Activation of the SspA serine protease zymogen of Staphylococcus aureus proceeds through unique variations of a trypsinogen-like mechanism and is dependent on both autocatalytic and metalloprotease-specific processing.* Journal of Biological Chemistry, 2007. **282**(47): p. 34129-34138.
11. Gustafsson, E. and J. Oscarsson, *Maximal transcription of aur (aureolysin) and sspA (serine protease) in Staphylococcus aureus requires staphylococcal accessory regulator R (sarR) activity.* FEMS Microbiology Letters 2008. **284**(2): p. 158-164.
12. Shaw, L., et al., *The role and regulation of the extracellular proteases of Staphylococcus aureus.* Microbiology, 2004. **150**(1): p. 217-228.
13. Shaw, L.N., et al., *Cytoplasmic control of premature activation of a secreted protease zymogen: Deletion of staphostatin B (SspC) in Staphylococcus aureus 8325-4 yields a profound pleiotropic phenotype.* Journal of Bacteriology, 2005. **187**(5): p. 1751-1762.
14. Shaw, L.N., et al., *Investigations into Sigma-B-modelated regulatory pathways governing extracellular virulence determinant production in Staphylococcus aureus.* Journal of Bacteriology, 2006. **188**(17): p. 6070-6080.
15. Martí, M., et al., *Extracellular proteases inhibit protein-dependent biofilm formation in Staphylococcus aureus.* Microbes and Infection. **12**(1): p. 55-64.
16. McGavin, M.J., et al., *Modification of the Staphylococcus aureus fibronectin binding phenotype by V8 protease.* Infection and Immunity, 1997. **65**(7): p. 2621-2628.
17. Dubin, G., *Extracellular proteases of Staphylococcus spp.* Biological Chemistry, 2002. **383**(7-8): p. 1075-1086.
18. Rice, K., et al., *Description of staphylococcus serine protease (ssp) operon in Staphylococcus aureus and nonpolar inactivation of sspA-encoded serine protease.* Infection and Immunity, 2001. **69**(1): p. 159-169.
19. Burlak, C., et al., *Global analysis of community-associated methicillin-resistant Staphylococcus aureus exoproteins reveals molecules produced in vitro and during infection.* Cellular Microbiology, 2007. **9**(5): p. 1172-1190.

20. Tamber, S. and A.L. Cheung, *SarZ promotes the expression of virulence factors and represses biofilm formation by modulating SarA and agr in Staphylococcus aureus.* Infection and Immunity, 2009. **77**(1): p. 419-428.
21. Gustafsson, E., *Studies on regulatory networks governing virulence gene transcription in staphylococcus aureus* in *Department of Microbiology, Tumor and Cell Biology*. 2009, Karolinska Institute, Stockholm: Stockholm.
22. Sibbald, M.J.J.B., et al., *Mapping the pathways to staphylococcal pathogenesis by comparative secretomics.* Microbiology and Molecular Biology Reviews, 2006. **70**(3): p. 755-788.
23. Köck, R., et al., *Methicillin-resistant Staphylococcus aureus (MRSA): Burden of disease and control challenges in Europe.* Eurosurveillance, 2011. **15**(41): p. 1-9.
24. Clatworthy, A.E., E. Pierson, and D.T. Hung, *Targeting virulence: A new paradigm for antimicrobial therapy.* Nature Chemical Biology, 2007. **3**(9): p. 541-548.
25. Guilfoile, P.A., Edward *Antibiotic Resistant Bacteria* Deadly Diseases and Epidemics. 2007, New York: Chelsea House Publications/ google books.
26. Heinzl, S., *Neue Antibiotika.* Bericht vom zweiten internationalen Symposium " Resistant Grampositive infections", Berlin, 2004.
27. Steed, M.E., C. Vidaillac, and M.J. Rybak, *Novel daptomycin combinations against daptomycin-nonsusceptible methicillin-resistant Staphylococcus aureus in an in vitro model of simulated endocardial vegetations.* Antimicrobial agents and chemotherapy, 2010. **54**(12): p. 5187-5192.
28. Oyston, P.C.F., et al., *Novel peptide therapeutics for treatment of infections.* Journal of Medical Microbiology, 2009. **58**(8): p. 977-987.
29. Hilpert, K., C.D. Fjell, and A. Cherkasov, *Short linear cationic antimicrobial peptides: screening, optimizing, and prediction.* Methods in molecular biology (Clifton, N.J.), 2008. **494**: p. 127-159.
30. Marr, A.K., W.J. Gooderham, and R.E.W. Hancock, *Antibacterial peptides for therapeutic use: obstacles and realistic outlook.* Current Opinion in Pharmacology, 2006. **6**(5): p. 468-472.
31. Chan, W.C., B.J. Coyle, and P. Williams, *Virulence regulation and quorum sensing in staphylococcal infections: Competitive AgrC antagonists as quorum sensing inhibitors.* Journal of Medicinal chemistry, 2004. **47**(19): p. 4633-4641.
32. Geisinger, E., T.W. Muir, and R.P. Novick, *agr receptor mutants reveal distinct modes of inhibition by staphylococcal autoinducing peptides.* Proceedings of the National Academy of Sciences of the United States of America, 2009. **106**(4): p. 1216-1221.
33. Chan, W.C., *Virulence Regulation and Quorum sensing in Staphylococcal Infections: Competitive ArgC Antagonists as Quorum Sensing Inhibitors.* Journal of Medicinal chemistry, 2004. **47, No. 19**(September 2004).
34. Tuteja, R., *Type I signal peptidase: An overview.* Archives of Biochemistry and Biophysics, 2005. **441**(2): p. 107-111.
35. Haydon, D.J., *An inhibitor of FtsZ with potent and selective anti-staphylococcal activity.* Science (2008);(321): p. 1673
36. Dubin, A., et al., *New generation of peptide antibiotics.* Acta Biochimica Polonica, 2005. **52**(3): p. 633-638.
37. George, E.A., R.P. Novick, and T.W. Muir, *Cyclic Peptide Inhibitors of Staphylococcal Virulence Prepared by Fmoc-Based Thiolactone Peptide Synthesis.* J. Am. Chem. Soc., 2008.

38. Gorske, B.C. and H.E. Blackwell, *Interception of quorum sensing in Staphylococcus aureus: A new niche for peptidomimetics.* Organic and Biomolecular Chemistry, 2006. **4**(8): p. 1441-1445.
39. Musk Jr, D.J. and P.J. Hergenrother, *Chemical countermeasures for the control of bacterial biofilms: Effective compounds and promising targets.* Current Medicinal Chemistry, 2006. **13**(18): p. 2163-2177.
40. Mayville, P., et al., *Structure-activity analysis of synthetic autoinducing thiolactone peptides from Staphylococcus aureus responsible for virulence.* Proceedings of the National Academy of Sciences of the United States of America, 1999. **96**(4): p. 1218-1223.
41. Thoendel, M., et al., *Peptide signaling in the Staphylococci.* Chemical Reviews. **111**(1): p. 117-151.
42. Mcdowell, P., et al., *Structure, activity and evolution of the group I thiolactone peptide quorum-sensing system of Staphylococcus aureus.* Molecular Microbiology, 2001. **41**(2): p. 503-512.
43. Jensen, R.O., et al., *Differential Recognition of Staphylococcus aureus Quorum-Sensing Signals Depends on Both Extracellular Loops 1 and 2 of the Transmembrane Sensor AgrC.* Journal of Molecular Biology, 2008. **381**(2): p. 300-309.
44. Shigenaga, A., et al., *Solid-phase synthesis and cyclative cleavage of quorum sensing depsipeptide analogues by acylphenyldiazene activation.* Synlett, 2006(4): p. 551-554.
45. Scott, R.J., Lu-Yun Lian, S. Hanna Muharram, Alan Cockayne, Stewart J. Wood, Barrie W. Bycroft, Paul Williams and Weng C. Chan, *Side-Chain-to-Tail Thiolactone Peptide Inhibitors of the Staphylococcal Quorum-Sensing System.* Bioorganic & Medicinal Chemistry Letters, 2003. **13**: p. 2449–2453.
46. Giacometti, A., *RNA III inhibiting peptide inhibits in vivo biofilm formation by drug resistant staphylococcus aureus.* Antimicrobial agents and chemotherapy, 2003. **47, No.6**: p. 1979-1983.
47. Balaban, N., et al., *Use of the quorum-sensing inhibitor RNAIII-inhibiting peptide to prevent biofilm formation in vivo by drug-resistant Staphylococcus epidermidis.* Journal of Infectious Diseases, 2003. **187**(4): p. 625-630.
48. Cirioni, O., et al., *RNAIII-inhibiting peptide affects biofilm formation in a rat model of staphylococcal ureteral stent infection.* Antimicrobial agents and chemotherapy, 2007. **51**(12): p. 4518-4520.
49. Simonetti, O., et al., *RNAIII-inhibiting peptide enhances healing of wounds infected with methicillin-resistant Staphylococcus aureus.* Antimicrobial agents and chemotherapy, 2008. **52**(6): p. 2205-2211.
50. Gordon Bruton a, Anthony Huxley a, Peter O'Hanlon a, Barry Orlek, *Lipopeptide substrates for SpsB, the Staphylococcus aureus type I signal peptidase: design, conformation and conversion to α-ketoamide inhibitors.* European Journal of Medicinal Chemistry 2003. **38**: p. 351-356.
51. Buzder-Lantos, P., et al., *Substrate based peptide aldehyde inhibits bacterial type I signal peptidase.* Bioorganic and Medicinal Chemistry Letters, 2009. **19**(10): p. 2880-2883.
52. Powers, M.E., *Type I Signal Peptidase and Protein Secretion in Staphylococcus epidermidis.* JOURNAL OF BACTERIOLOGY, 2011. **Jan. 2011**: p. 340–348.
53. Jang, M.-Y., *Synthesis of novel 5-amino-thiazolo[4,5-d]pyrimidines as E. coli and S. aureus SecA inhibitors.* Bioorganic & Medicinal Chemistry Letters, 2011. **19**: p. 702-714.
54. Kudryavtsev, K.V., *Probing of the cis-5-phenyl proline scaffold as a platform for the synthesis of mechanism-based inhibitors of the Staphylococcus aureus sortase SrtA isoform.* Bioorganic & Medicinal Chemistry Letters, 2009). **17**: p. 2886–2893.

55. Maresso, A.W. and O. Schneewind, *Sortase as a target of anti-infective therapy.* Pharmacological Reviews, 2008. **60**(1): p. 128-141.
56. Wang, W., R. White, and Z. Yuan, *Proteomic study of peptide deformylase inhibition in Streptococcus pneumoniae and Staphylococcus aureus.* Antimicrobial agents and chemotherapy, 2006. **50**(5): p. 1656-1663.
57. Driessen, A.J.M.N., Nico *Protein Translocation Across the Bacterial Cytoplasmic Membrane.* The Annual Review of Biochemistry, 2008. **77**: p. 643–67.
58. Biswas, L., et al., *Role of the twin-arginine translocation pathway in Staphylococcus.* Journal of Bacteriology, 2009. **191**(19): p. 5921-5929.
59. Natale, P., T. Brüser, and A.J.M. Driessen, *Sec- and Tat-mediated protein secretion across the bacterial cytoplasmic membrane "Distinct translocases and mechanisms"*. 2008.
60. Rigel, N.W. and M. Braunstein, *A new twist on an old pathway - Accessory secretion systems.* Molecular Microbiology, 2008. **69**(2): p. 291-302.
61. Sundaramoorthy, R., P.K. Fyfe, and W.N. Hunter, *Structure of Staphylococcus aureus EsxA Suggests a Contribution to Virulence by Action as a Transport Chaperone and/or Adaptor Protein.* Journal of Molecular Biology, 2008. **383**(3): p. 603-614.
62. Burts, M.L., A.C. DeDent, and D.M. Missiakas, *EsaC substrate for the ESAT-6 secretion pathway and its role in persistent infections of Staphylococcus aureus.* Molecular Microbiology, 2008. **69**(3): p. 736-746.
63. Yamada, K., et al., *Analysis of twin-arginine translocation pathway homologue in Staphylococcus aureus.* Current Microbiology, 2007. **55**(1): p. 14-19.
64. Khoon, L.Y. and V. Neela, *Secretome of Staphylococcus aureus.* African Journal of Microbiology Research, 2010. **4**(7): p. 500-508.
65. du Plessis, D.J.F., Nico Nouwen, Arnold J.M. Driessen, *The Sec translocase.* Biochimica et Biophysica Acta, 2010.
66. Papanikou, E., S. Karamanou, and A. Economou, *Bacterial protein secretion through the translocase nanomachine.* Nat Rev Micro, 2007. **5**(11): p. 839-851.
67. Sarvas, M., et al., *Post-translocational folding of secretory proteins in Gram-positive bacteria.* Biochimica et Biophysica Acta - Molecular Cell Research, 2004. **1694**(1-3 SPEC.ISS.): p. 311-327.
68. Paetzel, M.K., Andrew ; Strynadka, Natalie C. J. ; Dalbey,Ross E. , *Signal Peptidases.* Chemical Reviews, 2002. **102**: p. 4549-4579.
69. Suree, N., et al., *The structure of the Staphylococcus aureus sortase-substrate complex reveals how the universally conserved LPXTG sorting signal is recognized.* Journal of Biological Chemistry, 2009. **284**(36): p. 24465-24477.
70. Sibbald, M.J.J.B., *The Staphylococcus aureus secretome*. 2010, University of Groningen: Enschede.
71. Quiblier, C., et al., *Contribution of SecDF to Staphylococcus aureus resistance and expression of virulence factors.* BMC Microbiology, 2011. **11**.
72. Sibbald, M.J.J.B., et al., *Synthetic effects of secG and secY2 mutations on exoproteome biogenesis in Staphylococcus aureus.* Journal of Bacteriology, 2010. **192**(14): p. 3788-3800.
73. Tjalsma, H., et al., *Proteomics of protein secretion by Bacillus subtilis: Separating the "secrets" of the secretome.* Microbiology and Molecular Biology Reviews, 2004. **68**(2): p. 207-233.
74. Brooks, H., B. Lebleu, and E. Vivˆ¨s, *Tat peptide-mediated cellular delivery: Back to basics.* Advanced Drug Delivery Reviews, 2005. **57**(4 SPEC.ISS.): p. 559-577.

75. Segers, K. and J. Anne, *Traffic jam at the bacterial sec translocase: Targeting the SecA nanomotor by small-molecule inhibitors.* Chemistry and Biology, 2011. **18**(6): p. 685-698.
76. Willing, B.P., S.L. Russell, and B.B. Finlay, *Shifting the balance: Antibiotic effects on host-microbiota mutualism.* Nature Reviews Microbiology, 2011. **9**(4): p. 233-243.
77. Nilsson, B.L.S., Matthew B., and Raines Ronald T. , *Chemical Synthesis of Proteins.* Annual Revview of Biophysics and Biomolecular Structure, 2005. **34** p.: 91–118.
78. Balalaie, S., M. Mahdidoust, and R. Eshaghi-Najafabadi, *2-(1H-benzotriazole-1-yl)-1,1,3,3-tetramethyluronium tetrafluoroborate as an efficient coupling reagent for the amidation and phenylhydrazation of carboxylic acids at room temperature.* Journal of the Iranian Chemical Society, 2007. **4**(3): p. 364-369.
79. Vive`s, E., P. Brodin, and B. Lebleu, *A truncated HIV-1 Tat protein basic domain rapidly translocates through the plasma membrane and accumulates in the cell nucleus.* Journal of Biological Chemistry, 1997. **272**(25): p. 16010-16017.
80. Vive`s, E., *Cellular utake of the Tat peptide: An endocytosis mechanism following ionic interactions.* Journal of Molecular Recognition, 2003. **16**(5): p. 265-271.
81. Gräslund, A., et al., *Mechanisms of cellular uptake of cell-penetrating peptides.* Journal of Biophysics, 2011.
82. Trabulo, S., et al., *Cell-penetrating peptides-mechanisms of cellular uptake and generation of delivery systems.* Pharmaceuticals, 2010. **3**(4): p. 961-993.
83. Langel, Ü., *Cell-penetrating peptides: Processes and applications*. Pharmacology and Toxicology Series, ed. C. Press. 2002, Florida, Boca Raton: CRC Press. 406.
84. Deshayes, S., et al., *Delivery of proteins and nucleic acids using a non-covalent peptide-based strategy.* Advanced Drug Delivery Reviews, 2008. **60**(4-5): p. 537-547.
85. Geueke, B., et al., *Bacterial cell penetration by B3-oligohomoarginines: Indications for passive transfer through the lipid bilayer.* ChemBioChem, 2005. **6**(6): p. 982-985.
86. Kloك, A., et al., *The cell-penetrating peptide octa-arginine is a potent inhibitor of proteasome activities.* European Journal of Pharmaceutics and Biopharmaceutics, 2009. **72**(1): p. 219-225.
87. Rajarao, G.K., *Peptide-mediated delivery of green fluorescent protein into yeasts and bacteria.* FEMS Microbiology Letters, 2002. **215**: p. 267-272.
88. Bhat, K.G., B.K. Hedge, and P.G. Shivananda, *A modified chemically defined medium for Staphylococcus aureus.* Indian Journal of Experimental Biology, 1993. **31**(12): p. 948-950.
89. Miedzobrodzki, et al., *Proteolytic Activity of Staphylococcus aureus Strains Isolated from the Colonized Skin of Patients with Acute-Phase Atopic Dermatitis.* European Journal of Clinical Microbiology & Infectious Diseases, 2002. **21**(4): p. 269-276.
90. Arvidson, S., T. Holme, and B. Lindholm, *Studies on extracellular proteolytic enzymes from Staphylococcus aureus. I. Purification and characterization of one neutral and one alkaline protease.* BBA - Enzymology, 1973. **302**(1): p. 135-148.
91. Arvidson, S., *Studies on extracellular proteolytic enzymes from Staphylococcus aureus. II. Isolation and characterization of an EDTA-sensitive protease.* BBA - Enzymology, 1973. **302**(1): p. 149-157.
92. Karlsson, A. and S. Arvidson, *Variation in extracellular protease production among clinical isolates of Staphylococcus aureus due to different levels of expression of the protease repressor sarA.* Infection and Immunity, 2002. **70**(8): p. 4239-4246.
93. Bjorklind, A. and S. Arvidson, *Influence of amino acids on the synthesis of an extracellular proteinase from Staphylococcus aureus.* Journal of General Microbiology, 1978. **107**(2): p. 367-375.

94. Saheb, S.A., *Purification and characterization of an extracellular protease from Staphylococcus aureus, inhibited by E.D.T.A.* Biochemie, 1976. **58**(7): p. 793-804.
95. Arvidson, S., T. Holme, and T. Wadstrom, *Formation of Bacteriolytic Enzymes in Batch and Continuous Culture of Staphylococcus aureus.* J. Bacteriol., 1970. **104**(1): p. 227-233.
96. Karlsson, A., et al., *Decreased amounts of cell wall-associated protein A and fibronectin-binding proteins in Staphylococcus aureus sarA mutants due to up-regulation of extracellular proteases.* Infection and Immunity, 2001. **69**(8): p. 4742-4748.
97. Karlsson-Kanth, A., et al., *Natural human isolates of Staphylococcus aureus selected for high production of proteases and Î±-hemolysin are ÏfB deficient.* International Journal of Medical Microbiology, 2006. **296**(4-5): p. 229-236.
98. Vive`s, E. and B. Lebleu, *One-pot labeling and purification of peptides and proteins with fluorescein maleimide.* Tetrahedron Letters, 2003. **44**(29): p. 5389-5391.
99. Singh, S., et al., *Addition of o-aminobenzoic acid during Fmoc solid phase synthesis of a fluorogenic substrate containing 3-nitrotyrosine.* Letters in Peptide Science, 2002. **9**(4-5): p. 221-225.
100. Yabuta, M., S. Onai-Miura, and K. Ohsuye, *Isolation and characterization of urea-resistant Staphylococcus aureus V8 protease derivatives.* Journal of Fermentation and Bioengineering, 1995. **80**(3): p. 237-243.
101. Breddam, K. and M. Meldal, *Substrate preferences of glutamic-acid-specific endopeptidases assessed by synthetic Peptide Substrates based on intramolecular fluorescence quenching.* European Journal of Biochemistry, 1992. **206**(1): p. 103-107.
102. Pieper, R., et al., *Comparative proteomic analysis of Staphylococcus aureus strains with differences in resistance to the cell wall-targeting antibiotic vancomycin.* Proteomics, 2006. **6**(15): p. 4246-4258.
103. Fischer, P.M., *Cellular uptake mechanisms and potential therapeutic utility of peptidic cell delivery vectors: Progress 2001-2006.* Medicinal Research Reviews, 2007. **27**(6): p. 755-795.
104. Solbiati, J., et al., *Processing of the N termini of nascent polypeptide chains requires deformylation prior to methionine removal.* Journal of Molecular Biology, 1999. **290**(3): p. 607-614.
105. De Beer, T., et al., *Molecular mechanism of NPF recognition by EH domains.* Nature Structural Biology, 2000. **7**(11): p. 1018-1022.
106. Conner, S.D. and S.L. Schmid, *Regulated portals of entry into the cell.* Nature, 2003. **422**(6927): p. 37-44.
107. Kawai, M., et al., *Cell-wall thickness: Possible mechanism of acriflavine resistance in meticillin-resistant Staphylococcus aureus.* Journal of Medical Microbiology, 2009. **58**(3): p. 331-336.
108. Zajic, G., A. Forge, and J. Schacht, *Membrane stains as an objective means to distinguish isolated inner and outer hair cells.* Hearing Research, 1993. **66**(1): p. 53-57.
109. Wan Long Zhu, S.Y.S., *Effects of dimerization of the cell-penetrating peptide Tat analog on antimicrobial activity and mechanism of bactericidal action.* Journal of peptide science, 2009. **15**(5): p. 345-352.
110. Vives, E., *Cellular utake of the Tat peptide: An endocytosis mechanism following ionic interactions.* Journal of Molecular Recognition, 2003. **16**(5): p. 265-271.
111. Ohara-Nemoto, Y., et al., *Characterization and molecular cloning of a glutamyl endopeptidase from Staphylococcus epidermidis.* Microbial Pathogenesis, 2002. **33**(1): p. 33-41.

112. Potempa, J., et al., *Proteolytic inactivation of α-1-anti-chymotrypsin. Sites of cleavage and generation of chemotactic activity.* Journal of Biological Chemistry, 1991. **266**(32): p. 21482-21487.
113. Potempa, J., W. Watorek, and J. Travis, *The inactivation of human plasma α1-proteinase inhibitor by proteinases from Staphylococcus aureus.* Journal of Biological Chemistry, 1986. **261**(30): p. 14330-14334.
114. Potempa, J., et al., *Staphylococcus aureus proteinase as mediators of inflammatory reaction.* The Staphylococci, Zbl Bakt, 1991(SUPPL. 21): p. 187-188.
115. Kwak, Y.K., et al., *Biological Relevance of Natural a-Toxin Fragments from Staphylococcus aureus.* Journal of Membrane Biology: p. 1-11.
116. Ziebandt AK, W.H., Rudolph J, Schmid R, Höper D, Engelmann S, Hecker M, *Extracellular proteins of Staphylococcus aureus and the role of SarA and sigma B.* Proteomics, 2001. **1**(1): p. 480-493.
117. Coleman, G., M. Aboshkiwa, and B. Al-Ani, *The effect of glucose on the expression of extracellular protein genes by Staphylococcus aureus strain V8.* FEMS Microbiology Letters, 1989. **61**(3): p. 247-250.
118. Ono, T., et al., *Comparison of conformations of κ-casein, para-κ-casein and glycomacropeptide.* Biochimica et Biophysica Acta - Protein Structure and Molecular Enzymology, 1987. **911**(3): p. 318-325.
119. Arvidson, S., *Hydrolysis of casein by three extracellular proteolytic enzymes from Staphylococcus aureus, strain V8.* Acta Pathologica et Microbiologica Scandinavica - Section B Microbiology and Immunology, 1973. **81 B**(5): p. 538-544.
120. Tsukatani, T., et al., *Colorimetric cell proliferation assay for microorganisms in microtiter plate using water-soluble tetrazolium salts.* Journal of Microbiological Methods, 2008. **75**(1): p. 109-116.
121. Lammers, A., P.J.M. Nuijten, and H.E. Smith, *The fibronectin binding proteins of Staphylococcus aureus are required for adhesion to and invasion of bovine mammary gland cells.* FEMS Microbiology Letters, 1999. **180**(1): p. 103-109.
122. Yabuta, M., N. Ochi, and K. Ohsuye, *Hyperproduction of a recombinant fusion protein of Staphylococcus aureus V8 protease in Escherichia coli and its processing by OmpT protease to release an active V8 protease derivative.* Applied Microbiology and Biotechnology, 1995. **44**(1-2): p. 118-125.
123. Houmard, J. and G.R. Drapeau, *Staphylococcal protease: a proteolytic enzyme specific for glutamoyl bonds.* Proceedings of the National Academy of Sciences of the United States of America, 1972. **69**(12): p. 3506-3509.
124. Berger, K., et al., *Quantitative proteome analysis in benign thyroid nodular disease using the fluorescent ruthenium II tris(bathophenanthroline disulfonate) stain.* Molecular and Cellular Endocrinology, 2004. **227**(1-2): p. 21-30.
125. Heidebrecht, F., et al., *Improved semiquantitative Western blot technique with increased quantification range.* Journal of Immunological Methods, 2009. **345**(1-2): p. 40-48.
126. Fu, H., C. Dahlgren, and J. Bylund, *Subinhibitory concentrations of the deformylase inhibitor actinonin increase bacterial release of neutrophil-activating peptides: A new approach to antimicrobial chemotherapy.* Antimicrobial agents and chemotherapy, 2003. **47**(8): p. 2545-2550.
127. Mader, D., et al., *Formyl peptide receptor-mediated proinflammatory consequences of peptide deformylase inhibition in Staphylococcus aureus.* Microbes and Infection. **12**(5): p. 415-419.
128. Fagerlund, A., T. Lindbäck, and P.E. Granum, *Bacillus cereus cytotoxins Hbl, Nhe and CytK are secreted via the Sec translocation pathway.* BMC Microbiology, 2010. **10**.

129. Kuroda, A., et al., *Isolation and characterization of light-dependent hemolytic cytotoxin from harmful red tide phytoplankton Chattonella marina.* Comparative Biochemistry and Physiology Part C: Toxicology & Pharmacology, 2005. **141**(3): p. 297-305.
130. Park, P.W., et al., *Binding and degradation of elastin by the staphylolytic enzyme lysostaphin.* International Journal of Biochemistry and Cell Biology, 1995. **27**(2): p. 139-146.
131. Facey, S.J. and A. Kuhn, *Biogenesis of bacterial inner-membrane proteins.* Cellular and Molecular Life Sciences, 2010. **67**(14): p. 2343-2362.
132. Xie, K. and R.E. Dalbey, *Inserting proteins into the bacterial cytoplasmic membrane using the Sec and YidC translocases.* Nature Reviews Microbiology, 2008. **6**(3): p. 234-244.
133. David, R., M.P.O. Richter, and A.G. Beck-Sickinger, *Expressed protein ligation: Method and applications.* European Journal of Biochemistry, 2004. **271**(4): p. 663-677.
134. Coin, I., M. Beyermann, and M. Bienert, *Solid-phase peptide synthesis: from standard procedures to the synthesis of difficult sequences.* Nat. Protocols, 2007. **2**(12): p. 3247-3256.
135. Malik, L., et al., *Automated 'X-Y' robot for peptide synthesis with microwave heating: Application to difficult peptide sequences and protein domains.* Journal of peptide science, 2010. **16**(9): p. 506-512.
136. Subiros-Funosas, R., et al., *Microwave irradiation and COMU: a potent combination for solid-phase peptide synthesis.* Tetrahedron Letters, 2009. **50**(45): p. 6200-6202.
137. Avdeeva, O.N., et al., *Construction of the 'minimal' SRP that interacts with the translating ribosome but not with specific membrane receptors in Escherichia coli.* FEBS Letters, 2002. **514**(1): p. 70-73.

1) List of Figures

2) TABLES

1 Appendix-I: Fmoc solid phase synthesis of the cell penetrating peptides

As described in chapter IV, three peptide constructs were described in Rajarao *et al*. [87]. These peptides were chemically generated by the Fmoc solid phase approach. They are shown in table 5.1

Table 5.1 List of the cell penetrating peptides synthesized by Fmoc solid phase peptide synthesis.

Construct	Sequence (labeled with F5M)	Molar mass (monoisotopic)	MALDI mass
Peptide-1	VLTNENPFSDPC(fluor)-amide	1759.6	1760
Peptide-2	RSNNPFRARC(fluor)-amide	1644.6	1645
Peptide-3	YGRKKRRQRRRC(fluor)-amide	2087.9	2089

1.1 Peptide-1

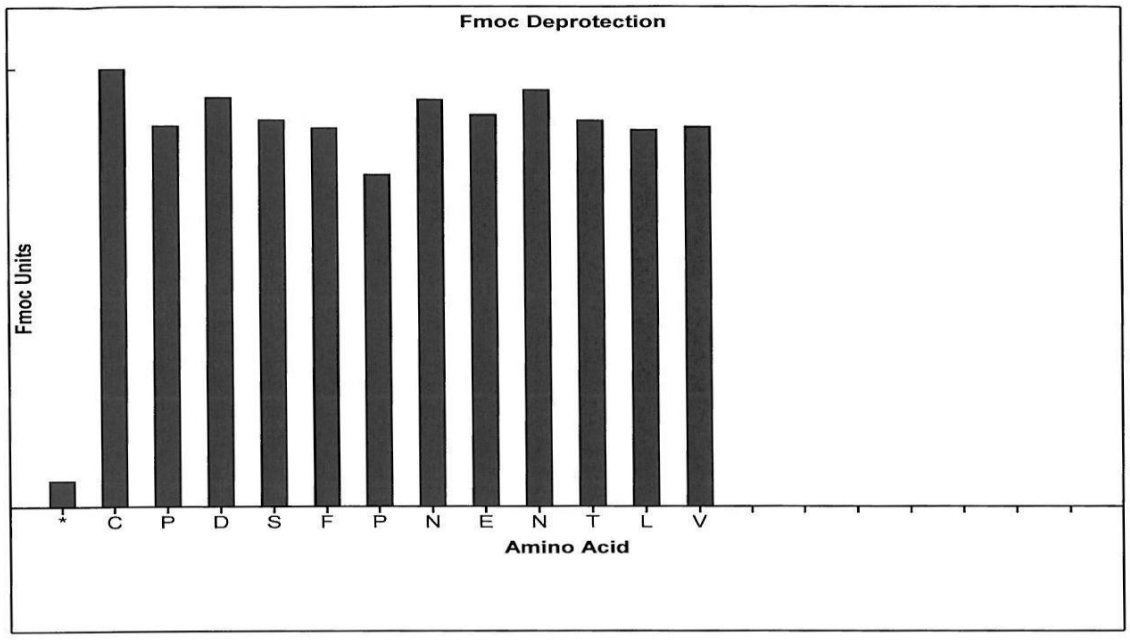

Figure 1 The Fmoc deprotection profile shows the successful synthesis process of peptide-1 by the Pioneer peptide syntheisizer.

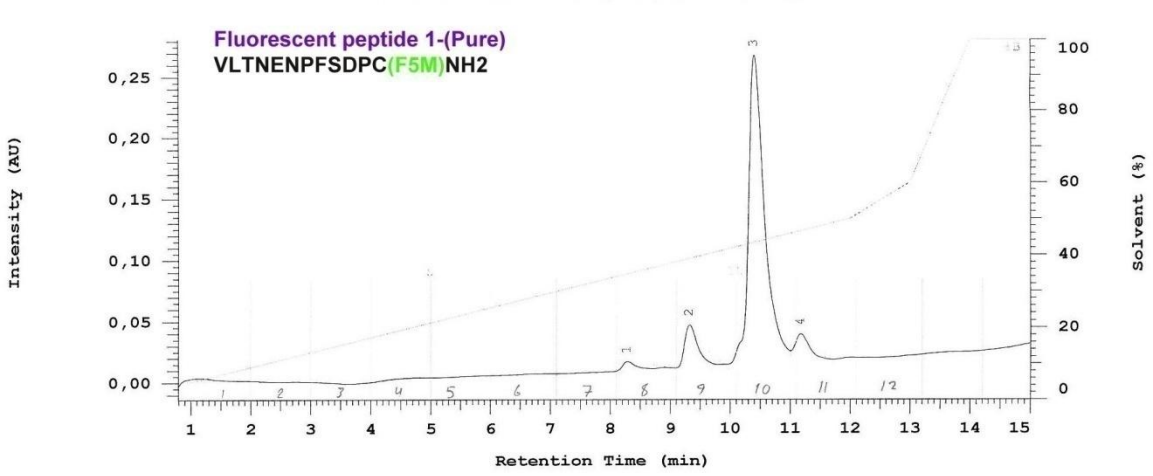

Figure 2 The HPLC chromatogram of the purified peptide-1 shows a major peak with some minor peaks.

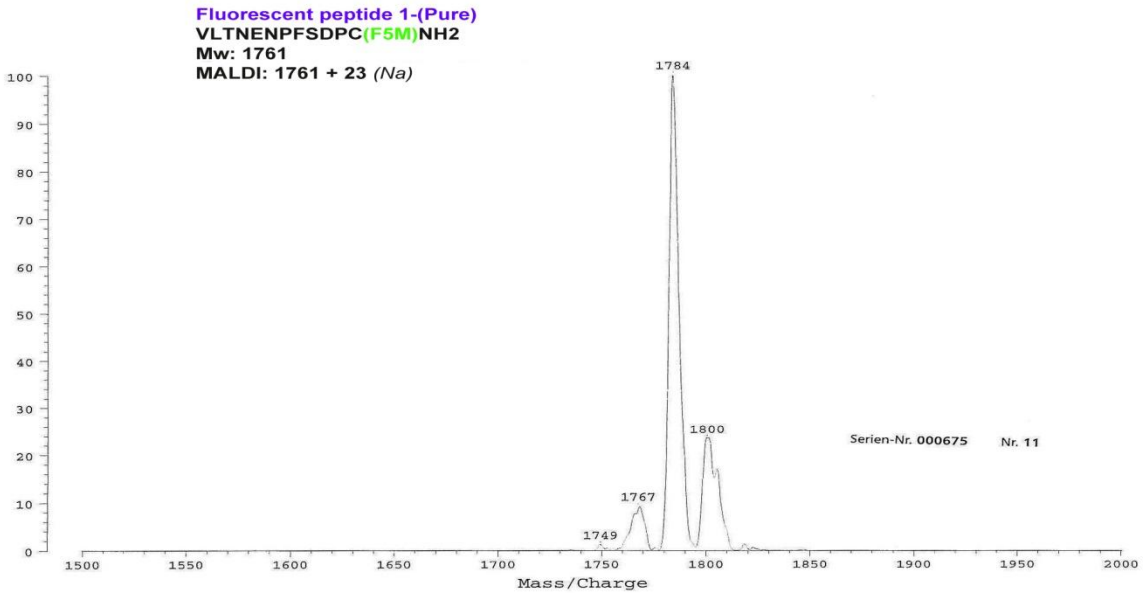

Figure 3 MALDI-TOF spectrum shows a measured mass of the purified peptide-1.

1.2 Peptide-2

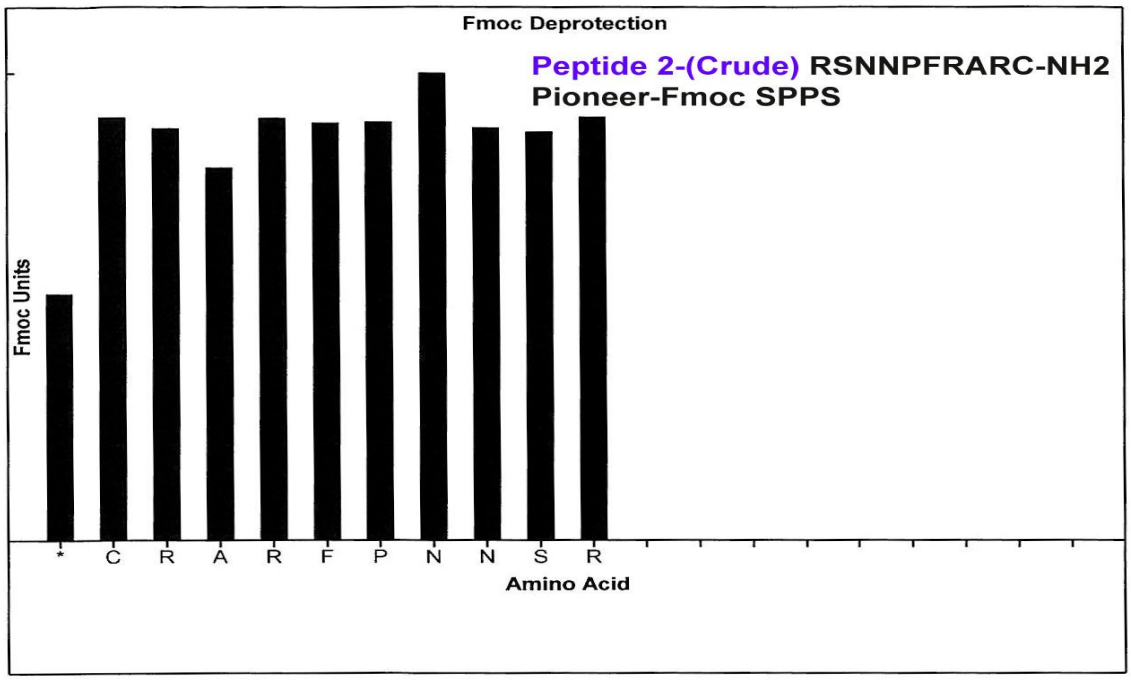

Figure 4 The Fmoc deprotection profile is an indication of successful synthesis of peptide-2 by the Pioneer peptide synthesizer.

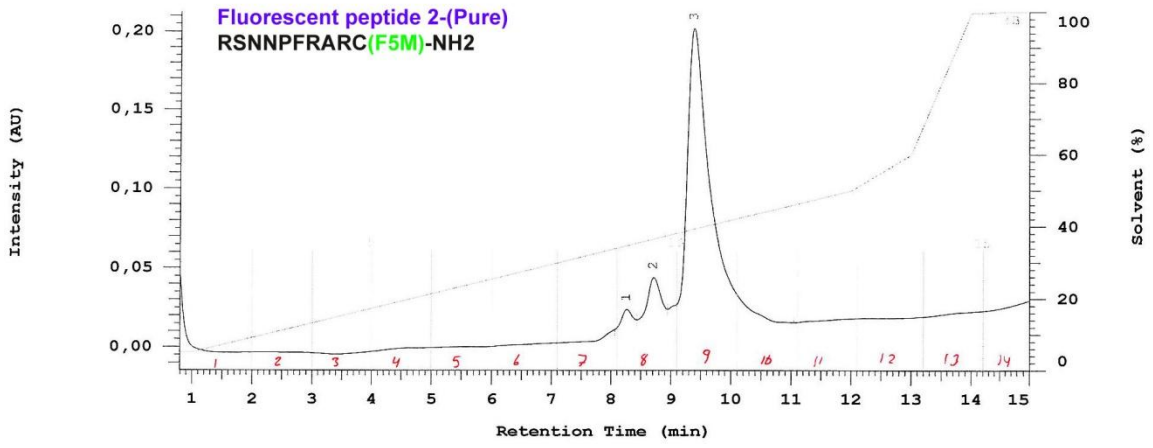

Figure 5 The HPLC chromatogram of the purified peptide-2 shows a major peak with two minor peaks.

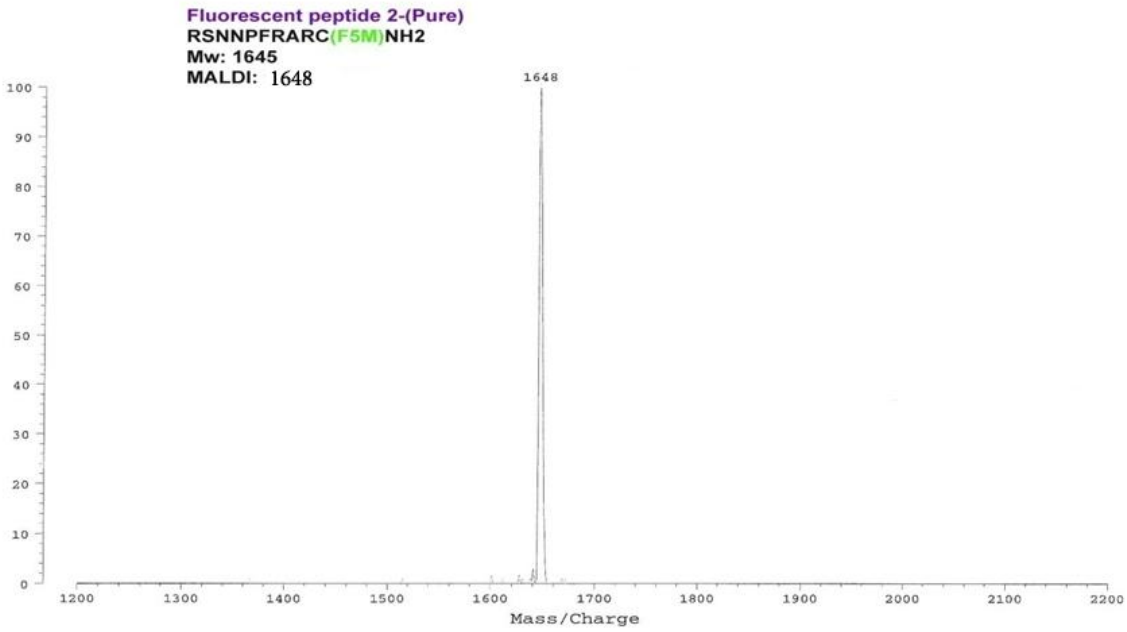

Figure 6 The MALDI-TOF spectrum shows the expected molecular mass of peptide-2.

1.3 Peptide-3

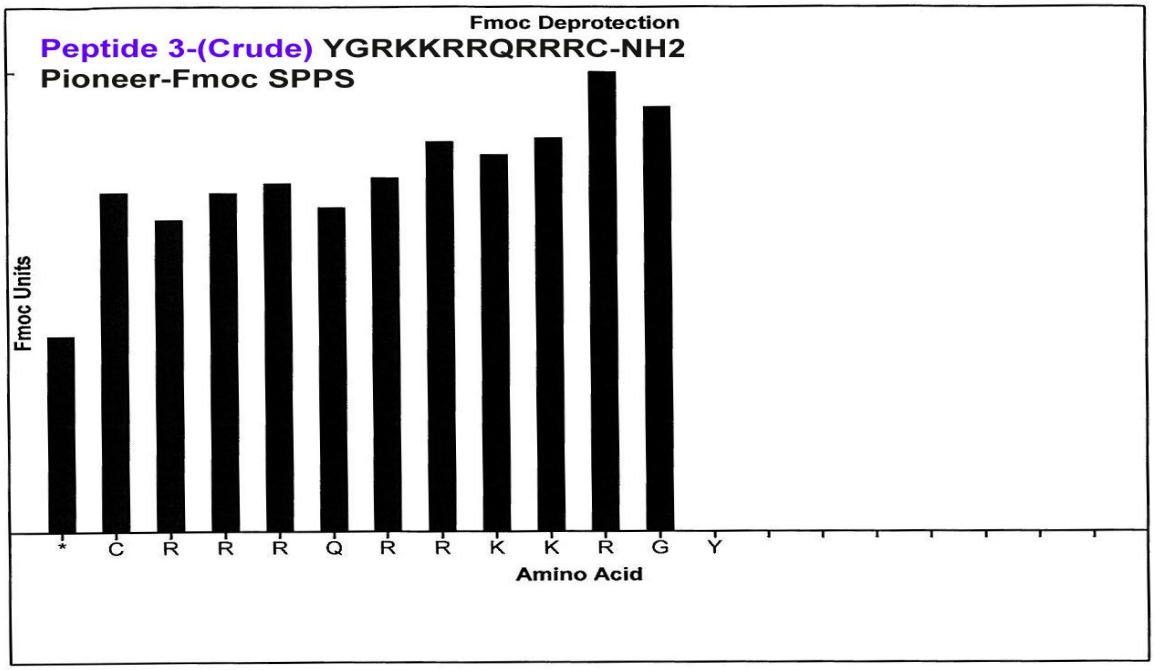

Figure 7 The Fmoc deprotection protocol of the Pioneer peptide synthesizer indicates the coupling of the amino acids of peptide-3.

.

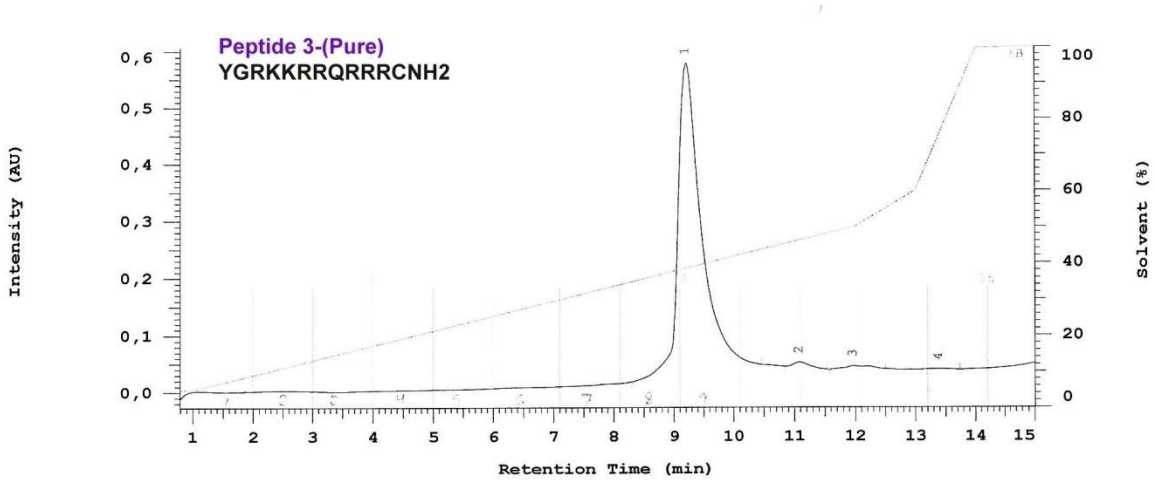

Figure 8 HPLC chromatogram of the purified peptide-3 before labeling with fluorescein-5-maleimide (F5M).

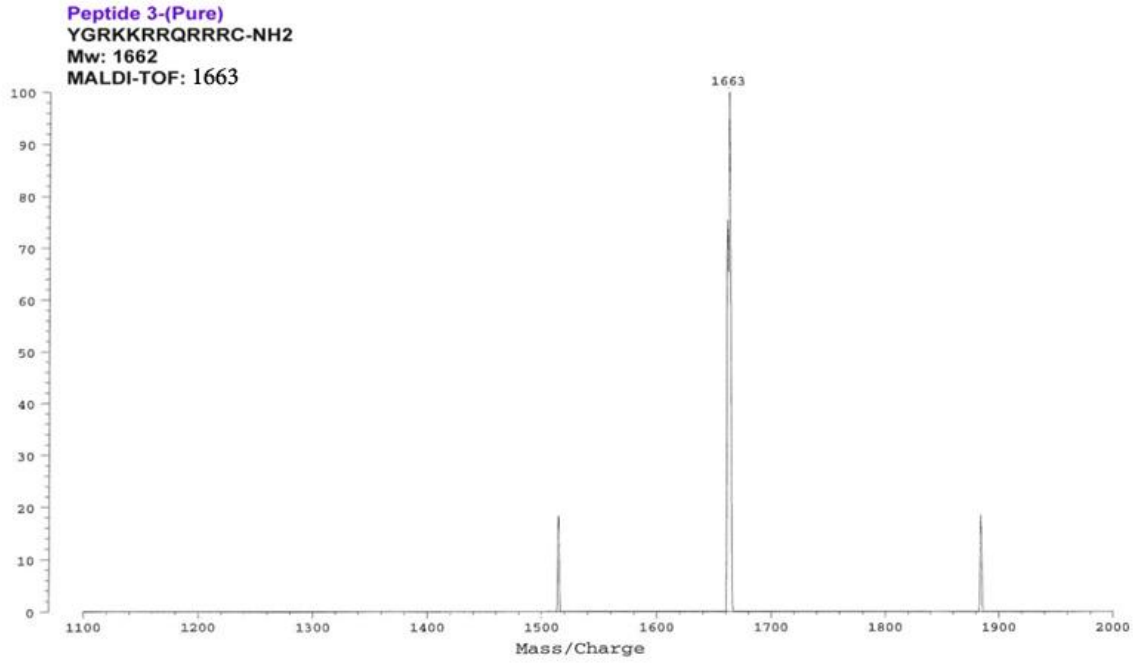

Figure 9 MALDI-TOF spectrum of peptide-3 (pure) before it was labeled with fluorescein-5-maleimide (F5M).

Peptide-3 was purified and chemically coupled to fluorescein-5-maleimide (F5M), then it was purified by RP-HPLC. Further analysis and mass determination confirmed the successful synthesis of fluorescent peptides. See figures 10 and 11.

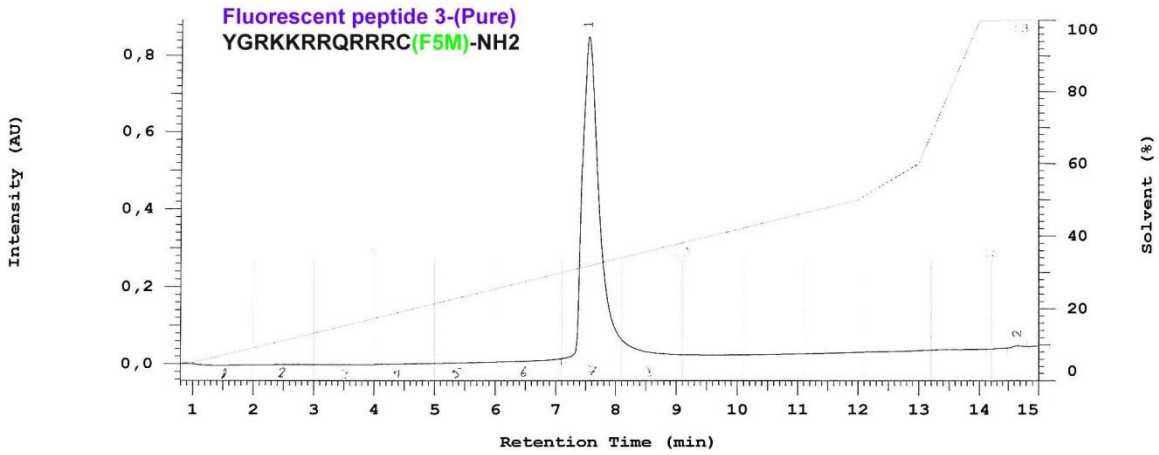

Figure 10 HPLC chromatogram of peptide-3 after labeling with fluorescein-5-maleimide.

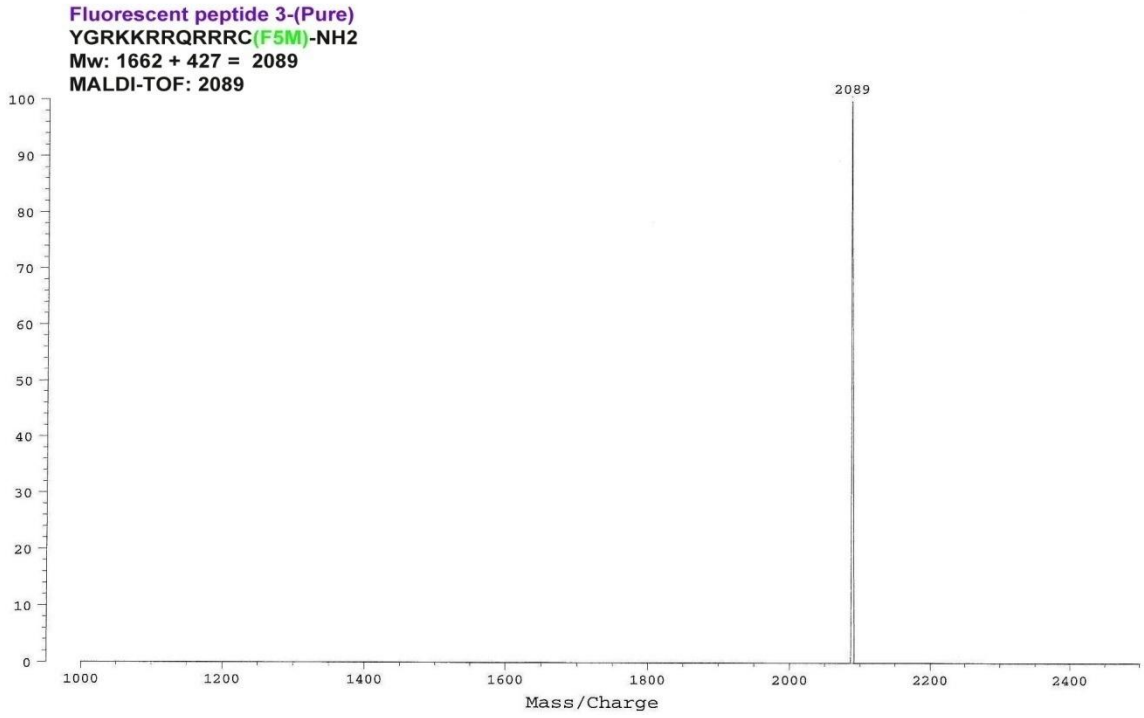

Figure 11 The MALDI-TOF spectrum shows the expected mass of the purified peptide-3.

2 Appendix-II: Fmoc solid phase synthesis of the potentially Sec- interfering peptides

Table 5.2 List of the potentially Sec- interfering peptides and their controls synthesized by Fmoc solid phase peptide synthesis.

Construct	Sequence	monoisotopic mass	Empirical mass
Peptide A	KGKFLKVSSLFVATLTTATLVSSPAANA-YGRKKRRQRRR-NH_2	4362.5	4362
Peptide B	MKGKFLKVSSLFVATLTTATLVSSPAANA-YGRKKRRQRRR-NH_2	4492.6	4493
Peptide C	For-MKGKFLKVSSLFVATLTTATLVSSPAANA-YGRKKRRQRRR-NH_2	4520.6	4521
Peptide D	YGRKKRRQRRRC-NH_2	1658.9	1662
Peptide E	KGKFLKVSSLFVATLTTATLVSSPAANA-NH_2	2820.6	2821
Peptide F	MKGKFLKVSSLFVATLTTATLVSSPAANA-NH_2	2951.7	2951
Peptide G	For-MKGKFLKVSSLFVATLTTATLVSSPAANA-NH_2	2979.6	2980
Peptide H	AAMGNSFVLSTLTKTKPAFLTLVASASVK-YGRKKRRQRRR-NH_2	4492.6	4494

2.1 Peptide A

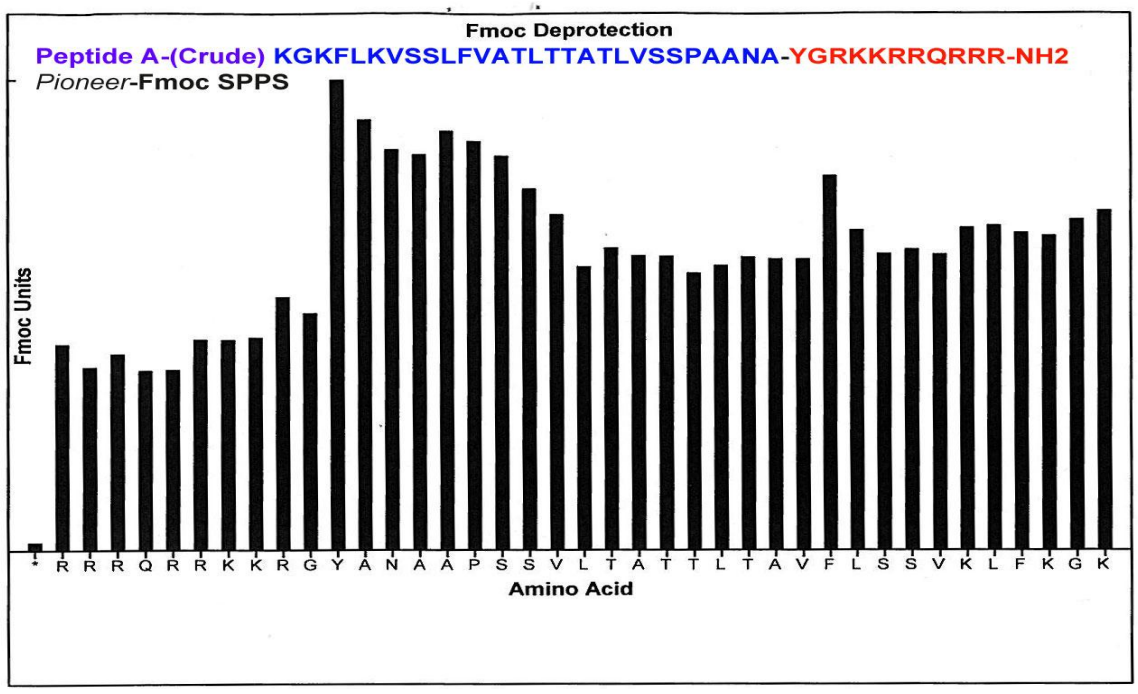

Figure 12 The Fmoc deprotection protocol of the Pioneer peptide synthesizer indicates successful amino acid couplings of peptide A.

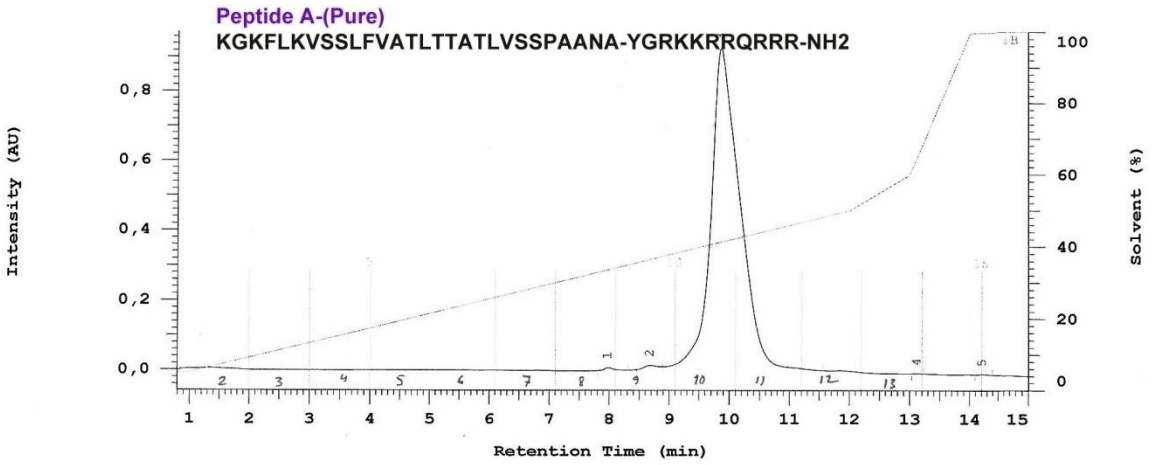

Figure 13 The HPLC chromatogram of the purified peptide A shows a single peak.

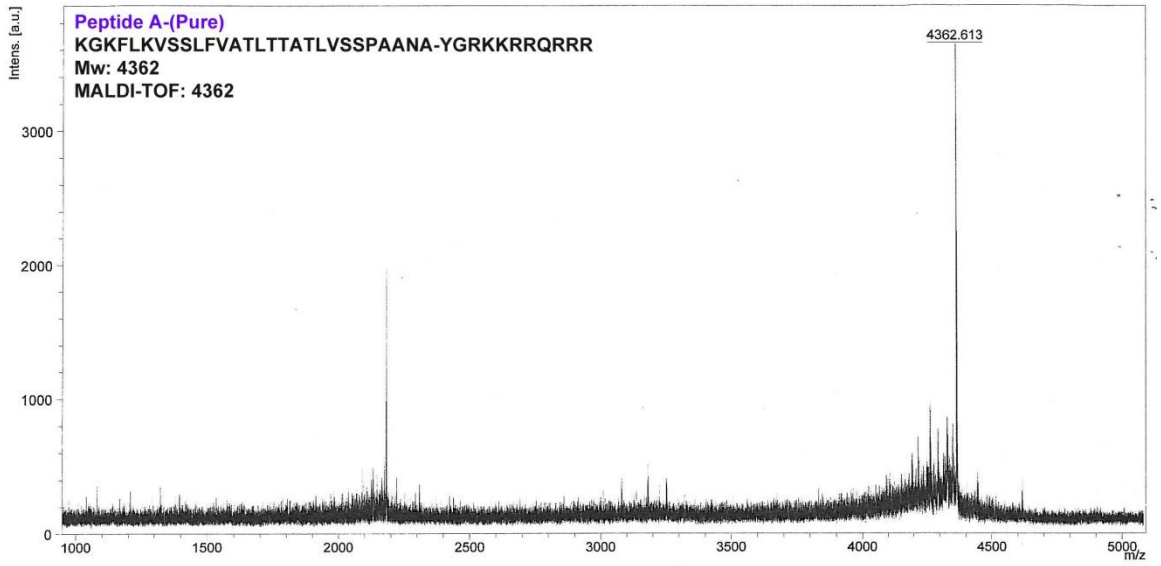

Figure 14 The MALDI-TOF spectrum shows the expected mass of the purified peptide A, while the small peak at m/z 2181 is the double-charged mass of peptide A.

2.2 Peptide B

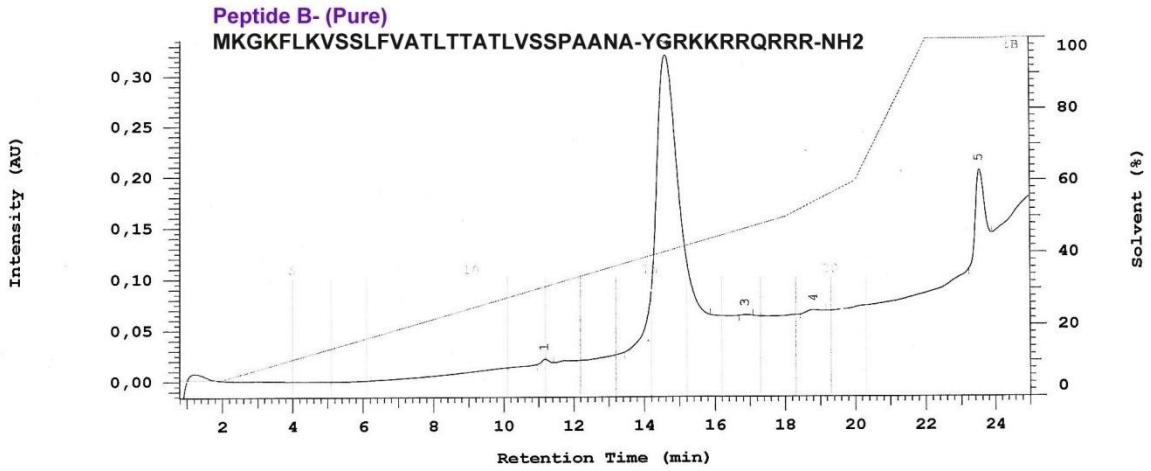

Figure 15 The HPLC chromatogram of the purified peptide B shows a majorproduct peak with a late peak of unkown identity.

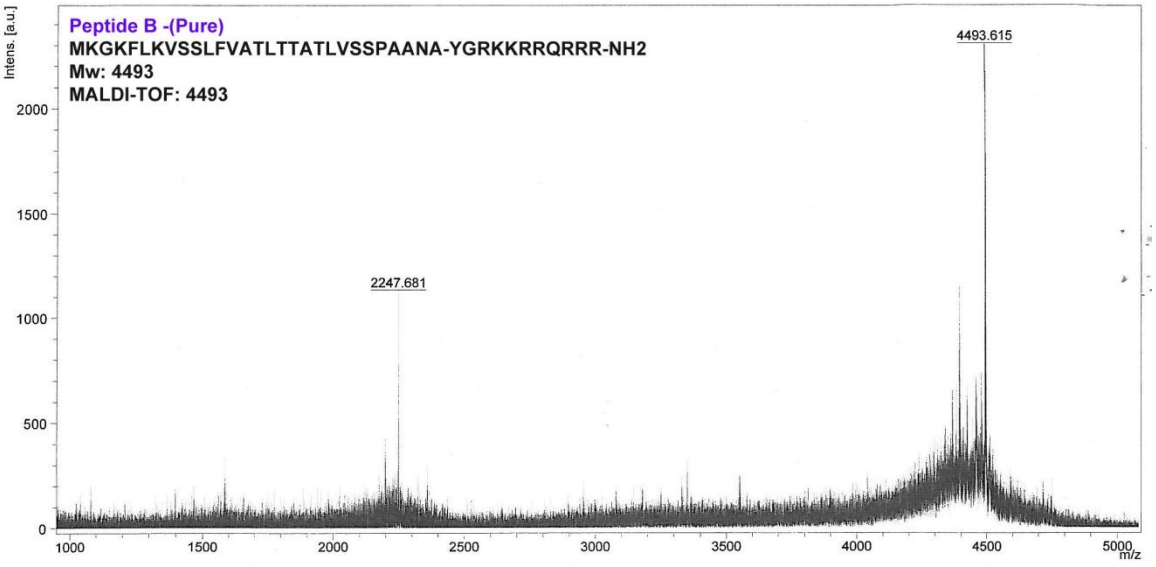

Figure 16 The MALDI-TOF spectrum shows the expected mass of the purified peptide B, while the mass at m/z 2247 is the double charged mass of peptide B.

2.3 Peptide C

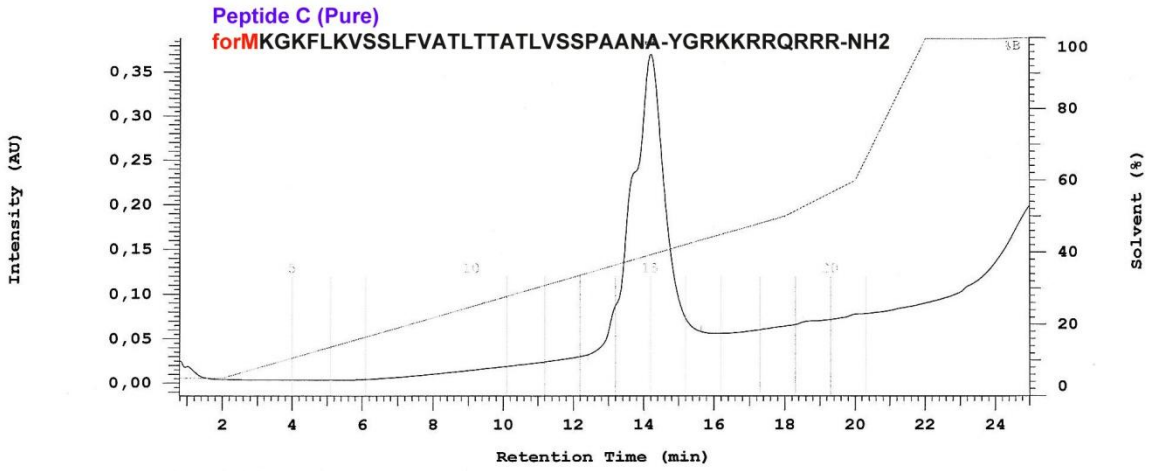

Figure 17 The HPLC chromatogram of the purified peptide C shows a single peak with a shoulder of a non-separable byproduct.

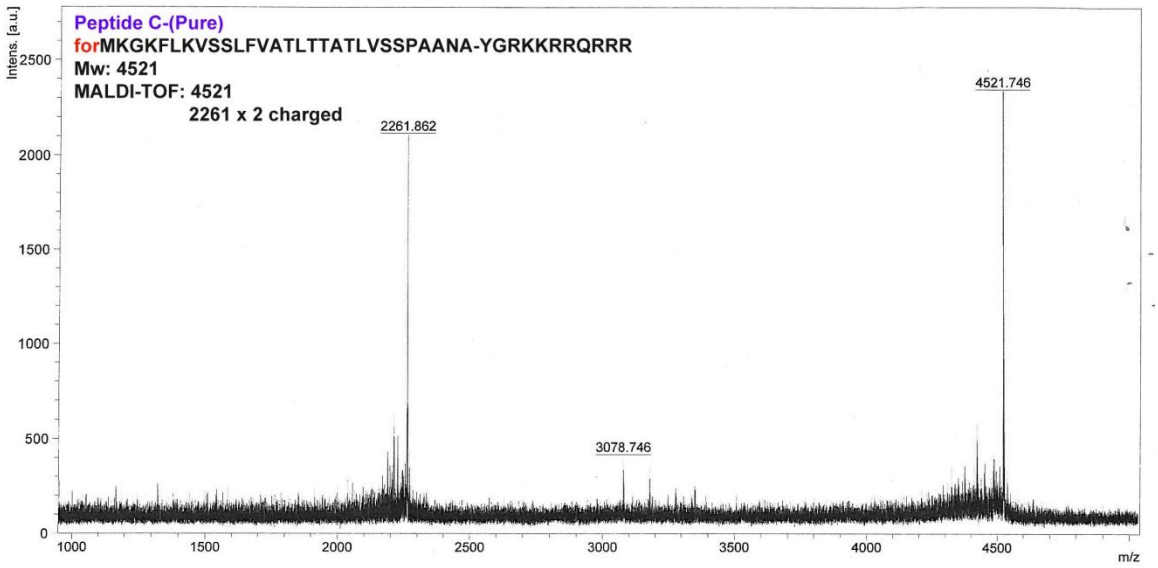

Figure 18 The MALDI-TOF spectrum shows a corresponding mass of the purified peptide C, while the peak at m/z 2261.86 is the double-charged mass of peptide C.

.

3 Appendix-III: Fmoc solid phase synthesis of the control peptides

3.1 Peptide D

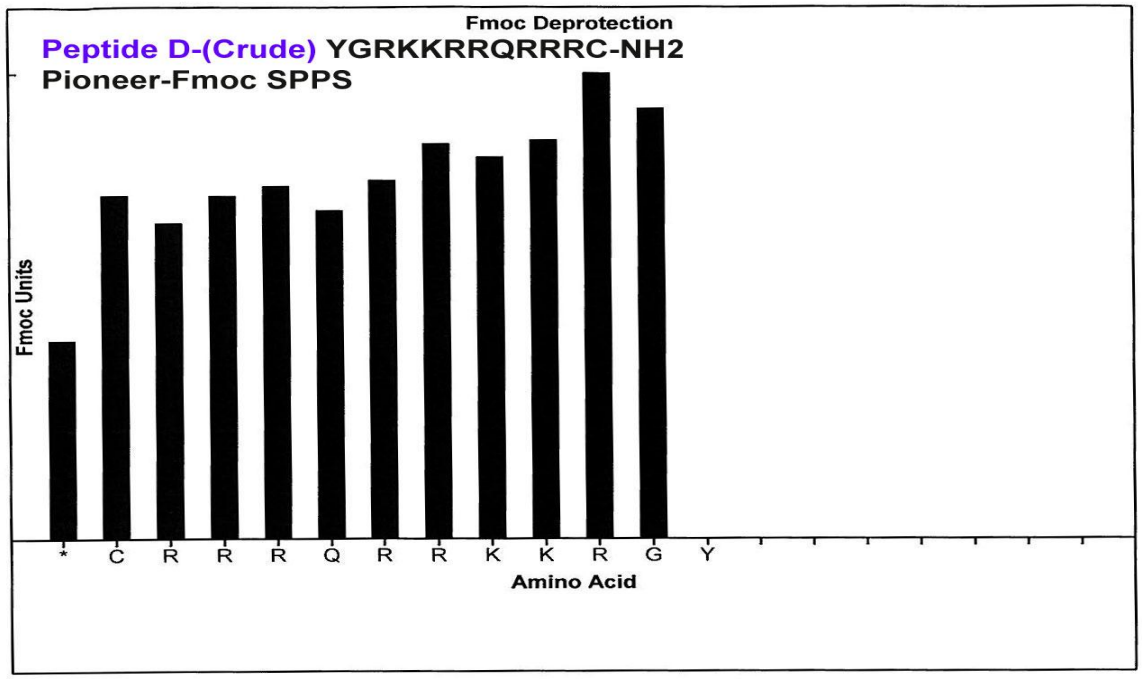

Figure 19 The Fmoc deprotection protocol of the Pioneer peptide synthesizerindicates a successful coupling of the amino acids of peptide D.

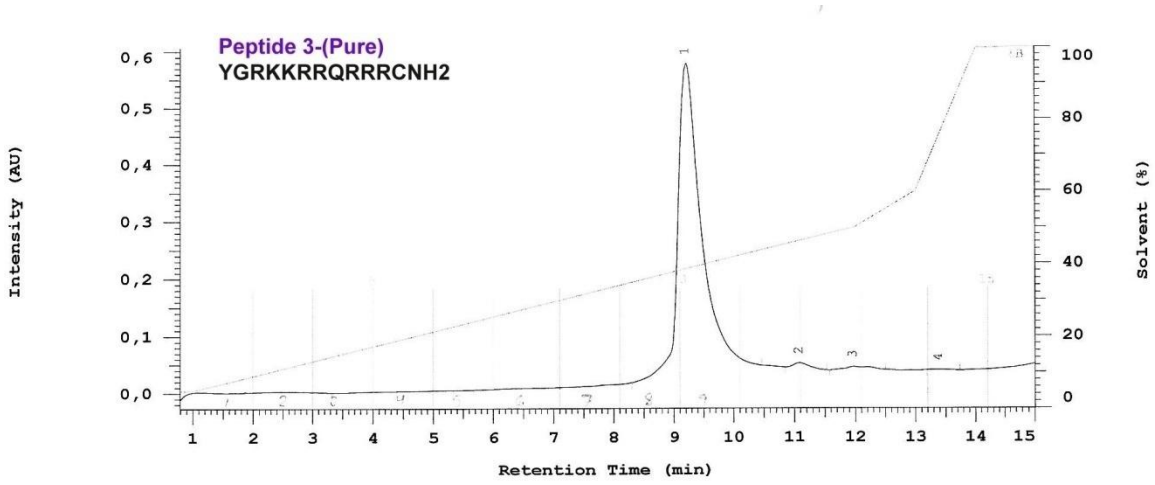

Figure 20 The HPLC chromatogram of the purified peptide D shows a single peak.

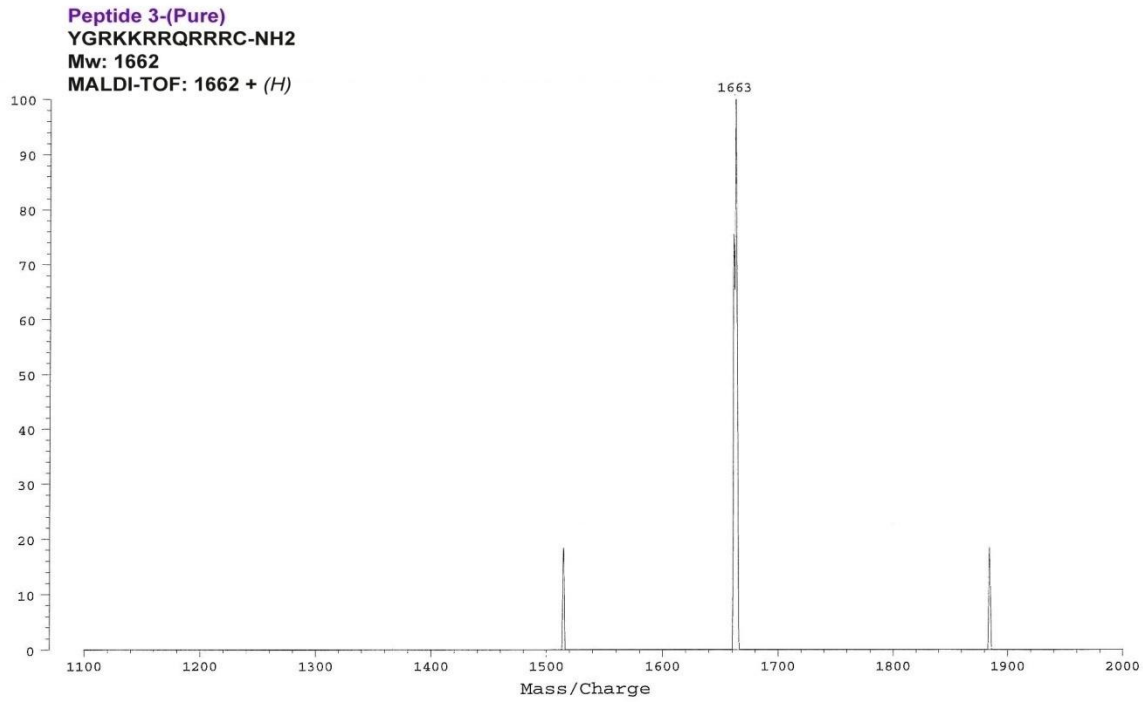

Figure 21 The MALDI-TOF spectrum shows the expected meausred mass of the purified peptide D at m/z 1663.

3.2 Peptide E

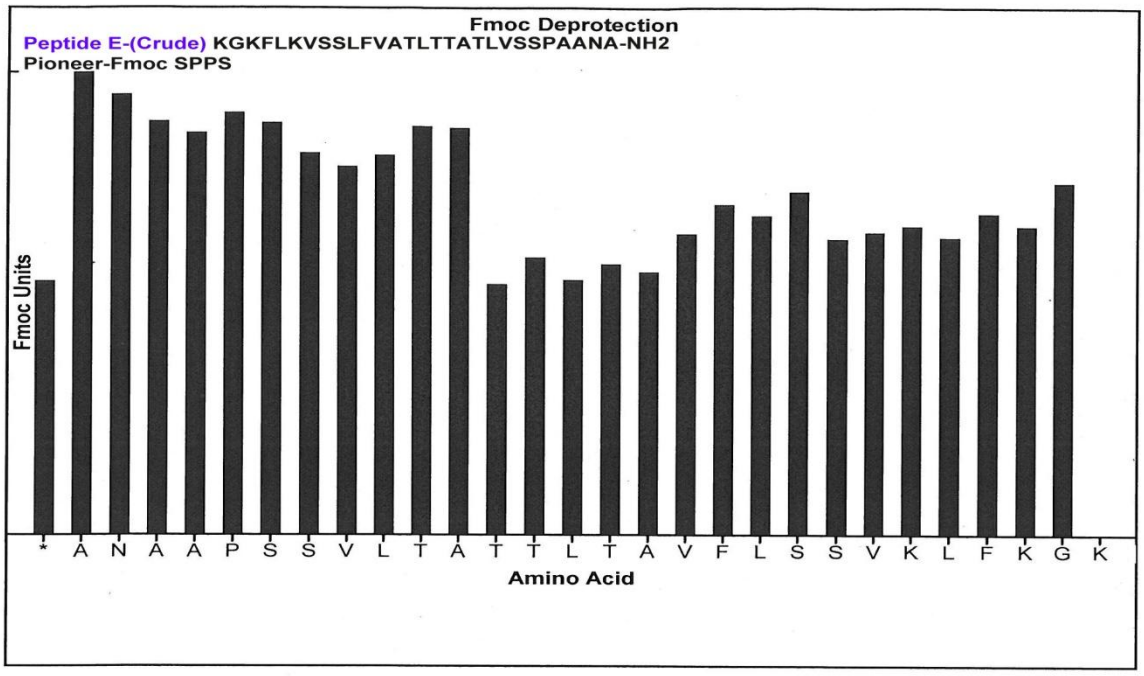

Figure 22 The Fmoc deprotection protocol of the Pioneer peptide synthesizer indicates a successful coupling of the amino acids of peptide E.

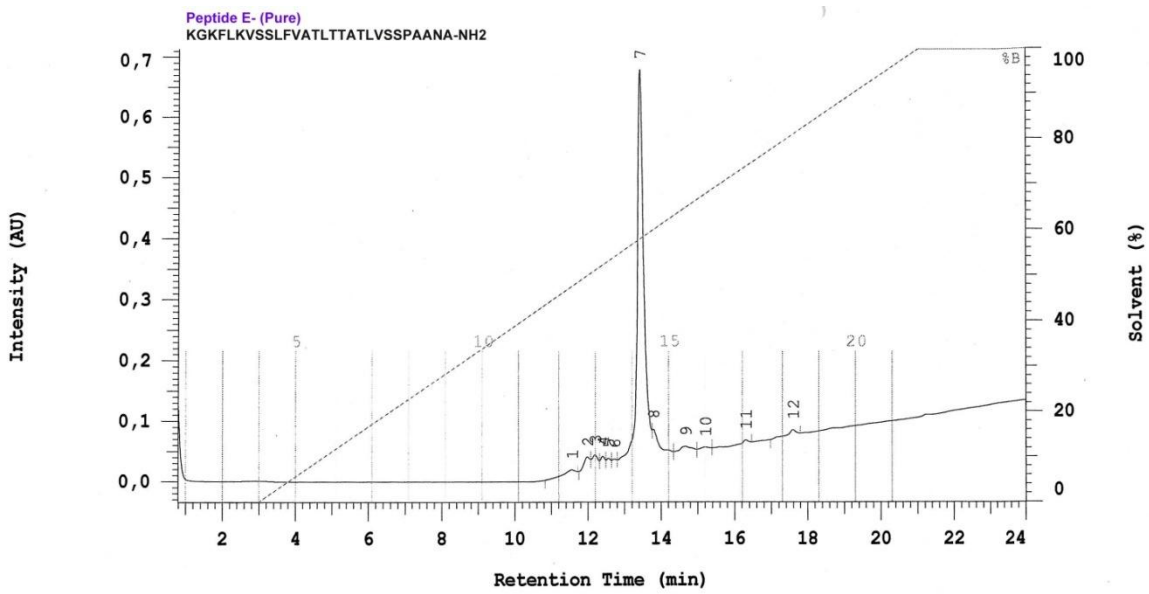

Figure 23 The HPLC chromatogram of the purified peptide E shows a single peak.

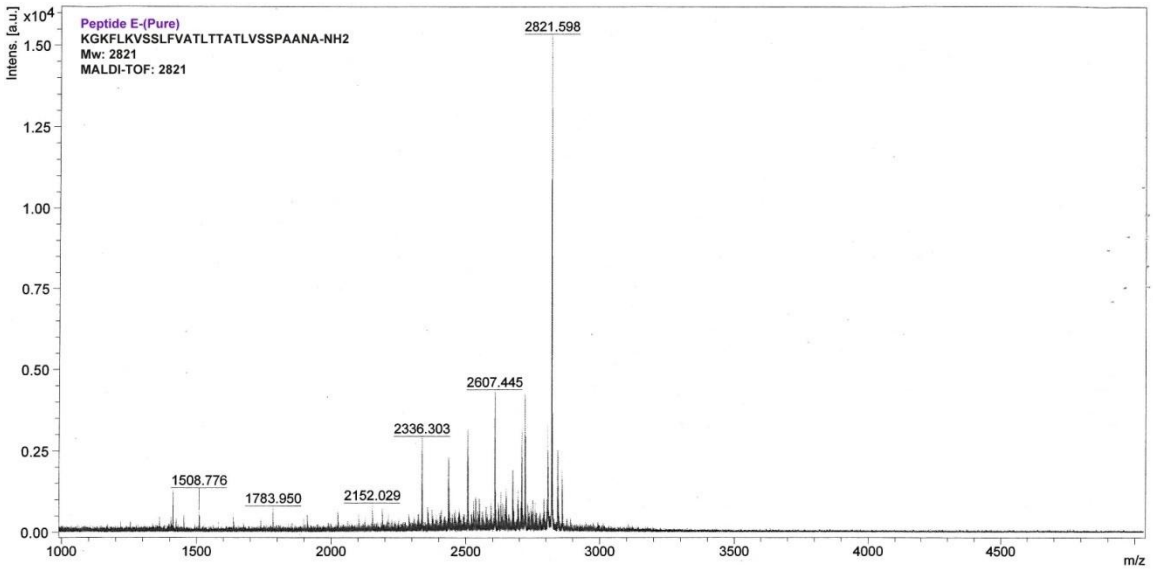

Figure 24 The MALDI-TOF spectrum shows the expected mass of the purified peptide E at m/z 2821 together with impurities.

3.3 Peptide F

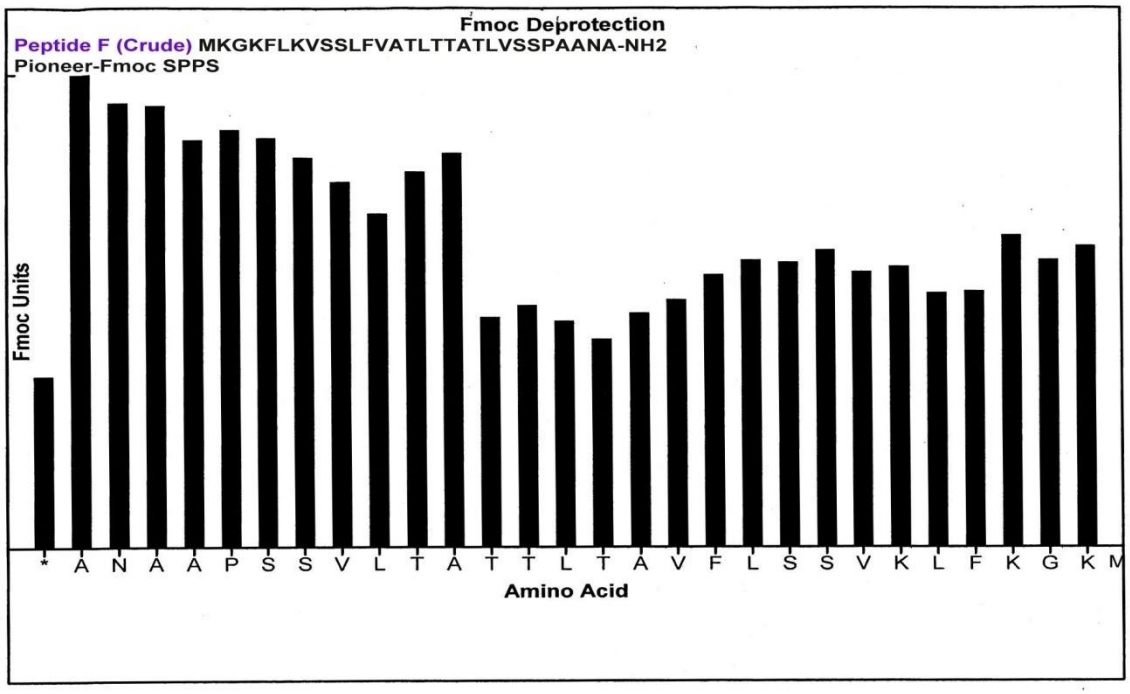

Figure 25 Fmoc deprotection protocol of the Pioneer peptide synthesizer: amino acid couplings of peptide F.

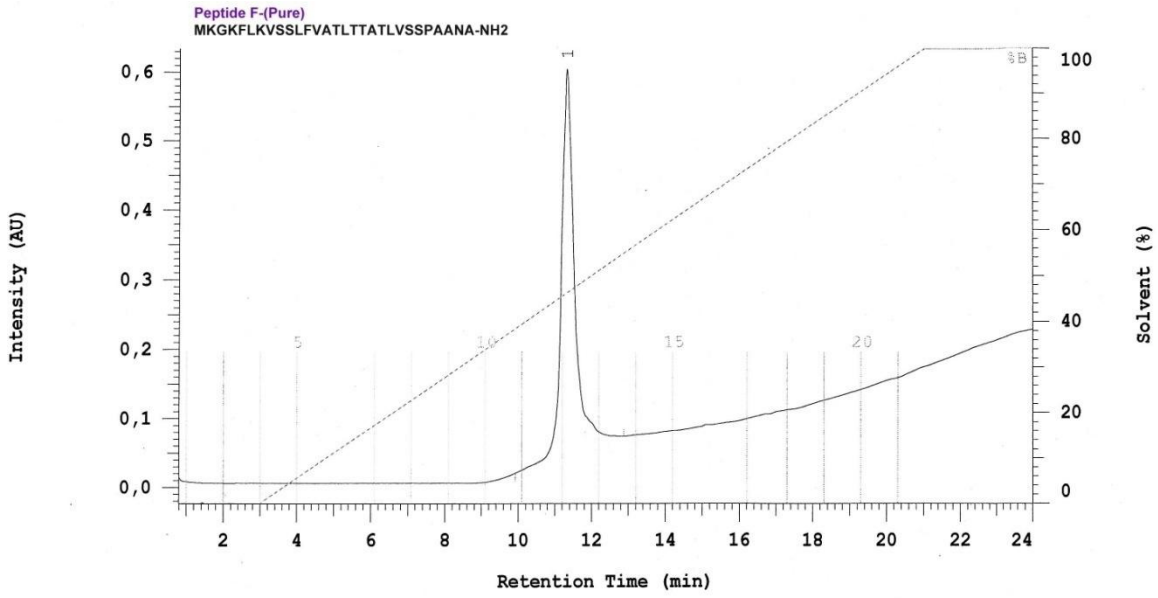

Figure 26 The HPLC chromatogram of the purified peptide F shows a single peak.

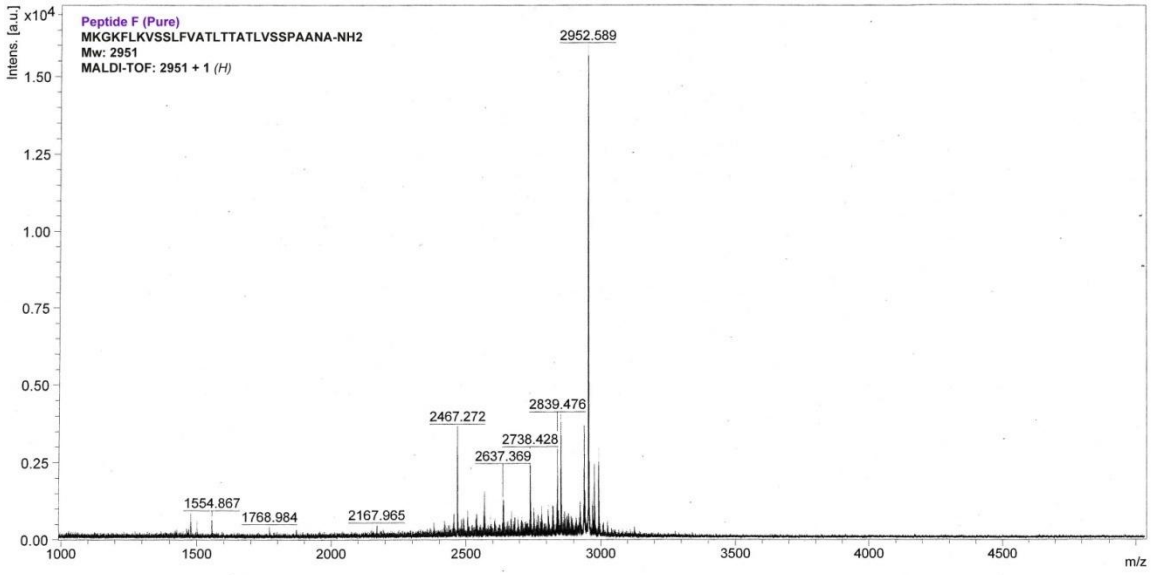

Figure 27 The MALDI-TOF spectrum shows the expected mass of the purified peptide F at m/z 2952 together with impurities.

3.4 Peptide G

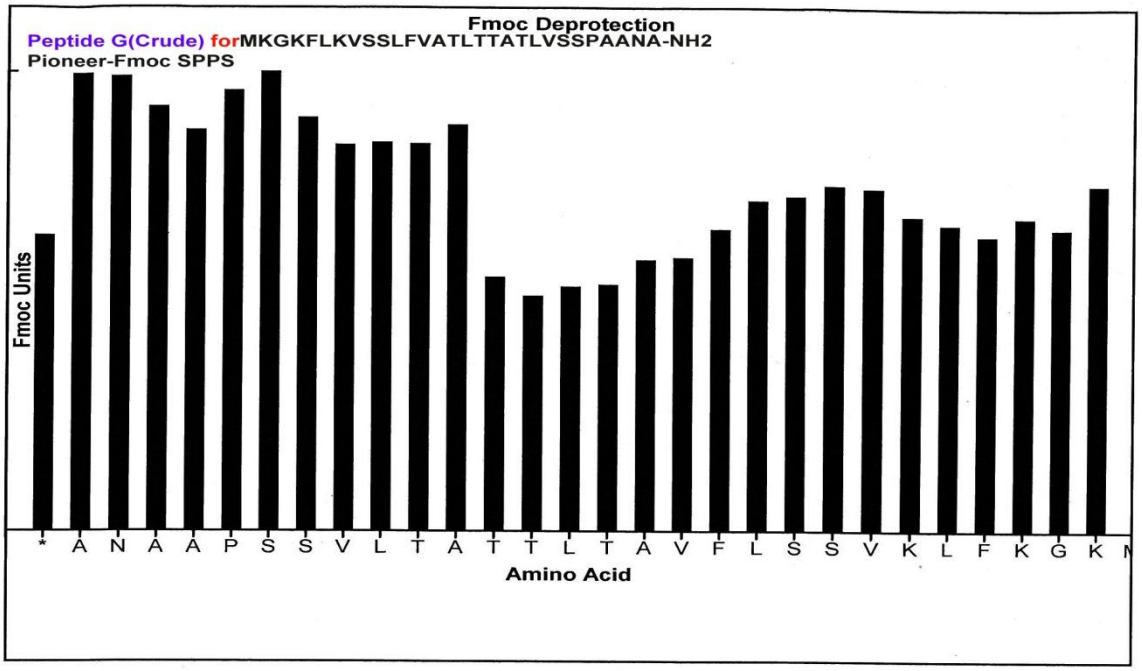

Figure 28 Fmoc deprotection protocol of the Pioneer peptide synthesizer: amino acid couplings of peptide G.

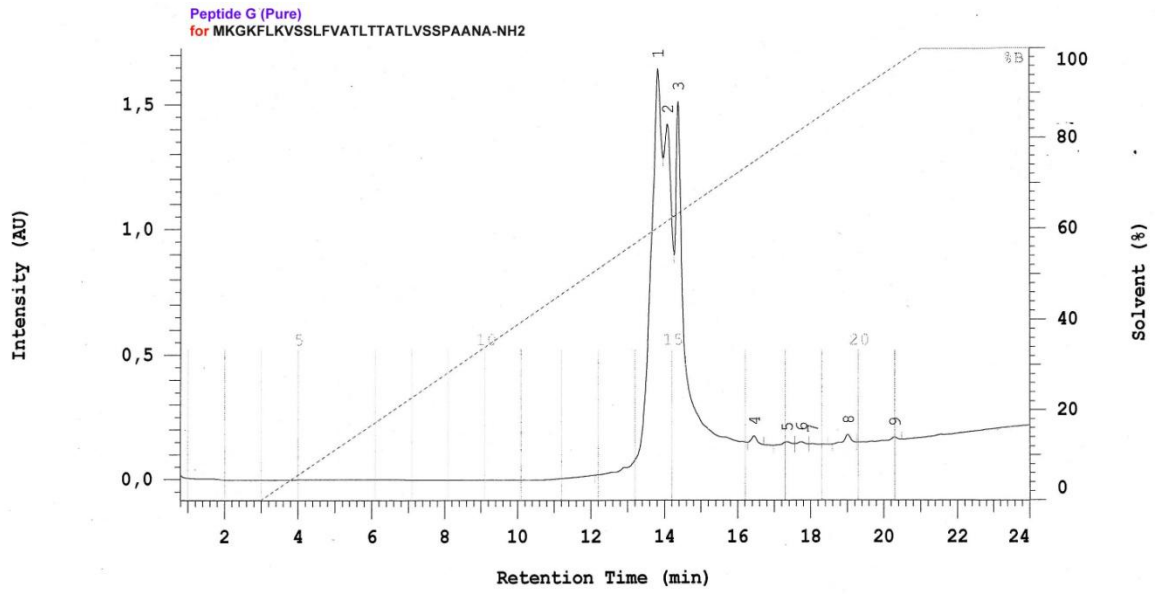

Figure 29 The HPLC chromatogram of the purified peptide G shows non-separable byproducts.

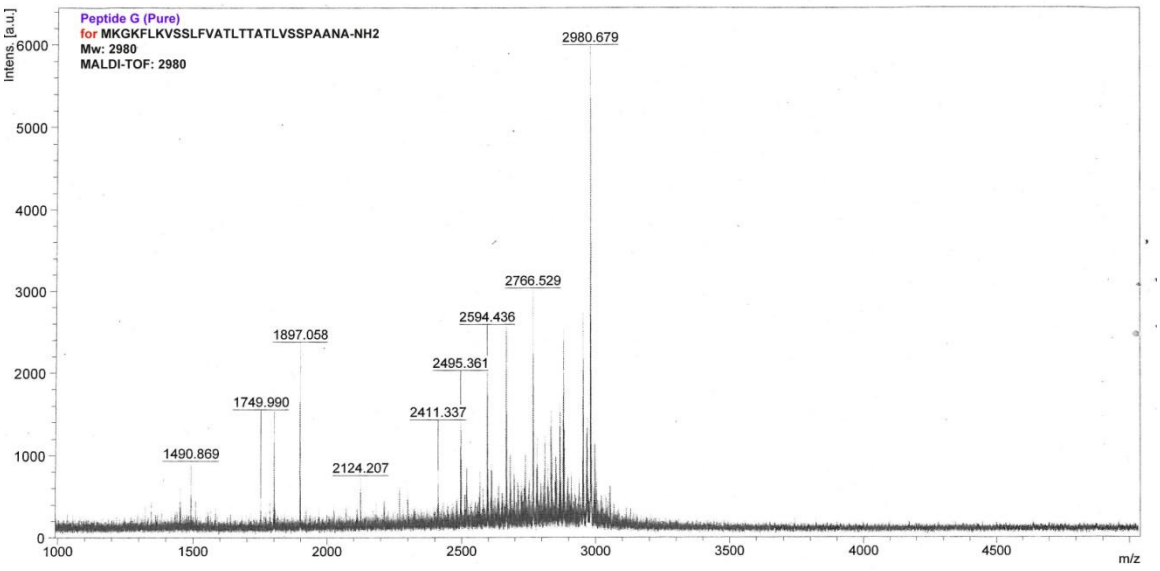

Figure 30 The MALDI-TOF spectrum shows a major peak of the purified peptide G at m/z 2980.

3.5 Peptide H

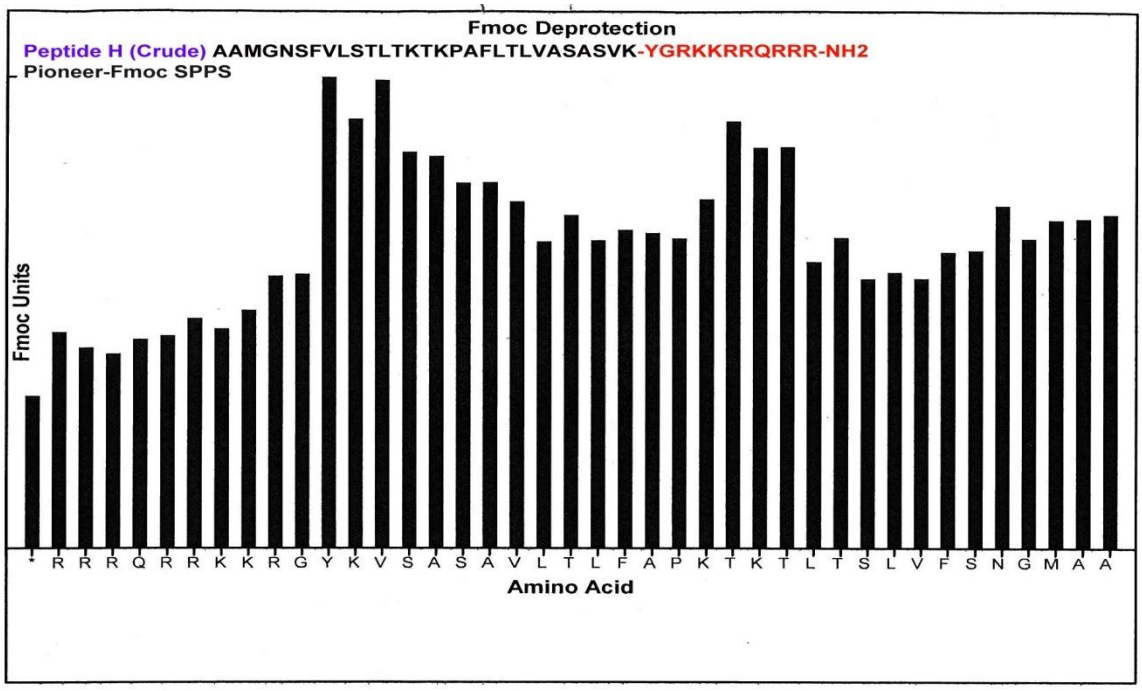

Figure 31 Fmoc deprotection protocol of the Pioneer peptide synthesizer: amino acid couplings of peptide H.

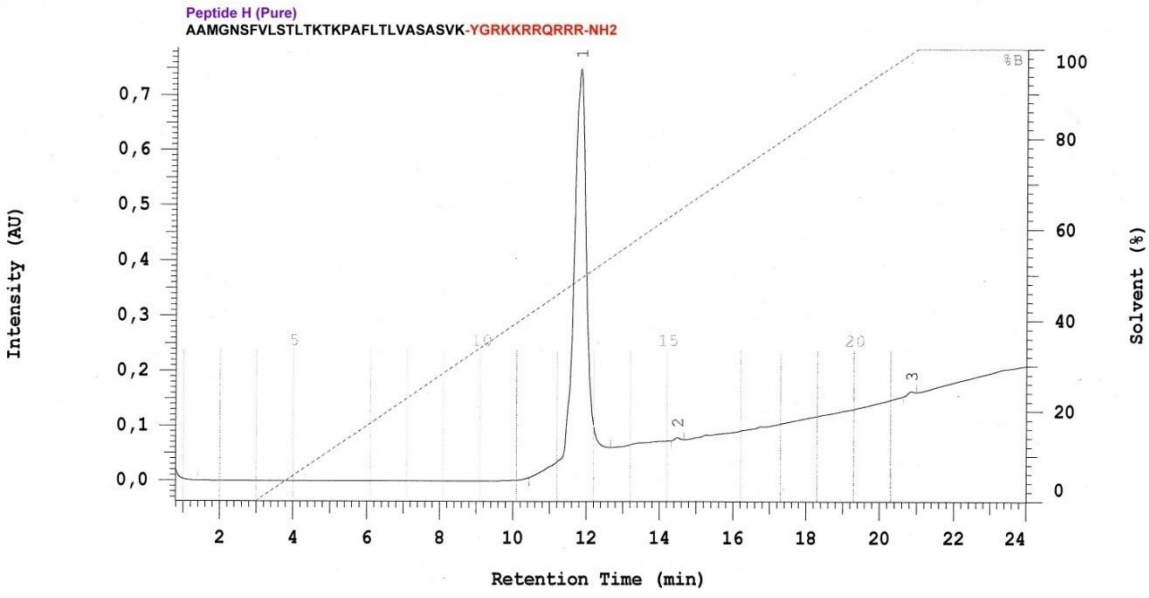

Figure 32 The HPLC chromatogram of the purified scrambled sequence (peptide H) shows a single peak.

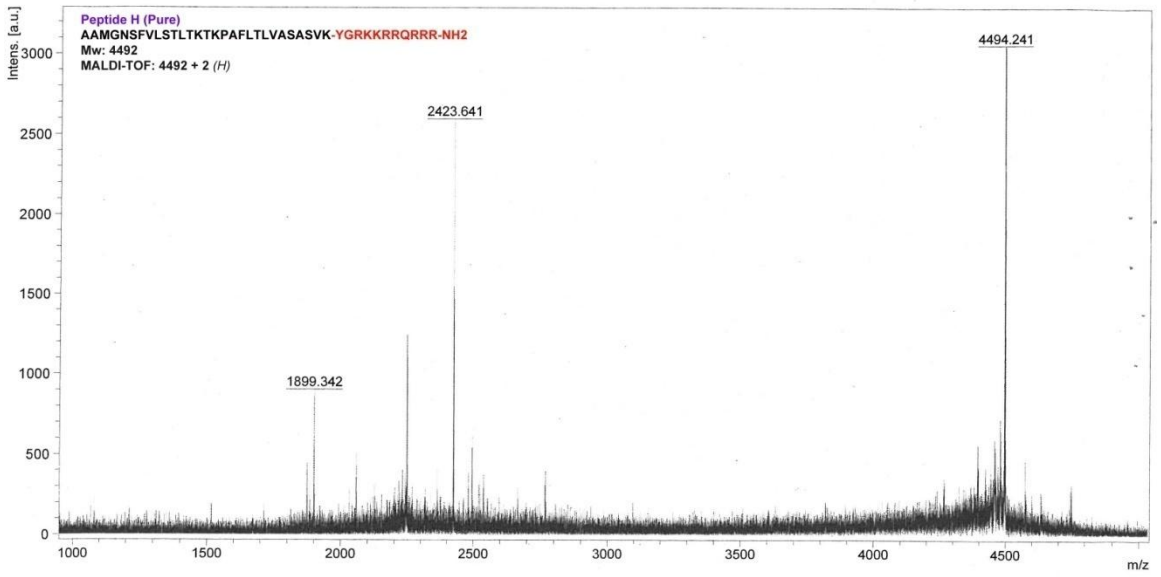

Figure Error! Use the Home tab to apply 0 to the text that you want to appear here.**33 The MALDI-TOF spectrum shows a major peak of the purified peptide H at m/z 4494.**

3.6 Peptide I

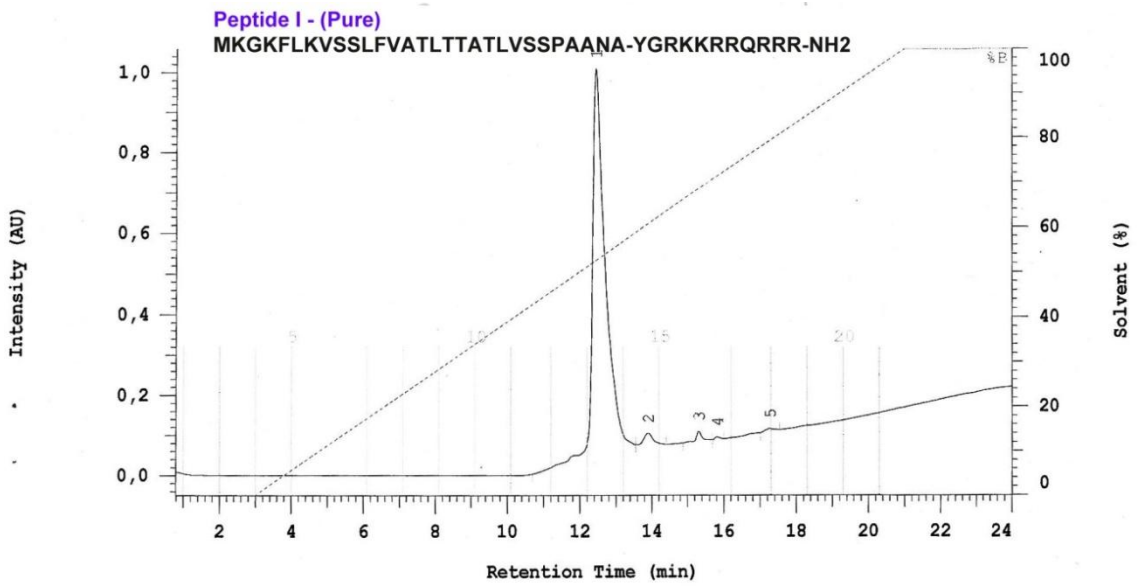

Figure 34.The HPLC chromatogram of the purified peptide I shows a major peak.

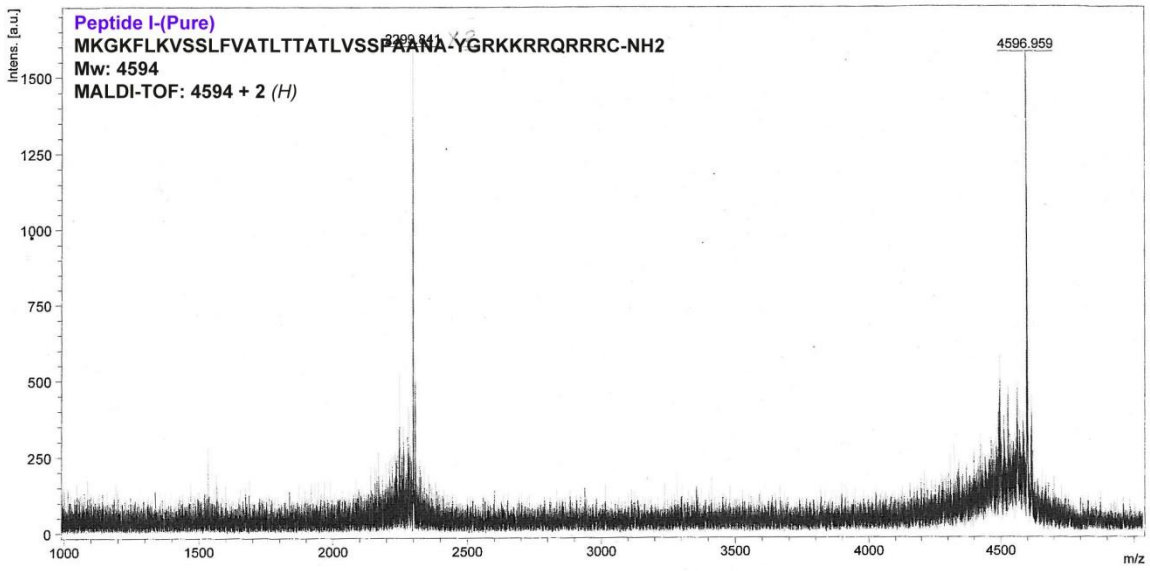

Figure 35 The MALDI-TOF spectrum shows the expected mass of the purified peptide I at m/z 4596, while the peak at m/z 2298 shows the double charged-mass of peptide I.

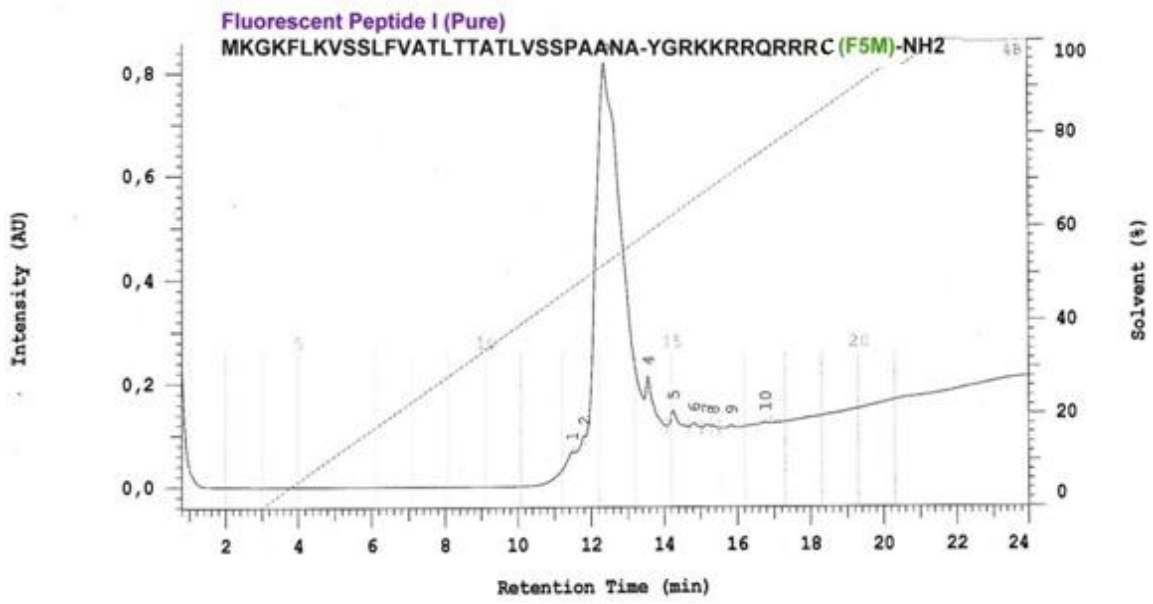

Figure 36 The HPLC chromatogram of the purified fluorescein-conjugated peptide B with added cysteine residue shows a major peak.

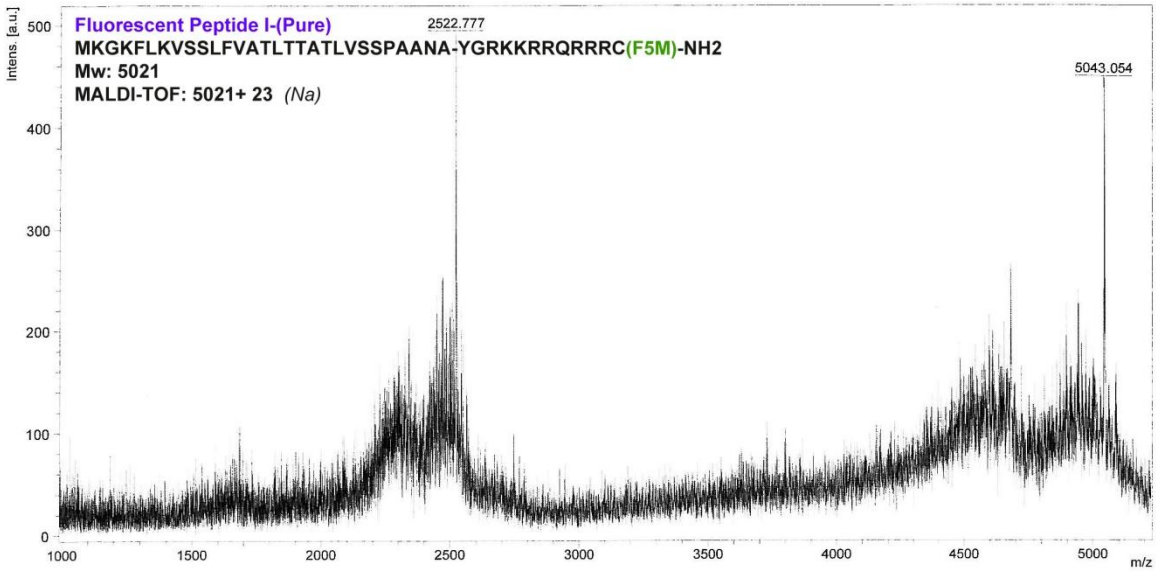

Figure 37 The MALDI-TOF spectrum shows two peaks of the purified fluorescein-conjugated peptide B at m/z 5043 and at m/z 2522 (double charged).

3.7 Peptide J (Peptide C with cysteine residue)

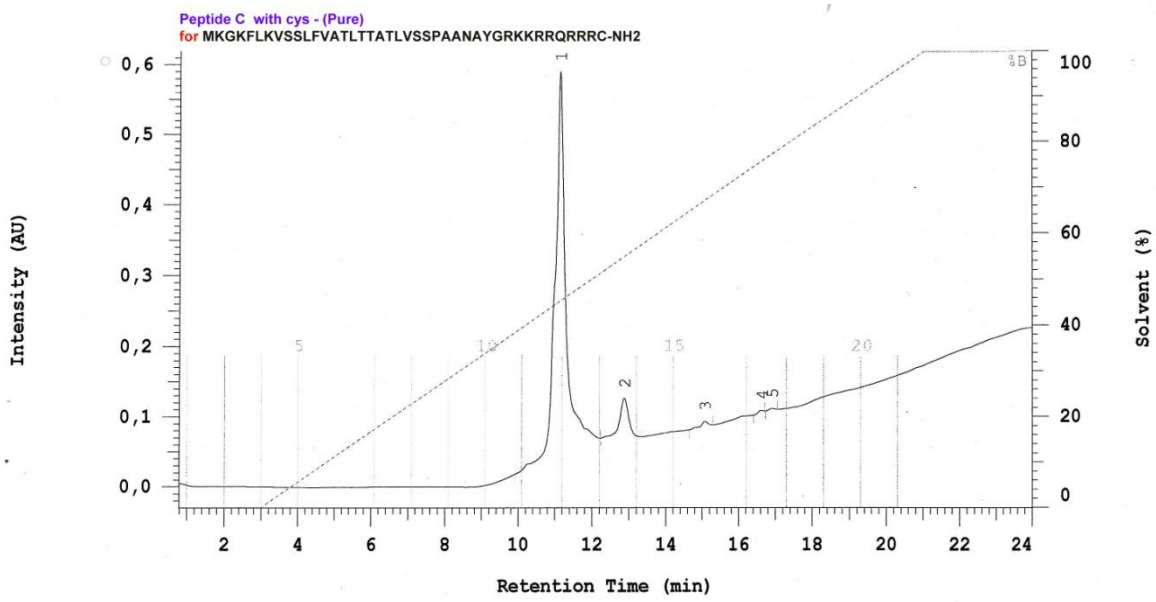

Figure 38 The HPLC chromatogram of the purified fluorescein-conjugated peptide C with added cysteine residue shows a single major peak with non-separable byproducts.

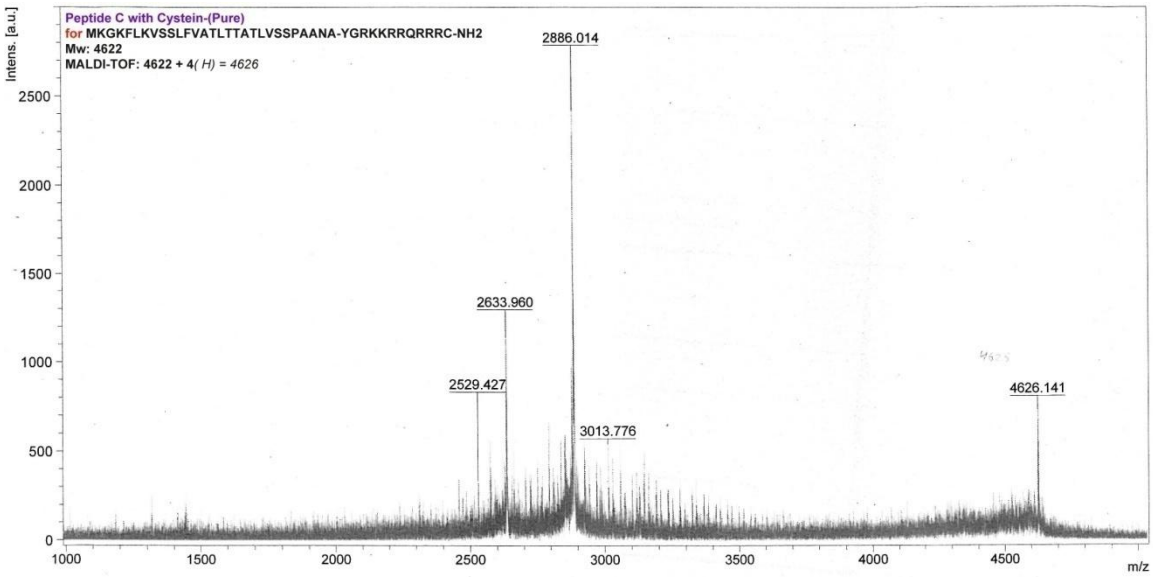

Figure 39 The MALDI-TOF spectrum shows a major mass of the purified peptide C with added cysteine residue together with impurities.

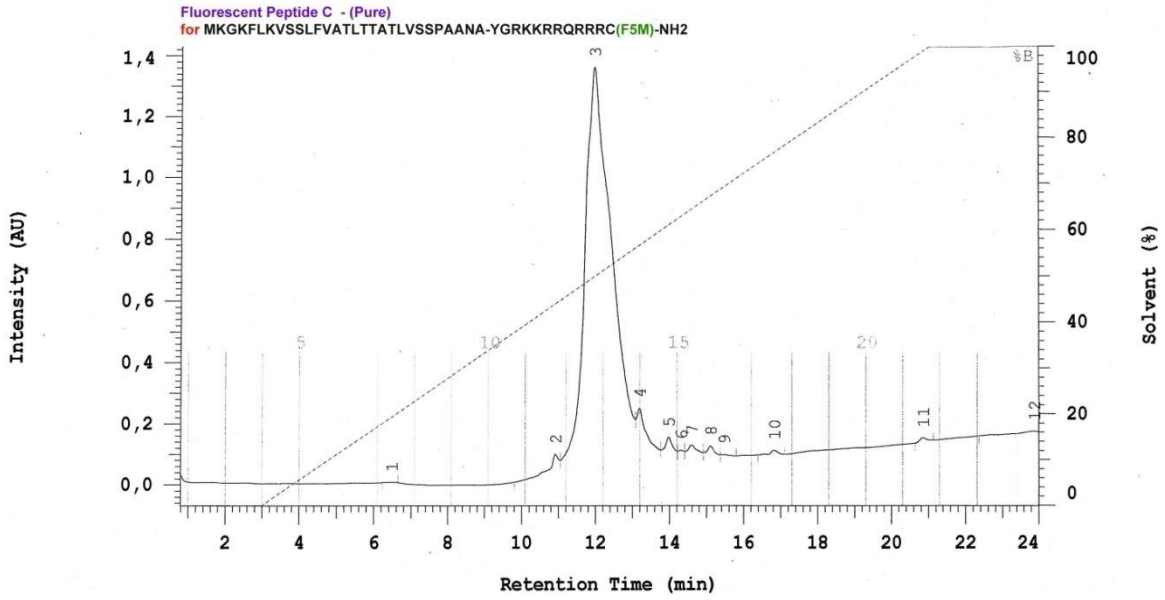

Figure 40 The HPLC chromatogram of the purified fluorescein-conjugated peptide C shows a major peak.

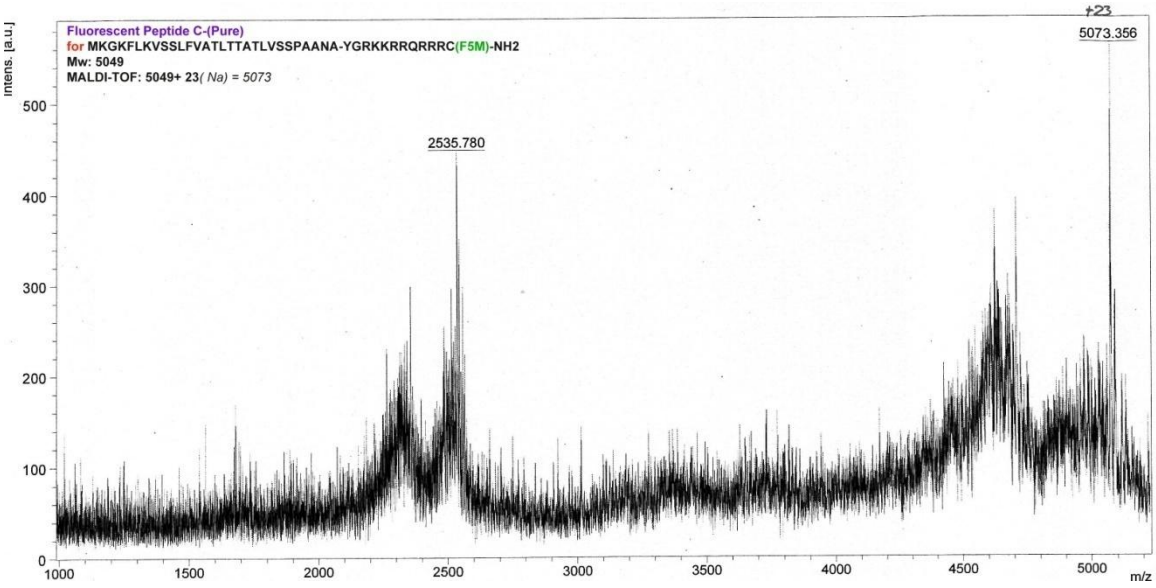

Figure 41 The MALDI-TOF spectrum shows peaks of the mono and double charged mass at m/z 5073.356 and m/z 2535.78 of the purified fluorescein-conjugated peptide C with added cysteine residue.

4 Appendix-IV: Testing the peptide uptake by *Staphylococcus aureus* V8 strain

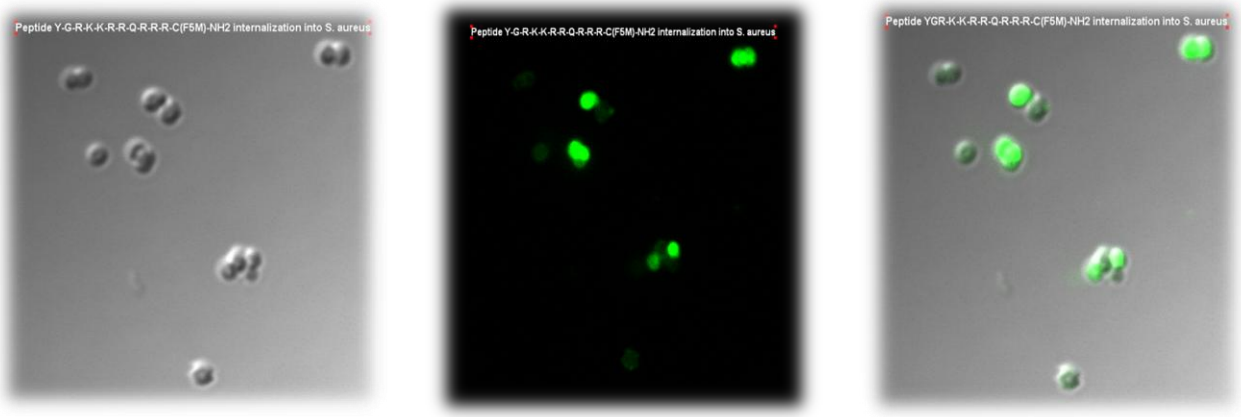

A B C

Figure 42 Images from the confocal laser microscope at a specific z-value.
The images show the 3D distribution of the fluorescent peptide-3 in *Staphylococcus aureus*. A *Staphylococcus aureus* cells visible filter. B Staphylococcal cells under the fluorescence filter (at λ520 nm). C shows the pictures A and B superimposed.

4.1 Fluorescence activated cell scanning (FACS) analysis:

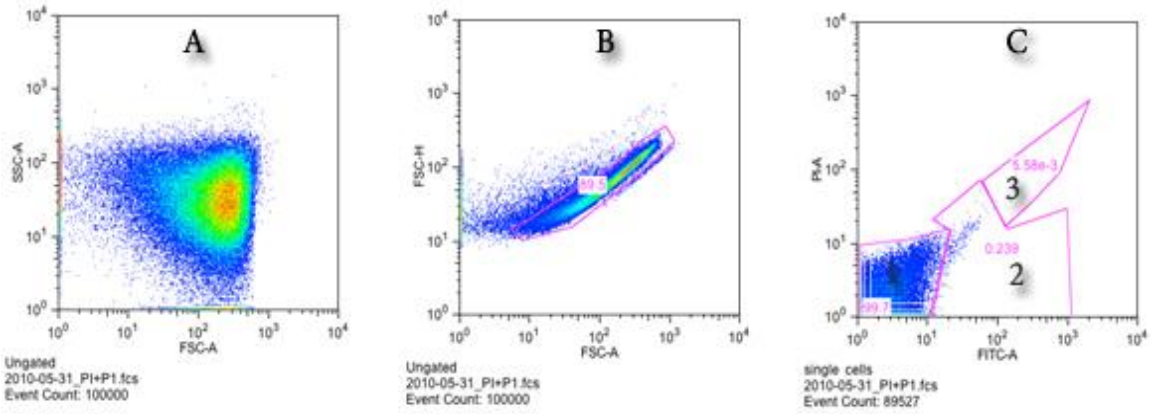

Figure 43 FACS analysis of staphylococcal cells incubated with peptide-1 and propidium iodide.
A: sideward fluorescence scattering (SSC) *vs*, forward scattering (FSC). B: gated populations from the labeled cell *vs*, dead cells. C: visual quantification of the population for the counted cells in the gated area. Area 1: background. Area 2: the counted live cells. Area 3: counted dead cells. All dot plots were produced by FlowJo software.

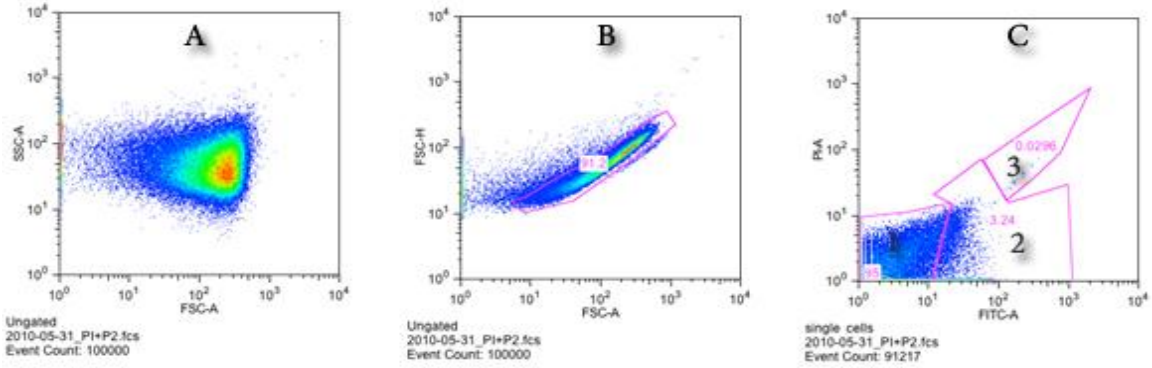

Figure 44 FACS analysis of staphylococcal cells incubated with peptide-2 and propidium iodide.
A: sideward fluorescence scattering (SSC) *vs*, forward scattering (FSC). B: gated populations from the labeled cell *vs*, dead cells. C: visual quantification of the population for the counted cells in the gated area. Area 1: background. Area 2: the counted live cells. Area 3: counted dead cells. All dot plots were produced by FlowJo software.

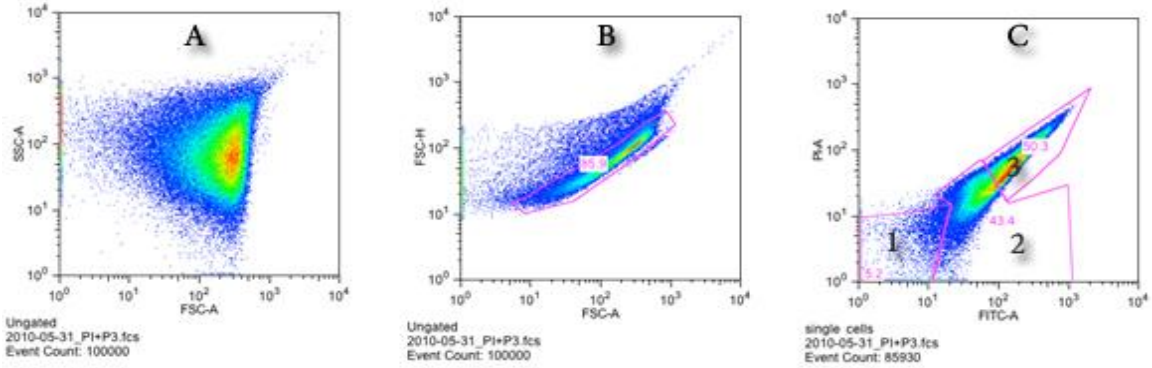

Figure 45 FACS analysis of staphylococcal cells incubated with peptide-3 and propidium iodide.
A: sideward fluorescence scattering (SSC) *vs*, forward scattering (FSC). B: gated populations from the labeled cell *vs*, dead cells. C: visual quantification of the population for the counted cells in the gated area. Area 1: background. Area 2: the counted live cells. Area 3: counted dead cells. All dot plots were produced by FlowJo software.

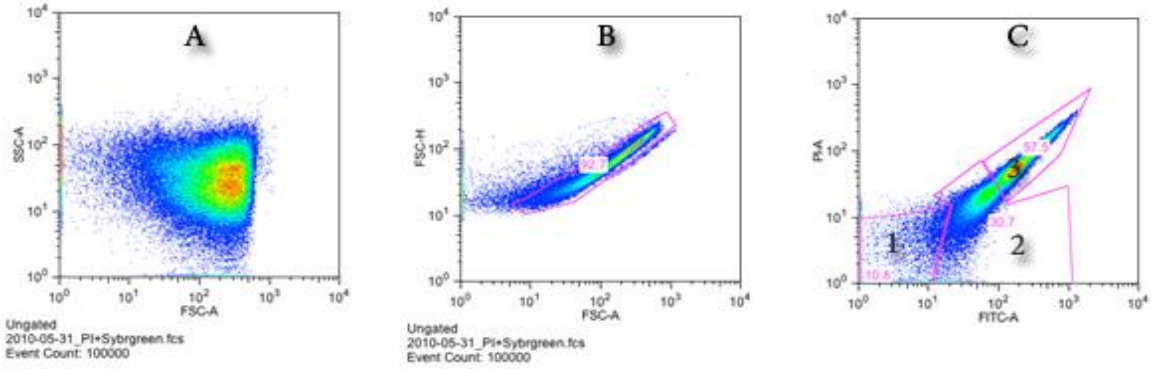

Figure 46 FACS analysis of staphylococcal cells incubated with SYBR-green (all live cells).
A: sideward fluorescence scattering (SSC) *vs*, forward scattering (FSC). B: gated populations from the labeled cell *vs*, dead cells. C: visual quantification of the population for the counted cells in the gated area. Area 1: background. Area 2: the counted live cells. Area 3: counted dead cells. All dot plots were produced by FlowJo software.

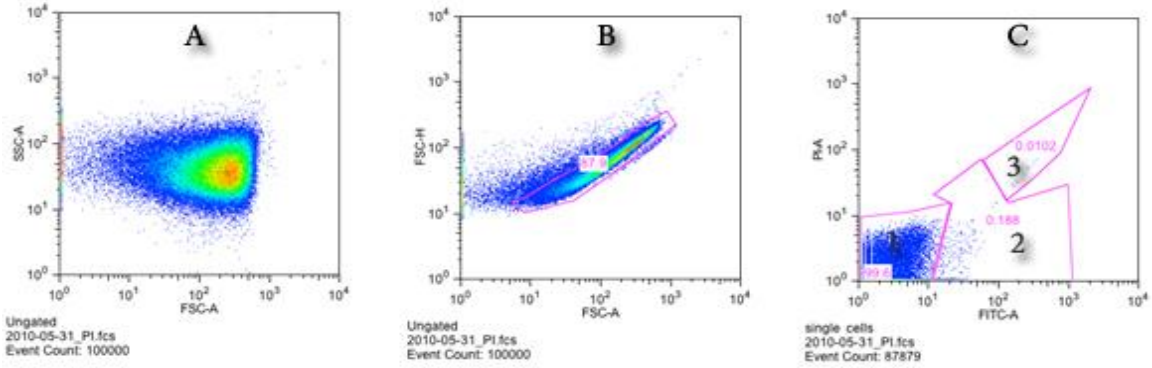

Figure 47 FACS analysis of staphylococcal cells incubated with propidium iodide (all dead cells).
A: sideward fluorescence scattering (SSC) *vs*, forward scattering (FSC). B: gated populations from the labeled cell *vs*, dead cells. C: visual quantification of the population for the counted cells in the gated area. Area 1: background. Area 2: the counted live cells. Area 3: counted dead cells. All dot plots were produced by FlowJo software.

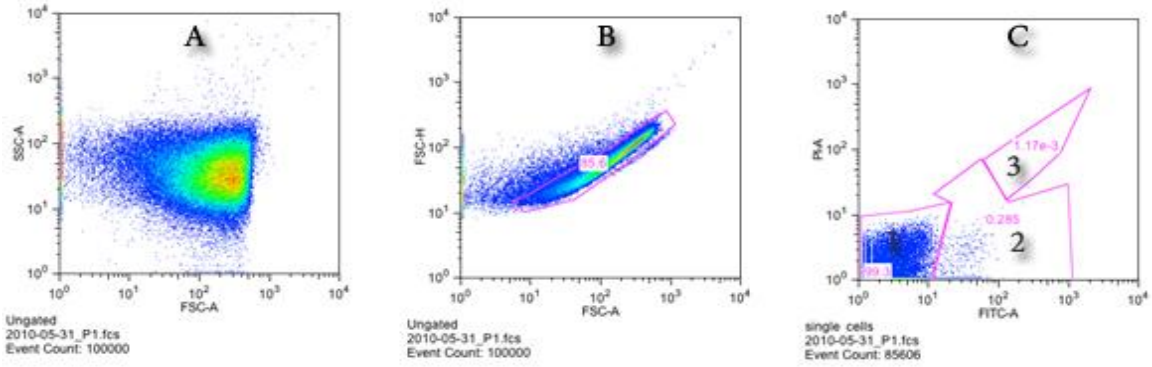

Figure 48 FACS analysis of staphylococcal cells incubated with peptide-1 only.
A: sideward fluorescence scattering (SSC) *vs*, forward scattering (FSC). B: gated populations from the labeled cell *vs*, dead cells. C: visual quantification of the population for the counted cells in the gated area. Area 1: background. Area 2: the counted live cells. Area 3: counted dead cells. All dot plots were produced by FlowJo software.

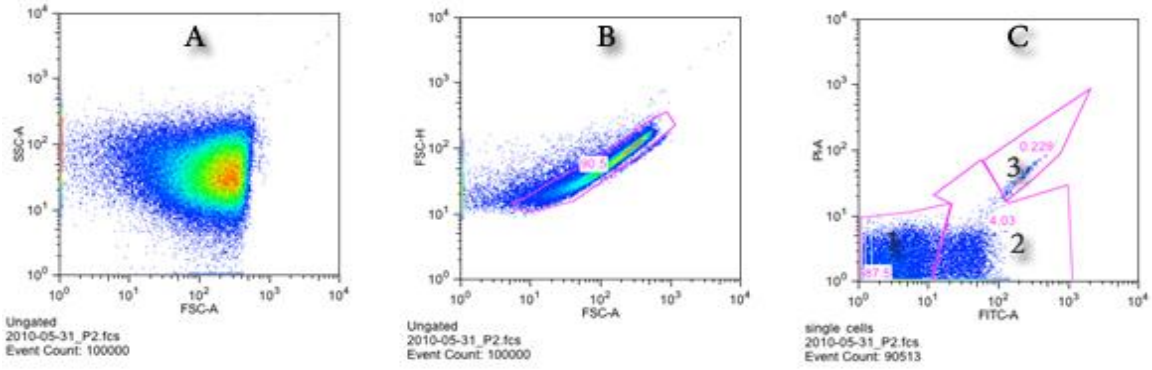

Figure 49 FACS analysis of staphylococcal cells incubated with peptide-2 only.
A: sideward fluorescence scattering (SSC) *vs*, forward scattering (FSC). B: gated populations from the labeled cell *vs*, dead cells. C: visual quantification of the population for the counted cells in the gated area. Area 1: background. Area 2: the counted live cells. Area 3: counted dead cells. All dot plots were produced by FlowJo software.

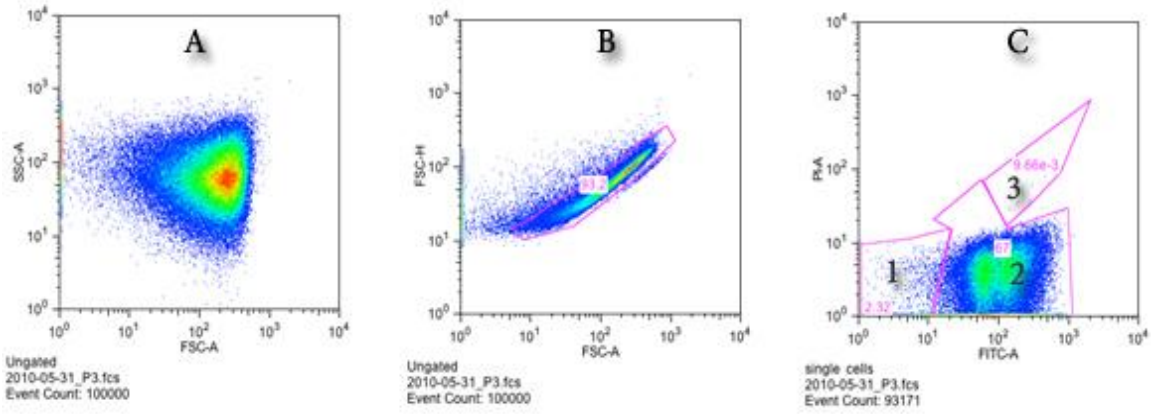

Figure 50 FACS analysis of staphylococcal cells incubated with peptide-3 only.
A: sideward fluorescence scattering (SSC) *vs*, forward scattering (FSC). B: gated populations from the labeled cell *vs*, dead cells. C: visual quantification of the population for the counted cells in the gated area. Area 1: background. Area 2: the counted live cells. Area 3: counted dead cells. All dot plots were produced by FlowJo software.

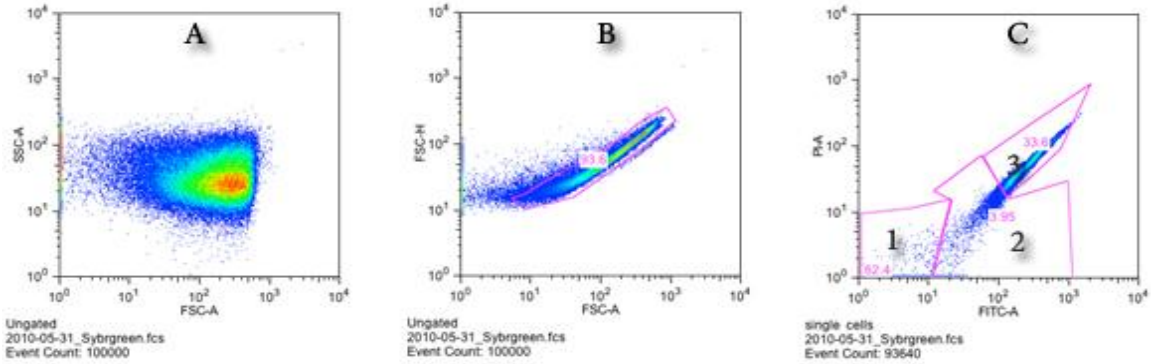

Figure 51 FACS analysis of staphylococcal cells incubated with SYBR-green (all cells).
A: sideward fluorescence scattering (SSC) *vs*, forward scattering (FSC). B: gated populations from the labeled cell *vs*, dead cells. C: visual quantification of the population for the counted cells in the gated area. Area 1: background. Area 2: the counted live cells. Area 3: counted dead cells. All dot plots were produced by FlowJo software.

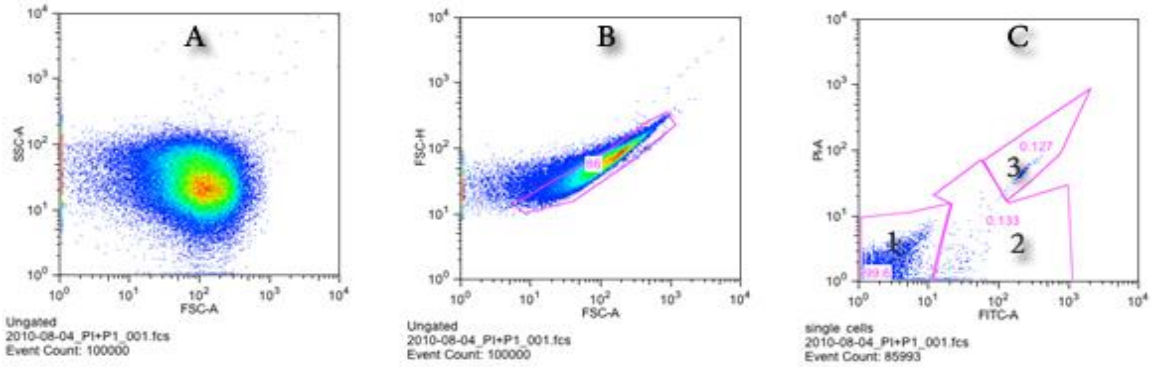

Figure 52 FACS analysis of staphylococcal cells incubated with peptide-1 and propidium iodide.
A: sideward fluorescence scattering (SSC) *vs*, forward scattering (FSC). B: gated populations from the labeled cell *vs*, dead cells. C: visual quantification of the population for the counted cells in the gated area. Area 1: background. Area 2: the counted live cells. Area 3: counted dead cells. All dot plots were produced by FlowJo software.

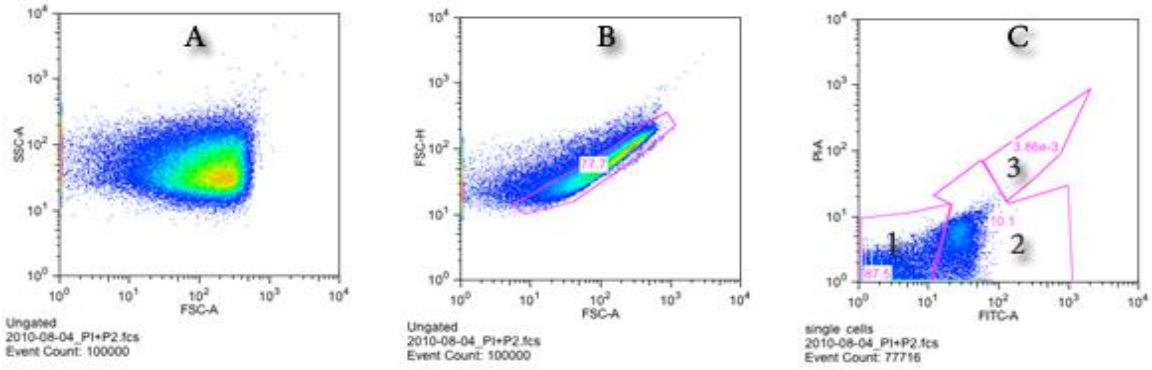

Figure 53 FACS analysis of staphylococcal cells incubated with peptide-2 and propidium iodide.
A: sideward fluorescence scattering (SSC) *vs*, forward scattering (FSC). B: gated populations from the labeled cell *vs*, dead cells. C: visual quantification of the population for the counted cells in the gated area. Area 1: background. Area 2: the counted live cells. Area 3: counted dead cells. All dot plots were produced by FlowJo software.

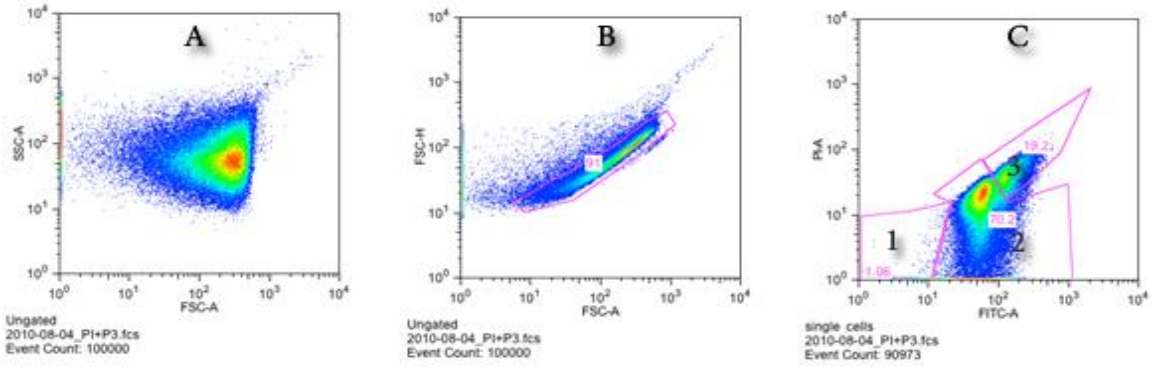

Figure 54 FACS analysis of staphylococcal cells incubated with peptide-3 and propidium iodide.
A: sideward fluorescence scattering (SSC) *vs*, forward scattering (FSC). B: gated populations from the labeled cell *vs*, dead cells. C: visual quantification of the population for the counted cells in the gated area. Area 1: background. Area 2: the counted live cells. Area 3: counted dead cells. All dot plots were produced by FlowJo software.

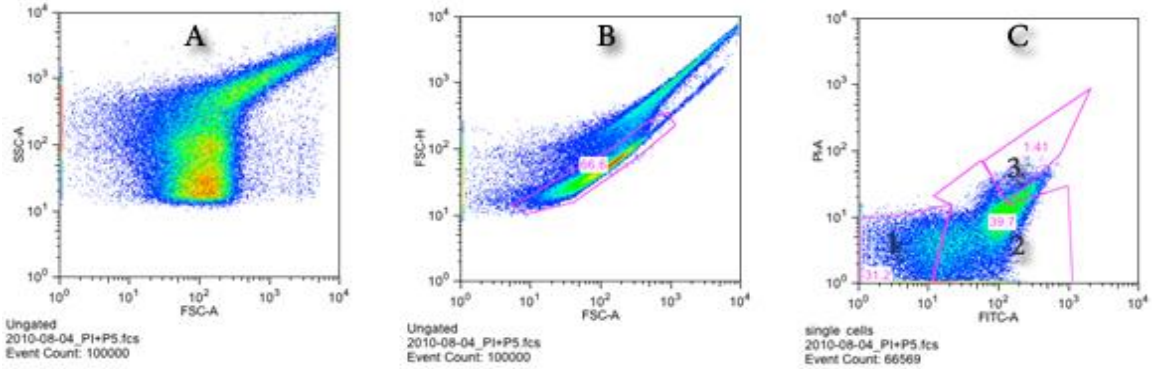

Figure 55 FACS analysis of staphylococcal cells incubated with peptide-J and propidium iodide.
A: sideward fluorescence scattering (SSC) *vs*, forward scattering (FSC). B: gated populations from the labeled cell *vs*, dead cells. C: visual quantification of the population for the counted cells in the gated area. Area 1: background. Area 2: the counted live cells. Area 3: counted dead cells. All dot plots were produced by FlowJo software.

5 Appendix-V: Fluorogenic assay to detect V8 protease in the supernatant using the substrate ABz-AFAFEVFY(NO_2)D

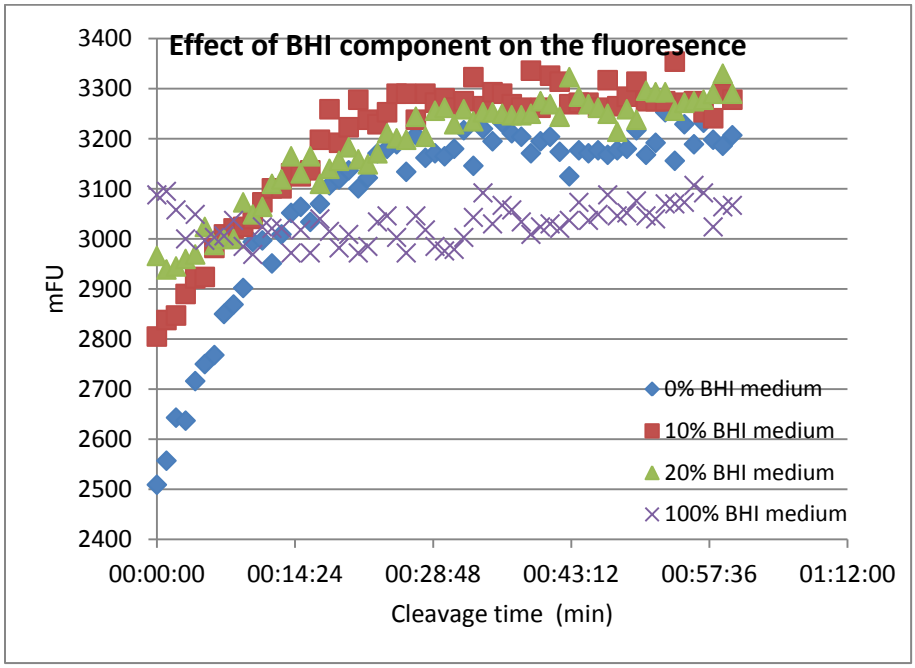

Figure 56 The competitive inhibitory effect of the BHI contents on the cleavage rate of the substrate in the supernatant.

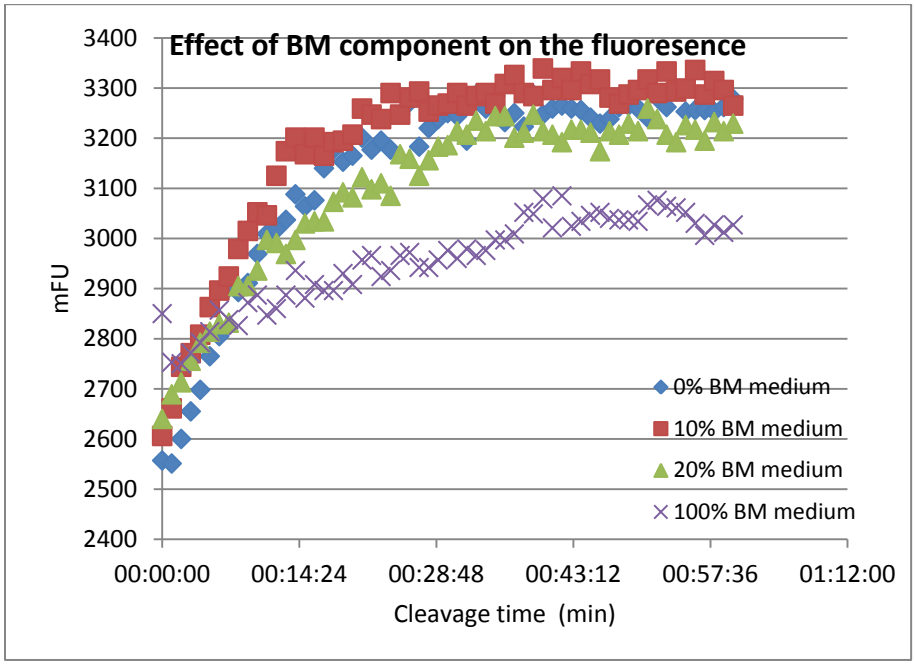

Figure 57 Increased reactivity of the cleavage was associated with diluting the supernatant in the fluorogenic assay (BM medium).

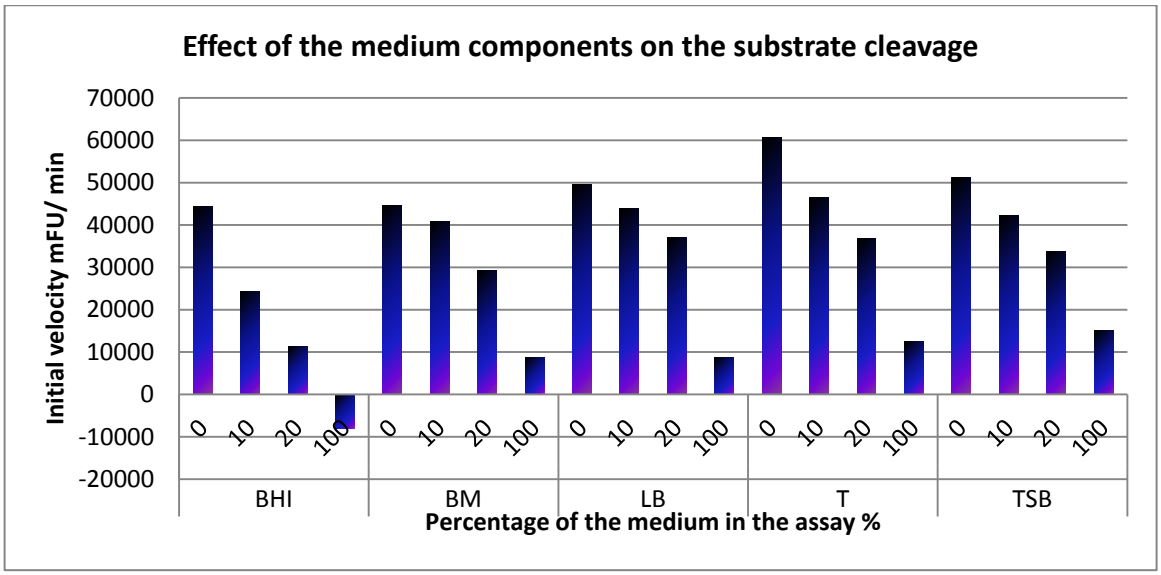

Figure 58 The effect of the medium components on the rate of cleaving the fluorogenic substrate by the secreted V8 protease.
The rate of cleavage of the fluorogenic substrate ABz-AFAFEVFY(NO_2)D decreased when the culture supernatants were diluted with HEPES buffer (0: only Hepes buffer, 10: supernatants were diluted 1:9, 20: supernatants were diluted 2:8, 100: supernatant was not diluted with HEPES. Five culture media were used: BHI, BM, LB, T, and TSB.

5.1 Studying the effect of the peptides on the secretion of the Sec-dependent protein (V8 protease)

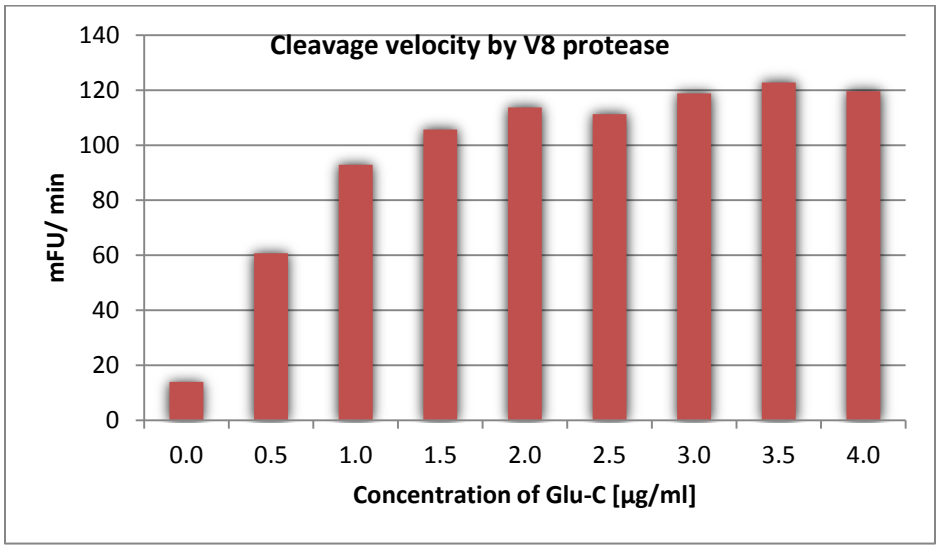

Figure 59 The reactivity of commercial V8 protease in the fluorogenic assay.
The initial velocity was represented by the fluorescence increase in the first 10 min of the reaction.

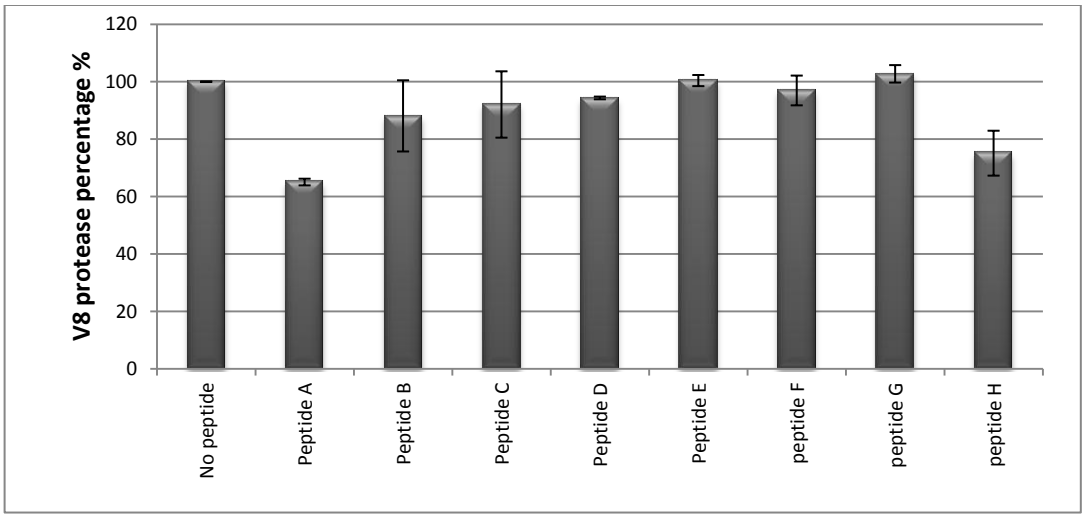

Figure 60 WB analysis of the secreted V8 protease in the supernatants.
The quantified bands of V8 protease in nine bacterial cultures non-treated/treated with 10 µM peptides A to H. The error bars represent the standard deviation values generated from three individual experiments.

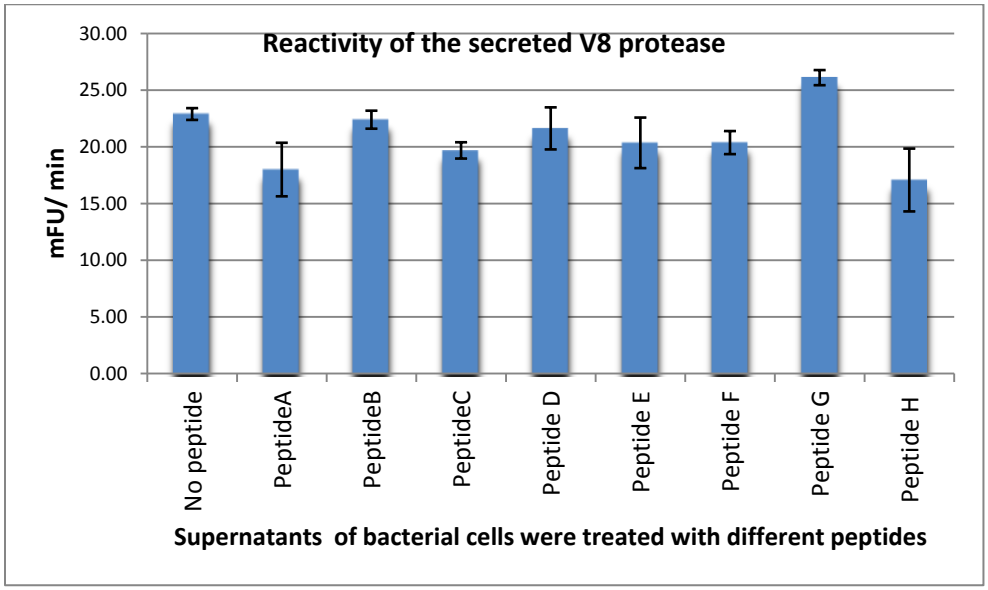

Figure 61 The reactivity of the secreted V8 protease in the supernatant as measured in the fluorogenic assay.
The initial velocity is represented by the fluorescence increase in the first 10 min of the reaction.

6 Appendix-VI: Sequence alignment analysis of the Sec secretion signal peptides from *Staphylococcus aureus*

The hallmark in the signal sequences of the Sec-dependent proteins is the Spase cleavage box AxAA at the C domain, in addition to the positively charged N domain and the hydrophobic H domain.

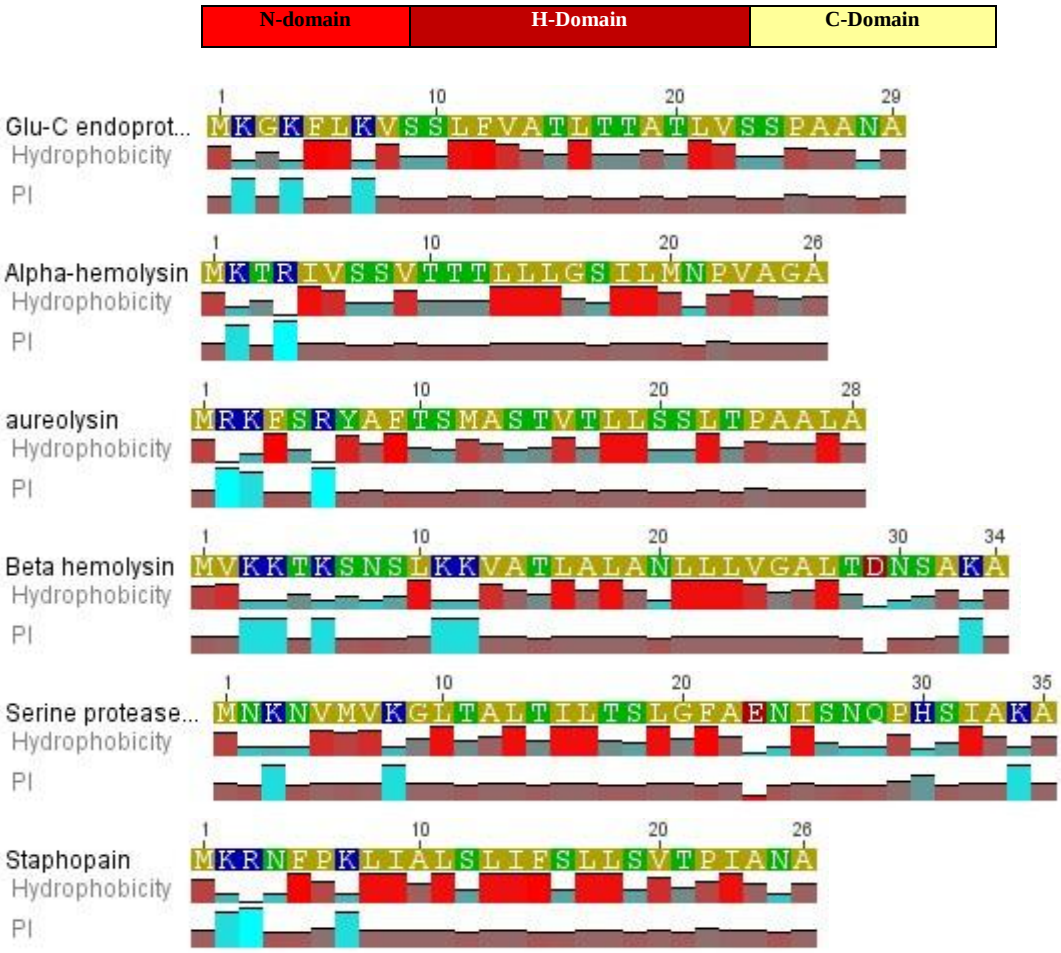

Figure 62 Multiple alignments of staphylococcal secretion signal peptides.

Multiple alignments of the staphylococcal secretion signal peptides are important tools in studying sequences. The basic information they provide is the identification of conserved sequence regions. This is very useful in designing experiments to test and modify the function of specific proteins, in predicting the function and structure of proteins and in identifying new members of protein families. By means of the software JALVIEW or the website http://www.ebi.ac.uk/Tools/sequence.html some useful parameters can be tested. The similarities

of the sequence alignment of both V8 protease and other staphylococcal signal peptides can be investigated as well. The multiple sequence alignment program ClustalW2 was used at the URL: http://www.ebi.ac.uk/Tools/msa/clustalw2/

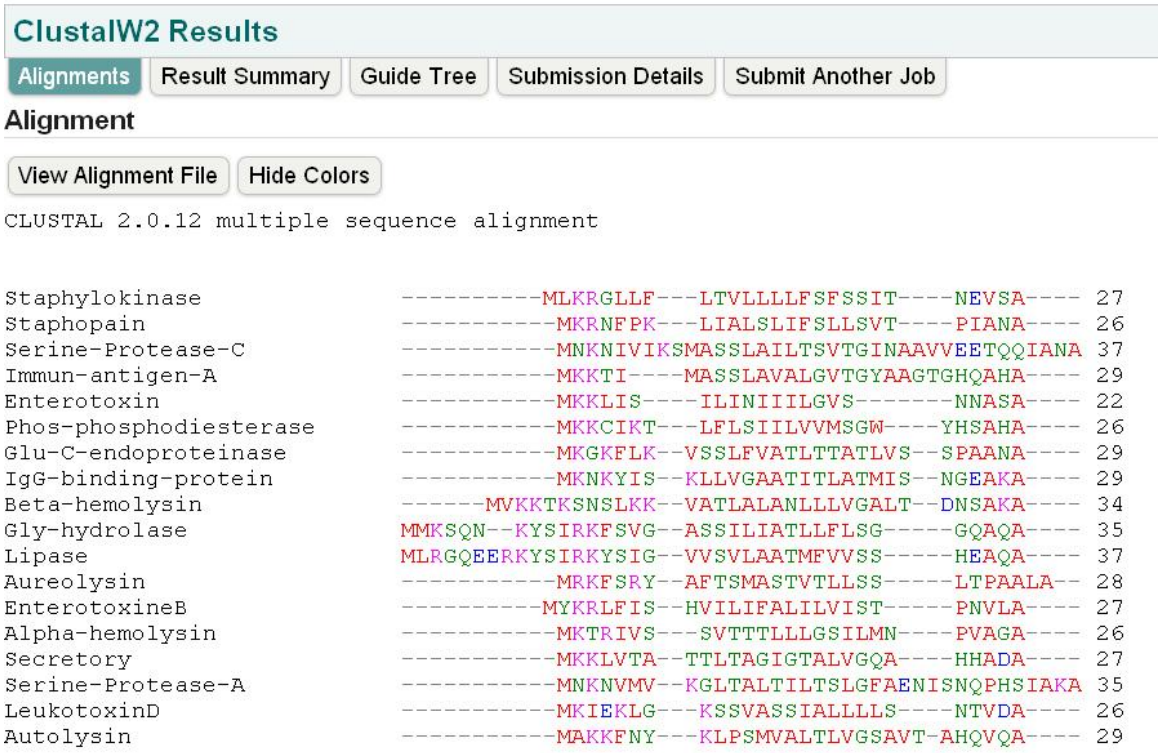

Figure 63 Signal peptide alignment of 18 Sec-dependent proteins from *Staphylococcus aureus*.

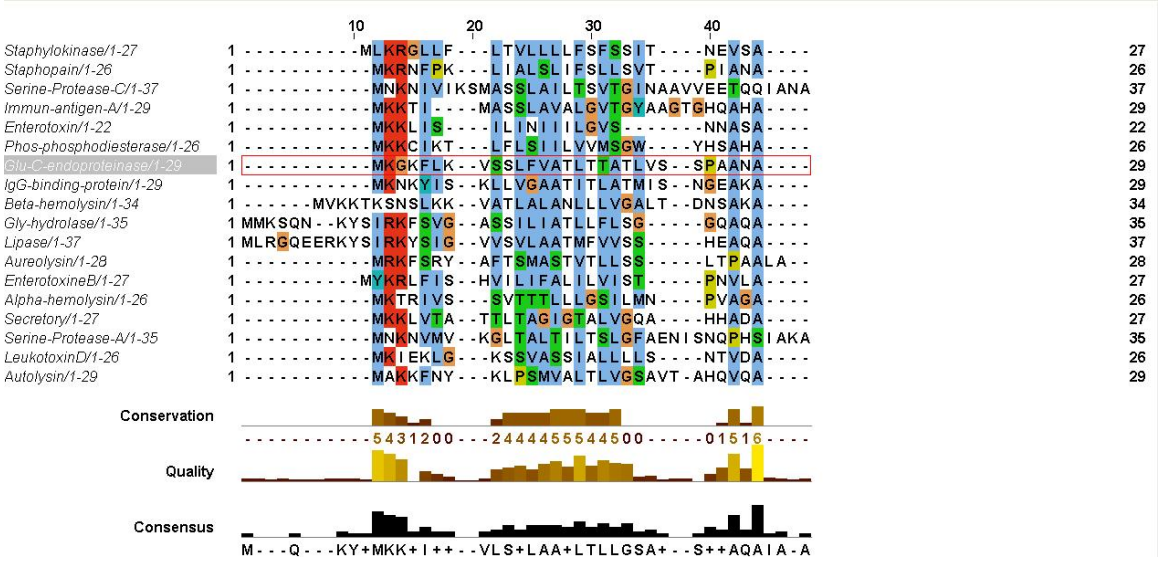

Figure 64 The similarity of hydrophobicity of the studied signal sequences.

Table 6.1 Analysis of signal peptide alignment of 18 Sec-dependent proteins known *in S. aureus.*
The table compares the degree of similarity using the peptide alignment for eighteen secretion signal sequences from *S. aureus.* The score is ordered from the highest to the lowest value of similarity. The signal sequences of the Gly-hydrolase and the lipase show the highest score at 45.71.

Sequence A	Length	Sequence B	Length	Score
Gly-hydrolase	35	Lipase	37	45.7143
Enterotoxin	22	Phos-phosphodiesterase	26	40.9091
Staphylokinase	27	Staphopain	26	38.4615
Glu-C-endoproteinase	29	IgG-binding-protein	29	37.931
Immun-antigen-A	29	Enterotoxin	22	36.3636
Serine-Protease-C	37	Staphopain	26	34.6154
Beta-hemolysin	34	Phos-phosphodiesterase	26	34.6154
Glu-C-endoproteinase	29	Beta-hemolysin	34	34.4828
Serine-Protease-C	37	Immun-antigen-A	29	34.4828
Gly-hydrolase	35	Aureolysin	28	32.1429
Serine-Protease-A	35	Enterotoxin	22	31.8182
Enterotoxin	22	Staphopain	26	31.8182
Beta-hemolysin	34	IgG-binding-protein	29	31.0345
IgG-binding-protein	29	Gly-hydrolase	35	31.0345
EnterotoxineB	27	Staphopain	26	30.7692
Immun-antigen-A	29	Phos-phosphodiesterase	26	30.7692
Serine-Protease-A	35	Staphylokinase	27	29.6296
Serine-Protease-A	35	Secretory	27	29.6296
Aureolysin	28	Secretory	27	29.6296
Glu-C-endoproteinase	29	Aureolysin	28	28.5714
Serine-Protease-C	37	Aureolysin	28	28.5714
Lipase	37	Aureolysin	28	28.5714
EnterotoxineB	27	Enterotoxin	22	27.2727
Beta-hemolysin	34	Enterotoxin	22	27.2727
LeukotoxinD	26	Enterotoxin	22	27.2727
Enterotoxin	22	Gly-hydrolase	35	27.2727
Enterotoxin	22	Secretory	27	27.2727
EnterotoxineB	27	LeukotoxinD	26	26.9231
Glu-C-endoproteinase	29	Alpha-hemolysin	26	26.9231
Glu-C-endoproteinase	29	Staphopain	26	26.9231
Serine-Protease-A	35	Staphopain	26	26.9231
Serine-Protease-C	37	LeukotoxinD	26	26.9231
Alpha-hemolysin	26	Staphylokinase	27	26.9231
Alpha-hemolysin	26	Secretory	27	26.9231
Beta-hemolysin	34	LeukotoxinD	26	26.9231
Beta-hemolysin	34	Staphopain	26	26.9231
LeukotoxinD	26	Immun-antigen-A	29	26.9231
LeukotoxinD	26	Autolysin	29	26.9231
LeukotoxinD	26	Gly-hydrolase	35	26.9231
LeukotoxinD	26	Aureolysin	28	26.9231
LeukotoxinD	26	Staphopain	26	26.9231
Immun-antigen-A	29	Staphopain	26	26.9231
Aureolysin	28	Staphopain	26	26.9231
Secretory	27	Phos-phosphodiesterase	26	26.9231
EnterotoxineB	27	Staphylokinase	27	25.9259
Glu-C-endoproteinase	29	Staphylokinase	27	25.9259
Glu-C-endoproteinase	29	Secretory	27	25.9259
Immun-antigen-A	29	Secretory	27	25.9259

Autolysin	29	Secretory	27	25.9259
Beta-hemolysin	34	Aureolysin	28	25.0
Autolysin	29	Aureolysin	28	25.0
Glu-C-endoproteinase	29	Immun-antigen-A	29	24.1379
Glu-C-endoproteinase	29	Autolysin	29	24.1379
Glu-C-endoproteinase	29	Lipase	37	24.1379
Serine-Protease-C	37	IgG-binding-protein	29	24.1379
Beta-hemolysin	34	Immun-antigen-A	29	24.1379
Immun-antigen-A	29	Autolysin	29	24.1379
Immun-antigen-A	29	IgG-binding-protein	29	24.1379
IgG-binding-protein	29	Lipase	37	24.1379
EnterotoxineB	27	Alpha-hemolysin	26	23.0769
Glu-C-endoproteinase	29	LeukotoxinD	26	23.0769
Serine-Protease-C	37	Alpha-hemolysin	26	23.0769
Serine-Protease-C	37	Phos-phosphodiesterase	26	23.0769
Alpha-hemolysin	26	Beta-hemolysin	34	23.0769
Alpha-hemolysin	26	Immun-antigen-A	29	23.0769
Alpha-hemolysin	26	Aureolysin	28	23.0769
Alpha-hemolysin	26	Staphopain	26	23.0769
Alpha-hemolysin	26	Phos-phosphodiesterase	26	23.0769
Autolysin	29	Phos-phosphodiesterase	26	23.0769
Gly-hydrolase	35	Staphopain	26	23.0769
Aureolysin	28	Phos-phosphodiesterase	26	23.0769
Serine-Protease-A	35	Serine-Protease-C	37	22.8571
Glu-C-endoproteinase	29	Enterotoxin	22	22.7273
Serine-Protease-C	37	Enterotoxin	22	22.7273
Alpha-hemolysin	26	Enterotoxin	22	22.7273
Autolysin	29	Enterotoxin	22	22.7273
Enterotoxin	22	IgG-binding-protein	29	22.7273
Enterotoxin	22	Lipase	37	22.7273
Enterotoxin	22	Staphylokinase	27	22.7273
EnterotoxineB	27	Serine-Protease-C	37	22.2222
EnterotoxineB	27	Autolysin	29	22.2222
EnterotoxineB	27	Lipase	37	22.2222
Serine-Protease-C	37	Secretory	27	22.2222
Beta-hemolysin	34	Staphylokinase	27	22.2222
Beta-hemolysin	34	Secretory	27	22.2222
Autolysin	29	Staphylokinase	27	22.2222
IgG-binding-protein	29	Secretory	27	22.2222
Gly-hydrolase	35	Secretory	27	22.2222
Serine-Protease-A	35	Aureolysin	28	21.4286
Immun-antigen-A	29	Aureolysin	28	21.4286
Glu-C-endoproteinase	29	Serine-Protease-A	35	20.6897
Glu-C-endoproteinase	29	Serine-Protease-C	37	20.6897
Glu-C-endoproteinase	29	Gly-hydrolase	35	20.6897
Serine-Protease-A	35	Immun-antigen-A	29	20.6897
Serine-Protease-A	35	Autolysin	29	20.6897
Serine-Protease-C	37	Autolysin	29	20.6897
Immun-antigen-A	29	Gly-hydrolase	35	20.6897
Autolysin	29	IgG-binding-protein	29	20.6897
Autolysin	29	Gly-hydrolase	35	20.6897
Autolysin	29	Lipase	37	20.6897
Glu-C-endoproteinase	29	Phos-phosphodiesterase	26	19.2308
Serine-Protease-A	35	Alpha-hemolysin	26	19.2308

Serine-Protease-A	35	LeukotoxinD	26	19.2308
Serine-Protease-A	35	Phos-phosphodiesterase	26	19.2308
Alpha-hemolysin	26	LeukotoxinD	26	19.2308
Alpha-hemolysin	26	Autolysin	29	19.2308
Alpha-hemolysin	26	IgG-binding-protein	29	19.2308
Alpha-hemolysin	26	Gly-hydrolase	35	19.2308
Alpha-hemolysin	26	Lipase	37	19.2308
LeukotoxinD	26	IgG-binding-protein	29	19.2308
LeukotoxinD	26	Lipase	37	19.2308
LeukotoxinD	26	Staphylokinase	27	19.2308
LeukotoxinD	26	Secretory	27	19.2308
LeukotoxinD	26	Phos-phosphodiesterase	26	19.2308
Autolysin	29	Staphopain	26	19.2308
IgG-binding-protein	29	Staphopain	26	19.2308
Gly-hydrolase	35	Phos-phosphodiesterase	26	19.2308
Lipase	37	Staphopain	26	19.2308
Staphylokinase	27	Phos-phosphodiesterase	26	19.2308
Staphopain	26	Phos-phosphodiesterase	26	19.2308
EnterotoxineB	27	Glu-C-endoproteinase	29	18.5185
EnterotoxineB	27	Serine-Protease-A	35	18.5185
EnterotoxineB	27	Beta-hemolysin	34	18.5185
EnterotoxineB	27	IgG-binding-protein	29	18.5185
EnterotoxineB	27	Gly-hydrolase	35	18.5185
EnterotoxineB	27	Aureolysin	28	18.5185
EnterotoxineB	27	Secretory	27	18.5185
Serine-Protease-C	37	Staphylokinase	27	18.5185
Gly-hydrolase	35	Staphylokinase	27	18.5185
Lipase	37	Secretory	27	18.5185
Aureolysin	28	Staphylokinase	27	18.5185
Enterotoxin	22	Aureolysin	28	18.1818
IgG-binding-protein	29	Aureolysin	28	17.8571
Serine-Protease-C	37	Beta-hemolysin	34	17.6471
Beta-hemolysin	34	Gly-hydrolase	35	17.6471
Serine-Protease-A	35	IgG-binding-protein	29	17.2414
Beta-hemolysin	34	Autolysin	29	17.2414
Immun-antigen-A	29	Lipase	37	17.2414
Serine-Protease-C	37	Gly-hydrolase	35	17.1429
Serine-Protease-C	37	Lipase	37	16.2162
EnterotoxineB	27	Phos-phosphodiesterase	26	15.3846
IgG-binding-protein	29	Phos-phosphodiesterase	26	15.3846
Lipase	37	Phos-phosphodiesterase	26	15.3846
Staphopain	26	Secretory	27	15.3846
EnterotoxineB	27	Immun-antigen-A	29	14.8148
Immun-antigen-A	29	Staphylokinase	27	14.8148
IgG-binding-protein	29	Staphylokinase	27	14.8148
Lipase	37	Staphylokinase	27	14.8148
Staphylokinase	27	Secretory	27	14.8148
Serine-Protease-A	35	Beta-hemolysin	34	14.7059
Beta-hemolysin	34	Lipase	37	14.7059
Serine-Protease-A	35	Gly-hydrolase	35	14.2857
Serine-Protease-A	35	Lipase	37	14.2857

7 Appendix-VII: Comparison of the cellular proteomes in the presence and absence of peptide A.

7.1 Supernatant proteins

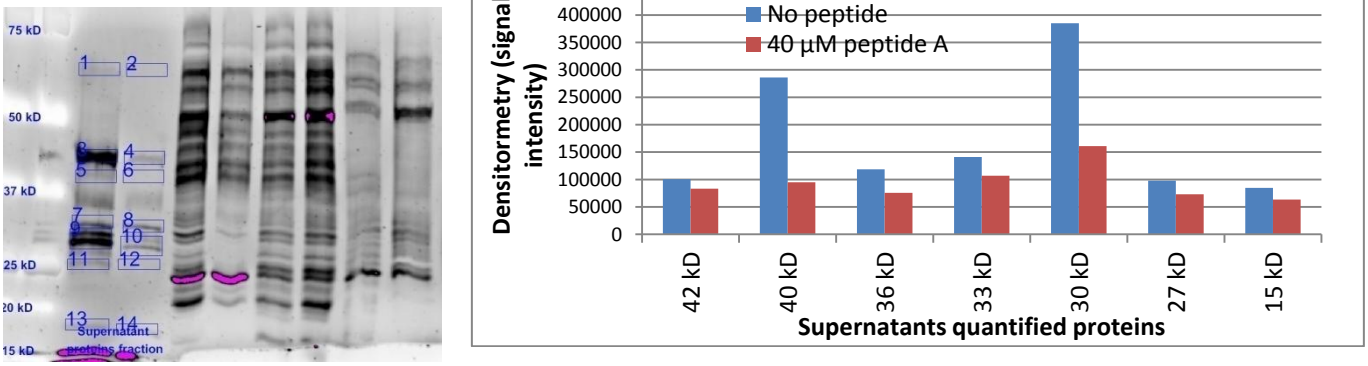

Figure 65 Comparison of the supernatant proteins between the peptide-treated and the non-treated cells.

7.2 Cell wall and periplasm proteins

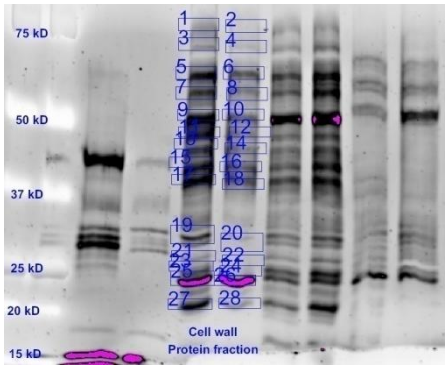

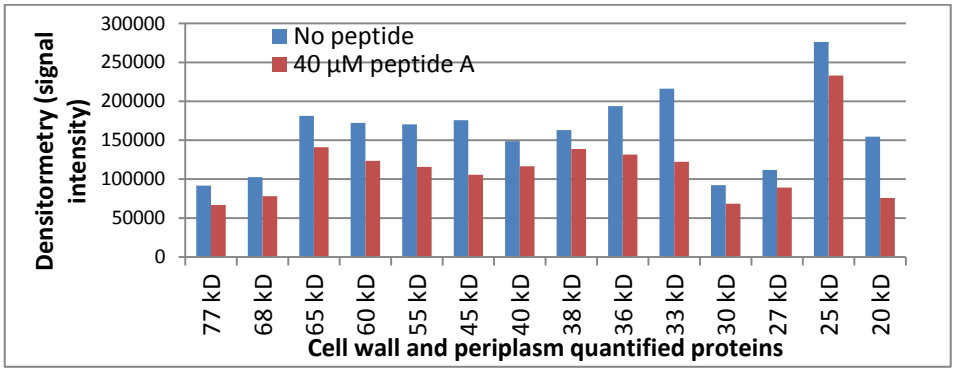

Figure 66 Comparison of the cell wall and periplasm proteins between the peptide-treated and the non-treated cells.

7.3 Cytosolic proteins

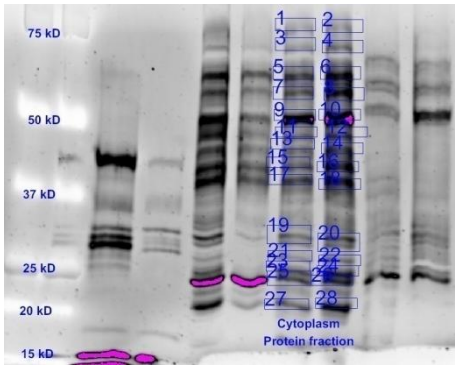

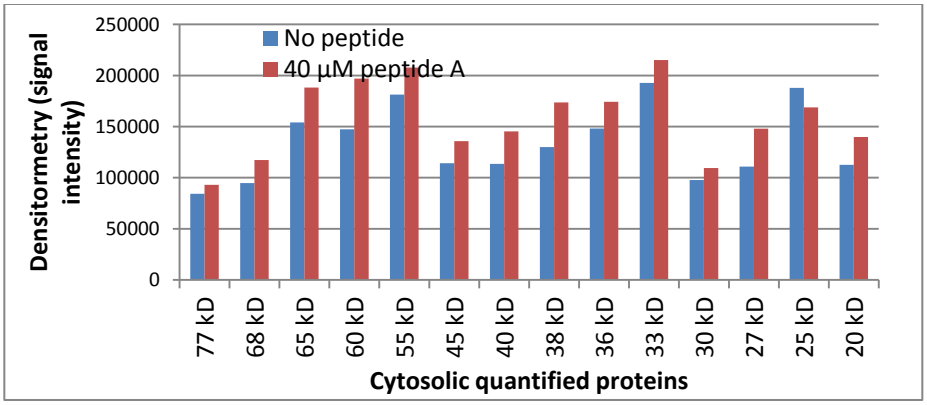

Figure 67 Comparison of the cytosolic proteins between the peptide-treated and the non-treated cells.

7.4 Membrane proteins

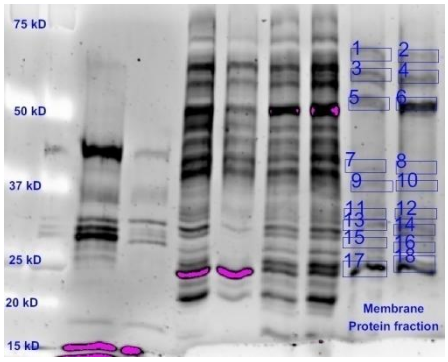

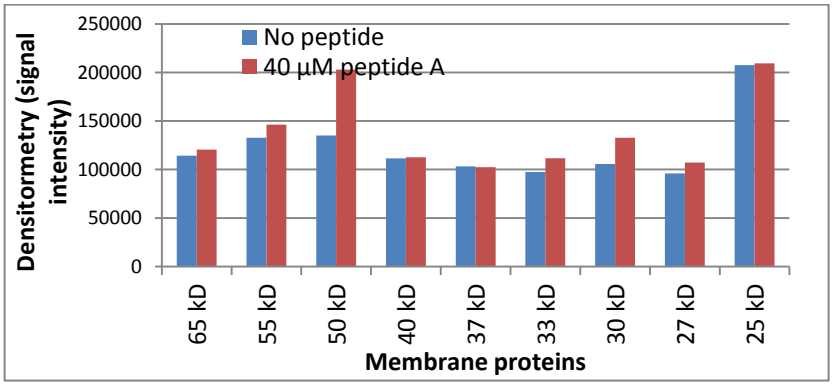

Figure 68 Comparison of the membrane proteins between the peptide-treated and the non-treated cells.

8 Appendix-VIII: Amino acids used in this study

Three letter code	One letter code	Description	Mw
Ala	A	L-Alanine	89.09
Arg	R	L-Arginine	174.2
Asn	N	L-Asparagine	132.12
Asp	D	L-Aspartic acid	133.1
Cys	C	L-Cystein	121.16
Gln	Q	L-Glutamine	146.15
Glu	E	L-Glutamic acid	147.12
Gly	G	L-Glycin	75.07
His	H	L-Histidine	155.16
Ile	I	L-Isoleucine	131.18
Leu	L	L-Leucine	131.18
Lys	K	L-Lysine	146.19
Met	M	L-Methionine	149.21
Phe	F	L-Phenylalanine	165.19
Pro	p	L-Proline	115.13
Ser	S	L-Serine	105.09
Thr	T	L-Thrionine	119.12
Trp	W	L-Tryptophane	204.23
Tyr	Y	L-Tyrosine	181.19
Val	V	L-Valine	117.15